

Doctoral thesis

Doctoral theses at NTNU, 2023:58

Lars Aaberg Stenvik

Pumping iron and manganese

Geochemistry and engineering of
groundwater well systems with challenging
redox conditions

NTNU
Norwegian University of Science and Technology
Thesis for the Degree of
Philosophiae Doctor
Faculty of Engineering
Department of Geoscience and Petroleum



Norwegian University of
Science and Technology

Lars Aaberg Stenvik

Pumping iron and manganese

Geochemistry and engineering of groundwater well systems with challenging redox conditions

Thesis for the Degree of Philosophiae Doctor

Trondheim, March 2023

Norwegian University of Science and Technology
Faculty of Engineering
Department of Geoscience and Petroleum



Norwegian University of
Science and Technology

NTNU

Norwegian University of Science and Technology

Thesis for the Degree of Philosophiae Doctor

Faculty of Engineering

Department of Geoscience and Petroleum

© Lars Aaberg Stenvik

ISBN 978-82-326-6385-9 (printed ver.)

ISBN 978-82-326-6879-3 (electronic ver.)

ISSN 1503-8181 (printed ver.)

ISSN 2703-8084 (online ver.)

Doctoral theses at NTNU, 2023:58

Printed by NTNU Grafisk senter

Abstract

Wells facilitate extraction of groundwater from aquifers, both for drinking water, irrigation, drainage and thermal energy purposes. For the latter case, wells can also be used to reinject the groundwater back into the aquifer. Groundwater wells' ability to supply or recharge satisfactory quantities and qualities of water is often altered with time. Especially, the redox sensitive elements iron and manganese are common problem causers. Dissolved and reduced iron and manganese will precipitate as (hydr)oxide minerals if oxidized. The precipitates form incrustations which clog the flow cross section, leading to lower water discharge capacity for a given hydraulic head drawdown (1), and cause coloring which is undesired from a water quality perspective (2).

Nine groundwater heat pump (GWHP) systems in Melhus, Norway have facilitated a field laboratory to study and monitor iron related clogging issues. The investigations have revealed the occurrence of both iron oxide and iron sulfide incrustations, sometimes even in the same well systems. This indicates redox conditions on the verge between post-oxic and sulfidic in the Melhus aquifer, evidenced by high dissolved iron ($\text{Fe}^{2+}=0.2\text{-}6.2$ mg/L) and low dissolved oxygen ($\text{DO}\leq 0.05$ mg/L) concentrations. Though co-occurring, iron oxides tend to encrust relatively low-saline (0.4-1.3 g/L), while iron sulfides mostly encrust high-saline (1.4-2.4 g/L) GWHP systems. The most severe iron oxide clogging has occurred at the Lena terrasse GWHP, where the iron-oxidizing bacteria (IOB) *Gallionella* and *Sideroxydans* have been detected. Lena terrasse is characterized by high Fe^{2+} (3.2-4.0 mg/L), and lower pH (7.3 ± 0.1) and higher groundwater pumping rate Q (9 ± 4 L/s) than most other GWHP systems in Melhus. Lower pH and DO are more favorable for IOB-aided than abiotic iron oxidation. This implies that iron oxidation risk assessment in anoxic aquifers should focus on hydrochemical and hydraulic conditions which promote biotic growth, rather than purely abiotic considerations.

Hydraulic monitoring at the Lena terrasse GWHP indicates that the pumped water is discharged by gravity (i.e., waterfall flow) from the heat exchanger down through the injection well (~20 m fall to the natural water table). This has two important implications: groundwater pipework pressurization will only increase the pumping power (i.e., costs) slightly (1), and incrustations will not increase the pumping costs before severely clogging the injection well filter (2). Pressurization of the piping system, by means of injection pipe constriction and air-release valves, will lower the risk of degassing and gas entrapment, and possibly air in-leakage. Though, the added pressure will have limited influence on CO_2 degassing and pH. Thus, iron incrustations must still be expected in a pressurized GWHP system.

Elevated manganese concentrations in the production wells at Ringerike waterworks first occurred after 19 years of operation (2006), increased for ~eight years (2006-2014), before stabilizing at a high level (2014-). The delayed occurrence is probably due to a sorption front progressing from the bank filtration area ~500 m away from the well field. The high manganese concentrations have necessitated a costly water treatment (~10 mill. EUR) due to unpleasant taste and color, but led to little or no well filter clogging. This is probably due to manganese's slower oxidation kinetics compared with iron. The changing water quality detected with time at both Melhus and Ringerike suggests that water quality should be monitored during operation of groundwater wells, both for qualitative (drinking water) and clogging (energy/drinking water) purposes. For bank filtrations schemes, an observation well in between the well field and bank filtration area is advised for early detection of sorption fronts.

GWHP systems are advised to optimize Q from hydrochemical, hydraulic and thermal monitoring data, to minimize clogging risk and maximize heat output vs. power input. This led to recommendations to minimize Q in the range 6-12 L/s for the Lena terrasse GWHP. Still, maintenance actions must be expected, especially in the heat exchanger and injection well. Heat exchanger rehabilitation (incl. flow reversal) is short-term economically and technically more favorable than injection well rehabilitation. The economically competitive and environmentally non-hazardous chemical sodium dithionite ($\text{Na}_2\text{S}_2\text{O}_4$) is proposed for improving well rehabilitation efficiency on mature iron oxides.

Preface

The PhD work has been carried out at the Department of Geoscience and Petroleum, Norwegian University of Science and Technology, with professor Bjørn Syvert Frenstad as the main supervisor. Adjunct professor Randi Kalskin Ramstad from the same department has been the co-supervisor.

The 4-year (2018-2022) PhD contract allocated time for both research (75%) and duty work (25%). The research activities have been part of the research project “Optimal resource utilization of groundwater for heating and cooling in Melhus” (ORMEL 2), and was funded by the Regional Research funds in Mid-Norway (grant-number 284965). The duty work comprised two main activities: lecturing, seminar supervision, and preparation of exam and seminar problems for TGB4205 – Hydrogeology (spring 2019-2022) (1), and preparation and supervision of the 1-2 weeks start-up project “Teknostart” (august 2019-2022) for new students at the department (2). Just over 300 hours participation in the Polish-Norwegian research project “CO₂-Enhanced Geothermal Systems for Climate Neutral Energy Supply” (EnerGizerS) and covid-19 related laboratory delays led to roughly four months of contract extension. This allocated time for a six-week research stay at the University of Huelva, Spain (autumn 2022).

Acknowledgements

It has been said about and by two great ‘trøndere’ (i.e., Mid-Norwegians), respectively:

“Jesus redder ... men ‘Ivers’ scorer på returen”

[Eng: “Jesus saves... but ‘Ivers’ (i.e., Odd Iversen (1945-2014), former Rosenborg striker) scores on the rebound”]

- *Unknown*,

written on a church wall in Mjøndalen, Norway

and

“Du kan itj skräem nånne te å bli god!”

[Eng: “You cannot frighten someone into improving!”]

- *Nils Arne Eggen (1941-2022)*,
former Rosenborg manager

I have found both these quotes from the football pitch adaptable to the pursue of a PhD. First, it craves a bit of the ‘Ivers’ mentality of not giving up although failing on the initial attempt to ‘score’ (e.g., damaging field equipment, claims of ‘scarce apotations’ by reviewers, etc.). I also testify to the legendary former Rosenborg manager Nils Arne Eggen’s ‘Godfot-teori’ (Eng: ‘good foot theory’), stating that well-being and cooperation is the key to success. This PhD would never have been realized without the mentoring, supervision, help, cooperation, and comfort provided by people constituting my work and social environment during the last few years.

I would like to start thanking my main supervisor, professor Bjørn Syvert Frenstad, and co-supervisor, associate professor Randi Kalskin Ramstad, both at the Department of Geoscience and Petroleum, NTNU. As supervisors, they have complemented each other fantastically, or as “R&B”: ‘Randi the rhythm’, always ready to put things in motion and fronting the ‘learning by doing’, and ‘Bjørn the blues’, always open to discuss new ideas, listening to lamentations, and motivate me when I felt discouraged. Thanks to the pleasant work environment provided by them I have been eager to learn and felt professionally capable during the vast majority of the last 4 ½ years.

A very important influence for me choosing to pursue a PhD at all was former PhD student and colleague Sondre Gjengedal. We first met as supervisor and student during my final year as a master’s student. I made a mediocre first impression, making Sondre aware that I did not have a driver’s license just ahead of the six-hour drive to Elverum, but the atmosphere improved when we discovered our shared love for groovy disco beats. Since then, Sondre has been an everlasting source of ground source

heat pump knowledge, guidance, and sparring. I owe many thanks to Sondre for the fruitful cooperation and all the good times, which have contributed significantly to this thesis.

This PhD has also benefitted from the collaboration within the ORMEL 2 research project. This includes professional sparring and field work assistance provided by Bernt Olav Hilmo, Mari Helen Riise and Henrik Holmberg at Asplan Viak AS, and discussions with researchers Atle Dagestad, Pål Gundersen and Guri Venvik at the Geological Survey of Norway (NGU). A special thanks is directed to Bernt Olav for introducing me to relevant case studies on iron and manganese in Norwegian groundwater works, and his guidance and our collaboration on this topic. Furthermore, field assistance was provided by Gjøvaag AS on camera inspections, Jan Ivar Ulfnes (Optiview) on the automation, surveillance, and regulation of Lena terrasse's groundwater heat pump system, and all the local janitors in Melhus. From the latter group, special thanks are directed to Gry Tangvik Amundsen for always welcoming our visits, and for sharing her 'hands on' experience.

The laboratories at Department of Geoscience and Petroleum, NTNU have been vital for data acquisition. First, staff engineer Håkon Myhren custom-designed, built, and repaired the highly useful flow-through cell used for hydrochemistry field measurements. Later, mineralogical and chemical analysis of incrustation samples were aided by senior engineers Laurentius Tjihuis and Torill Sørløkk. The tireless assistance and discussions with Laurentius and Torill have been vital, both for data quality and motivational purposes. Staff engineer Kjetil Eriksen's scanning electron microscopy (SEM) analyses provided important clues on the activity of iron-oxidizing bacteria. I would like to thank all of them for always being ready to help during the last few years.

Also, people from outside the research project and NTNU have contributed to the completion of this thesis. David Banks, senior research fellow at University of Glasgow, provided supervision at an early stage of the PhD work including updating me on the state of the art of open loop ground source heat pumps and chemical well rehabilitation. Researcher Clara Sena and professor emeritus Per Aagaard, both at Department of Geosciences, University of Oslo, have contributed with discussions on geochemistry, PHREEQC programming guidance and critical pre-review of manuscripts. Ulrich Wolfgang Weber, former PhD student from the same department, generously came to Melhus all the way from Oslo just to perform field measurements of gas concentrations. PHREEQC guidance and troubleshooting was furthermore aided by David Parkhurst, scientist emeritus at US Geological Survey, channeled through the 'PHREEQC Users Discussion Forum'. Fruitful discussions and guidance on well incrustations were initiated at conferences and continued through email correspondence with Niels Hartog, principal scientist at KWR water research institute, Netherlands, and Georg Houben, head of department at the Federal Institute for Geosciences and Natural Resources (BGR), Germany. I would like to thank each one of them for taking time to share their knowledge and expertise.

During the finalization of the thesis, University of Huelva, Spain provided excellent conditions for a six-week 'writing retreat'. Many thanks to the everyone at the 'Tharsis' research group, and especially to my host professor Manuel Olías, at the Department of Earth Sciences for warmly welcoming me.

Outside the work environment, I would like to thank my mother and father, Berit and Gunnar, for supporting my pursue for a PhD, both morally and materially before and during the 4-year period. Materially, it includes office facilities during the last one and a half year after moving to Oslo. I offer many thanks to my colleague there, Henri, for cheerful breaks in the park. I also owe great thanks to my sister Ragnhild for her affectionate character and openness.

Lastly, and most appreciably, I would like to say "miles gracias" to my dearest friend Marte for sticking with me during all these years. The appreciation is not so much for her support in doing the PhD work as for her demands to put down the work in time (and her surprising claim that there are more important things to life than groundwater!). Surely, this has contributed to improve both the thesis and my quality of life during the last few years. I am forever thankful for this, Marte my dear!

Nomenclature

<i>Latin letters</i>	<i>Explanation</i>	<i>SI unit</i>
B	Linear (pressure) loss coefficient	[s/m ²]
c	Dissolved concentration of gas/solid in water	[M]
C	Non-linear (pressure) loss coefficient	[s ² /m ⁵]
COP	Coefficient of performance (i.e., ratio between heat output and power input)	[-]
d	Diameter	[m]
Eh	Redox potential with respect to the standard hydrogen electrode	[V]
Fr	Froude number (i.e., ratio between inertia and gravitational forces)	[-]
h	Hydraulic head (i.e., sum of elevation, pressure and velocity head)	[m]
k	Homogenous rate constant for oxidation of iron	[mol/s]
k'	Heterogenous rate constant for oxidation of iron	[/mol/s]
K_{ads}	Adsorption coefficient	[-]
K_H	Henry's constant	[Pa·m ³ /mol]
L	Length	[m]
LMTD	Logarithmic mean temperature difference (of heat exchange)	[K]
LOI	Loss on ignition	[-]
n	Number of data points	[-]
p	Pressure	[Pa]
P	Heat output or exchanged	[W]
Q	Volumetric flow/pumping rate of groundwater	[m ³ /s]
R	Manganese retardation factor (i.e., ratio between groundwater flow and manganese transport rate)	[-]
s	Hydraulic head drawdown through well filters or heat exchanger	[m]
t	Time	[s]
T	Temperature	[K]
U	Heat transfer coefficient (of heat exchange between fluids)	[W/K/m ²]
V	Volume	[m ³]
W	Power input	[W]
<i>Greek letter</i>	<i>Explanation</i>	<i>SI unit</i>
τ	Shear stress exerted by flow on heat exchanger plates	[Pa]
<i>Constants</i>	<i>Explanation</i>	
$c_p \approx 4.184$ kW/K/kg	Specific heat capacity of water (at $T = 20$ °C)	
$g \approx 9.81$ m/s ²	Gravitational acceleration	
$\rho \approx 1$ g/cm ³	Density of pure water at ($T = 4$ °C)	

<i>Abbreviation</i>	<i>Explanation</i>
ATES	aquifer thermal energy storage (i.e., GWHP system with additionally seasonal heat storage)
GP	groundwater pump
GSHP	ground source heat pump (i.e., heat pump utilizing subsurface as heat source or sink)
GWHP	groundwater heat pump (i.e., open-loop ground source heat pump utilizing an aquifer)
HE	heat exchanger
HP	heat pump
IOB	iron-oxidizing bacteria (i.e., group of bacteria contributing to the oxidation of iron)
IRB	iron-reducing bacteria (i.e., bacteria contributing to the reduction of iron)
NGU	Geological Survey of Norway
NTNU	Norwegian University of Science and Technology
SOB	sulfur-oxidizing bacteria (i.e., bacteria contributing to the oxidation of sulfur)
SRB	sulfate-reducing bacteria (i.e., bacteria contributing to the reduction of sulfate)

Table of contents

Abstract.....	i
Preface	iii
Acknowledgements.....	iii
Nomenclature.....	v
1. Introduction.....	1
1.1. Background.....	2
1.2. Thesis context	3
1.3. Thesis structure and research questions	3
2. Theory.....	5
2.1. Ground source heat pump systems.....	5
2.2. Redox geochemistry of iron and manganese	7
2.3. Clogging of groundwater wells and heat exchangers	11
3. Study areas.....	17
3.1. Melhus.....	17
3.2. Ringerike.....	19
4. Materials and methods	23
4.1. Water quality.....	23
4.2. Incrustation composition and remediation	25
4.3. PHREEQC modeling	28
4.4. Hydraulic and thermal monitoring of GWHP systems	29
5. Results.....	31
5.1. Brief comments on published papers	31
5.2. Additional results	36
6. Discussion.....	41
6.1. How to reduce the negative effects of pumping iron and manganese.....	53
7. Conclusions.....	55
7.1. Further work.....	57
References.....	59
Appendices.....	66

Section of original papers

Paper I: Stenvik, L. A., & Hilmo, B. O. (2020). Jern- og manganproblematikk ved grunnvannsuttak med eksempler fra Ringerike og Sunndal vannverk [Eng: Iron and manganese in groundwater works – review of problems and case studies from Ringerike and Sunndal]. *Vann*, 55(2), 151-161.

Paper II: Stenvik, L. A., Gjengedal, S., Ramstad, R. K., & Frengstad, B. S. (2022). Hydrochemical and biotic control on iron incrustations in groundwater heat pump systems: Case study from a saline, anoxic aquifer in Melhus, Norway. *Geothermics*, 100, 102349. <https://doi.org/10.1016/j.geothermics.2022.102349>

Paper III: Gjengedal, S., Stenvik, L. A., Storli, P.-T. S., Ramstad, R. K., Hilmo, B. O., & Frengstad, B. S. (2019). Design of Groundwater Heat Pump Systems. Principles, Tools, and Strategies for Controlling Gas and Precipitation Problems. *Energies (Basel)*, 12(19), 3657. <https://doi.org/10.3390/en12193657>

Paper IV: Gjengedal, S., Stenvik, L. A., Ramstad, R. K., Ulfsnes, J. I., Hilmo, B. O., & Frengstad, B. S. (2021). Online remote-controlled and cost-effective fouling and clogging surveillance of a groundwater heat pump system. *Bulletin of Engineering Geology and the Environment*, 80, 1063–1072. <https://doi.org/10.1007/s10064-020-01963-z>

Paper V: Stenvik, L. A., Gjengedal, S., Ramstad, R. K., & Frengstad, B. S. (2022). How to avoid gas clogging in groundwater heat pump systems: a case study from the Lena terrasse system in Melhus, Norway. *Bulletin of Engineering Geology and the Environment*, 81(4), 152. <https://doi.org/10.1007/s10064-022-02652-9>

Paper VI: Stenvik, L. A., Ramstad, R. K., & Frengstad, B. S. (2022). Optimizing Submersible Pump Regulation of a Clogging Prone Groundwater Heat Pump System in Melhus, Norway. *Science and Technology for the Built Environment*. <https://doi.org/10.1080/23744731.2022.2136901>

Paper VII: Stenvik, L. A. (2022). Laboratorietesting av en kjemikalie som reduserer og løser opp jernoksid-utfellinger. Vurdering av anvendbarhet til rensing av grunnvannsbrønner [Eng: Laboratory testing of a chemical which reduces and dissolves iron oxide incrustations. Assessment of applicability to well rehabilitations]. *Vann*, 57(3).

Paper VIII: Stenvik, L. A., Hilmo, B. O., & Frengstad, B. S. (2022). Elevated manganese concentrations in groundwater wells after longtime abstraction with bank filtration. *Hydrogeology Journal*. <https://doi.org/10.1007/s10040-022-02538-w>

1. Introduction

The importance of groundwater for drinking water and thermal energy purposes is likely to increase in the 21st century, due to growing water demands (United Nations, 2022) and the energy transition from fossil fuels to renewables (Bloemendal et al., 2015). *Aquifers* (i.e., groundwater reservoirs) contain 99% of all liquid freshwater resources on Earth. This makes groundwater a key factor in delivering drinking water to a growing world population facing increasing water scarcity (United Nations, 2022). Furthermore, aquifers are excellent thermal energy storages. Thus, groundwater extraction and injection may serve renewable, low-environmental impact and cost-reducing heating and cooling. Around 15% of the world’s population lived in areas with high potential for the *aquifer thermal energy storage* (ATES) technology at the beginning of the 21st century. Although this portion is predicted to decrease to ~5% in the second half of the century, aquifers still demonstrate a substantial and not fully utilized potential for heating and cooling applications (Bloemendal et al., 2015).

Groundwater wells facilitate extraction and injection of groundwater from/to aquifers for both drinking water and thermal energy purposes. Therefore, groundwater-based water supply and heating/cooling rely on sustainable operation of groundwater well systems. Groundwater wells may face a variety of water quality challenges during operation, see Figure 1.1. These challenges can be divided into problems for the longevity of well-functioning (1), and water quality issues related to human health and aesthetics (2) (Ellingsen, 1992). Thermal energy systems only need to consider problems related to well-functioning, while drinking water wells additionally must secure a satisfactory water quality for their consumers.

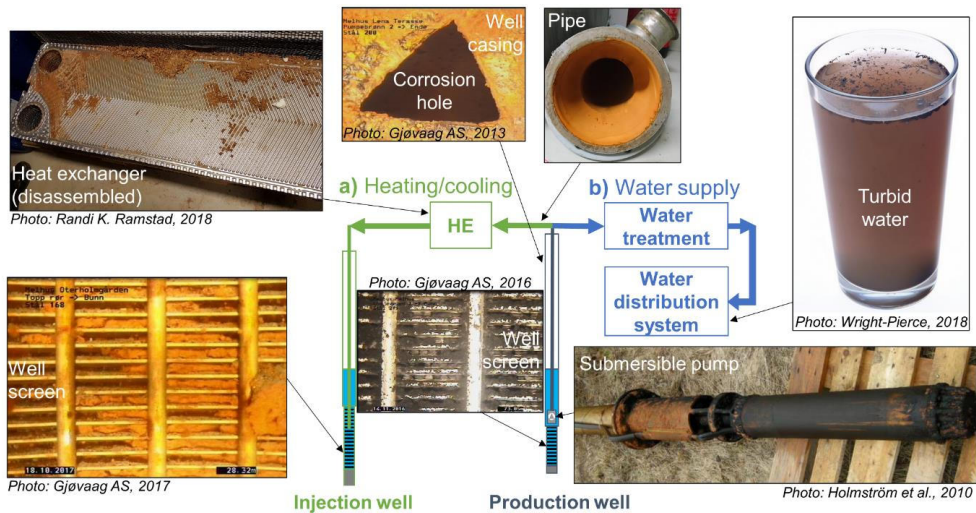


Figure 1.1 Typical operational problems related to groundwater quality in **a** heating and cooling and **b** water supply systems.

The predominant well-functioning problems are corrosion and clogging. Corrosion involves electrochemical oxidation of metallic iron, leading to deterioration of well steel. Clogging is caused by initially dissolved and suspended substances in the groundwater, which then precipitate and deposit in the well system. These precipitates and deposits will incrust and clog well filters, pumps, pipes, etc., and increase the groundwater pumping costs and/or decrease the well yield. Especially, incrustations of iron and manganese oxides, both from natural and corrosion origin, is a worldwide phenomenon impeding groundwater well performance (Lindblad-Påsse, 1986, van Beek, 1989, Banks, 1992, Walter, 1997, McLaughlan, 1992, Bakema, 2001, Houben and Treskatis, 2007, Dimkić et al., 2012).

The pathogenic water quality is generally better for groundwater than surface water sources, due to filtration and degradation processes in the aquifer and natural protection from pollution (Gaut, 2011, Kvitsand et al., 2017). However, groundwater may contain elevated dissolved concentrations of inorganic compounds, for instance poisonous arsenic (Smedley and Kinniburgh, 2002) and fluoride (Frengstad et al., 2002), and iron and manganese. The latter two mainly represent aesthetic concerns, causing undesired color, smell and taste of the water (Ellingsen, 1992).

This thesis will deal with both groundwater quality and clogging issues in thermal energy and drinking water well systems. Primarily, the thesis will focus on clogging issues in *groundwater heat pump* (GWHP, i.e., groundwater and thermal energy extraction-injection systems without energy storage) systems, but groundwater quality and clogging issues related to iron and manganese in groundwater works will also be discussed.

1.1. Background

Groundwater is relatively sparsely utilized for drinking water and thermal energy purposes in Norway. Only 15% of Norwegian drinking water are withdrawn from aquifers, compared with 60-100% in the other Nordic countries (Kløve et al., 2017) and ~50% globally (United Nations, 2022). An even lower percentage (<0.1%) of the more than 60,000 ground sourced thermal energy systems in Norway involve groundwater extraction and injection (Midttømme et al., 2020).

The sparse groundwater utilization in Norway can partly be explained by the preconditions. Larger groundwater extraction and injection schemes require a permeable aquifer of sufficient size (and temperature) to yield the required quantity of groundwater (and thermal energy) (Houben and Treskatis, 2007, Snijders and Drijver, 2016). Thin and/or impermeable soil covers, and mainly crystalline bedrocks, have limited larger Norwegian groundwater works to (glacio)fluvial deposits consisting of unconsolidated sand and gravel. Water supply in any medium-sized Norwegian cities (~15,000-25,000 inhabitants, e.g., Lillehammer, Hønefoss (Ringerike), Kongsberg and Elverum) rely on induced bank filtration from local rivers to increase the groundwater abstraction capacity (Frengstad and Dagestad, 2008). The Norwegian (glacio)fluvial deposits are also suitable for thermal energy purposes, but with a large discrepancy between potential and realization (Midttømme et al., 2020).

For Norwegian groundwater wells it is common practice to perform quantitative well tests and water quality measurements prior to start of operation. If the well yield and quality are deemed satisfactory, the well is put into operation with little or no monitoring or maintenance planned. As a result, well problems often develop unnoticed beyond repair, making abandoning or drilling of new wells the only viable solution (Banks, 1992, Stenvik, 2020). Lack of experience and aversion against chemical rinsing could partly explain rehabilitations' inability to restore the clogged wells (Hilmo and Gurigard, 2017). Sparse monitoring data also make troubleshooting of problem genesis difficult, and the learning outcome from well failures limited.

Examples comprise iron oxide clogging issues at Sunndalsøra waterworks (Vestland, 2010), and the occurrence of elevated manganese concentrations in the abstracted groundwater after long time operation at Ringerike (Hilmo, 2007) and Lillehammer waterworks (Holmström et al., 2010). The manganese issues at Ringerike and Lillehammer have necessitated water treatment facilities costing ~10 mill. EUR (Brugger and Paskert, 2020) and ~25 mill. EUR (Holmøy, 2020), respectively.

The modest interest in groundwater sourced heating and cooling is probably due to the reported and partly unsolved iron oxide clogging issues in pioneering systems at Oslo airport, Gardermoen (Eggen and Vangnes, 2005, Rike, 2011, Woyessa, 2012) and Melhus (Riise, 2015). For instance, the gradual abandoning of the groundwater sourced heating and cooling at Oslo airport, meanwhile increasingly exploiting the municipal district heating system, cannot be termed 'good advertisement' for the technology.

The examples from both the drinking water and heating and cooling sector demonstrate the need for more hydrogeological competency involved during groundwater extraction and injection. Especially, increasing iron and manganese knowledge seems important for improving the sustainability of groundwater exploitation. This also explains the motivation (1) and aim (2) for this PhD thesis, which are...

... making groundwater utilization more reliable and attractive both for drinking water and thermal energy applications (1) by increasing the understanding of iron and manganese's geochemical behavior and related operational issues in groundwater well systems (2).

1.2. Thesis context

Riise (2015) demonstrated the lack of professional expertise involved in the design, operation and maintenance of nine GWHP systems established in Melhus town center, Mid-Norway. This review set the agenda for the research project *Optimal resource utilization of groundwater for heating and cooling in Melhus and Elverum* (ORMEL) which spanned for three years between 2015-2018. This project was a collaboration between Norwegian University of Science and Technology (NTNU), Asplan Viak AS, Geological Survey of Norway (NGU), and Melhus and Elverum municipality. The objective of the ORMEL project was to gain knowledge for sustainable utilization of the aquifers in Melhus and Elverum for thermal energy purposes. Special emphasis was put on hydrogeological characterization of the aquifers, and GWHP system design and monitoring with regards to clogging (Ramstad et al., 2020, Gjengedal, 2021).

Water quality studies carried out before and during the ORMEL project revealed elevated dissolved iron and manganese concentrations and high salinities in all GWHP system in Melhus (Solberg et al., 2014, Riise, 2015, Brøste, 2017). This could to some extent explain the clogging issues, but not fully settle their genesis, possibly catalyzing effects (e.g., by iron-oxidizing bacteria), and remediation strategies.

The unsolved issues set the stage for a sequel research project: *Optimal resource utilization of groundwater for heating and cooling in Melhus* (ORMEL 2). This was a collaboration between NTNU, Asplan Viak AS, NGU, Gjøvaag AS, University of Oslo (UiO), Gjøvaag AS and Melhus municipality, between 2018 and 2021. ORMEL 2 contained two work packages: one related to planning of a joint GWHP solution for the town center in Melhus, and one concerning operational issues arising from high iron and manganese concentrations. This PhD thesis is part of the latter work package.

1.3. Thesis structure and research questions

There are three main research topics in this PhD thesis: iron and manganese geochemistry (A), degassing and gas entrapment in GWHP systems (B), and operation and rehabilitation of groundwater heat pump (GWHP) systems (C). Four **research questions** have been formulated:

- I) *How do the geochemical signatures of iron and manganese influence groundwater well operation?*
- II) *How important is the microbiology for the GWHP incrustations in Melhus, and which factors control the bacterial activity?*
- III) *How do vacuum pressures amplify GWHP operational problems, and which design measures are feasible to prevent degassing and gas entrapment?*
- IV) *How can groundwater pumping and maintenance procedures be adjusted to reduce clogging risk and improve GWHP system economy?*

The first question (I) is relevant for and will be answered based on data from both water supply and GWHP systems, while the latter three (II-IV) mainly deal with GWHP systems. The research questions are sought answered in eight original papers and two additional results (i.e., not published previously).

The thesis structure is visualized in Figure 1.2. Horizontal arrows indicate the work process from research topics and questions, via methodology, to results. Diagonal arrows demonstrate that the methodology and results for research topic B and C are partly based on data and analyses from research topic A and A-B, respectively.

Chapter 2 presents relevant theory for the main research topics (A-C), before the thesis' study areas, methodology and results are described in chapter 0-5. The results (published papers and additional results) will be discussed with emphasis on the research questions in chapter 6, leading to recommendations in chapter 6.1 and conclusions in chapter 7. Written and oral scientific contributions not incorporated in the main thesis outline are presented in Appendix A.

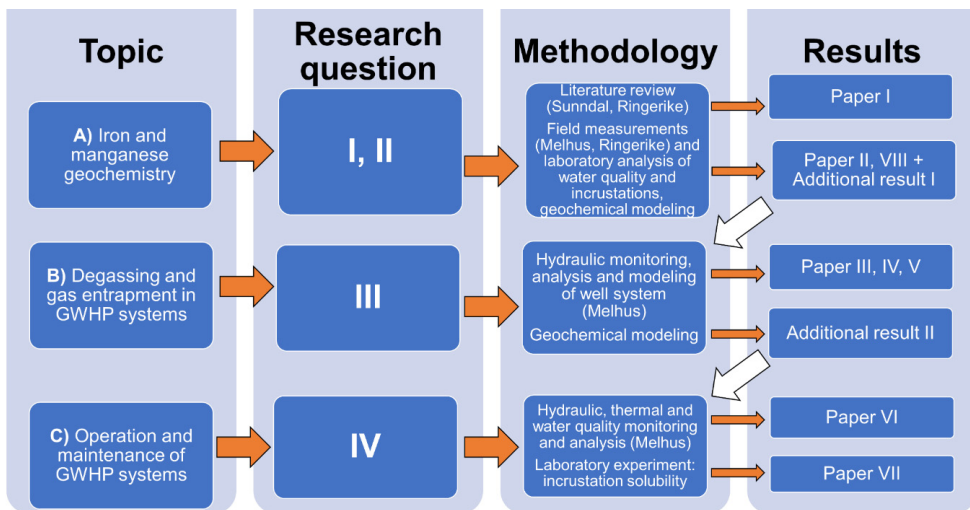


Figure 1.2 Thesis structure and research questions.

2. Theory

This chapter will introduce relevant literature for the thesis work, including description of the ground source heat pump (GSHP) technology with emphasis on groundwater heat pump (GWHP) systems, iron and manganese geochemistry, and clogging of groundwater well systems. The latter chapter will focus on mechanisms, impact and detection, and preventive measures, especially with regards to iron-related clogging. Bank filtration theory is not included in this chapter but described in Paper I and VIII.

2.1. Ground source heat pump systems

Ground source heat pump (GSHP) systems utilize shallow parts of the subsurface (< 200 m depth or so) as a heat source and/or sink for buildings. The thermal energy in shallow parts of the subsurface is mainly solar heat. The insulating rock and/or soil cover will lead to slow heat absorption during summer, and limit the heat loss during winter. Consequently, the subsurface temperature will be more or less constant from a few meters depth, and resemble the long-term annual average air temperature (Banks, 2012). In Norway, this typically yields temperatures $\leq 6\text{ }^{\circ}\text{C}$ in the shallow subsurface (Kirkhusmo and Sønsterud, 1988), which means a heat pump is needed to “pump up” the temperature to a level usable for the consumer ($25 \leq T \leq 60\text{ }^{\circ}\text{C}$) (Banks, 2012).

Compared with an ambient air source heat pump, the constant temperature in the ground provides stable operating conditions which are favorable for the longevity of the heat pump. The stable operating conditions also yield a high coefficient of performance (COP = heat output / power input) $\sim 2.5\text{--}3.3$, which corresponds to 60–70% energy savings compared with conventional electrical heating (NGU, 2020). Thus, the subsurface represent a renewable, economically favorable and reliable energy resource, which is almost universally available for GSHP utilization. However, the preferred GSHP technology, either a *closed* or *open* loop system, depends on site conditions.

Closed loop GSHP systems comprise circulating a heat carrying fluid (i.e., typically water mixed with glycol) in a closed plastic pipe through the subsurface, and a heat pump unit at terrain level, see Figure 2.1. In heating mode, heat is transferred from the closed loop to the heat pump evaporator. This inflicts a temperature reduction to the heat carrying fluid, and heat transfer from the ambient rock/soil to the cooled down heat carrying fluid during the following loop through the subsurface. Solely energy (i.e., not mass) is exchanged with the subsurface in the closed loop configuration, making *conduction* the main mode of heat transfer.



Figure 2.1 Closed loop ground source heat pump (GSHP) technologies: vertical boreholes (*left*) and horizontal collector pipes (*right*). Illustrations by Norman Energiteknikk AS, modified in Gjengedal (2021).

Since the drilling costs are lower and the thermal conductivities are higher in hard rock than soil, vertical closed loop systems in boreholes are preferential in areas with a thin soil cover. These boreholes are often termed *energy wells*, since only energy is extracted. In areas with a thick cover of impermeable soil (e.g., clay) and/or limited heating/cooling demand, horizontal closed loop collector pipes can be established in 1-2 m deep dug ditches. In heating mode, the vertical and horizontal closed loop

configurations in Norway will typically yield 30-40 W/m “active borehole” (i.e., portion below water table) and 15-30 W/m collector pipe, respectively (NGU, 2020).

Due to the closed loop systems’ nearly universal applicability, they represent the most common GSHP technology worldwide (Banks, 2012). In Norway, >90% (Midttømme et al., 2016) of the of the 60,000 installed GSHP systems are energy wells in crystalline rocks (Midttømme et al., 2020).

In **open loop GSHP systems** both groundwater and energy are extracted from the geological formation. The groundwater functions as the heat carrying fluid, which transfers heat to/from a heat exchanger in connection with a heat pump. Accordingly, the technology relies on *convective* heat transfer to/from the subsurface. The heat P_{HE} extracted from/added to the groundwater in the heat exchanger can be described with the equation (as quoted in Stene, 2001)

$$P_{HE} = Q * c_p * \Delta T_{gw} \quad (2.1)$$

where Q is the groundwater discharge rate (e.g., kg/s \approx l/s), c_p is the specific heat capacity of water (\approx 4.2 J/g/°C for T=0-10 °C), and ΔT_{gw} is the groundwater temperature change through the heat exchanger.

Equation 2.1 demonstrates that the open loop configuration requires a sufficiently permeable geological formation (i.e., allowing higher groundwater extraction rates Q) (1), and a high enough groundwater temperature to allow temperature reductions without freezing the groundwater (2). This limits the applicability of open loop GSHPs to aquifers of unconsolidated sand and gravel, sandstone and karstic/highly fractured carbonates (Snijders and Drijver, 2016), and abandoned mine galleries (Ramos et al., 2015). Furthermore, regions with permafrost and ground temperatures close to 0 °C should be avoided (Banks, 2012).

A *groundwater heat pump* (GWHP) system is an open loop GSHP technology which utilizes an aquifer as its heat source and/or sink, see Figure 2.2. The groundwater loop contains three basic components: a screened production well (1), a heat exchanger in loop with the heat pump unit (2), and a screened injection well/drain to the local stormwater system (3). The production well contains a submersible pump which pumps the groundwater up to the heat exchanger. The indirect heat exchange to the heat pump by means of a *secondary circuit* between the heat pump and the heat exchanger (Figure 2.2) is common for open loop systems to avoid clogging of the heat pump unit itself (Banks, 2012). The heat exchanged groundwater is then either recharged to the aquifer through the injection well, or discharged to the local stormwater drain.

If the GWHP system reinjects the groundwater, the injection well(s) must be placed sufficiently far away from the production well to avoid *thermal breakthrough*. This occurs if the injected water reaches the production well prior to acquiring the natural aquifer temperature (i.e., by heat transfer between the injected water and the aquifer). Placing the injection well downstream the production would reduce the risk of thermal breakthrough. This also implies that GWHP systems benefit from an inclined water table, inducing high aquifer flow rates and convective heat transfer to/from the well field (Snijders and Drijver, 2016)

Aquifer thermal energy storage (ATES) systems are GWHP systems where a hot and cold storage are built up around each part of the well doublet. This is done by installing submersible pumps in both wells, and reversing the flow between winter and summer. Thus, a hot storage builds up around the well which functions as an injection well during the summer. This heat can be utilized during winter when the flow is reversed. Followingly, instead of dedicated production and injection well(s), ATES systems operate with hot and cold wells. Balance between the heating and cooling demand reduces the risk of thermal breakthrough (Snijders and Drijver, 2016). Since ATES systems attempt to store the thermal energy, they benefit from a horizontal water table inducing lower groundwater flow rates (Bloemendal and Hartog, 2018).

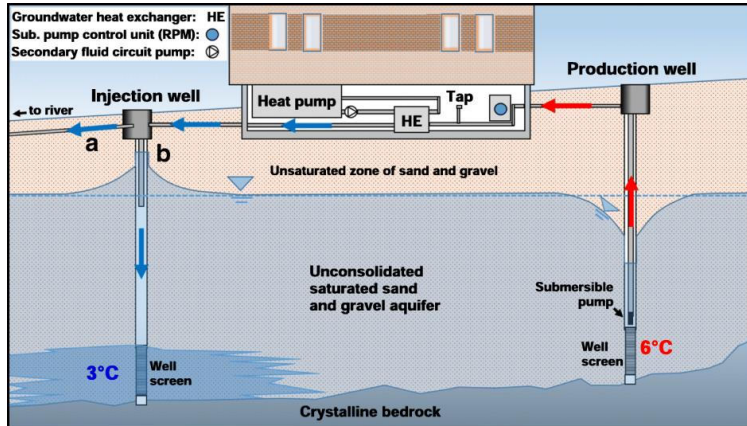


Figure 2.2 Typical Norwegian groundwater heat pump (GWHP) designs, with **a** groundwater discharge to river/stormwater drains, or **b** groundwater reinjection to the aquifer. *HE* heat exchanger. Geological conditions are representative for Melhus, Norway (Gjengedal et al., 2020).

Open loop systems are especially beneficial for buildings with high heating and/or cooling demands. This is exemplified with the Lena terrasse apartment complex's GWHP system in Melhus, Norway. The GWHP system provides up to 350 kW heating and hot water to the 119 apartments, whereof 260 kW being ground sourced heat. The well system consists of one production well (36.4 m) pumping $Q = 5\text{-}13$ L/s groundwater ($T \sim 6$ °C) to the heat exchanger, and recharging the groundwater by means of one injection well (36.5 m). It would crave 25-35 closed loop 250 m-boreholes¹ delivering 30-40 W/m active borehole (NGU, 2020) to cover the same heating demand. The drilling of 6250-8750 total borehole meters would cost more and restrain larger areas than the two GWHP wells. Consequently, large GWHP systems have shorter payback times and are more suitable to densely populated areas than energy wells.

On the downside, open loop systems are usually less operationally reliable and require more monitoring and maintenance actions than closed loop systems. This is due to the elevated groundwater flow associated with open loop systems, which increases the risk of thermal breakthrough, clogging and corrosion (Banks, 2012). Especially, clogging by iron oxide incrustations is a major problem documented, and often not properly solved, in GWHP and ATEs systems (Bakema, 2001, Eggen and Vangsnes, 2005, Lerm et al., 2011, Riise, 2015, Possemiers et al., 2016, Burté et al., 2019). Operational challenges and geological prerequisites may explain why only ~ 30 open loop GSHP systems are currently active in Norway (Midttømme et al., 2020).

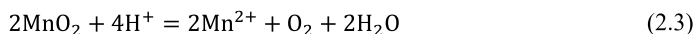
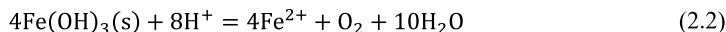
2.2. Redox geochemistry of iron and manganese

Iron and manganese are abundant elements in the earth's crust, averaging 5.6% and 0.1% of its weight, respectively (Haynes, 2016). The elements are present in many rock forming minerals such as silicates (e.g., pyroxenes and amphiboles), oxides (e.g., goethite), carbonates (e.g., siderite) and sulfides (e.g., pyrite) (Appelo and Postma, 2005). Because of the elements' ubiquitous availability in soils and aquifers, the dissolved concentrations of iron and manganese in groundwater are largely controlled by hydrochemical conditions.

Both iron and manganese are redox sensitive elements. In *oxic* environments, oxygen (O_2) will be the thermodynamically preferred oxidant, which will oxidize reduced iron (Fe^{2+}) and manganese (Mn^{2+}), and form practically insoluble ferric (Fe^{3+}) and manganese ($Mn^{3+/4+}$) oxide minerals (Berner, 1981). This

¹ Approximate average borehole depth for Norwegian vertical closed loop systems consisting of ≥ 4 boreholes in 2018 and 2019 (Midttømme et al., 2020).

is exemplified with *ferrihydrate* ($\text{Fe}(\text{OH})_3$) (eq. 2.2) and *pyrolusite* (eq. 2.3) (as quoted in Stumm and Morgan, 1996)



The **thermodynamic equilibrium** constant $K_{\text{Fe}(\text{OH})_3}$ defines the steady state concentration ratio for the reaction in eq. 2.2 (as quoted in Stumm and Morgan, 1996)

$$K_{\text{Fe}(\text{OH})_3} = \frac{[\text{Fe}^{2+}]'^4 \cdot [\text{O}_2]'}{[\text{H}^+]'^8} \quad (2.4)$$

where brackets with apostrophes indicate equilibrium concentrations (or activities) and $[\text{H}_2\text{O}] = [\text{Fe}(\text{OH})_3] = 1$ by convention. However, equilibrium conditions are seldom achieved in dynamic systems like aquifers. Instead, the measured concentrations (in brackets) will yield an *ion activity product* ($\text{IAP}_{\text{Fe}(\text{OH})_3}$) (as quoted in Stumm and Morgan, 1996)

$$\text{IAP}_{\text{Fe}(\text{OH})_3} = \frac{[\text{Fe}^{2+}]^4 \cdot [\text{O}_2]}{[\text{H}^+]^8} \quad (2.5)$$

The *saturation index* (SI) defines the logarithmic ratio between the measured and calculated $\text{IAP}_{\text{Fe}(\text{OH})_3}$ and the experimentally determined $K_{\text{Fe}(\text{OH})_3}$ (as quoted in Stumm and Morgan, 1996)

$$\text{SI} = \log \left(\frac{\text{IAP}_{\text{Fe}(\text{OH})_3}}{K_{\text{Fe}(\text{OH})_3}} \right) \quad (2.6)$$

The saturation index can thus define three different conditions with respect to dissolution and precipitation of iron oxides:

- $\text{SI} > 0$, the solution will be *oversaturated* with respect to ferrihydrate, and tend to precipitate iron oxides (i.e., eq. 2.2 will proceed from right to left)
- $\text{SI} < 0$, the solution will be *undersaturated* with respect to ferrihydrate, and tend to dissolve ferrihydrate (i.e., eq. 2.2 will proceed from left to right)
- $\text{SI} = 0$, the solution will be *saturated*, and tend to neither dissolve nor precipitate iron oxides (i.e., eq. 2.2 in equilibrium)

From this, we can deduce that higher pH will offer more hydroxide ions for dissolved iron and manganese to react and form (hydr)oxide minerals. Conversely, iron and manganese will be the preferred oxidants in environments shut off from the atmosphere (i.e., due to limited oxygen supply). The oxides will then be reduced to soluble ferrous ($\text{Fe}(\text{II})$) and manganous ($\text{Mn}(\text{II})$) species. This is termed a *post-oxic* redox environment, according to Berner's (1981) classification. Iron and manganese may precipitate as siderite (FeCO_3) and rhodochrosite (MnCO_3), respectively, in post-oxic, neutral-basic pH environments with high inorganic carbon contents.

If ferric and manganic oxides are depleted, sulfate will be the preferred oxidant. Sulfate will then be reduced to sulfide. These redox conditions are termed a *sulfidic*, according to Berner's (1981) classification. Dissolved iron and sulfide will react to form iron sulfide minerals, for instance pyrite (FeS_2) and mackinawite (FeS).

The thermodynamic equilibrium constants can be used to visualize *equilibrium* speciation of elements as a function of Eh/pe and pH (Garrels and Christ, 1965). Eh and pe represent the redox potential and the conceptual activity of free electrons, respectively. Higher Eh/pe correspond to more oxidic conditions. Some thermodynamic differences between iron and manganese are illustrated in the Eh-pH diagrams

in Figure 2.3: First, manganese oxides require higher Eh (i.e., more oxic conditions) to form than iron oxides. Second, iron sulfides are much more likely to form than manganese sulfides. These geochemical features influence the behavior of iron and manganese in aquifers, as will be discussed in chapter 6.

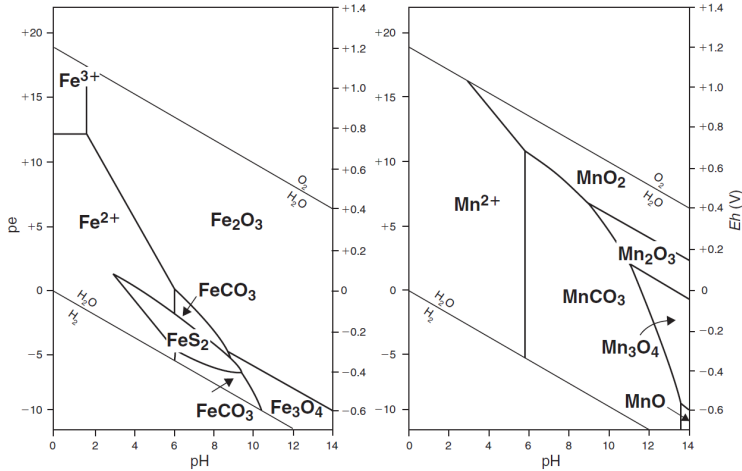


Figure 2.3 Eh(pe)-pH diagram for iron (left) and manganese (right), for $T = 25^\circ\text{C}$, total inorganic carbon = 1 M, total sulfur = 10^{-6} M. Solid-solution boundaries are drawn at $[\text{Fe}^{2+}] = 10^{-6}$ M (Krauskopf, 1979, modified in Appelo and Postma, 2005).

While SI calculation (eq. 2.6) and Eh-pH diagrams (Figure 2.3) only provide information about which iron and manganese speciation will tend to occur. Chemical **kinetics** seeks to answer how long it takes for the equilibria to be reached. The oxidation of iron proceeds through different pathways and by different mechanisms, making its kinetic description challenging. Initially, iron ions may be oxidized by reaction with oxygen in solution (i.e., *homogenous* oxidation). The rate of homogenous oxidation of iron can be described with the equation (Stumm and Lee, 1961):

$$-\frac{d[\text{Fe}^{2+}]}{dt} = k[\text{Fe}^{2+}][\text{O}_2][\text{H}^+]^{-2} \quad (2.7)$$

where k is the homogenous rate constant and parentheses indicate concentrations. Oxidation of iron is the rate controlling step of iron oxide formation at circumneutral pH. The squared dependence on H^+ -concentration indicates that the iron oxidation rate will increase rapidly with pH until oxygen diffusion becomes the rate controlling step of iron oxide formation at $\text{pH} > 8$. The oxidation rate (i.e., the rate constant k) may be catalyzed or inhibited by different ions in solution. Some metal ions (e.g., Cu^{2+} and Mn^{2+}) and anions (e.g., H_2PO_4^-) will catalyze the oxidation (Stumm and Lee, 1961), but the oxidation rate generally slows down as salinity increases (Sung and Morgan, 1980).

The oxidation of iron may also occur at solid surfaces (i.e., *heterogenous* oxidation), most notably once iron ions are adsorbed to iron oxides. The *autocatalytic* effect of iron oxides on oxidation of iron has been experimentally determined and described by Tamura et al. (1976):

$$-\frac{d[\text{Fe}^{2+}]}{dt} = (k[\text{O}_2][\text{H}^+]^{-2} + k'K_{\text{ads}}[\text{O}_2][\text{H}^+]^{-1}[\text{Fe}^{3+}])[\text{Fe}^{2+}] \quad (2.8)$$

where k' is the heterogenous rate constant, K_{ads} is the adsorption constant for ferrous iron onto iron oxides, and Fe^{3+} is oxidized and precipitated iron (i.e., only a conceptual concentration). In eq. 2.8 the left and right part represent the homogenous and heterogenous reaction, respectively. The autocatalytic reaction rate increases with pH, O_2 , and concentration of dissolved (Fe^{2+}) and oxidized (Fe^{3+}) iron. The relative importance of heterogenous vs. homogenous oxidation is greater at lower pH, due to the reactions' linear and squared dependence on H^+ -concentrations, respectively.

The practical applicability of eq. 2.8 is restricted by the difficulty in determining $[\text{Fe}^{3+}]$ (Houben, 2004). Theoretically, $[\text{Fe}^{3+}]$ can be defined as the time integrated of eq. 2.7 (i.e., the total oxidized iron). However, the amount of oxidized iron that is contributing to autocatalysis may reach a maximum after some time, since the iron oxide precipitates will enclose each other and limit the solid surface-solution interface. Alternatively, $[\text{Fe}^{3+}]$ can be defined to be constant with time. Despite the practical limitations, eq. 2.8 demonstrates that iron oxidation rate will increase with time as more iron has been oxidized.

The heterogenous rate of iron oxidation can be further catalyzed in the presence of *iron-oxidizing bacteria* (IOB) which thrive at solid surfaces such as iron oxides. IOB genera comprises a wide range of bacteria, acquiring energy and carbon for growth from different sources. This includes *chemolithoautotrophs* (e.g., the genera *Gallionella* and *Sideroxydans*) requiring energy from oxidation of iron and an inorganic carbon source, and *heterotrophs* (e.g., the genus *Leptothrix*) which oxidizes iron *facultatively* (i.e., co-occurring, not a prerequisite for growth) and craves an organic carbon source.

The IOBs' preferred habitats also vary considerably, see Table 2.1, but generally they contribute to broaden the environmental conditions which facilitate oxidation of iron. Especially, they are active under post-oxic conditions on the verge between Fe^{2+} oxidation and Fe^{3+} reduction, see Figure 2.3 (Lindblad-Påsse, 1986). Søgaard et al. (2000) used the homogenous framework (eq. 2.7) to demonstrate that the rate constant k was ~ 60 times higher for hydrochemical conditions which triggered IOB growth. Consequently, preferential growth conditions for IOB (Table 2.1) may trigger more intense oxidation of iron than conditions which seem more preferential abiotically (i.e., high pH and O_2 , see eq. 2.7 and 2.8).

Table 2.1 also demonstrates that the IOBs' preferred growth habitats are often not properly settled. Followingly, their catalyzing effect on iron oxidation often remain uncertain. Before IOBs were typically detected visually by microscopy (Houben and Treskatis, 2007). More recently, the development of DNA technology has facilitated more in-depth studies of IOBs and other bacteria's influence on iron oxidation in different environmental settings (Lerm et al., 2011, Burté et al., 2019, Houben and Sander, 2020).

Table 2.1 Optimum growth conditions of the most common IOB bacteria in groundwater wells. *Neutrophilic* prefers circum-neutral pH, *salt tolerant* tolerates more salt than the other genera, but bacterial activity decreases as salinity increases. *N/A* facultative bacteria which can grow without iron

Genera (species)	T (°C)	pH	Eh (mV)	O_2 (mg/L)	Fe^{2+} (mg/L)	TDS ^a (g/L)	Stalks?	Source
<i>Gallionella (ferruginea)</i>	8-16	6.0-7.6	200-300	0.1-1	5-25	< 5	Yes	Hanert (2006)
<i>Sideroxydans (littotrophicus)</i>	-	<i>Neutrophilic</i>	-	-	-	<i>Salt tolerant</i>	No	Emerson and Moyer (1997)
<i>Leptothrix</i>	-	6.5-8 (7.3-7.5) ^b	-	0.1-10	<i>N/A</i>	< 2	Yes	Eggerichs et al. (2014)

^{a)} from McBeth et al. (2013).

^{b)} Optimum values in parenthesis

The abiotic oxidation kinetics of manganese has been demonstrated to be both homogenous and heterogenous (Morgan, 1967), thus resembling the autocatalytic oxidation of iron (eq. 2.8). Correspondingly, the oxidation rate of manganese can also be accelerated by bacteria (e.g., *Leptothrix discophora* SS1) (Zhang et al., 2002). However, oxidation of manganese is generally much slower than the oxidation of iron (Stumm and Morgan, 1996). Comparison of data from von Langen et al. (1997) and Houben (2004) indicate that abiotic, homogenous oxidation kinetics of iron are 10^6 to 10^8 times faster than for manganese at the same temperature, pH, and concentrations of oxygen and iron/manganese. The comparison of biotic rates is more complicated since the bacteria's catalysis is dependent on growth habitat. Still, comparison of data from Søgaard et al. (2000) and Zhang et al. (2002) suggest faster biotic oxidation of iron than manganese, although the difference between the two seems lower than for the abiotic, homogenous case.

2.3. Clogging of groundwater wells and heat exchangers

Clogging describes the process of precipitation, sedimentation and degassing of substances initially dissolved or suspended in the water phase, impelling increased frictional resistance to flow. This chapter will present genesis, impact and detection, and remediation by operation and rehabilitation of the most common clogging types in groundwater well systems, particularly in well filters and heat exchangers. Special emphasis will be given to clogging by iron incrustations and gas, since these are the main topics in this thesis.

Genesis

Clogging is categorized as either (Bakema, 2001, Houben and Treskatis, 2007)

- *(bio)chemical*, from changes in chemical equilibria or rates, often aided by microbes,
- *mechanical*, from erosion and deposition of sediments,
- *biological* (or *biofouling*), from microbes building biofilms and slimes, or
- *gas*, from degassing or gas in-leakage to the groundwater pipes

Iron oxide incrustations are the most common **chemical clogging** phenomena in groundwater wells (Houben and Treskatis, 2007). Production wells typically abstract groundwater from different redox zones, either vertically (van Beek, 1989) or laterally (Stuetz and McLaughlan, 2004). This can lead to mixing of incompatible reductive, iron-rich and oxic, oxygen-rich water, which will induce oxidation and precipitation of the initially reduced, dissolved iron. Locally elevated groundwater flow rates in and around the groundwater well system also lead to a high nutrient supply, which facilitates the growth of microorganisms (e.g., iron-oxidizing bacteria) (Huisman and Olsthoorn, 1983, in Houben and Treskatis, 2007). This explains why intense incrustation by iron oxides have been detected in drinking water (van Beek, 1989, Banks, 1992, Walter, 1997, Dimkić et al., 2012, Bustos Medina et al., 2013), irrigation (Stuetz and McLaughlan, 2004), dewatering (Weidner et al., 2012), and open loop GSHP wells (Lindblad-Påsse, 1986, Bakema, 2001, Lerm et al., 2011, Woyessa, 2012, Riise, 2015, Possemiers et al., 2016, Burté et al., 2019).

For well systems extracting groundwater with more reducing conditions, iron sulfides may precipitate and clog the well filters, etc. (Oldmeadow and Marinova, 2011, Lerm et al., 2011). Alternatively, iron oxides may form in the top and iron sulfides in the bottom of long production well screens, but generally iron sulfide are less common than iron oxides in groundwater well systems (Houben and Treskatis, 2007)

The risk of **erosion and transport of sediments** from the aquifer formation to the production well filter or into the GWHP system (i.e., *sand production*) also magnifies with increasing groundwater flow velocities. A criterion for maximum average entrance velocity $v_e = Q/A_{eff}$, where Q is pumping rate and A_{eff} is the total area of the well screen slots, is typically set to mitigate this problem (Houben, 2015). Still, improper sizing of screen slots and gravel pack relative to the grain size distribution of the formation (1), insufficient well development (2), and/or clogging of the production well filter (3) may lead to sand production although the entrance velocity criterion is/was initially met (Bakema, 2001). The eroded and transported sediments may deposit and clog production wells (van Beek et al., 2009b), heat exchangers (Kerner, 2011) and injection wells (Olsthoorn, 1982).

The build-up of **biofilms** in and around groundwater well systems is also facilitated by locally elevated flow rates (i.e., higher nutrient supply). The bacteria responsible for the formation of fluffy, slimy biofilms are often termed *slime-forming bacteria* (SLYM). (Cullimore, 2008).

According to *Henry's law*, groundwater contains dissolved **gas** concentrations (c_g) proportional to the partial pressures (p_g) of gases ($g = N_2, O_2, CO_2$, etc.) in contact with the water-phase (as quoted in Stumm and Morgan, 1996)

$$p_g = K_{H,g} \cdot c_g \quad (2.9)$$

where $K_{H,g}$ is the temperature dependent Henry's constant for gas g . Pressure drops thus may lead to degassing of initially dissolved gases. Well systems containing injection wells (e.g., GWHP systems) are prone to vacuum pressures if the flow down the injection pipe is not properly constricted (Sniegocki and Reed, 1963). This involves risk of degassing, and additionally air in-leakage through improperly sealed parts of the pipework. Open loop GSHP systems also involve temperature changes. Still, the small ΔT (~ 3 K) for GWHP systems make pressure drops the main degassing concern (Bakema, 2001).

The fate of gas bubbles is determined by the balance between drag and buoyancy forces. Drag forces will tend to carry the gas bubbles with the water flow. Meanwhile, buoyancy forces will tend to lift the gas bubbles to local high points in the aquifer or well system. The *Froude number* (Fr) describes the ratio between the two forces (as quoted in Çengel and Cimbala, 2010)

$$Fr = \frac{q}{\sqrt{g \cdot L_c}} \quad (2.10)$$

where q is the volumetric flow rate Q divided by the flow cross section A , g is the gravitational acceleration, and L_c is a characteristic length (e.g., the diameter of a cylindrical pipe). The bubbles will be carried with the flow if Fr is larger than a critical Froude number Fr_c . Fr_c has been determined experimentally to be largest for downward inclined, smaller for horizontal, and smallest for downward vertical pipes (Zukoski, 1966). If $Fr < Fr_c$, gas bubbles formed from degassing or air in-leakage, or gas initially present in pipes (i.e., from before start of operation), will be entrapped to form gas pockets clogging the pipework (Corcos, 2003).

Impact and detection

Frictional resistance to flow impels hydraulic head losses (h_L , i.e., drops in pressure, velocity and/or elevation head) (Çengel and Cimbala, 2010). Accordingly, groundwater flow towards/from a pumping/injection well leads to a water table drawdown s dependent on flow rate Q (Jacob, 1947, in Kruseman et al., 1990)

$$s = BQ + CQ^2 \quad (2.11)$$

where B and C are the linear and non-linear loss coefficients, respectively. Clogging leads to higher frictional resistance (i.e., higher B - and C -values), and lower *specific well yields* Q/s . The increasing head losses will also increase the required pumping head (h_p) and pump power consumption (W_{GP}) (as quoted in Çengel and Cimbala, 2010):

$$W_{GP} = \frac{\rho \cdot g \cdot Q \cdot h_p}{\eta} \quad (2.12)$$

where ρ is the water density, g is gravitational acceleration, and η is the groundwater pump efficiency. Thus, well clogging will first result in increased pumping costs for a given Q . Later, the pump may struggle to sustain the same Q , as the coupled h_p exceeds the pump's capacity (Houben and Treskatis, 2007).

Step-discharge tests are common to assess the hydraulic performance of groundwater wells. The tests comprise pumping a well at different steps (i.e., Q), and measuring the corresponding pressure drawdown (s) in the same well. These data facilitate the fitting of B - and C -values to eq. 2.11 (Kruseman et al., 1990). Regular step-discharge tests can thus be used to monitor clogging of production and injection wells (Houben and Treskatis, 2007), and even heat exchangers (Gjengedal et al., 2020). For iron oxide clogged wells, the autocatalytic oxidation of iron (eq. 2.8) will gradually accelerate the build-up of flow resistance with time, see Figure 2.4. This underlines that continuous monitoring is important, even for wells which initially do not seem to suffer from clogging (Houben, 2004).

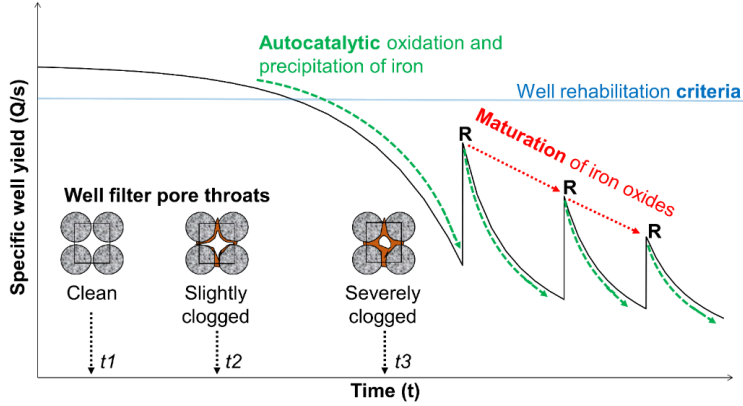


Figure 2.4 Specific well yield with time for a groundwater well filter clogged by iron oxide incrustations. Accelerated decrease in Q/s with time due to autocatalytic oxidation of iron, and less efficient rehabilitations with time due to iron oxide maturation. Modified from Houben (2004).

Clogging will also impede the heat transfer in the heat exchanger of the open loop GSHP system. This is because the thermal conductivity of clogging materials (i.e., both incrustations and gas) is much lower than the steel alloys of heat exchanger (Müller-Steinhagen, 2010). The *heat transfer coefficient* U [$W/m^2/K$] describes the heat exchanger's thermal performance (as quoted in Stene, 2001):

$$U = \frac{P_{HE}}{A * LMTD} \quad (2.13)$$

where P_{HE} is the heat transfer in the heat exchanger, A is the total heat exchange area, and LMTD is the *logarithmic mean temperature difference*, defined by the equations (as quoted in Stene, 2001):

$$LMTD = \frac{\Delta T_a - \Delta T_b}{\ln(\Delta T_a / \Delta T_b)} \quad \text{if } \Delta T_a \neq \Delta T_b \quad (2.14)$$

$$LMTD = \frac{\Delta T_a + \Delta T_b}{2} \quad \text{if } \Delta T_a = \Delta T_b \quad (2.15)$$

where ΔT_a and ΔT_b are the temperature difference between groundwater and the secondary fluid at the heat exchanger's groundwater inlet and outlet, respectively (Figure 2.5). Heat exchanger clogging would impel a reduction in U and increase in LMTD) for a given heat transfer P_{HE} , see Figure 2.5. Consequently, the heat pump evaporation temperature will also decrease, leading to a ~3-4% decrease in heat delivered from the heat pump ($P = P_{HE} + W_{HP}$, where W_{HP} is the heat pump compressor work) and ~2-3% decrease in heat pump's *coefficient of performance* ($COP_{HP} = P / W_{HP}$) (Stene, 2001).

Thermal monitoring thus represents an alternative approach to monitor heat exchanger clogging. Tracking of the U -value (eq. 2.13) with time would crave temperature measurements at the inlet and outlet of the heat exchanger's hot (groundwater circuit) and cold side (secondary circuit) (1), and flowmeter measurements of Q (2), facilitating calculation of P_{HE} (eq. 2.1) (Kerner, 2011).

Hydraulic and thermal monitoring can detect clogging but cannot fully unravel clogging type and genesis. For this purpose, analysis of water quality and incrustation composition are helpful. Measurements of hydrochemistry, suspended solid content and bacterial activity aids in risk assessment, while *in situ* (e.g., camera inspection) or laboratory analysis (e.g., mineralogical, chemical) will elaborate on clogging extent and genesis (Houben and Treskatis, 2007).

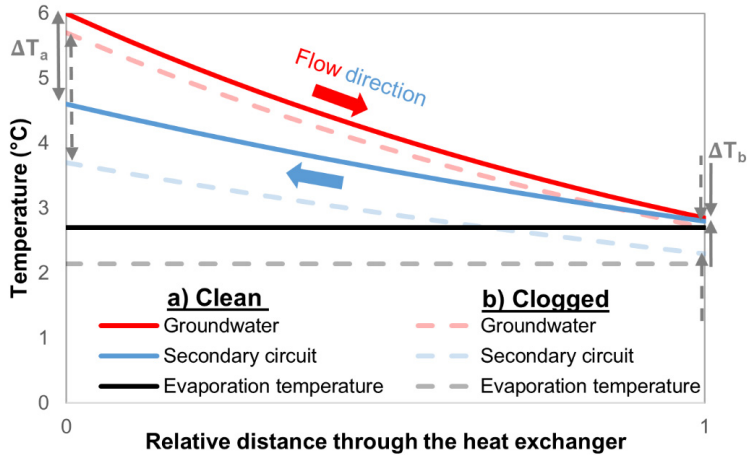


Figure 2.5 Temperature profiles of groundwater and secondary circuit (i.e., glycol-water mixture) through the heat exchanger, and corresponding evaporation temperatures of the heat pump working fluid for clean (a) and clogged (b) heat exchanger. Groundwater and secondary circuit data from the Lena terrasse GWHP in Melhus, Norway, and evaporation temperature calculated assuming $U \cdot A = 163\text{-}164$ W/K for the heat pump evaporator.

Gas may impact well operations in multiple ways. Gas pockets will impel a *waterfall flow*, with added hydraulic head (h_L) losses equal to the elevation difference between top and bottom of the gas pocket (Corcos, 2003). It can also obstruct and rapidly clog well filters, especially in the injection well (Bakema, 2001), and lower the thermal performance of the heat exchanger (eq. 2.13) (Müller-Steinhagen, 2010). Indirectly, the increase in pH from degassing of CO_2 and vacuum-induced oxygen in-leakage through improperly sealed pipes may increase the risk of iron oxide formation (eq. 2.2) Thus, determining gas' overall impact craves a combination of hydraulic, thermal and water quality analyses.

Operation and rehabilitation

The pumping rate Q is an important operational parameter for a groundwater well, influencing both pumping costs and clogging risk (Houben and Treskatis, 2007). Pumping costs justify minimizing Q (eq. 2.12). Clogging will increase the hydraulic head losses and pumping power. Thus, operating the pump at a Q which reduces the clogging rate may be economically favorable. Q 's influence on heat transfer and heat pump operation must also be considered for GWHP systems (Stene, 2001).

The optimum Q varies with type and location of the clogging material. Thus, it is difficult to give general advice on groundwater pump operation. For instance, van Beek et al. (2009a) advice pumping production wells with frequent shut-on/-offs to remove particles in the well filter (1), and continuously to restrict vertical redox mixing impelling iron oxide incrustations (2). These advises are given for abstraction only systems (e.g., water supply). In a GWHP system, there is a pronounced risk that the particles settle in the heat exchanger or the injection well. The time t dependent injection well clogging (drawdown) s_{inj} by particles has a squared dependence on Q (Olsthoorn, 1982):

$$\frac{ds_{inj}}{dt} \propto Q^2 \quad (2.16)$$

The increasing turbulence from higher flow rates (i.e., higher Reynolds numbers) have also been shown to kinetically accelerate the precipitation of calcite (Zeppenfeld, 2005) and iron oxide (Du et al., 2018) in laboratory experiments. This may explain why production well filters have been observed to be more heavily incrustated in sections of higher inflow velocities (Houben, 2006). High groundwater flow rates in and around the groundwater well system also facilitates high nutrient supply, and good growth conditions for biofouling (Huisman and Olsthoorn, 1983, in Houben and Treskatis, 2007). Lowering the Q is thus advised to decelerate biological, chemical and mechanical clogging of wells.

Contrarily, the wall shear stress τ of a plate heat exchanger (Kerner, 2011):

$$\tau = \frac{s_{HE} \cdot d_h}{4L_{HE}} \quad (2.17)$$

is advised to be high (> 25 Pa) to avoid sedimentation of fine particles and biofilms (Novak, 1981, 1982, Kerner, 2011). Here, s_{HE} is the heat exchanger pressure drop, d_h is the hydraulic mean diameter of the heat exchanger channels and L_{HE} is the effective (diagonal) heat exchanger plate length. s_{HE} increases with Q . Thus, the wall shear stress criterion can be met by increasing the pumping rate Q .

A higher Q could also be beneficial with regards to gas clogging. First, a higher Q will increase the head losses throughout the groundwater circuit. This requires a higher pumping head h_p , which will contribute to keep the groundwater pipes pressurized. Followingly, the risk of gas in-leakage and degassing induced by vacuum pressures will be lowered. The higher Q will also increase the drag forces on the gas bubbles, thus reducing the risk of gas entrapment. Pressurization and gas evacuation can also be achieved by constricting the end of the injection pipe (Olsthoorn, 1982) and installing air-release valves at local high points (Corcos, 2003). If not in place, increasing Q can be justified from a gas formation and gas entrapment point of view.

For an open loop GSHP system, lowering the pumping rate will crave a larger temperature change ΔT_{gw} in the heat exchanger to maintain the same heat transfer P_{HE} (eq. 2.1: $P_{HE} = Q \cdot c_p \cdot \Delta T_{gw}$). In heating mode, care must be taken not to freeze the groundwater or secondary circuit fluid. Conversely, a higher pumping rate Q will lead to a lower ΔT_{gw} , which will increase the secondary circuit and heat evaporation pumping temperature, see Figure 2.5. This will lower the required heat pump compressor power (W_{HP} , i.e., converts to heat) (Stene, 2001), making Q a fit parameter to maximize the GWHP system's total COP:

$$COP = \frac{P_{HE} + W_{HP}}{W_{HP} + W_{GP} + W_{SC}} \quad (2.18)$$

where W_{SC} is the pump power consumption of the pump circulating the secondary circuit fluid.

All the above-described aspects influenced by the groundwater pumping rate is summarized in Figure 2.6. Lowering the pumping rate can easily be justified for groundwater abstraction-only schemes (i.e., which are less prone to vacuum pressures) without heat exchange. However, for systems comprising groundwater extraction, heat exchange and injection (e.g., GWHP systems), the optimization of Q should be based on hydraulic, thermal and geochemical monitoring data.

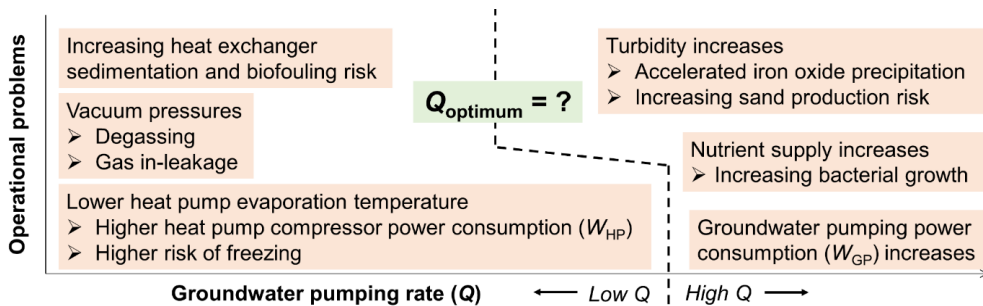


Figure 2.6 Operational aspects of GWHP systems related to Q (Stenvik et al., 2022d).

Although improving the operation, the well owner must expect regular maintenance and rehabilitation actions to secure the longevity of the well system. The timing and type of actions is of great significance. Rehabilitation is categorized as either mechanical, chemical or thermal (Houben and Treskatis, 2007). The appropriate method is dependent on both the type of incrustation, and legal, technical and safety constraints. It should thus be customized to individual well systems, and be based on thorough investigations of incrustation type and extent.

The well incrustation material may be more difficult to remove with time. Iron oxides incrustations mature with time, from soft, amorphous ferrihydrite ($\text{Fe}(\text{OH})_3$) to hard, crystallized *goethite* (FeOOH) with time (Schwertmann and Murad, 1983). This means that iron oxide clogging will accelerate and become more difficult to loosen with time, see Figure 2.4. In practice it is often difficult to remove all incrustations during rehabilitation, especially the material located far outside the well screen. The consequence of not removing all iron oxide incrustations could be a rapid decline in well yield after rehabilitation, due to the autocatalytic effect of iron oxide surfaces on oxidation of iron (eq. 2.8) (Houben and Treskatis, 2007).

Therefore, well rehabilitation is advised to be executed at an “early stage” and thoroughly. A certain %-drop in specific well yield Q/s (i.e., typically 10-30%) is often used as the well rehabilitation criterion (Driscoll, 1989, McLaughlan, 2002, Houben and Treskatis, 2007, Hilmo and Gurigard, 2017). The most thorough well cleaning is achieved by deploying a combination of mechanical and chemical rehabilitation techniques, according to Houben and Treskatis (2007).

The chemical *sodium dithionite* ($\text{Na}_2\text{S}_2\text{O}_4$) has proven effective in reducing and dissolving iron oxides. Laboratory experiments of common well rehabilitation chemicals demonstrated that sodium dithionite was the most effective in dissolving mature, synthetic iron oxides (Houben, 2003b). Sodium dithionite together with the complexing agents has been patented as *Aixtractor*[®] 2.0. This chemical has proven effective in rehabilitating iron oxide incrustated wells in combination with hydraulic “gravel washing”, see Figure 2.7 (Stuyfzand, 2007, Wolffgramm et al., 2010, Beckedorf et al., 2016).

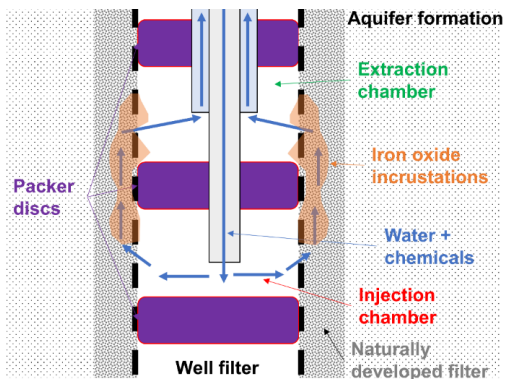


Figure 2.7 Combined hydraulic and chemical well filter cleaning. Modified from Detay (1997, in Houben and Treskatis, 2007).

Heat exchanger rehabilitations can be carried out by *cleaning-in-place* (CIP) procedures circulating a rinsing fluid through (without disassembling) the heat exchanger. It is also possible to carry out preventive maintenance by increasing and reversing the flow through the heat exchanger (Müller-Steinhagen, 2010). Generally, rehabilitation and maintenance of heat exchangers are cheaper and more technically and environmentally convenient than well rehabilitations. Thus, concentrating clogging problems in heat exchangers instead of production and injection wells could be beneficial for GWHP system.

3. Study areas

The PhD work involved field measurements and sampling from two study sites, groundwater heat pump systems in Melhus town center (1) and Ringerike groundwater works located at Kilemoen, Ringerike (2). This excludes Sunndal waterworks, which was only covered by a literature review.

3.1. Melhus

Melhus town center has ~7000 inhabitants (Statistics Norway, 2022), and locates 20 km south of Trondheim, Mid-Norway, see Figure 3.1. The town center is situated 15-20 meters above sea level in the lowermost part of the Gauldalen valley. Due to its location on top of the Melhus aquifer, GWHP systems provide heating and cooling to many of the town center's larger buildings.

The Melhus aquifer

The Melhus aquifer is an unconsolidated glaciofluvial deposit from ~12,500 years ago (Younger Dryas). In this period the glacier stagnated into the fjord bottom where the town center of Melhus now locates, see Figure 3.1. At the ice margin, glacial meltwater flushed out and deposited a distinguished ridge of sand and gravel in the fjord (Vorren and Mangerud, 2006). The deposit was not built up to sea level, making it a *subaqueous delta* deposit. As the glacier retreated, seawater inundated the valley floor and covered the glaciofluvial deposit with thick marine clay. In total this has left up to 320 meters of unconsolidated sediments in lower Gauldalen (Tassis et al., 2016)

Melting of the Fennoscandian ice sheet led to isostatic uplift in the Holocene. The town center of Melhus rose above seawater ~3000-4000 years ago according to local shore displacement curves (Reite et al., 1999). Glaciofluvial sand and gravel barely outcrops to the surface in the study area (Figure 3.1). 2D resistivity profiles and geotechnical drilling logs have revealed up to 60 meters thickness of glaciofluvial sand and gravel, below up to 120 meters of marine clay (Solberg et al., 2014, Hellestveit, 2018). The up to 90 m high and 500 meters wide Melhus ridge, crossing the Gaula valley from the east bank of River Gaula and two kilometers eastwards, is the most characteristic feature of the Melhus aquifer deposit today (Reite, 1990).

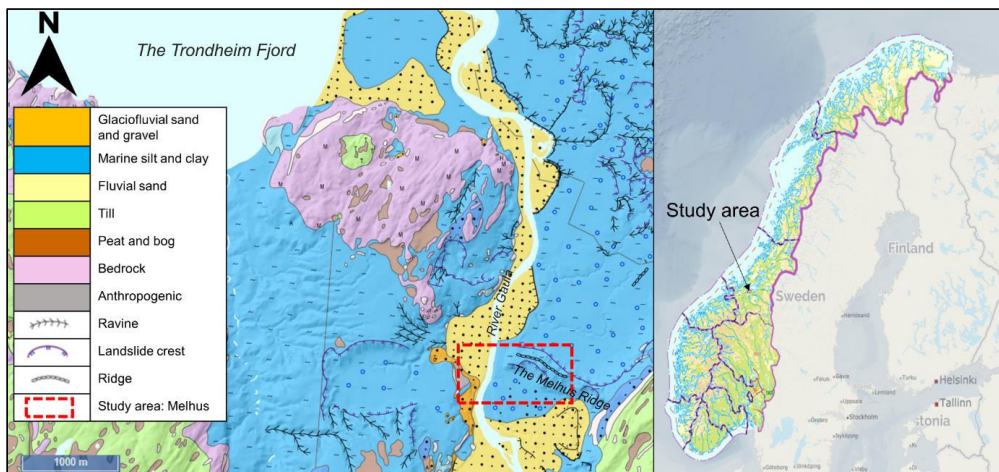


Figure 3.1 Quaternary map of lower parts of the Gauldalen valley, with study area outlined (red lines) (*left*). Study area is depicted in greater detail in Figure 3.2. Location of study area is also shown on a map of Norway (*right*).

The Melhus aquifer dips southwards from the Melhus ridge down below Melhus town center, see Figure 3.2. The thickness of and depth to the aquifer varies with distance from the Melhus ridge. The glaciofluvial layer is thicker and the marine clay layer is thinner closer to the ridge. The aquifer's marine genesis and thick clay cover has left the aquifer with a saline and anoxic groundwater quality (Solberg et al., 2014, Brøste, 2017). The thick clay cover has also questioned if (and where) River Gaula

recharges the Melhus aquifer. The two water bodies seem to be in hydraulic contact based on correlating water levels (Hellestveit, 2018). The water level further indicates that the aquifer is both confined and unconfined, depending on distance from the Melhus ridge, see Figure 3.2b. The Melhus aquifer's extent, high hydraulic conductivities ($1.1 \cdot 10^{-4} < K_{95\%}^2 < 2.0 \cdot 10^{-2}$ m/s) and temperatures ($5 < T < 9$ °C) has made it a promising heat source/sink for buildings in Melhus town center.

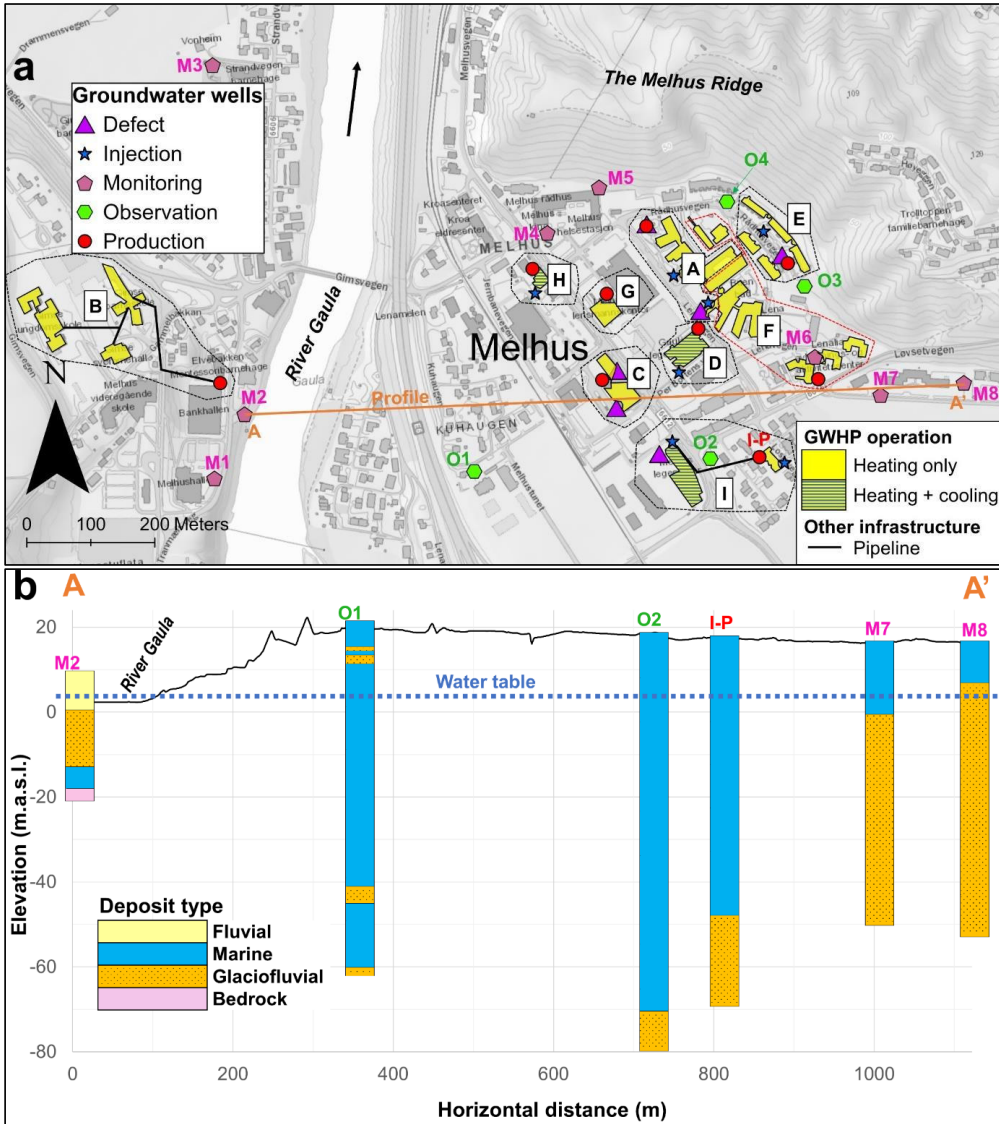


Figure 3.2a Map of Melhus town center, including GWHP connected buildings and groundwater wells. *Defect* clogged and abandoned wells, *Monitoring* wells with (CTD-)Divers (van Essen instruments) continuously monitoring temperature, pressure (and electric conductivity), *Observation* wells without continuous monitoring, and **b** quaternary geology profile based on well logs from Hellestveit (2018).

² Calculated from $n = 103$ sediment samples estimated with Kozeny-Carman's formula in Hellestveit (2018).

GWHP systems in Melhus town center

The Melhus aquifer has been exploited for heating and cooling of apartments, nursery homes, grocery stores and schools since 1999. The aquifer has been accessed by means of groundwater heat pump (GWHP) systems with and without injection wells, see Table 3.1. As per September 2021, a total of nine GWHP systems are/have been in operation in the town center. The depths of the production wells and pumping rates relate to the thickness of the clay cover and heating/cooling demand ($P = 70\text{--}340$ kW), respectively (Riise, 2015).

All GWHP systems in Melhus have to some extent suffered from clogging, with most issues occurring in well filters and heat exchangers. This has resulted in multiple rehabilitation and even reconstruction actions (Table 3.1), leading to several defect and abandoned wells within the study area (Figure 3.2a). Initially, the GWHP systems were established without hydrogeological expertise, and with improper monitoring, which explains why many problems have developed beyond repair (i.e., requiring reconstruction). A review by Riise (2015) disclosed iron oxide incrustations as the main clogging mechanism. This initiated a more scientific and professionally grounded approach to the clogging issues, followed up in the research projects ORMEL (2015-2018) and ORMEL 2 (2018-2021).

Table 3.1 Basic information about the GWHP systems in Melhus, see Figure 3.2. Q = groundwater pumping rate. bgl = below ground level. Pumping rate data is partly retrieved from Riise (2015). *Inj.* injection, *rehab.* rehabilitation, *reconst.* reconstruction. Table modified from Stenvik et al. (2022b).

GWHP system (Start of operation)	Production well screen (meters bgl)	Q (l/s)	Inj. well(s)	Clogging measures ^c (#)	
				Rehab.	Reconst.
A) Buen (2013-)	36-44 (29.5-32.5 ^a)	8-9 ^b	2	1	2
B) Gimse (2009-)	19-34	6-7	-	2	0
C) Høvdingen (2015-2020)	66-69 (65-68 ^a)	7.5	2	0	2
D) Idegården (2008-)	46-60	6.5	1	2	0
E) Lena terrasse (2003-2006, 2015-)	30-36 (27-37 ^a)	5-13 ^b	1	8	3
F) Lenavegen 3 (1999- 2013,2014-)	39.5-43 (17.5-23.5 ^a)	15-16	-	0	2
G) Melhuset (1999-)	24.5-34.5	4	-	1	0
H) Oterholmgården (2010-)	36-38	5.5	1	2	0
I) Thoragården ^d (2013-)	73-78 (79.5-83 ^a)	4-5	2	0	1

^{a)} Defect/replaced production wells. bgl = below ground level

^{b)} Variable speed drive (VSD) groundwater pump

^{c)} Clogging measures in wells, heat exchangers or submersible pumps per September (2021).

^{d)} Sometimes referred to as two GWHPs (Losjevegen and Thoragården), but the systems share production well.

3.2. Ringerike

Ringerike municipality locates just northwest of the capital Oslo in Southeastern Norway, see Figure 3.3. The municipality has ~31 000 inhabitants, whereof just over half of the population live in the city of Hønefoss (Statistics Norway, 2022). Ringerike waterworks supplies most of the municipality's inhabitants with groundwater from the Kilemoen aquifer. This makes it Norway's third largest groundwater works with respect to produced quantity (Norwegian Food Safety Authority, 2021).

The Kilemoen aquifer

The Kilemoen aquifer consists of unconsolidated sand and gravel deposited in an ice marginal delta during the Holocene deglaciation (~10,500 years ago) (Vorren and Mangerud, 2006). The aquifer water table is governed by the adjacent River Begna, recharging the aquifer to a saturated thickness > 30 meters (Vestland, 2012). Blocks of dead ice melted to form kettle holes at Kilemoen during the deglaciation, see Figure 3.4. Shorter vertical distance to the aquifer water table in these kettle holes (i.e., only a few meters) imposes reduced well drilling costs. This hydrogeological setting was deemed favorable for the municipal waterworks' extraction wells (Ellingsen and Finsrud, 1990).

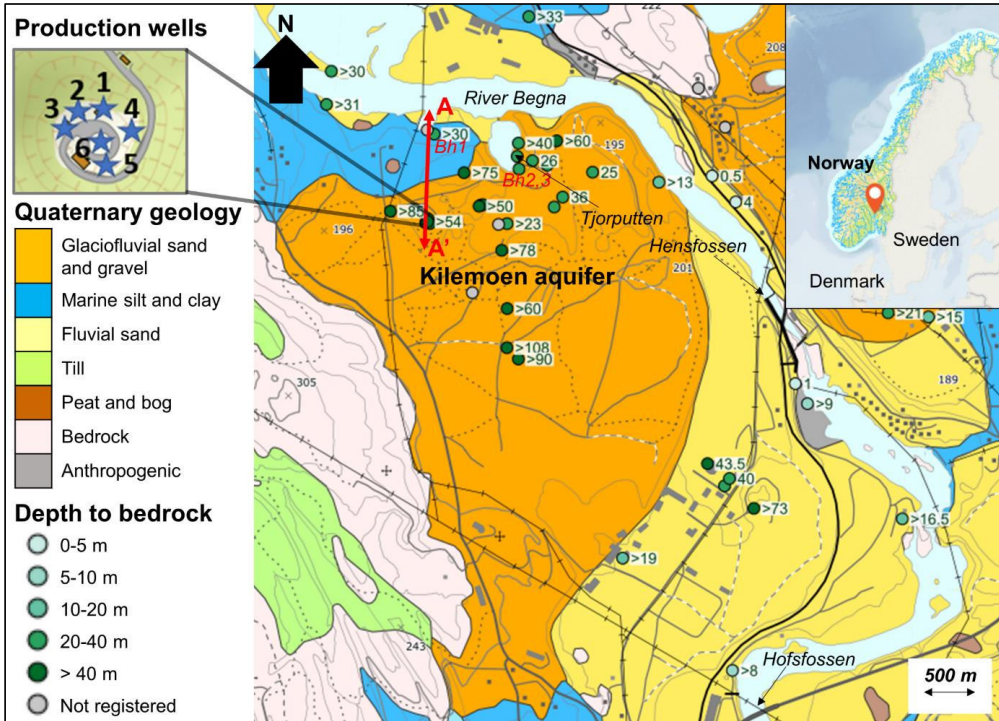


Figure 3.3 Quaternary geology map of the study area in Ringerike, including location map (top right) and enlarged section displaying Ringerike waterworks' well field (top left). Modified from Stenvik et al. (2022c).

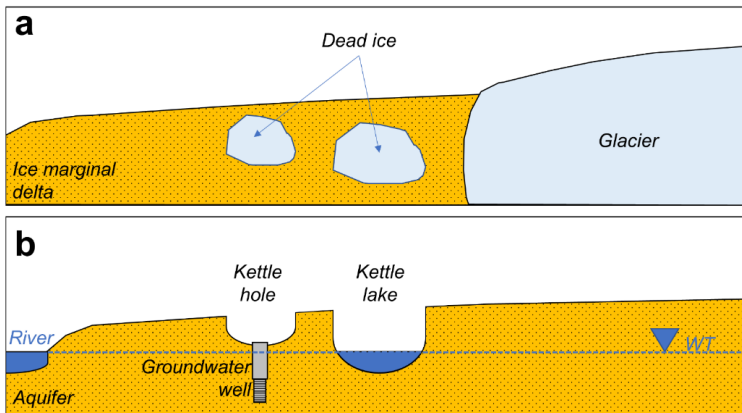


Figure 3.4a Ice marginal delta with dead ice which forms **b** kettle holes/lakes after melting. Kettle holes represent interesting prospects for groundwater extraction. *WT* water table.

Ringerike waterworks

Ringerike waterworks started extracting groundwater from a kettle hole at Kilemoen in 1987, see Table 3.2. Initially, three production wells (PW1-3) were established to cover the water demand of $Q = 80\text{--}90$ L/s (Ellingsen and Finsrud, 1990), see Figure 3.3. The waterworks relies on induced bank filtration from River Begna to increase the extraction capacity. Most of the infiltration is assumed to occur north of the well field and in Tjørputten (Vestland, 2012), see Figure 3.3.

After problems with increasing manganese concentrations in 2006, three more wells were drilled in the kettle hole in 2007 (PW4-5) and 2009 (PW6). These wells were shallower than PW1-3 to ensure extraction of oxic groundwater with low manganese concentrations. PW4 has partly been out of operation due to sand production, while PW5-6 mostly have delivered groundwater of satisfactory quality. However, during periods when one or more of PW1-3 were taken out of operation, manganese concentrations also rose in PW5-6. This vulnerability finally led to the construction of a 100 mill. NOK (~10 mill. EUR) manganese treatment facility in 2018, which ever since has delivered water of satisfactory quality to the water distribution system (Brugger and Paskert, 2020).

Still, the sudden increase in manganese concentrations after 19 years of operation had not been fully explained. This set the stage for a literature review (Stenvik and Hilmo, 2020) and in-depth analysis (Stenvik et al., 2022c) from Ringerike waterworks.

Table 3.2 Basic information about production wells in kettle hole at Ringerike waterworks. Table from Stenvik et al. (2022c).

Well	Operational since (year)	Total depth (m)	Screened depth (m)	Q (L/s)
PW1	1987	47	27-47	16-21
PW2	1987	43	23-43	16-21
PW3	1987	47	27-47	16-21
PW4	2007	33	23-33	- ^a
PW5	2007	27	16-26	14-19
PW6	2009	33	23-33	14-19

^{a)} Currently not in operation due to problems with sand production.

4. Materials and methods

4.1. Water quality

The groundwater extracted by the GWHP systems in Melhus and drinking water wells at Ringerike were analyzed for hydrochemistry. Additionally, dissolved gas and suspended solids were measured in some GWHP systems in Melhus, see Table 4.1. All materials and instruments used during water quality sampling and measurements were carefully cleaned with deionized water before, between and after sampling/measurements.

Table 4.1 Overview of hydrochemical data retrieved from Melhus and Ringerike. b.g.l. = below ground level. Loc. = location. PW = production well

Period	Study area	Sampling location [Filter depth (meters b.g.l.)]	Type of analysis	Analyses ^a (#/loc.)
2019-2021	Melhus	GWHP A [36-44], B [19-34], C [66-69], D [46-60], E [30-36], F [40-43], G [25-35], I [73-78]	Hydrochemistry	4-8
2020	Melhus	GWHP A [36-44], D [46-60], E [30-36]	Dissolved gas	1
2020-2021	Melhus	GWHP H [36-38], Well M6 [18-24]	Hydrochemistry	1
2021	Melhus	GWHP E [30-36]	Suspended solids	2
2021	Ringerike	PW1 [27-47], PW2 [23-43], PW3 [27-47], PW5 [16-26], PW6 [23-33]	Hydrochemistry	1

^{a)} Refers to number of sampling dates (i.e., number of measurements/sampling batches per location)

Hydrochemistry

The field parameters pH (WTW Sensolyt 900-P), dissolved oxygen (DO) (WTW FDO 925), redox potential (Eh) (WTW Sensolyt ORP 900-P), electrical conductivity (EC) (WTW TetraCon 925/C) and temperature (T) (all instruments above) were measured by sensors submerged in a *flow-through cell*, see Figure 4.1. The flow-through cell was constructed at the mechanical lab at Department of Geoscience and Petroleum, NTNU, and facilitated continuous measurement in a constant set-up for each sampling point. The closed chamber restricted the contact between atmospheric gas and groundwater. This was vital for the measurements carried out in Melhus, where the groundwater was anoxic, and thus prone to atmospheric disturbance.

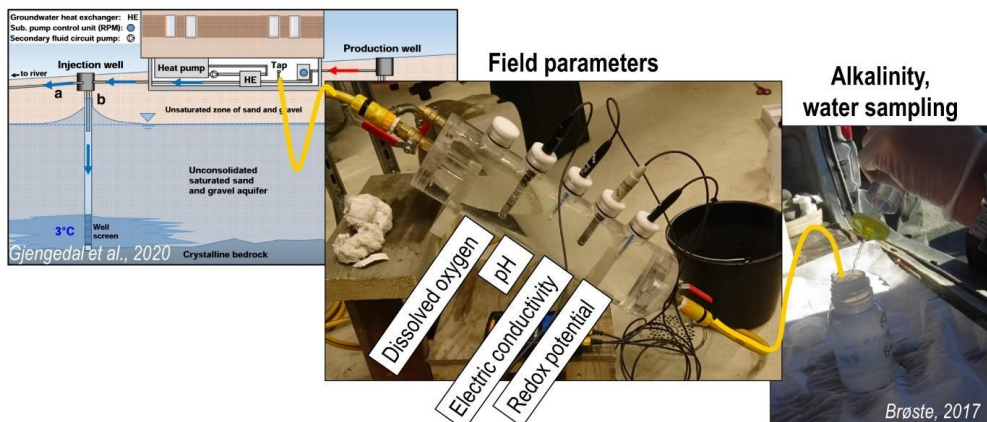


Figure 4.1 Field parameter electrodes submerged in a flow-through cell leading water from a water tap before/after the heat exchanger of a groundwater heat pump system. Alkalinity measurements and water sampled were taken from water flowing out of the flow-through cell.

Water was discharged through the flow-through cell at a rate ~ 0.1 - 0.2 L/s for \sim two hours, during which time most of the parameters did stabilize. However, the Eh measurements were sluggish, and did not stabilize during measurement at any field site. The Eh did not even stabilize during 5-6 days of continuous measurement at the Thoragården GWHP system, see Figure 4.2. This is probably due to the coexistence of multiple active redox couples, and underlines the limited precision of Eh measurements

(Appelo and Postma, 2005). Still, the Eh measurements were deemed useful to get an overview of the redox environment, and for comparison of the redox levels internally between the GWHP systems in Melhus and between the production wells at Ringerike waterworks. See Appendix B for calibration routines.

Alkalinity was measured with “Gran titration” (Merck MColorTest). Three consecutive measurements were carried out and averaged for each sampling location.

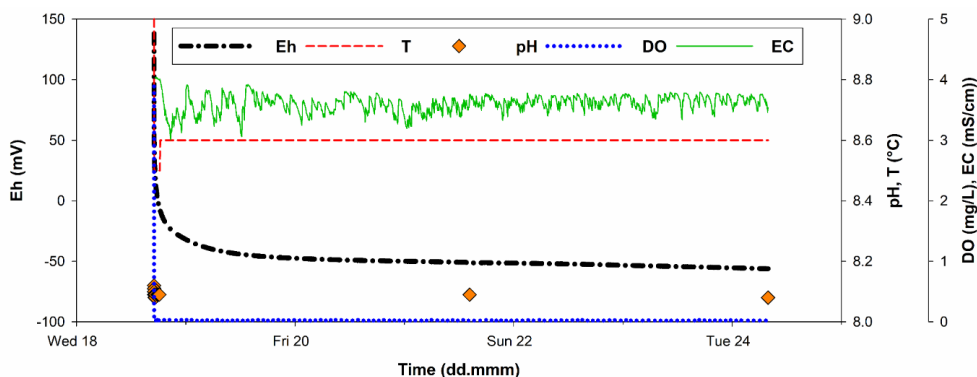


Figure 4.2 Continuous measurement of the field parameters over 5-6 days (November 2020) at Thoragården’s GWHP system (“T” in Figure 3.2a). Eh redox potential, T temperature, DO dissolved oxygen, and EC electrical conductivity.

Water samples were taken for each location being field measured. Water was sampled from the same container of water used for alkalinity measurements, to convene electrical charge balance calculations. Two water samples were taken from each sampling site, one for cations and one back up/for anions. Both samples were filtered (0.45 μm) *in situ* and digested with 65% HNO_3 *in situ* in the lab. All samples were analyzed by ICP-MS (Element 2 - ICP-HR-MS, Agilent 8800). Only one batch of anion samples were analyzed by ion chromatography (Metrosep A Supp 7 - 250/4.0), because of the groundwater’s low levels of nitrate (< 0.5 mg/L) and the ICP-MS instruments’ ability to analyze chloride. At least one sampling campaign from each Melhus’ GWHP system (except Oterholmgården) included both 0.45 μm -filtered and unfiltered samples. This was done to differentiate between dissolved (filtered, i.e., Fe^{2+}) and total (unfiltered, i.e., including both Fe^{2+} and suspended Fe^{3+} -compounds) iron. All analyses were performed at the Department of Chemistry, NTNU.

Quality control of the water samples included calculation of electrical charge balance between cations and anions, regular ICP-MS analysis of blanks and standards by the laboratory staff, triplicate ICP-MS analysis of each water sample, and assuring no time trends from drift in and differences between the two ICP-MS instruments. Water samples displaying electrical charge balance errors $> \pm 5\%$ were re-analyzed or left out from further analysis for Melhus. Electrical imbalance $\leq 10\%$ was deemed acceptably accurate for the more dilute groundwater from Ringerike. The analytical precision of the laboratory ICP-MS instruments was assured by low triplicate root square deviations (RSD < 10%) for major anions, cations, iron and manganese. Chloride triplicates from Ringerike were the only exceptions, displaying RSD values up to 15%, probably due to low concentrations ($\text{Cl}^- < 1 \text{ mg/L}$). The time trends in/between instruments (Element 2 - ICP-HR-MS, Agilent 8800) were evaluated by plotting measured concentrations vs. analytical sequence and meta data on batch number/instrument type, see Appendix B. This was inspired by a procedure in Eggen et al. (2019). Appendix B also contains calculations which justify the comparison between water samples taken before and after the heat exchangers of GWHP systems during operation.

Dissolved gas

A portable mass spectrometric system (miniRuedi) (Brennwald et al., 2016) was used to analyze *in-situ* the groundwater's content of the natural gases N₂, CO₂, O₂, Ar, He, Kr. Data were retrieved from the GWHPs Buen, Idegården and Lena terrasse during operation in November 2020. Of these, only data from Lena terrasse is presented here. H₂S gas was detected qualitatively from smell of rotten eggs.

Suspended solids and hydrochemistry during step-discharge tests

The suspended solids content and hydrochemistry was measured during step-discharge tests (chapter 2.3) at the Lena terrasse GWHP system ("E" in Figure 3.2a) to assess how changing pumping rates influenced the water quality.

Suspended solids content was measured both by a turbidity meter (WTW Turb® 430 T) and manual particle counting of water samples brought to the laboratory. Water samples were taken at each step (pumping rate) of two step-discharge tests (16 September 2021, 1 October 2021). Due to the high iron precipitation potential of the groundwater, the laboratory analyses were performed within few hours (i.e., the same day) after sampling.

Hydrochemistry was measured by a combination of water samples and field measurements as described above, see chapter 4.1 "Hydrochemistry") during two step-discharge tests (8 October 2019, 14 May 2020). Field measurements were performed continuously for both these step discharge tests. On 8 October 2019, water samples were taken at four different steps (85%, 90%, 95% and 100% of maximum pumping speed), while only one water sample was taken 14 May 2020 (70%). Between the two tests, the pH meter was changed from a "field electrode" (WTW SenTix 980) to a "process electrode" (WTW Sensolyt 900-P), which was supposed to be more suited to endure the elevated pressures in the flow-through cell. Data from 8 October 2019 were left out from the original sampling program (i.e., presented in Stenvik et al. (2022b)) to improve the comparability between measurements.

4.2. Incrustation composition and remediation

Analyses of incrustations in the GWHP systems in Melhus have been performed both by laboratory analysis of samples retrieved in the field (Table 4.2) and camera inspections (Appendix C). The laboratory analyses can be divided into mineralogical and chemical analyses (1) and organic and microbiological analyses (2). The incrustation investigations have not been carried out routinely. This was due to the difficulty of sampling and camera inspecting GWHP systems in operation.

Table 4.2 Incrustation samples and laboratory analyses. Pipe filter = periodically cleaned filter in groundwater pipe circuit prior to heat exchanger (HE), pipe = abandoned pipe after reconstruction, tap = water tap in groundwater pipeline. All samples collected and analyzed by Stenvik et al. (2022b), except where noted.

#	GWHP system	Sample Location	Year	Type	Analysis [year]
1	A – Buen	Pipe filter	2019	Solid	XRD [2019], ICP-MS [2020], LOI [2020]
2		Pipe filter	2021 ^b	Solid	DNA [2022] ^b
3	B – Gimse	Pipe	2020	Solid	XRD [2020], ICP-MS [2020]
4	C – Høvdningen	Pipe filter	2019	Solid	XRD [2020], ICP-MS [2020], LOI [2020]
5	D – Idegården	Pipe filter	2020	Solid	XRD [2020], ICP-MS [2020], LOI [2020]
6	E – Lena terrasse	HE	2018	Solid	XRD [2018], ICP-MS [2020], LOI [2020]
7		HE	2019	Dissolved	ICP-MS [2019]
8		Pipe	2021 ^b	Solid	SEM [2021] ^b
9		Injection pipe (top)	2021 ^b	Solid	DNA [2022] ^b
10		Injection pipe (bottom)	2021 ^b	Solid	DNA [2022] ^b
11	F – Lenavegen 3	Pipe	2017 ^a	Solid	XRD [2017] ^a , ICP-MS [2020], LOI [2020]
12		Tap	2020	Solid	XRD [2020], LOI [2020]
13	G – Melhuset	Pipe	2019	Solid	XRD [2020], ICP-MS [2020], LOI [2020]
14	H – Oterholmgården	HE	2021	Dissolved	ICP-MS [2021]
15	I – Thoragården	Tap	2020	Solid	XRD [2020], ICP-MS [2020], LOI [2020]

^{a)} Collected/analyzed by Brøste (2017)

^{b)} Not previously published

Mineralogy and chemistry

X-ray diffraction (XRD) was performed to analyze the incrustation mineralogy. The samples were mortared and dried (35/65 °C) prior to analysis (Bruker D8 Advance) in the mineralogy laboratory at the Department of Geoscience and Petroleum, NTNU. The analyses were often just qualitative, due to low samples crystallinity which inhibited quantification of mineral phases.

ICP-MS analysis were performed to settle the incrustation samples' chemical composition. Solid samples for ICP-MS analysis were dissolved in nitric acid (HNO₃) and filtered prior to analysis (Perkin Elmer ELAN DRC II) in the mineralogy laboratory at the Department of Geoscience and Petroleum, NTNU. Results from ICP-MS analysis could be used to estimate the relative abundance (%) of iron hydroxides in the samples, assuming all dissolved iron stemmed from ferrihydrite (Fe(OH)₃):

$$\text{Fe(OH)}_3 [\%] = \frac{m_{\text{Fe}}[\text{mg}] \cdot \frac{M_{\text{Fe(OH)}_3}}{M_{\text{Fe}}}}{m_{\text{sample}}[\text{mg}]} \cdot 100\% \quad (4.1)$$

where m_{Fe} is the mass of dissolved iron detected during ICP-MS, $M_{\text{Fe(OH)}_3}$ is the molar weight of ferrihydrite (= 106.87 g/mol), M_{Fe} is the molar weight of iron (=55.85 g/mol), and m_{sample} is the sample mass dissolved in HNO₃. Eq. 4.1 were used for ochreous samples where XRD had already confirmed the presence of crystalline goethite (FeOOH).

ICP-MS analysis of incrustations which had already been dissolved during heat exchanger rehabilitation with citric acid were filtered (0.45 μm) and then analyzed (Element 2 - ICP-HR-MS, Agilent 8800) in the chemistry lab at the Department of Chemistry, NTNU. These ICP-MS analyses could be used to determine how much incrustations had been removed during rehabilitation, and compare how much incrustations had formed in different GWHP systems (i.e., Lena terrasse and Oterholmgården).

Organic matter and microbiology

Loss on ignition (LOI) was used to estimate the amount of organic matter in the incrustation samples. Samples were mortared and dried (105 °C) prior to analysis, which consisted of igniting the samples (400 °C) for four hours in a Nabertherm B180 oven. The LOI was measured as the percentage weight loss after versus prior to ignition:

$$\text{LOI}(\%) = \frac{m_{105}[\text{g}] - m_{400}[\text{g}]}{m_{105}[\text{g}]} \cdot 100\% \quad (4.2)$$

where m_{105} is the incrustation sample weight after drying and m_{400} is the weight after ignition. The ignition temperature is conservative compared with the 500-600 °C suggested by Skøien (2000). This was a precaution not to ignite minerals such as pyrite which ignites at 430-450 °C (Mackenzie, 1970). The LOI was used as an indicator of organic matter formed by bacterial activity in the incrustations (McLaughlan, 1992). This interpretation was justified from low humus concentrations (color grading ≤ 3 mg Pt/l) measured in groundwater from the Melhus aquifer (Brøste, 2017). Thus, probably only a small fraction of the organic matter in the incrustations was formed and transported from outside the well filter.

The bacterial activity was measured more directly by biological activity reaction tests (BART). The tests comprised sampling water from GWHP systems and adding it to separate incubators with nutrients designated for iron-oxidizing bacteria (IOB), slime-forming bacteria (SLYM) and sulfate-reducing bacteria (SRB) growth. Semi-quantitative estimation of type and number of bacteria in the incubators could be performed by observation of days until and type of reaction. Tests were both taken during continuous pumping and shortly after the submersible groundwater pump had been switched off and on. Bacteria detected during BART sampling were assumed to stem from GWHP incrustations, since these bacteria prefer inhabiting solid surfaces rather than the water-phase (Cullimore, 2008).

Scanning electron microscopy (SEM, Hitachi SU-6600) was performed to identify iron-oxidizing bacteria. The analysis comprised inspecting SEM images looking for IOB's characteristic visual features, and comparing observations with previous studies (Houben and Treskatis, 2007, McBeth et al., 2013, Burté et al., 2019). SEM analysis was performed on one sample taken from a replaced valve (Figure 4.3a) in the groundwater pipeline at Lena terrasse. The sample was air-dried at 65°C and carefully attached to a carbon tape, not to damage the bacteria structures in the samples, as recommended in Houben and Treskatis (2007). The analysis was performed at the Department of Geoscience and Petroleum, NTNU.

A metagenome analysis was used to accurately identify the DNA present in iron oxide and iron sulfide incrustations. Incrustations from the Buen (Figure 4.3b) and Lena terrasse GWHP (Figure 4.3c and d) were sampled by sterilized spoons and conserved in a solution containing 96% ethanol in a freezer (-40 °C) prior to transport to Blue Biolabs GmbH in Berlin, Germany. Here, bacterial DNA was extracted, amplified, purified, and then analyzed and phylogenetically classified with the Kraken reference database (Wood and Salzberg, 2014).



Figure 4.3 Incrustations sampled for **a** SEM analysis and **b-d** DNA sequencing. Samples from **a** replaced valve in groundwater pipe before heat exchanger at Lena terrasse, **b** groundwater pipe filter before heat exchanger at Buen, **c** top and **d** bottom of injection pipe (flexible hose) at Lena terrasse.

Camera inspections

Camera inspections were performed by the local water and wastewater entrepreneurs Gjøvaag AS. A wired camera (iPEK Rovion CCTV) was lowered down through the well to be inspected, meanwhile video recording. The video was live monitored in the inspection car, which facilitated focusing the inspection to areas of special interest. This included assessment of corrosion holes, welding joints, well screen dimensions, incrustations, and sump filter sediments. Submersible pumps and injection pipes had to be removed from the wells before camera inspection. Thus, most camera inspections were performed during rehabilitations (i.e., mostly in injection wells) and in abandoned (i.e., clogged) wells. The videos were analyzed by comparison with previous literature description of incrustations (Houben and Treskatis, 2007) and laboratory analyses, see Figure 4.4.

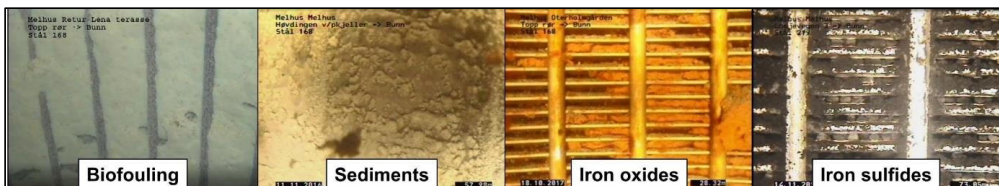


Figure 4.4 Interpreted observations from camera inspections (Stenvik et al., 2022b).

Rehabilitation records

Records on rehabilitation actions in Melhus' GWHP systems were collected both from Riise (2015) and directly from janitors. Clogging causes were settled based on rehabilitation descriptions, and hydrochemical and incrustation analyzes (chapter 4.1 and 4.2).

Testing of sodium dithionite ($\text{Na}_2\text{S}_2\text{O}_4$) on iron oxide incrustations

A laboratory experiment was carried out testing (sodium) dithionite's ($\text{Na}_2\text{S}_2\text{O}_4$) ability to reduce and dissolve iron oxide incrustations from the heat exchanger at Lena terrasse's GWHP (sample 6 in Table 4.2). The experiment was inspired by Houben (2003b) who demonstrated dithionite's exceptional capability of dissolving both amorphous and mature synthetic iron oxides in a laboratory experiment testing several common rinsing chemicals.

The experiment comprised mixing equimolar amounts of dithionite and bicarbonate (50 mmol) in a beaker containing 0.5 L water, and then adding 87 mg iron oxide incrustations (~ 1 mmol) to the beaker. Nitrogen gas (N_2) bubbling into the solution ensured oxygen levels remained low during the experiment, while a magnetic stirrer kept the solution in motion. Water samples (2 mL) were taken prior to and every ten minutes of the experiment. The samples were then filtered (0.2 μm), digested (0.1 M HNO_3), and analyzed for Fe^{2+} content by ICP-MS (Perkin Elmer ELAN DRC II). The Fe^{2+} results were recalculated to amount of dissolved iron oxides (eq. 4.1). During the two hours of experiment, regular measurement (\sim every 40 minutes) of pH (WTW Sensolyt 900-P), dissolved oxygen (WTW FDO 925), electrical conductivity (WTW TetraCon 925/C) and temperature (all sensors) ensured the dissolution process went according to plan. The experiment was performed in the mineralogy laboratory at the Department of Geoscience and Petroleum, NTNU.

4.3. PHREEQC modeling

The software PHREEQC v. 3.7.3 (Parkhurst and Appelo, 2013) was deployed for geochemical calculations and modeling by use of various PHREEQC modules and the PHREEQC.DAT database. Calculations of speciation, electrical balance between cations and anions, and saturation indices for mineral phases were performed with the SOLUTION module for all measured hydrochemistry (field measurements, water samples). Furthermore, more advanced modeling was performed to assess degassing's effect on pH in Lena terrasse's GWHP system (1), and simulate sorption retardation of manganese transport in the Kilemoen aquifer where Ringerike waterworks locate (2).

Degassing's effect on pH in the Lena terrasse GWHP system

A simplified gas model was developed to assess how much CO_2 degassing and coupled pH increase should be expected for Lena terrasse's and similar GWHP systems. This work was significantly aided by the constructive comments from David L. Parkhurst, scientist emeritus at US Geological Survey (USGS), channeled through the PhreeqcUsers Forum (<https://www.phreeqcusers.org/>).

The model used hydrochemistry measured from Lena terrasse (chapter 4.1) equilibrated with a gas phase, using the SOLUTION and GAS_PHASE modules. Two different redox uncoupled gas compositions (i.e., gas pressures) and two different initial distributions between volume of gas (V_g) and water (V_w) yielded a total of four models (A-D), see Table 4.3. These models were meant to resemble groundwater pipes (i.e., closed system) with high ($p_{\text{gas}} = 1.41$ atm) and low dissolved gas concentrations ($p_{\text{gas}} = 1$ atm), and with initially 0% ($V_g/V_w = 0$) and 50% ($V_g/V_w = 1$) gas phase present. Higher relative V_g/V_w ratios were not expected to occur at Lena terrasse based on calculated Froude numbers (eq. 2.10) (Stenvik et al., 2022a).

The four models were then subjected to pressure changes ($p = 0.1$ -1.4 atm) with the REACTION_PRESSURE module to simulate pipe pressure's effect on gas pressures (p_{N_2} , p_{CO_2} , $p_{\text{O}_2^*}$), relative gas phase volume (V_g/V_w) and pH. Temperature was kept constant ($T = 4.6$ °C) to simplify the models. This was justified from the modest groundwater temperature reductions ($\Delta T = 2$ -5 K) in the GWHP systems in Melhus. See full script in Appendix D.

Table 4.3 Gas pressure data used for PHREEQC modeling. p_{N_2} , p_{CO_2} , p_{O_2} = partial pressures, p_{gas} = total gas pressure, V_g = gas volume, V_w = water volume.

Model	p_{N_2} (atm)	p_{CO_2} (atm)	$p_{O_2}^*$ (atm)	p_{gas} (atm)	Source	Initial V_g/V_w
A	0.98 ^a	0.0115 ^b	0.01 ^a	1.00	Lena terrasse GWHP	0
B	0.98 ^a	0.0115 ^b	0.01 ^a	1.00	Lena terrasse GWHP	1
C	1.40	0.0146	0.00	1.41	Universal 95 th percentile ^c	0
D	1.40	0.0146	0.00	1.41	Universal 95 th percentile ^c	1

^a Sum of nitrogen (O₂) and argon (Ar) gas, due to PHREEQC's lack of Ar geochemical data, and their similar solubilities (Sander, 2015)

^{a)} from portable mass spectrometric (miniRuedi) measurements (chapter 4.1, "Dissolved gas")

^{b)} calculated from pH and alkalinity measurements (chapter 4.1, "Hydrochemistry")

^{c)} based on a review of groundwater gas pressures by Lüders et al. (2016)

The models were verified by hydrochemical field measurements of pH, temperature and dissolved oxygen, and pressure monitoring (see "p3" in Figure 4.5). Additionally, the effect of changing temperatures on pH (i.e., independent of the carbonate system) was evaluated through a PHREEQC script utilizing the REACTION_TEMPERATURE module. The temperature modeled pH (pH_T) was plotted versus observed pH (pH_{obs}) to assess how much of the pH change could be attributed to temperature change alone. The remaining observed pH change (ΔpH_{obs}) was verified versus the pressure modeled pH change (ΔpH_{mod}).

Manganese sorption retardation at Ringerike waterworks

A simplified advection-reaction model simulating the effect of sorption on manganese transport in the Kilemoen aquifer, Ringerike waterworks was developed by use of the EXCHANGE and ADVECTION modules. Three separate models were created for production well 1-3, based on hydrochemistry (chapter 4.1) and soil composition (clay and organic matter content). The soil composition data were quite sparse. Thus, the models involved quite significant uncertainty, but still were deemed useful to assess the probability of sorption contributing to manganese retardation in the aquifer. See Stenvik et al. (2022c) for in-depth description of methodology and PHREEQC script.

4.4. Hydraulic and thermal monitoring of GWHP systems

Generally, the groundwater circuits of GWHP systems in Melhus have been sparsely monitored. Some systems have manual manometers, flowmeters, energy meters and temperature sensors installed, but often the instruments are lacking or defect. One notable exception is the Lena terrasse GWHP.

Lena terrasse

Hydraulic and thermal parameters have been monitored continuously (i.e., every minute) at the Lena terrasse GWHP since April 2019, as proposed and described by Gjengedal et al. (2020, 2021), see Figure 4.5.

The hydraulic monitoring scheme was designed to enable detection of clogging in production wells, injection wells and heat exchangers from pressure ($p1$ - $p4$) and flow rate (Q) measurements. Aquifer water table variations ($p0$) were monitored by a CTD-Diver (van Essen instruments) in a nearby observation well (Figure 3.2, see "M5" ~300 m from Lena terrasse). These data were used to calibrate natural water table variations at Lena terrasse (i.e., measured at $p1$ and $p4$ when the subsurface groundwater pump was turned off). This facilitated pressure drawdown calculations for the production and injection well. Additionally, measurements of the groundwater pump's power consumption (W_{GP}) was monitored.

The thermal monitoring constituted measurement of power input (W_{HP}) and heat output (P), and temperature measurements before/after the heat exchanger both for the groundwater and ethylene glycol circuit ($T1$ - $T4$). The temperature measurements also facilitated calculation of the heat delivered from the groundwater to the glycol circuit (P_{HE} , eq. 2.1). Theoretically, P_{HE} together with $T1$ - $T4$ could be

used to calculate the heat transfer coefficient U , which is even more sensitive to clogging than pressure measurements (p_2-p_3) (Kerner, 2011). However, the temperature sensors at Lena terrasse had low accuracy, which impeded thermal clogging detection.

Step-discharge tests were performed semi-monthly between August 2019 and April 2022 to relate pressure drawdowns in the wells ($s_{prod/inj}$) and the heat exchanger (s_{HE}), and W_{GP} to pumping rate Q (eq. 2.11 and 2.12). Plotting s_i and W_{GP} with time for a fixed Q (e.g., 8 L/s) eased the tracking of clogging. The continuous monitoring and step-discharge tests facilitated optimization of the submersible pump operation Q , both with regards to the GWHP system's total coefficient of (heat) performance (2.18) and clogging.

A synthetic model of the pressure profile along the groundwater circuit of a GWHP system with similar design as Lena terrasse identified the top of the injection pipe as the most vulnerable to vacuum pressures (Gjengedal et al., 2019). Therefore, a manual manometer (Hasvold) was installed in this part of the GWHP system, and manually read off (p^*) during one step-discharge test (11 March 2021). See Stenvik et al. (2022a) for accuracy of instruments used for hydraulic and thermal monitoring.

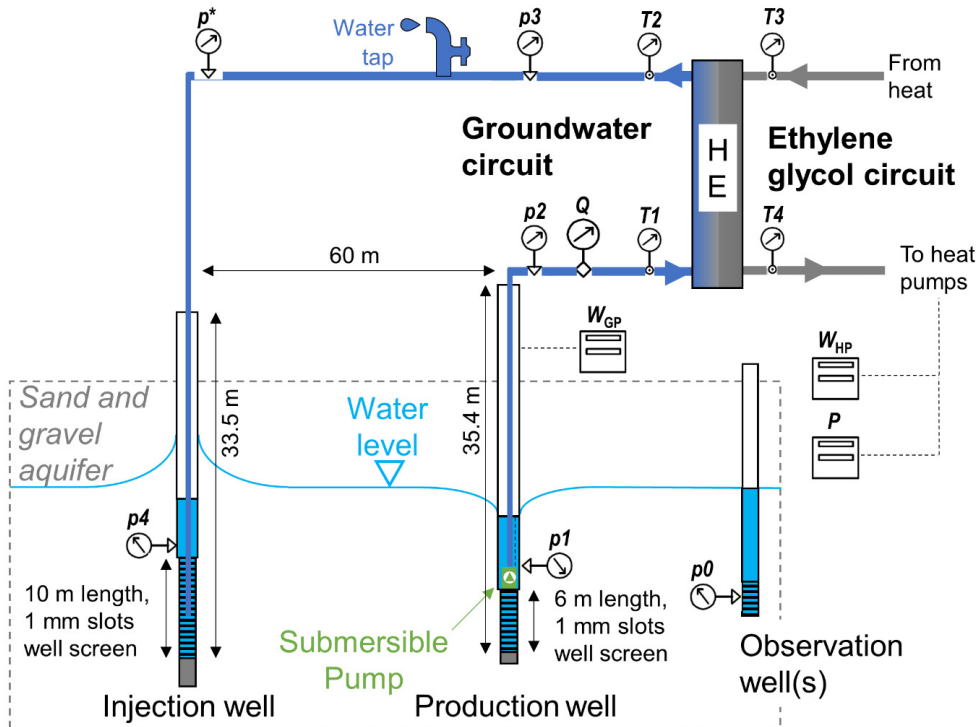


Figure 4.5 Hydraulic and thermal monitoring scheme at Lena terrasse GWHP system. Modified from Gjengedal et al. (2021) and Stenvik et al. (2022d).

5. Results

The results section includes brief comments on motivation and outcome from eight published peer-reviewed papers (chapter 5.1), and two unpublished additional results which will be described in greater detail (chapter 5.2).

5.1. Brief comments on published papers

Paper I: Stenvik, L. A., & Hilmo, B. O. (2020). Jern- og manganproblematikk ved grunnvannsuttak med eksempler fra Ringerike og Sunndal vannverk [Eng: **Iron and manganese in groundwater works – review of problems and case studies from Ringerike and Sunndal**. In Norwegian]. *Vann*, 55(2), 151-161.

Iron and manganese are often co-cited when referring to groundwater well clogging and water quality issues. Although the co-citation can be justified by the elements similar redox behavior, they also differ with regards to how easily and how fast they are oxidized. Banks (1992) documented Norwegian drinking water wells suffering from iron and manganese clogging and how the clogging issues were (not) handled. However, there are sparse published data on the status as per 2020. This motivated a literature review to shed light on whether iron and manganese's differing geochemistry affected well operational problems, and how the problems are handled nationally. The review included two case studies: Ringerike waterworks abstracting groundwater with elevated manganese concentrations and Sunndal waterworks abstracting groundwater with high manganese concentrations.

The different problem evolution, issues, and handling at Sunndal and Ringerike waterworks demonstrates the differences between iron and manganese in a groundwater abstraction perspective. Iron is more easily oxidized, and therefore represent a bigger risk of well filter and water pipe clogging. Meanwhile, manganese craves more oxygen and time to be oxidized, and therefore often first compose inconvenience upon arrival to the consumers. The lower tendency to become oxidized also make water treatment to remove manganese more costly.

The problems in both Ringerike and Sunndal were first noticed after developing partly beyond repair. This indicated deficient monitoring of water quality, which also made troubleshooting challenging. A questionnaire on operational problems and monitoring in Norwegian groundwater works with iron-and/or manganese-rich raw water was prepared and dispatched to relevant municipalities to uncover whether the case studies from Ringerike and Sunndal were representative (see Appendix A). Furthermore, the delayed breakthrough of manganese in the bank filtration abstraction wells at Ringerike set the stage for a more in-depth analysis (i.e., in Paper VIII).

Paper II: Stenvik, L. A., Gjengedal, S., Ramstad, R. K., & Frengstad, B. S. (2022). **Hydrochemical and biotic control on iron incrustations in groundwater heat pump systems: Case study from a saline, anoxic aquifer in Melhus, Norway**. *Geothermics*, 100, 102349. [doi:10.1016/j.geothermics.2022.102349](https://doi.org/10.1016/j.geothermics.2022.102349)

All nine groundwater heat pump systems in Melhus, Norway have to some extent suffered from clogging by incrustations. This makes the Melhus aquifer an excellent field laboratory to study clogging process. Previous studies have disclosed iron oxides as the main, but not only, incrustation type (Riise, 2015, Brøste, 2017, Gjengedal et al., 2020). Still, the clogging genesis and triggers (e.g., oxygen in-leakage/-mixing and iron-oxidizing bacteria (IOB)) are yet to be unraveled. This motivated a systematic field measurement and sampling campaign of GWHP process water with a flow-through cell (i.e., for reliable oxygen measurements) and biological activity reaction tests (BART, i.e., for estimation of IOB activity), together with analysis of incrustation composition by camera inspection and sampling for laboratory analysis.

The analysis revealed that oxidation of iron, and subsequent formation of iron oxide incrustation, could occur despite anoxic conditions (≤ 0.05 mg O₂/L). Also, black incrustations which previously were assumed to be manganese oxides, turned out to be iron sulfides, while only trace concentrations of manganese ($< 0.5\%$ Mn) were found in the incrustations. Thus, the clogging potential of manganese seems limited (cf. Paper 1). It also points to a more reducing regime in the Melhus aquifer than previously assumed, implying that bacteria probably play an important role in oxidation of iron. This was substantiated by BART tests confirming higher IOB activity in the GWHP systems than in the aquifer formation. The apparent importance of IOB further motivated a DNA analysis for genetic characterization of the microbial community in the iron incrustations (see Additional result (AR) 1, chapter 5.2).

Sediment deposits and biological slimes were also found along with the iron incrustations, underlining the importance of thorough investigations to characterize the clogging pathway and pick the appropriate remedy (e.g., the right rinsing chemicals).

Paper III: Gjengedal, S., Stenvik, L. A., Storli, P.-T. S., Ramstad, R. K., Hilmo, B. O., & Frengstad, B. S. (2019). **Design of Groundwater Heat Pump Systems. Principles, Tools, and Strategies for Controlling Gas and Precipitation Problems.** *Energies (Basel)*, 12(19), 3657.

According to the standard Eh-pH phase-diagram, oxidation and precipitation of iron can be triggered by increasing Eh and pH (Garrels and Christ, 1965). In well clogging perspectives, oxidation of iron is often attributed to more oxic conditions (i.e., higher Eh) in and around the well system. There has been limited emphasis on pH's influence, despite the homogenous oxidation of iron kinetics having a square dependence on pH (Stumm and Lee, 1961).

pH is closely related to the carbonate system. Dissolved CO₂ gas will form carbonic acid, with increasing solubility at higher pressures and lower temperatures. Contrarily, pressure drops and increasing temperatures will lower the gas solubility, which could impose CO₂ degassing and pH increase. During discharge through a GWHP system, both pressure and temperature changes. This inspired a conceptual fluid mechanical analysis of the GWHP design in Melhus, focusing on which part(s) of the system being most at risk for CO₂ degassing and simple design measures to reduce the degassing risk.

The analysis showed that the GWHP system design in Melhus is prone to vacuum pressure, especially on the injection side of the heat exchanger. This leads to CO₂ degassing risk, with the biggest risk associated with the top of the injection pipe. The GWHP systems in Melhus mostly operate in heating mode. Thus, temperature reduction through the heat exchanger entails a slightly increasing CO₂ solubility, but overall negligible compared with the degassing risk from the pressure drop. The exact influence on pH was not estimated due to lack of hydraulic and hydrochemical data.

The study suggests installing a backpressure valve, re-injecting the groundwater at same depth or deeper than the extraction depth, and lowering the top part of the groundwater circuit in the GWHP (e.g., by installing the heat exchanger in a drain below ground level). However, the analysis was impeded by the lack of real hydraulic and hydrochemical data, and not considering the fate of the degassed gas (i.e., being entrapped or carried along with the water flow). The acquisition of hydrochemical (Paper III) and hydraulic (Paper V) from Lena terrasse's GWHP enabled a more quantitative analysis of gas clogging (Paper VI) and its influence on pH (Additional result 2).

Paper IV: Gjengedal, S., Stenvik, L. A., Ramstad, R. K., Ulfesnes, J. I., Hilmo, B. O., & Frengstad, B. S. (2021). **Online remote-controlled and cost-effective fouling and clogging surveillance of a groundwater heat pump system.** *Bulletin of Engineering Geology and the Environment*, 80, 1063–1072.

A hydraulic and thermal monitoring scheme was installed at the Lena terrasse GWHP system in April 2019, based on a design proposed by Gjengedal et al. (2020). The continuous and online monitoring allowed remote control and analysis of the system's operation. Analysis of the first half year of operation with different monitoring strategies prompted a paper describing the set-up, and the set-up's capabilities and limitations with regards to clogging detection.

The analysis showed that the clogging of the production and injection wells and the heat exchanger could easily be detected hydraulically with a three-step step-discharge test. However, the temperature sensors were too inaccurate to measure clogging of the heat exchanger thermally. The analysis also demonstrated step-discharge tests' potential to evaluate the success of rehabilitations (e.g., heat exchanger cleaning) and optimize the GWHP operation (e.g., with regards to vacuum pressures and pumping costs), although the latter was outside the scope of this paper.

Paper V: Stenvik, L. A., Gjengedal, S., Ramstad, R. K., & Frengstad, B. S. (2022). **How to avoid gas clogging in groundwater heat pump systems: a case study from the Lena terrasse system in Melhus, Norway.** *Bulletin of Engineering Geology and the Environment*, 81(4), 152.

Gas clogging is often described as a concern for open-loop ground source heat pump systems (GWHP/ATES), leading to recommendations to keep the groundwater circuit pressurized (Bakema, 2001, Banks, 2012, Snijders and Drijver, 2016). However, limited published literature exists on case studies assessing the risk of and describing how to mitigate gas clogging. “Will CO₂ degas?”, “What will happen with the degassed gas?”, and “How much backpressure (i.e., pumping costs) is needed to avoid degassing?” were all questions which remained unanswered in Paper IV and other literature. The monitoring scheme described in Paper V enabled a more specific analysis of risk and mitigation of gas clogging at Lena terrasse's GWHP system.

The study shows that there is risk of both degassing and gas entrapment at Lena terrasse, due to vacuum pressures and too low flow velocities in the piping system. Pressure measurements indicate that the groundwater is cascaded from the heat exchanger down through the injection well (~20 m elevation difference between the heat exchanger and the natural water table). This causes suction pressures on the injection side of the heat exchanger. The groundwater piping system is only fully pressurized when the injection well is intensely clogged and the pumping rate is high. The risk of gas entrapment also decreases at high pumping rates. However, the drawbacks of allowing intense injection well clogging and high pumping rates are numerous (e.g., pumping costs, sand production risk, faster mineral precipitation kinetics, etc.).

Instead it is advised to install multiple injection pipes or an adjustable backpressure valve at the end of the injection pipe to supply the appropriate amount of backpressure at various pumping speeds (i.e., heat demands) and injection well filter clogging states. A pressure transducer in the top of the injection well (i.e., pressure minimum according to Paper IV) is recommended to adjust the supplied backpressure. The extra pumping costs associated with the added head loss will be minimal, since the GWHP system already cascades the water down through the injection well. Entrapped gas can be released by air-release valves at high-points instead of by increasing pumping rate. Altogether, the proposed scheme this involves minimal extra operational costs, but will crave extra investment in the GWHP building phase.

The potential benefits of maintaining the GWHP system pressurized has not been quantified in this paper. Qualitatively, the risk of oxygen in-leakage and CO₂ degassing will decrease when the GWHP

is pressurized, but neither seem to represent the major iron oxidation trigger in Melhus (Paper III, Additional result II). Thus, it is important to note that pressurizing the GWHP system does not necessarily solve all GWHP clogging problems. However, the paper indicates how pressurizing could be included as an affordable precaution in future GWHP system designs.

Paper VI: Stenvik, L. A., Ramstad, R. K., & Frengstad, B. S. (2022). **Optimizing Submersible Pump Regulation of a Clogging Prone Groundwater Heat Pump System in Melhus, Norway.** *Science and Technology for the Built Environment*.

The regulation of the submersible groundwater pump is a key aspect of GWHP operation which both affects the heat performance and clogging risk. The GWHP owners typically would like to know whether they should operate the pump at high or low and constant or variable speed. Unfortunately, one cannot answer these questions on a general basis. This is because different GWHP components (wells vs. heat exchanger), clogging issues (e.g., iron oxides vs. sand production) and energy consumptions (heat pump vs submersible pump) imply different, and often contradictory, regulation strategies. Therefore, the submersible pump regulation must be custom-fitted to each GWHP system. The vast monitoring data from Lena terrasse on both water quality (Paper III) and hydraulic and thermal parameters (Paper V, VI) facilitated optimization of its groundwater pumping scheme.

Although the recommendations are site-specific for Lena terrasse's GWHP, the paper demonstrates the value of monitoring data from different disciplines, and how they can be used in an interdisciplinary analysis. This also points to the need for interdisciplinary expertise from both hydrogeology, geochemistry, hydraulics, and thermal engineering to optimize GWHP system design and operation. Also, the analysis indicates that despite improved operation, the GWHP owner must be prepared to carry out rehabilitation actions from time to time. The frequent (i.e., yearly) need for cleaning of the injection well suggest new rehabilitation techniques should be tested, paving the way for Paper VIII.

Paper VII: Stenvik, L. A. (2022). Laboratorietesting av en kjemikalie som reduserer og løser opp jernoksid-utfelling. Vurdering av anvendelighet til brønnrensing [Eng: **Laboratory testing of a chemical which reduces and dissolves iron oxide incrustations. Assessment of applicability to well incrustations.** In Norwegian]. *Vann*, 57(3).

The use of chemicals during rehabilitation of groundwater wells has been very sparse in Norway, despite international experience point to a combination of mechanical and chemical rinsing as the most effective (Houben and Treskatis, 2007). This is probably both to a (sound) skepticism to contaminate aquifers with process chemicals, and limited technical knowledge.

Sodium dithionite ($\text{Na}_2\text{S}_2\text{O}_4$) is a chemical which has proved efficient in reducing and dissolving synthetic iron oxides (Houben, 2003b). Its residues are already present in the natural environment, and it works under neutral pH. Environmentally, it is therefore also favorable compared to other rinsing chemicals (e.g., strong, organic acids). Therefore, a laboratory experiment inspired by Houben (2003b) was carried out with sodium dithionite, only this time with real iron oxide incrustations from Lena terrasse's GWHP system. The reducing agent's applicability to cleaning of Norwegian groundwater wells was discussed, both with regards to its dissolving efficiency and economic competitiveness, environmental concerns, and technical obstacles.

Sodium dithionite proves efficient in dissolving iron oxides and/or separating them from silicate sediments, it is economically competitive with thermal well rehabilitation (i.e., Norwegian state-of-the-art rehabilitation), few environmental concerns (i.e., when no complexing agents are added), but with certain technical obstacles (i.e., no experience with *multichambered gravel washers* in Norway). It is therefore recommended to retrieve technical expertise from countries with practical experience on multichambered gravel washers (e.g., Germany and Finland), and test the chemical on GWHP wells in aquifers where the environmental impact will be limited (e.g., the confined Melhus aquifer).

Paper VIII: Stenvik, L. A., Hilmo, B. O., & Frengstad, B. S. (2022). Elevated manganese concentrations in groundwater wells after longtime abstraction with bank filtration. *Hydrogeology Journal*.

Drinking water wells experiencing increasing manganese concentrations after longtime operation with bank filtration have been documented in multiple wells in Norway, Canada and USA. This has commanded costly water treatment facilities (> €10 million) at Lillehammer and Ringerike waterworks, Norway, though without a full disclosure of problem cause. This motivated a more in-depth analysis of problem evolution for Ringerike waterworks, and the search for operational strategies to avoid similar unexpected water quality issues elsewhere.

A review of bank filtration geochemistry highlights that sorption may attenuate iron and manganese temporarily, but not in long term (Farnsworth and Hering, 2011). This led to formulation of a hypothesis that sorption had delayed the breakthrough of manganese at in the Kilemoen aquifer, Ringerike. To test this hypothesis a simplified advection-reaction model inspired by Oren et al. (2007) was developed, and verified versus observed data from Ringerike waterworks.

The simplified advection-reaction model showed that sorption was a plausible, and deemed the most probable, explanation to the delayed breakthrough of manganese at Ringerike waterworks. However, it is highlighted that significant uncertainty adheres to this conclusion due to the lack of sediment composition and water quality monitoring data. The operational scheme at Ringerike waterworks with bank filtration in a glaciofluvial aquifer is representative for many of the larger groundwater works in Norway. The establishing of an observation well between the bank filtration and production well area is recommended for these schemes to detect sorption fronts at an early stage, and estimate when/whether the sorption front will break through at the production well(s). This will allocate more time for developing and testing of *in situ* aquifer remedies, and reduce the risk of sudden, unexpected water treatment investments for the well owners.

5.2. Additional results

Additional result I: DNA sequencing of incrustations

SEM analysis of an iron oxide incrustation retrieved from Lena terrasse's GWHP (Figure 4.3a) revealed structural features which could resemble iron-oxidizing bacteria, see Figure 5.1. However, neither the characteristic twisted stalks associated with *Gallionella* nor the hollow stems of *Leptothrix* could be distinguished from the SEM photos. This demonstrated the need for a more accurate analytical method to ascertain the type(s) of IOBs and other bacteria in the GWHP system.

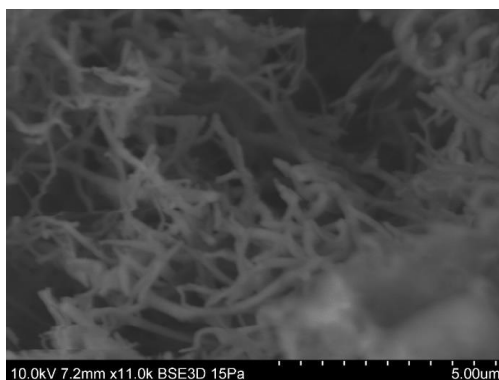


Figure 5.1 SEM photo of iron oxide incrustations from replaced valve at Lena terrasse in December 2020.

DNA analysis of two out of three samples sent to Blue Biolabs GmbH in Berlin, Germany gave meaningful results. The sample from Buen's GWHP was contaminated, probably due to too long storage time prior to analysis, and therefore left out of further analysis. The results from the two samples retrieved from Lena terrasse's injection pipe are presented in Figure 5.2. Both samples contain complex biofilms contributing to multiple processes, including iron oxidation and reduction, sulfate oxidation and reduction, and nitrogen and organic recycling.

The difference in appearance of the two samples from Lena terrasse's injection well are reflected in the microbial community. Most strikingly, the ratios between both iron-oxidizing and iron-reducing bacteria (IOB/IRB) (1), and sulfate-oxidizing and sulfate-reducing bacteria (SOB/SRB) (2) are higher in sample 1. This points to a more oxic regime in the top than in the bottom of the injection pipe, although the water passing through the top passes through the bottom only 10-15 seconds later.

The iron-oxidizing bacteria (IOB) species detected in largest abundance were *Sideroxydans litotrophicus* (1.4%, 1.4%), *Gallionella capsiferromans* (0.8%, -) and *Ferriphaselus amnicola* (0.5%, 0.2%), with percentages referring to sample 1 and 2, respectively. Similar relative abundance of *Sideroxydans* (0.3-2.9%) were detected for the iron oxide clogged ATES system at Oslo airport Gardermoen, Norway (Rike, 2011). Still, these concentrations were notably lower than the *Sideroxydans* predominance (40-80%) detected in iron oxide clogged water supply wells in North Germany (Houben and Sander, 2020). This indicates a more diverse biofilm in the Lena terrasse GWHP and Gardermoen ATES than in the North-German drinking water wells.

The ATES system coupled to the Reichstag building in Berlin, Germany is comparable to Lena terrasse's GWHP, both with regards to groundwater chemistry, incrustation types and bacteria genera, see Table 5.1. The Reichstag ATES has also experienced iron oxide and sulfide clogging aided by the IOB *Gallionella* and SRBs, respectively. Of these, the iron oxide clogging has been the most severe (Wolfgramm et al., 2010), which fits Lena terrasse where iron oxides are also deemed the most problematic issue (Stenvik et al., 2022b).

Both systems in Table 5.1 have also detected sulfide-oxidizing bacteria (SOB). Accelerated growth of the SOB *Thiothrix* occurred at the Reichstag ATEs in 2008 (Wolfgramm et al., 2010). *Thiothrix* is known for building “white gelatinous sulfur slime” (Ford and Tucker, 1975), which led to rapid clogging of a filter prior to the heat exchanger at the Reichstag ATEs (Wolfgramm et al., 2010). The white biofilm detected during camera inspection of Lena terrasse’s injection well in 2018 (Figure 4.4) fit the description of *Thiothrix* biofouling, though only the SOB *Thiobacillus* was detected by the DNA sequencing performed at Lena terrasse.

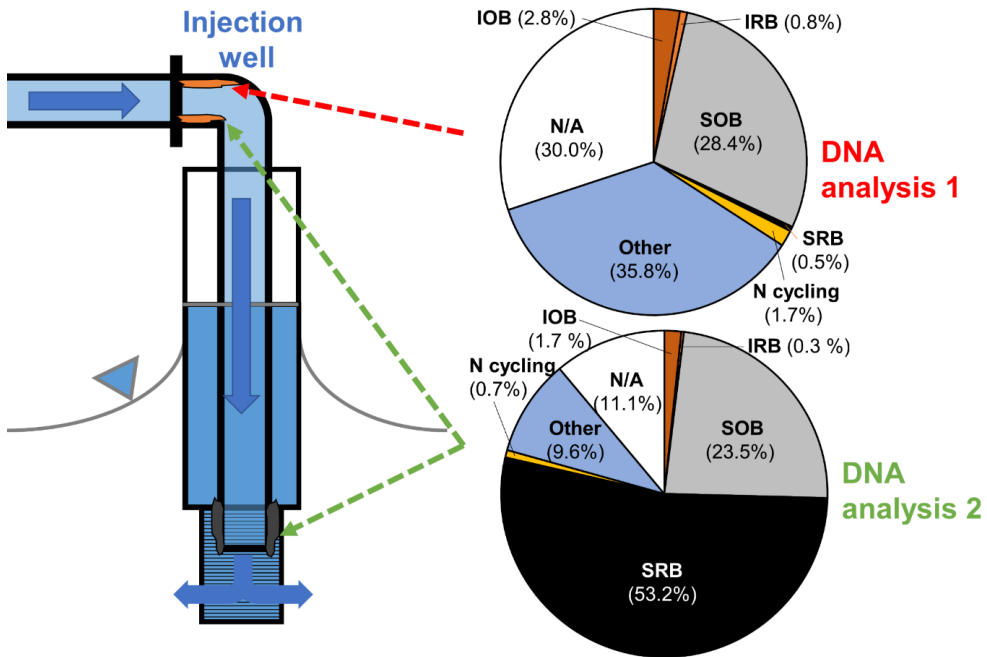


Figure 5.2 DNA sequencing results of two incrustation samples: from the top of the injection pipe (i.e., hose) (1), and from the top and bottom (mixed) of the injection pipe (2). *IOB* iron-oxidizing bacteria, *IRB* iron-reducing bacteria, *SOB* sulfate-oxidizing bacteria, *SRB* sulfate-reducing bacteria, *N* nitrogen, *N/A* not analyzed.

Table 5.1 Comparison of hydrochemistry, bacteria genera (gen) and incrustations (incr) at the Reichstag ATEs in Berlin, Germany and the Lena terrasse GWHP in Melhus, Norway. *TDS* total dissolved solids, *IOB* iron-oxidizing bacteria, *SRB* sulfate-reducing bacteria, *SOB* sulfate-oxidizing bacteria, *Fe-S* iron sulfides (undefined type), *Fe-Ox* iron oxides (undefined type)

Site	T (°C)	pH	Eh (mV)	O ₂ (mg/L)	Fe ²⁺ (mg/L)	NO ₃ ⁻ (mg/L)	SO ₄ ²⁻ (mg/L)	TDS (g/L)	Gen	Incr
Berlin * a	11±8	7.2±0.4	120±47	0.14±0.14	2.1±0.4	0.1-0.3	191±25	0.7±0.0	IOB	Fe-Ox
	29±16	7.2±0.2	91±46	0.14±0.14	1.0±0.2		259±25	29±4	SOB SRB	Fe-S
Melhus b	4±2	7.3±0.1	107±33	0.04±0.01	3.5±0.6	0.0-0.3	201±25	1.2±0.1	IOB IRB SOB SRB	Fe-Ox Fe-S

* Hydrochemistry measured in cold (first row) and heat (second row) storage

a) from the Reichstag building’s ATEs system. Data from Opel et al. (2014) (hydrochemistry) and Lerm et al. (2011) (genera) and Wolfgramm et al. (2010) (incrustations)

b) from Lena terrasse’s GWHP. Data from Riise (2015) and Asplan Viak (nitrate) and Stenvik et al. (2022b) (other hydrochemistry + incrustations)

The accelerated *Thiothrix* growth in Berlin occurred somewhat mysteriously since the hydrochemistry and the rest of the biotic environment remained stable. Lerm et al. (2011) speculate whether a slightly milder winter than normal in 2007/2008, causing higher average temperatures in the groundwater circuit, could explain the increased SOB activity. In 2018, the continuous hydraulic and thermal monitoring scheme was not in place at Lena terrasse. However, energy meter readings from the heat pump in 2016-2021 may indicate a higher average injection temperature prior to the biofilm build-up in October 2018, see Figure 5.3 (i.e., due to less heat extraction). The white biofilm has not been observed at Lena terrasse ever since October 2018. This indicates that relatively small habitat changes could influence the bacterial activity significantly.

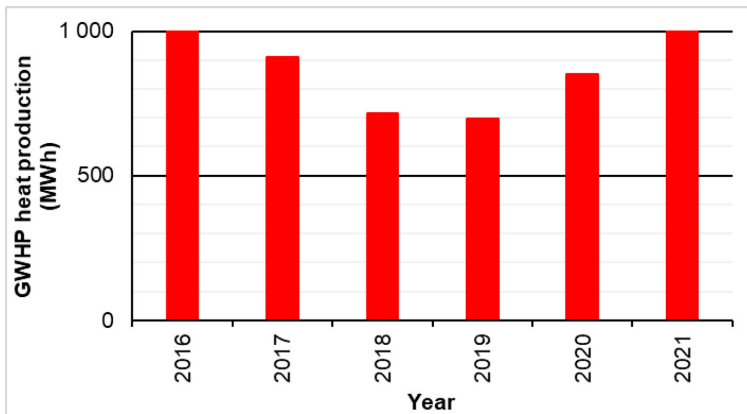


Figure 5.3 Energy meter data from the heat pump at Lena terrasse’s GWHP system. Modified from Ramstad and Stenvik (2020).

It is uncertain whether the sulfide incrustations observed at the bottom of the injection pipe at Lena terrasse represents a new clogging regime. There were observed increasing iron sulfide concentrations in incrustations in some wells at the Reichstag ATES in Berlin after several years of operation (2007, i.e., eight years after start of operation in 1999) (Wolfgramm et al., 2010). What may resemble iron sulfide incrustation were also detected in the bottom of the injection well screen prior to well rehabilitation in March 2020 at Lena terrasse (Figure 5.4). Though, XRD and ICP-MS analysis of the flushed out incrustations from well rehabilitation in May 2020 indicated presence of goethite and no mackinawite (FeS) and limited amounts of sulfur despite high iron concentrations, respectively (Stenvik et al., 2022b). The injection well is therefore still believed to mainly suffer from iron oxide incrustations, but the sulfides may add to the problem and function as a nutrient source for SOB clogging and IOBs.



Figure 5.4 Camera inspection from bottom (32.7 m below well top) of Lena terrasse GWHP’s injection well screen (23.5-33.5 m below well top).

Additional result II: Degassing's influence on pH

The modeled pH increases are largest for cases when gas is initially present in the pipes ($V_g/V_w = 1$), see Figure 5.5. This can be explained by CO_2 's ~ 70 times higher solubility than N_2 at $T = 4.6^\circ\text{C}$ (Sander, 2015), meaning the CO_2/N_2 ratio will be much higher in the water than the gas phase. It also means that the total CO_2 (i.e., in water + gas phase) will be much higher in a waterfilled than a 50/50 gas- and water-filled pipe. Consequently, CO_2 will constitute a larger proportion of the gas phase during degassing of an initially water-filled pipe, which equals a larger $p\text{CO}_2$ and lower pH values. One could argue that this is an artificial effect of how the gas phase composition is presumed in the model. Furthermore, the magnitude of the partial pressure measured by the miniRuedi are uncertain since the instrument is primarily used for measuring relative gas composition. However, the simulations provide insight to how gases in a closed system respond to pressure reductions, serve as a reference for verification of observed pH responses to pipe pressure.

All four cases in Figure 5.5 demonstrate that the pH increases with an exponential rate as pipe pressures drop. For the Lena terrasse GWHP, the minimum pressure measured in the top of the injection well was $p = 0.9$ bar. Subtracting the pressure sensor's accuracy (± 0.064 bar), yields worst case pipe pressure $p \geq 0.8$ bar (Stenvik et al., 2022a). This translates to a modeled pH increase in the range $0.00 < \Delta\text{pH}_{\text{mod}} \leq 0.12$, with largest pH change estimated for the scenario $p_{\text{gas},0} = 1.41$ atm and $V_{g,0}/V_{w,0} = 1$ (Figure 5.5d).

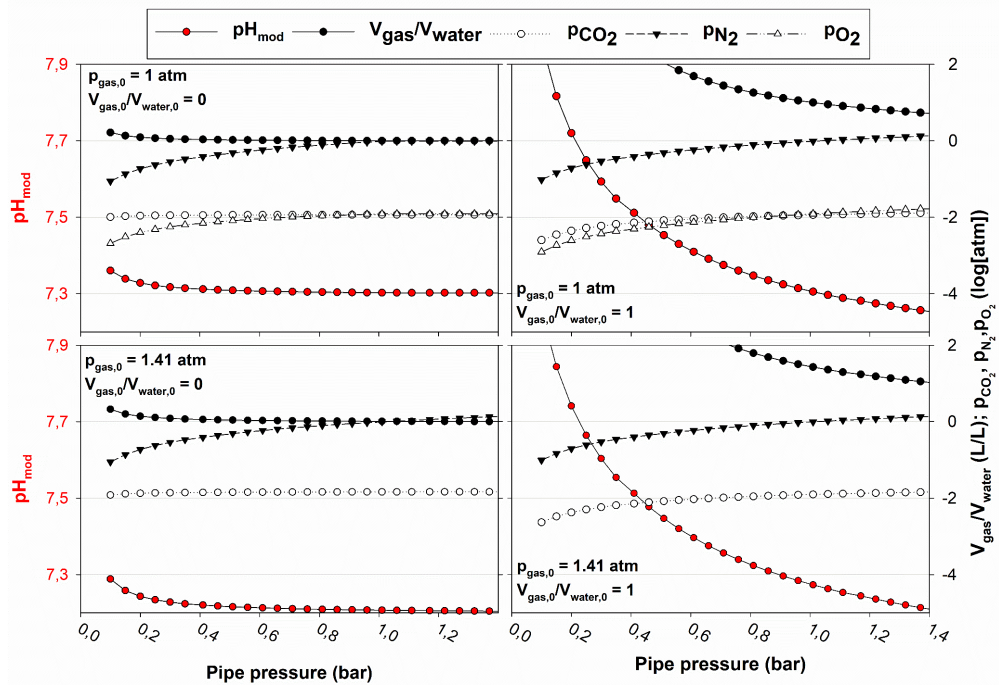


Figure 5.5 PHREEQC simulations displaying pH, relative gas to water volume (V_g/V_w), and gas pressures ($p\text{N}_2$, $p\text{CO}_2$, $p\text{O}_2$) versus GWHP absolute pipe pressure for four cases (A-D, see Table 4.3).

The pH measurements during two step-discharge tests were used to verify the changes in pH with pressure, see Figure 5.6. During the step-discharge test 08.10.19 a significant pH increase is observed when the pipe pressure becomes negative (i.e., relative to the atmospheric). Removing the temperature effect leads to a maximum observed pH increase $\Delta\text{pH}_{\text{obs}} = 0.14$ when the pipe pressure decreases from 1.1 to 0.9 bar ($\Delta p_3 = 0.2$ bar). Although the $\Delta\text{pH}_{\text{obs}} = 0.14$ is larger than the modeled pH increase ($0.00 < \Delta\text{pH}_{\text{obs}} \leq 0.04$) in the same pressure interval, it can still be deemed as modest pH changes.

The injection well was more severely clogged, and thus provided more backpressure to the groundwater pipes during the step-discharge test 14.05.20 (Stenvik et al., 2022d). This explains the higher pressures (p_3) and minimal pH changes recorded during this test. For both tests, stable dissolved oxygen concentrations (≤ 0.06 mg/L) confirmed no air in-leakage to the flow-through cell precluding the pH measurements.

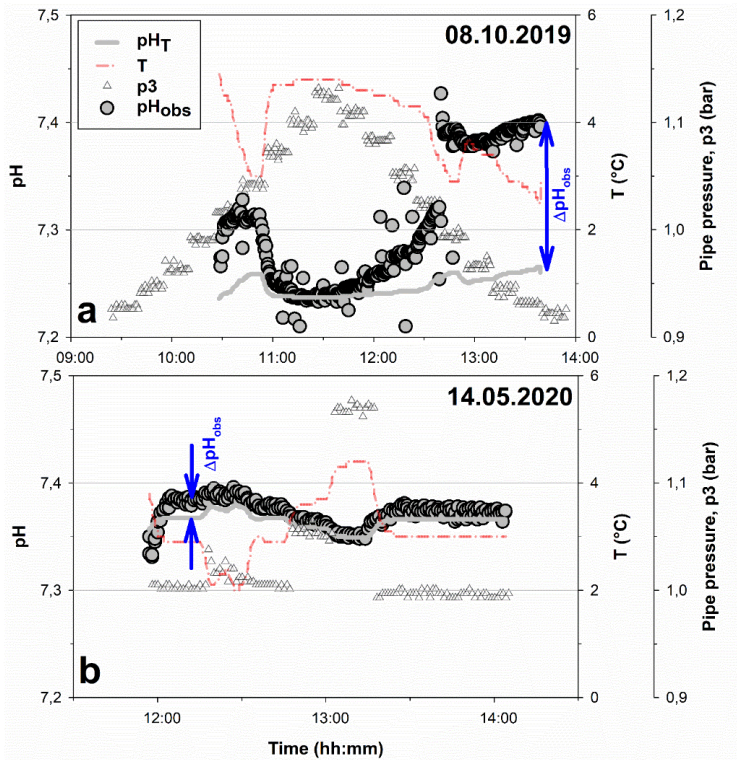


Figure 5.6 Measurement of temperature (T), absolute pipe pressure after the heat exchanger (p_3) and pH (pH_{obs}) during two step-discharge tests **a** 08.10.2019 and **b** 14.05.2020. Temperature induced changes to pH (pH_T) are modeled in PHREEQC.

Although a pH change $\Delta pH = 0.14$ may seem small, its effect on the iron oxidation kinetics can be substantial. For homogenous iron oxidation, this can lead to $\sim 90\%$ increased rate, due to its square dependence on $[OH^-]$ (eq. 2.7). If heterogenous iron oxidation dominates, $\Delta pH = 0.14$ equals a $\sim 40\%$ kinetic rate increase (eq. 2.8), which is still considerable. However, the most severe iron oxide clogging in Melhus has occurred at Lena terrasse GWHP ($pH \sim 7.3$), despite 60% (eq. 2.8) to 310% (eq. 2.7) faster abiotic oxidation rates estimated at Oterholmgården's GWHP ($pH \sim 7.7$). This assumes the same reaction constants (k, k') in the two GWHP systems, which probably is an erroneous assumption.

Søgaard et al. (2000) demonstrated that the introduction of iron-oxidizing bacteria in water treatment facilities could increase the oxidation rate equivalent to a 60-fold increase in the homogenous oxidation rate constant k (eq. 2.7). This occurred despite poorer hydrochemical conditions abiotically (i.e., higher pH and lower dissolved oxygen content). Thus, whether the hydrochemistry is favorable for IOBs or not may influence the iron oxidation rate more than the hydrochemistry's direct impact on abiotic iron oxidation. IOBs have been detected in GWHP systems in Melhus (Stenvik et al., 2022b, additional result 1). This justifies changing focus from CO_2 degassing's to IOB's influence on iron oxidation kinetics.

6. Discussion

The discussion will be structured according to research questions presented in chapter 1.3.

I) *How do the geochemical signatures of iron and manganese influence groundwater well operation?*

Stenvik et al. (2022b) demonstrated that the GWHP clogging issues in Melhus mostly were related to iron (oxide/sulfide) incrustations, while manganese was only present in trace concentrations (0-0.3%). Parts of this iron dominance is explained by the higher concentrations of iron (0.2-6.2 mg/L) than manganese (0-0.7 mg/L). However, it is mainly due to Fe^{2+} 's higher tendency to be oxidized and form oxide minerals or precipitate with reduced sulfur to form sulfides, compared with Mn^{2+} (chapter 2.2).

The higher required redox potential (> 0.5 V, see Figure 2.3) for the oxidation of manganese also explains why Ringerike waterworks' operational issues have occurred *after* passing the production well filters. Despite relatively high oxygen (0.3-6.7 mg/L) and manganese (≤ 1 mg/L) concentrations in the extracted water, this has not been sufficient to cause oxidation of manganese and cause severe clogging of the well filters. This is underlined by measured redox potentials ($0.3 \leq \text{Eh} \leq 0.4$ V) of the extracted water lower than required for the oxidation of manganese (Stenvik et al., 2022c).

Instead, the main problems have occurred in the water distribution system. Here, oxygenation during water treatment and longer residence times have allowed comprehensive oxidation and precipitation of manganese. This has caused black particles and stains, as first noticed at Leiv Vidar sausage factory (Lile, 2006). The "resistance" against being oxidized also explains the expensive (> 10 mill. EUR) manganese treatment plants that have been deemed necessary at both Ringerike and Lillehammer waterworks to be able to immobilize the manganese (Brugger and Paskert, 2020, Holmøy, 2020).

The redox characteristics of iron and manganese can also explain the delayed occurrence of elevated manganese, and not iron, at Ringerike waterworks. The water table oscillations caused by groundwater pumping will entrap gas bubbles, leading to oxygenation of the aquifer formation enclosing the production wells (Farnsworth and Hering, 2011). Since iron requires less oxygen than manganese to be oxidized, the iron-oxidizing zone will locate farther away from the production well than the manganese-oxidizing zone. This will allow more time for the rapid oxidation of iron, than for the slow oxidation of manganese (Stumm and Morgan, 1996). This also explains why *VYREDOX treatment* (i.e., *in situ* oxygen injection to the aquifer to force oxidation and precipitation of iron and manganese prior to extraction) is more effective for iron than for manganese (Hallberg and Martinell, 1976).

The sequence of preferred oxidants (O_2 , NO_3^- , $\text{Mn}^{3/4+}$ -oxides, Fe^{3+} -oxides, SO_4^{2-} , CO_2) (Stumm and Morgan, 1996) has certain implications for aquifers where redox conditions become more reducing with time. The preference of manganese over iron means elevated manganese (Mn^{2+}) concentrations are expected to occur before elevated iron (Fe^{2+}) concentrations. This has also been the case for most of the Norwegian municipal groundwater works which have experienced both iron and manganese concentrations above respective drinking water limits, see Figure 6.1. Higher drinking water limit for iron than manganese could partly explain the trend. However, this is believed to be counteracted by the higher earth crust abundance of iron than manganese (Haynes, 2016). Higher crustal concentration may also explain the one occurrence of elevated iron concentrations before elevated manganese. The main tendencies however correspond with the theoretical redox framework.

Iron concentrations have remained low at Ringerike waterworks meanwhile manganese concentrations increased (2006-2014) and stabilized at a high level (2014-). This indicates that the redox conditions in the Kilemoen aquifer, Ringerike is not becoming more reducing with time, and backs up sorption as the most probable cause of delayed, elevated manganese concentrations.

The actual sorption capacity of the Kilemoen aquifer remains uncertain, due to lack of sediment composition data. Clay and total organic carbon (TOC) concentrations can be used to estimate the cation exchange capacity (Breeuwsma et al., 1986) Recent TOC analyses of aquifer sediments from a deposit (Gardermoen) of the same age as Kilemoen displays lower values ($0.13 \pm 0.03\%$, $n = 20$) (Waade, 2022) than the ones used for the numerical sorption model ($0.19 \pm 0.06\%$, $n = 2$) (Stenvik et al., 2022c). Followingly, the Kilemoen aquifer's sorption retardation capacity ($R_{sorp} = 45 \pm 17$) may be overestimated in Stenvik et al. (2022c). Still, even with the new TOC data the sorption retardation capacity will be considerable ($R_{sorp} = 34 \pm 14$).

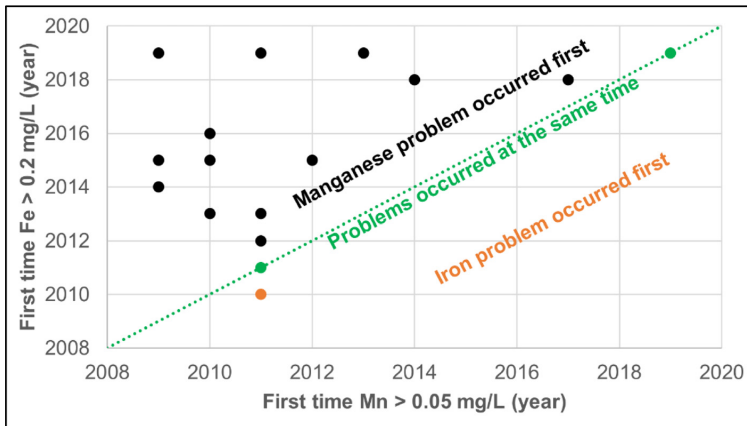


Figure 6.1 First occurrence of elevated iron (> 0.2 mg/L) vs manganese (> 0.05 mg/L) in Norwegian municipal groundwater wells which have experienced problems with both. Data from Norwegian Food Safety Authority.

Time trends with regards to iron and manganese have also been detected for the Lena terrasse GWHP system in Melhus. These hydrochemical changes are likely to stem from the production well's proximity to one of the injection wells at Buen GWHP (~140 m away), see Figure 3.2. The hydraulic gradient from Buen's injection to the Lena terrasse's production well induces a relatively fast groundwater flow. This explains why the water quality at Lena terrasse gradually has become more like the saline, iron- and manganese-rich water quality at Buen, see Figure 6.2.

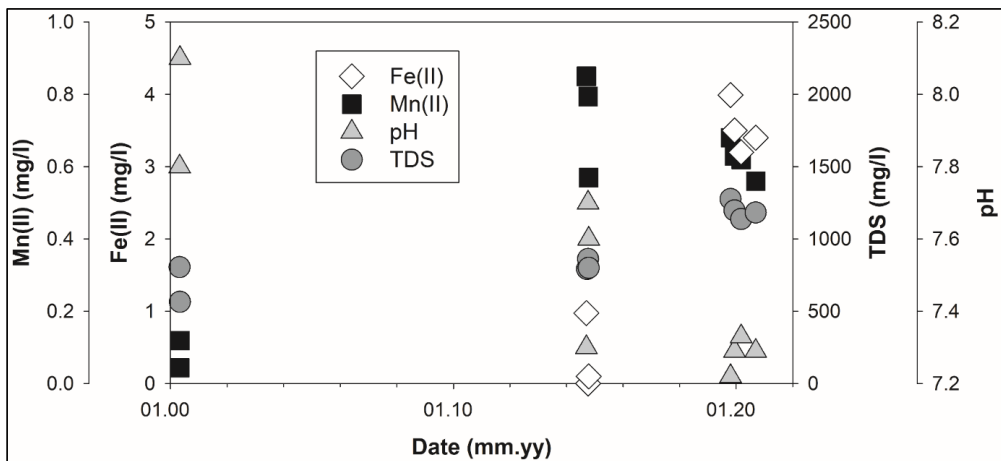


Figure 6.2 Dissolved iron (Fe(II)) and manganese (Mn(II)) (left side axes), pH and total dissolved solids (TDS) (right side axes) plotted versus time in for wells in the Lena terrasse area (year 2000) and Lena terrasse GWHP wells (years 2014-). Data from Storrø (2000), Riise (2015) and Stenvik et al. (2022b).

The observed water quality changes at Ringerike and Melhus underline the importance of hydrochemical monitoring. Thorough monitoring of the water quality during operation facilitates sooner detection and easier diagnosis of the problem cause. Both the groundwater works in Ringerike and the GWHP systems in Melhus were initially sparsely monitored, both hydrochemically and hydraulically. This led to problems evolving partly beyond repair, and made diagnosis of problem genesis challenging (Stenvik et al., 2022b, Stenvik et al., 2022c). New groundwater extraction (and injection) schemes are therefore advised to continue measuring hydrochemistry during operation, even though the water quality may be deemed acceptable initially.

The observed problems at Ringerike and in Melhus also involve some design implications on where to locate (1) and how to operate (2) GWHP systems:

- *Location* The absence of manganese clogging issues at Ringerike indicates that less operational problems are expected for GWHP than drinking water wells in glaciofluvial bank filtrations settings. This is because pure water quality issues are less important for GWHP systems than groundwater works. Alternatively, the GWHP systems could be placed between the waterworks' bank filtration area and the production well field. In this case, the GWHP system could function as an observation well, and facilitate early detection of manganese sorption fronts (Stenvik et al., 2022c). Furthermore, care should be taken not to place production and injection wells of separate GWHP system and differing water qualities too close to each other.
- *Operation* In GWHP systems already operating close to each other, lowering the groundwater pumping rate (Q) would reduce or delay the risk of breakthrough of a different water quality, and furthermore reduce pumping costs. However, clogging risk, heat exchanger and heat pump operation, vacuum pressure, and groundwater freezing risk, must also be considered before concluding on how to operate the groundwater pump (Stenvik et al., 2022d)

II) *How important is the microbiology for the GWHP incrustations in Melhus, and which factors control the bacterial activity?*

Research question A.2 will first be sought answered by comparison of two different GWHP systems in Melhus: Lena terrasse (E) and Oterholmgården (H), see Figure 3.2. Iron oxide incrustations and iron-oxidizing bacteria activity have been detected in both systems, but clogging issues have been much more pronounced at Lena terrasse. This is demonstrated from comparison of the dissolved iron concentrations in the rinsing fluid after heat exchanger rehabilitations, see Table 6.1.

Table 6.1 Data from heat exchanger (HE) rehabilitations at Lena terrasse and Oterholmgården. t_{clogged} time since new HE/last cleaning, Fe_{rins} iron dissolved during cleaning, V volume of rinsing fluid (i.e., rehabilitated HE + pipes), $m_{\text{Fe}} = Fe * V$, $Fe - pH - DO$ average dissolved iron, pH and dissolved oxygen of pumped groundwater, respectively, k homogenous rate constant estimated with hydrochemical data (Stenvik et al., 2022b) and eq. 2.7.

GWHP system	Rehabilitations		Rinsing fluid			Hydrochemistry			
	Date	t_{clogged} (years)	Fe_{rins} (mg/L)	V (L)	m_{Fe} (g)	Fe^{2+} (mg/L)	pH	O_2 (mg/L)	k (M/min)
E) Lena terrasse	08.10.2019	~1.0	1458	~200	~300	7.3	0.04	~ $3 * 10^{-13}$	
	21.01.2021	~1.3	3187	~200	~650				~ $5 * 10^{-13}$
H) Oterholmgården	17.03.2021	~6-11	74	~60 ^a	~5	7.7	0.03	~ $1 * 10^{-16}$	

^{a)} Estimated from comparison of maximum heat delivery (P) (Riise, 2015)

The comparison of heat exchanger rehabilitation data from the Lena terrasse and Oterholmgården GWHP indicates > 1000 times higher k at Lena terrasse than Oterholmgården (Table 6.1). This is based on a manipulated form of eq. 2.7: $k = m_{\text{Fe}} [H^+]^2 / ([Fe^{2+}][O_2])$. The k ratios are much higher than the literature k variations reviewed by Houben (2004).

Differences in k could be explained by variation in salinity (Sung and Morgan, 1980) (1), inorganic catalyzer concentrations (e.g., Mn^{2+} , Cu^{2+} , $H_2PO_4^-$) (Stumm and Lee, 1961) (2), and nitrate concentrations (3). Nitrate is the preferred iron oxidant in the absence of oxygen (Houben and Treskatis,

2007). Lena terrasse and Oterholmgården display similar salinities (ionic strength ~ 0.02 M). The inorganic catalyzers' variation is relatively modest in the Melhus aquifer ($0.04 \leq \text{Mn}^{2+} \leq 0.7$ mg/L), $\text{Cu}^{2+} < 3$ $\mu\text{g/L}$, $\text{H}_2\text{PO}_4 < 0.1$ mg/L) (Brøste, 2017, Stenvik et al., 2022b). The nitrate levels are generally low in the Melhus aquifer and comparable for Lena terrasse and Oterholmgården, see Figure 6.3. Followingly, the observed k variability cannot be explained by abiotic factors. This justifies turning focus towards heterogenous oxidation of iron aided by iron-oxidizing bacteria.

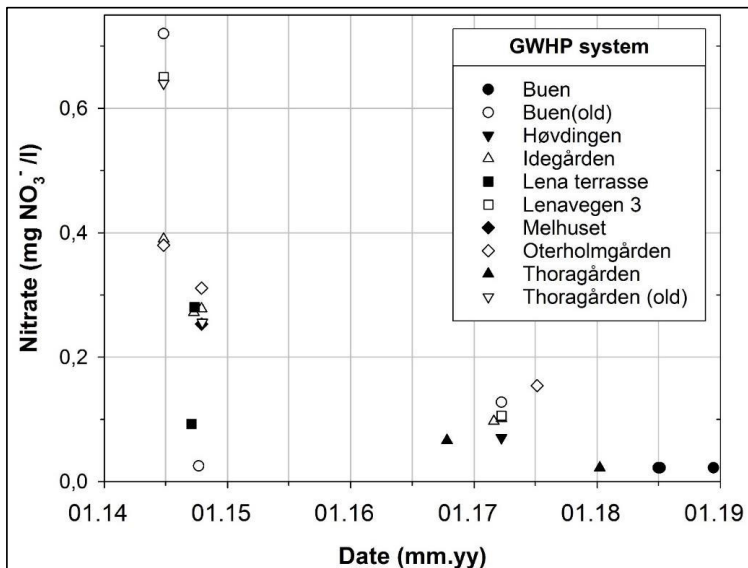


Figure 6.3 Nitrate concentrations from previous studies (Solberg et al., 2014, Riise, 2015, Brøste, 2017) and Asplan Viak AS (2018-2019).

The hydrochemical and hydraulic conditions seem more ideal for IOB growth at Lena terrasse than Oterholmgården, see Figure 6.4. Especially, higher Fe^{2+} , lower pH, higher Eh and higher Q could explain a more rapid growth at Lena terrasse. “Moderate” IOB activities were determined semi-quantitatively with biological activity reaction tests (BART) at both GWHP systems. However, the amount of incrustated iron (Table 6.1) and the number of rehabilitation/reconstruction actions (Table 3.1) are much higher for Lena terrasse than Oterholmgården. This indicates that the IOB activity in fact is higher at Lena terrasse, and questions the reliability of BART tests for quantifying the IOB presence.

The DNA analyses from Lena terrasse confirm the presence of IOBs (*Gallionella*, *Sideroxydans*), but additionally finds bacteria associated with iron reduction (IRB), sulfide oxidation (SOB) and sulfate reduction (SRB). This adds complexity to the analysis in Stenvik et al. (2022b), which hypothesized that oxides and sulfides occurred in separate GWHP systems governed by their salinity and pH.

The co-occurrence of IOB, IRB, SOB and SRB indicates bacterial symbiosis on the verge between post-oxic and sulfidic hydrochemical conditions. For instance, *Gallionella* have been demonstrated to benefit from the presence of SRB (Ghiorse, 1984), which provide nutrients (i.e., Fe^{2+} in sulfides) for growth (Lütters-Czekalla, 1990). The coexistence of iron oxides and sulfides have also been detected in other well systems (Houben, 2003a, Lerm et al., 2011) and water treatment plants (Søgaard et al., 2000).

Lerm et al. (2011) hypothesized that small differences in the physical environment (e.g., temperature) could drive changes to the microbial community on the verge between post-oxic and sulfidic redox conditions. The high iron and sulfate concentrations at Lena terrasse (Figure 6.4) provide nutrients for both IOB and SRB bacteria. This may explain the variations in the microbial community, and its ability to assist build-up of both iron oxide and iron sulfide incrustations, within the same GWHP system.

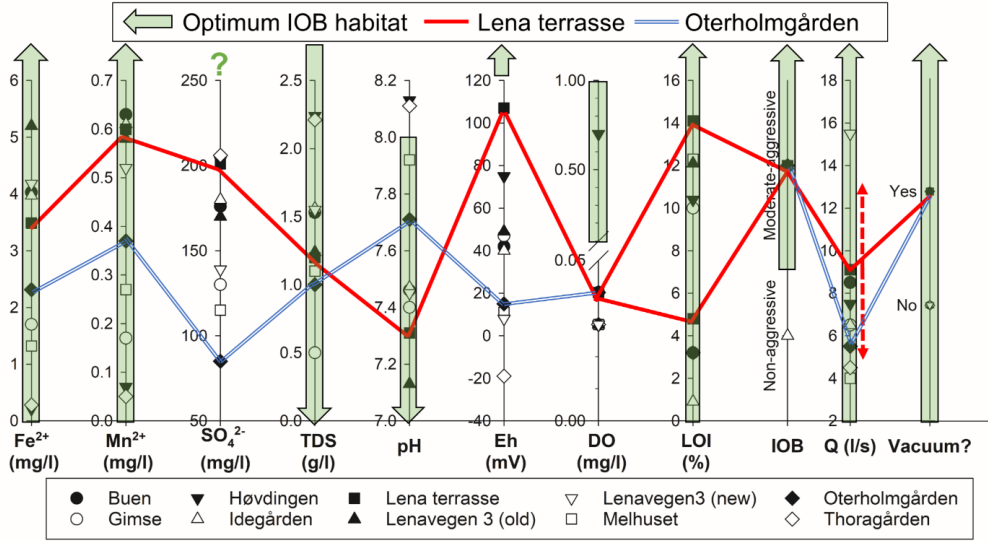


Figure 6.4 Optimum growth habitat for iron-oxidizing bacteria (IOB) (partly based on Table 2.1) vs. conditions at Lena terrasse’s and Oterholmgården’s GWHP systems (Stenvik et al., 2022b, Stenvik et al., 2022a, Stenvik et al., 2022d). *Dotted arrows* operational conditions which sometimes occur. *Green arrows* directed towards conditions more favorable for IOBs. Modified from Stenvik et al. (2022b).

Anyhow, the presence of both iron oxide and iron sulfide incrustations within the same aquifer and even the same GWHP system justifies thorough analysis of the clogging material prior to rehabilitation. This is especially important if chemical rehabilitation techniques are to be deployed. Acids (e.g., hydrochloric acid (HCl)) will dissolve both oxides and sulfides (Houben and Treskatis, 2007). However, the reducing agent sodium dithionite ($\text{Na}_2\text{S}_2\text{O}_4$) is the most effective and most environmentally gentle solvent of iron oxides (Houben, 2003b). This chemical would however not dissolve iron sulfides, which would require an oxidizing agent (e.g., sodium hypochlorite (NaClO) or hydrogen peroxide (H_2O_2)) to be dissolved (van Beek and Kooper, 1980, Lerm et al., 2011). The thermal and hydraulic rehabilitation technique, which is more common in Norway (Hilmo and Gurigard, 2017), work for both iron oxides and sulfides. Still, thorough investigations of the clogging material (e.g., by camera inspection) would be valuable to know the extent of clogging, and to assess operation and maintenance remedies.

III) How do vacuum pressures amplify GWHP operational problems, and which design measures are feasible to prevent degassing and gas entrapment

Hydraulic monitoring of the Lena terrasse GWHP has revealed direct gas clogging (Stenvik et al., 2022a). The gas clogging impels a *waterfall flow* from the highest point in the groundwater circuit (i.e., the heat exchanger) down through the injection pipe. The associated hydraulic head losses upon injection ($h_{L, \text{inj}}$) will equal (Figure 6.5)

$$h_{L, \text{inj}} = h_{\text{wt}} \quad \text{if } h_{L, \text{filter}} + h_{L, \text{pipe}} \leq h_{\text{wt}} \quad (6.1)$$

or

$$h_{L, \text{inj}} = h_{L, \text{filter}} + h_{L, \text{pipe}} \quad \text{if } h_{L, \text{filter}} + h_{L, \text{pipe}} > h_{\text{wt}} \quad (6.2)$$

where h_{wt} is the elevation difference between the top point and the injection well water level (~ 20 m at Lena terrasse), and $h_{L, \text{filter}}$ and $h_{L, \text{pipe}}$ are the head loss through the injection well filter and pipe, respectively (Figure 6.5).

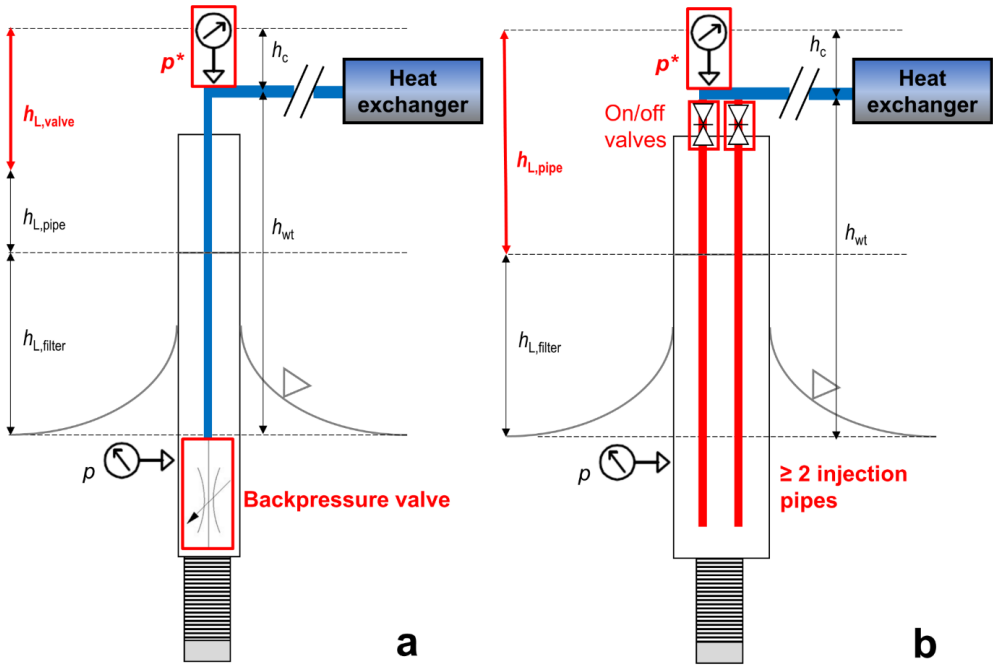


Figure 6.5 Hydraulics of injection wells, with current design (*black*) and two advised designs (**a**, **b**) for pressurizing the flow (*red*). $h_{L,i}$ head losses through component i = *filter* injection well filter, *pipe* injection pipe and *valve* backpressure valve, h_{wt} elevation difference between natural water level and top of groundwater circuit, h_c overpressure criterion, p pressure monitoring. Modified from Stenvik et al. (2022a).

Equation 6.1 and 6.2, and $h_{L,inj}$'s impact on the required pumping head, demonstrate that (Figure 6.5)

1. *injection well filter incrustations* (e.g., by iron oxides) leading to higher $h_{L,filter}$ will not increase the required pumping power (i.e., costs) before the criterion in eq. 6.2 is met, and that
2. *pressurizing the GWHP system* by increasing the frictional resistance in/at the end of the injection pipe(s) ($h_{L,pipe}$, $h_{L,valve}$) will only increase the required pumping head slightly ($\sim h_c$).

where $h_{L,valve}$ is the head loss impelled by the backpressure valve and h_c is the chosen overpressure criterion.

Point 1 have important implications for injection well filter monitoring and rehabilitation. First, incrustations may build up unnoticed if only pump power consumption (W_{GP}), and not injection well water level, is monitored. It also means that injection well rehabilitation will not be economically advantageous on short-term (i.e., meanwhile eq. 6.1 is valid). This does not justify delaying injection well rehabilitations, because mature incrustations will be harder to remove. However, it may explain why injection well clogging often has developed unnoticed and/or not been rehabilitated 'in time' in Melhus.

Point 2 indicates that pumping costs will not be severely increased from pressurizing the GWHP system. Figure 6.5 demonstrate two different ways of pressurizing, by means of an adjustable backpressure valve at the end of the injection pipe (a) and multiple injection pipes with on/off valves (b). Variations in pumping rate (Q) and injection well clogging will influence $h_{L,filter}$ and $h_{L,pipe}$. This craves adjustments to the added backpressure not to exaggerate the pumping costs. For instance, the added backpressure ($h_{L,valve}$ or $h_{L,pipe}$) must be reduced as the injection well filter clogs, and increased after well rehabilitations. Pressure monitoring (p^*) at the top of the injection well should be included to ensure the overpressure criterion h_c is met, but not significantly exceeded.

The placing of the p^* in Figure 6.5 presumes that the top of the injection well represents the pressure minimum in the groundwater circuit (Gjengedal et al., 2019, Stenvik et al., 2022a). This is true if the elevation difference between the injection well top and the top of the groundwater circuit h is small. However, if h is large and exceeds the head loss h_L imposed from pressurized flow between the top point and the injection well, then the pressure minimum will locate at the former location, see Figure 6.6a. Consequently, pressure monitoring (p^*) to accommodate h_c should be placed at the actual top of the groundwater circuit (e.g., right after the heat exchanger). Still, the set up in Figure 6.6a. will demand larger added backpressure, a longer groundwater circuit and higher pumping costs. Therefore, designs where the top of the injection well represents the pressure minimum will be beneficial both with regards to construction and pumping costs.

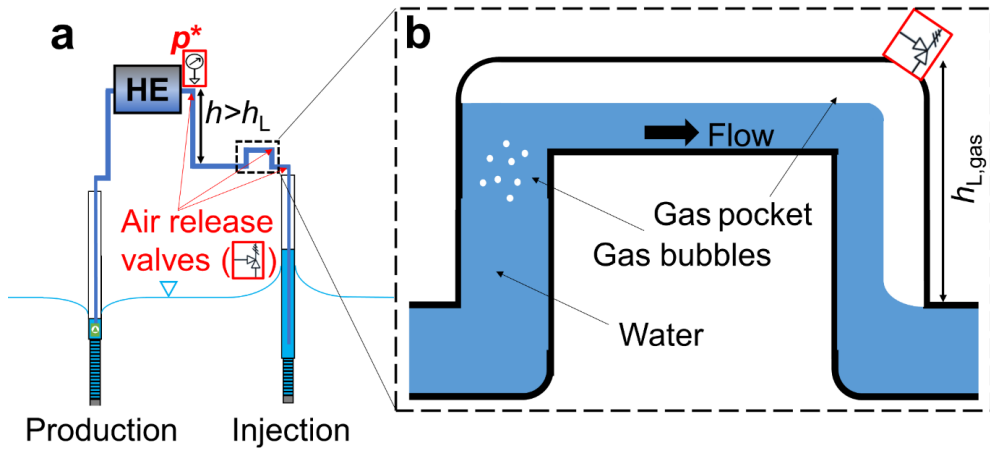


Figure 6.6a Pressure monitoring p^* at the pressure minimum and locations where air release valves must be installed, and **b** gas accumulation and head losses ($h_{L,gas}$) associated with upward-downward bends. h elevation difference and h_L head loss between top of groundwater circuit and injection well top, HE heat exchanger. Modified from Stenvik et al. (2022a).

Pressurizing the GWHP system will not necessarily remove all gas from the groundwater pipes. Stenvik et al. (2022a) demonstrated that the Froude numbers (eq. 2.10) in Lena terrasse's GWHP were too small to carry gas bubbles along with the pipe flow. Therefore, air release valves should be installed at all local top points to evacuate entrapped gas, see Figure 6.6b. Additionally, each gas-filled upward-downward bend will involve a head loss ($h_{L,gas}$) equal to the elevation difference between the top and bottom of the gas pocket. Thus, the number of bends should be minimized both for GWHP systems with (1) and without (2) dedicated pressure control. This will reduce number of air release valves required (1) and accumulated $h_{L,gas}$ (2), respectively.

The thermal impact from gas clogging at Lena terrasse's GWHP could not be quantified due to faulty temperature sensors ($T1$ - $T4$ in Figure 4.5). Still, the detection of a gas pocket in the pipes located directly after the heat exchanger (Stenvik et al., 2022a) indicates that the GWHP could benefit thermally from pressurization and air release from the pipes.

It is uncertain whether vacuum pressure-induced air in-leakage is a major issue for the GWHP systems in Melhus. Elevated dissolved oxygen concentrations ($DO = 0.2$ - 2.4 mg/L) stemming from a leaky pipe filter (Høvdingen) and corrosion damage (Idegården) have been detected. Apart from these two exceptions, solely anoxic ($DO \leq 0.05$ mg/L) conditions have been measured in the groundwater from sampling taps right before/after the heat exchanger (Stenvik et al., 2022b). However, the air in-leakage may be more severe closer to the injection well top, where the pressures are assumed to be lower. Unfortunately, no water has been sampled from these locations.

Figure 6.7a demonstrates that iron oxides tend to occur in the GWHP systems in Melhus with lower pipe pressures. This is based on all pressure measurements performed in the GWHP systems, either by continuous monitoring or by manual manometers. This could be explained by more air in-leakage occurring in pipes with lower pressures. If so, the air in-leakage could explain why injection well clogging is a larger problem than production well clogging in Melhus (Ramstad et al., 2020), since pressures decrease in the pipe flow direction.

The lower pressures in the iron oxide incrustated GWHPs could also be an indirect effect, since these well systems generally are shallower than the iron sulfide incrustated GWHPs (Table 3.1). Shorter groundwater circuits would require less pumping head, and consequently lower pipe pressures. Instead, the incrustation type could relate to the water quality, which is typically less saline in the shallower systems (Figure 6.4). Thus, it may not be a cause-and-effect relationship between pressure and incrustation type.

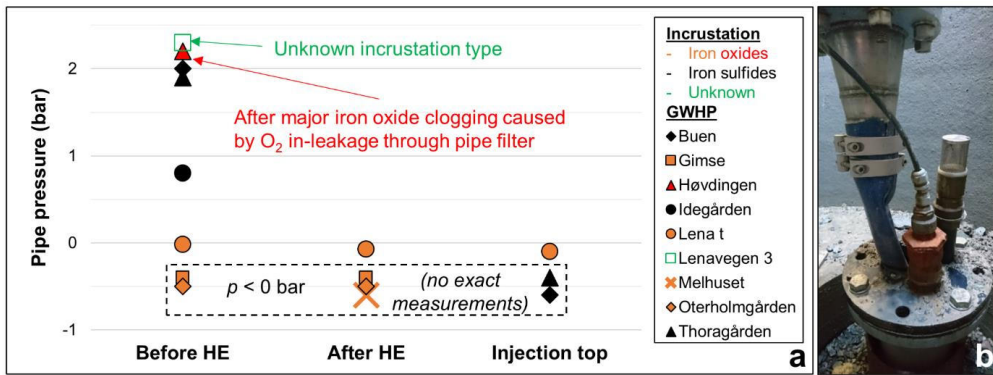


Figure 6.7a Pipe pressure vs incrustation type, and **b** observation of vacuum in injection pipe (hose) in one of Buen GWHP system's injection wells (see injection well closest to defect well at system "A" in Figure 3.2).

The importance of (vacuum) pressure for iron incrustation type and intensity is further questioned by observations of...

- negative pressures in iron sulfide incrustated GWHP systems, for instance at Buen where contraction of the flexible injection hose indicated pressures below the atmospheric (Figure 6.7b), and
- iron oxide incrustation being much more intense at Lena terrasse than Oterholmgården (Table 3.1, Table 6.1), even though both have detected vacuum pressures (Figure 6.7a).

Furthermore, the ATEs system connected to the Reichstag building in Berlin has experienced iron oxide incrustations despite pressurizing the piping system with N₂ gas at 0.4-0.9 bar overpressure (Lerm et al., 2011). The influence of CO₂ degassing on iron oxidation was also deemed minor in Additional result 2 (chapter 5.2). Therefore, pressurizing the GWHP system cannot be expected to fix the iron oxide clogging problems.

The modest increase in operational costs, together with the expected improved hydraulic and thermal performance, still makes pressurizing the GWHP system recommendable. The investment costs have not been considered, but are assumed to be economically viable, at least for the design in Figure 6.5b. However, the GWHP owner must still expect regular maintenance actions, since chemical, mechanical and biological incrustations are expected to persist pressurization. Apart from the already recommended hydrochemical, hydraulic and thermal monitoring to detect clogging, this justifies focusing on operation and maintenance procedures to extend periods between and effectiveness of rehabilitation actions.

IV) How can groundwater pumping and maintenance procedures be adjusted to reduce clogging risk and improve GWHP system economy?

Operation of the groundwater pump

Stenvik et al. (2022d) demonstrated how the combination of hydraulic and thermal monitoring and water quality data could be used to optimize the groundwater pumping rate of Lena terrasse's GWHP system. This forms the basis for the discussion of research question IV.

With regards to COP (eq. 2.18), the analysis showed that the benefit of decreasing groundwater pumping costs is larger than the drawback of the coupled decrease in evaporation temperature. This justifies decreasing the pumping rate Q but adjusting it to the heat demand (P_{HE}) to avoid freezing the groundwater (eq. 2.1) or the secondary circuit fluid (Figure 2.5).

The optimization of Q becomes more complex when also considering clogging. Both the injection well and the heat exchanger at Lena terrasse suffer from significant clogging, with clogging rate being independent of Q in the typical pumping range ($Q = 6-12$ L/s), see Figure 6.8. Pumping rates above this range were shown to increase the suspended solids loading, with associated injection well clogging risk. Contrarily, $Q < 6$ L/s increased the heat exchanger clogging rate, see May-June 2021 in Figure 6.8 (Stenvik et al., 2022d).

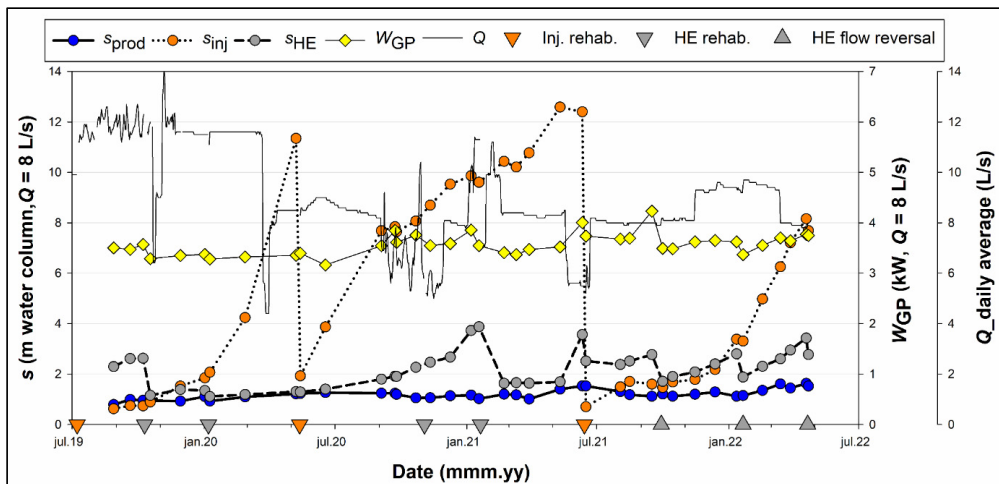


Figure 6.8 Monitoring of pressure drawdown (s) of production well (*prod*), injection well (*inj*) and heat exchanger (*HE*), and submersible groundwater pump power consumption (W_{GP}), between August 2019 and April 2022. Data points are calculated from step-discharge test results (B_i - and C_i -values) to the reference groundwater pumping rate $Q = 8$ L/s (eq. 2.11 and 2.12). *Rehab.* rehabilitation. Modified from Stenvik et al. (2022d).

Recommendations to reduce Q for injection wells (eq. 2.16) (Olsthoorn, 1982) and increase Q for plate heat exchangers (eq. 2.11, 2.17) (Kerner, 2011) may at first glance seem counterintuitive. Higher flow velocities will lead to more drag force acting on suspended particles and shear stresses acting on sediments (e.g., in well filter pack). This means suspended particles will tend to remain suspended, and deposited particles will tend to become eroded. However, due to the radial flow out of the injection well, the velocities will decrease out through the well filter, eventually facilitating sedimentation of suspended solids. Meanwhile, the velocities will remain more constant through the plate heat exchanger. This may explain the different focuses: avoiding sediment transport in/to injection wells and avoiding sedimentation in heat exchangers.

The wells (both production and injection) and the heat exchanger also respond differently to Q variation. Figure 6.9 shows the specific capacity of the wells and the heat exchanger after vs. before step-discharge

tests. Evidently, the wells seem to benefit from changing the pumping rate after longer periods with semi-constant Q (Figure 6.8). The step-discharge could function as a ‘light-version’ of filter development, thus mobilizing particles which have settled in the filter packs. On the other hand, heat exchangers seem to become slightly impeded by the step-discharge tests. This could be due to the temporarily increased sediment transport during elevated flow rates, followed by lower pumping rates facilitating sedimentation. However, only slightly impeded heat exchanger performance and the ease and low costs of heat exchanger flow reversals or rinsing compared with well rehabilitation, advocates for continuing step-discharge testing the GWHP system. It may even argue for testing out a pumping scheme involving more Q variation.

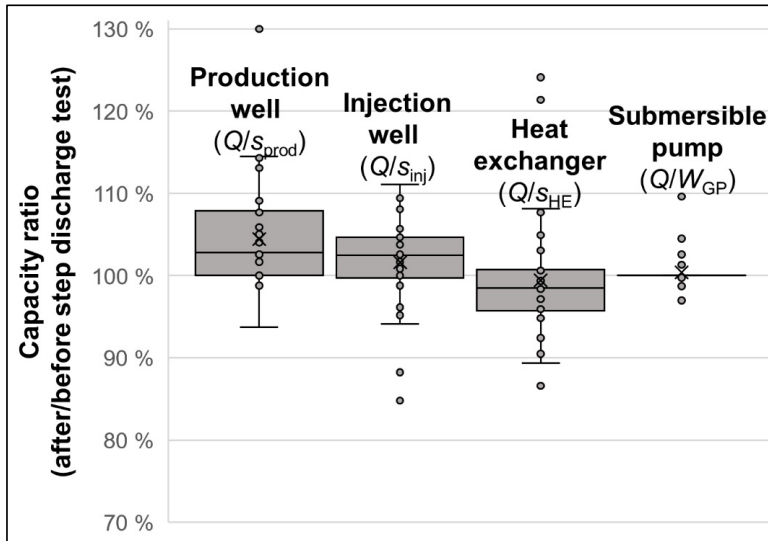


Figure 6.9 Comparison of the specific well/heat exchanger capacity (Q/s_i) for $i = \text{prod, inj and HE}$, and specific pump yield (Q/W_{GP}), after divided by before step-discharge tests ($n = 34$). Data from Stenvik et al. (2022d).

Varying the pumping rate is recommended for wells suffering from mechanical, but not chemical, incrustations (van Beek et al., 2009a). This is due to the risk of increasing the vertical mixing of shallow, oxic and deep, iron-rich water. However, at Lena terrasse’s GWHP the water quality remains stable, independent of the pumping rate (Stenvik et al., 2022d). This indicates that vertical redox mixing is not a major issue, and that varying the pumping rate could reduce the mechanical clogging risk without worsening the iron oxide clogging problem.

The recommended pumping scheme could also be affected by the GWHP design and neighboring GWHP systems:

If the GWHP design includes a strategy to pressurize and avoid gas entrapment (Figure 6.5, Figure 6.6), Q can be lowered without risking vacuum pressures, degassing and air in-leakage. Pressurization also allows turning off the groundwater pump without emptying water from the piping system, and the associated vacuum and air in-leakage risk. Followingly, the groundwater pump can be turned off during periods with low heating/cooling demands and cut pumping costs, instead of continuously pumping like most of the GWHP systems in Melhus do today. The pump shut-off periods can also cut off the nutrient supply to bacteria in the well filters. Adding disinfectants to the wells during shut offs may further inhibit bacteria growth, but the bacteria are likely to reappear provided that the nutrients (i.e., iron) are still present (Houben and Treskatis, 2007). Thus, disinfections cannot replace well rehabilitations.

The presence of neighboring GWHP systems could induce water quality changes, see Figure 6.2. This suggests lowering the pumping rate to delay the breakthrough of a new water quality type.

Altogether, the optimization of the groundwater pumping is complex. The optimization based on Lena terrasse's GWHP should not be considered a "one size fits all"-solution. However, the workflow and considerations may serve as an example for improving the operation of other GWHP systems.

Rehabilitation of wells and heat exchangers

The GWHP wells in Melhus are probably not rehabilitated frequently enough. According to Houben and Treskatis (2007) one should expect to rehabilitate a well in an unconsolidated sand and gravel aquifer every 1-5 years. Presuming an economic well service life of ≥ 25 years, one would expect rehabilitation/reconstruction action ratios in the range $\geq 4-24$. In Melhus, the rehabilitation/reconstruction ratio is 1.3, see Figure 6.10. This means far less rehabilitations and/or too many reconstructions have been carried compared with the expected range. Considering the challenging redox water quality in the Melhus aquifer, this suggests that more rehabilitations should be carried out in GWHP systems in Melhus in the future. The number of well reconstructions is also deemed to be reduced with more successful rehabilitations.

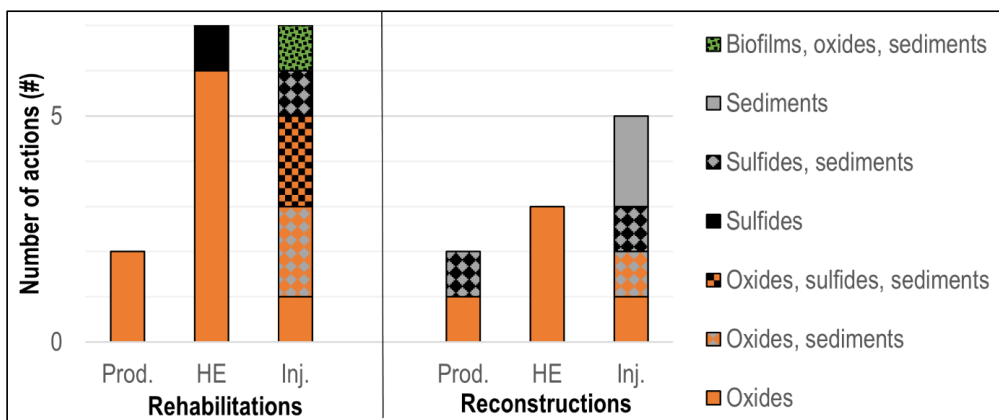


Figure 6.10 Rehabilitation and reconstruction actions in Melhus' GWHP systems distributed by problem location and type. Data from janitor logs, Riise (2015), Brøste (2017) and Stenvik et al. (2022b).

Well rehabilitations' varying degree of success of in Melhus could explain their infrequent execution. Several different incrustation types and compositions have been detected, see Figure 6.10, although some uncertainty adheres to the classification. Especially the injection wells have experienced a wide variety of problems. Up until now, mechanical (e.g., jetting and airlift pumping) and thermal (i.e., steaming) rehabilitations have been deployed regardless of problem type. Probably, including a chemical rehabilitation step with custom-fitted rinsing chemicals would improve the rehabilitations' efficiency (Houben and Treskatis, 2007).

The general aversion to add chemicals to aquifers in Norway may be altered by a responsible and scientific based implementation. Sodium dithionite ($\text{Na}_2\text{S}_2\text{O}_4$) is the most effective reducer and solvent of iron oxides (Houben, 2003b). Chemical well cleaning with dithionite buffered with bicarbonate yields the non-hazardous rest products sodium (Na^+), sulfate (SO_4^{2-}) and bicarbonate (HCO_3^-), in addition to the dissolved incrustations. Of these, the latter may be the most hazardous rest products from rehabilitation, due to iron oxides' high contents of trace elements (Houben and Treskatis, 2007).

Figure 6.11 displays trace element concentrations in incrustations from Melhus' GWHP systems. Although the contents vary considerably, the highest detected concentrations of Ni, Cu, Zn and Pb constrain their disposal at landfills (Regulation on organic fertilizers, 2003). The trace element contents may also restrict the discharge of dissolved incrustations to local stormwater systems, but this is decided on municipal level. This demonstrates that chemical well rehabilitation with sodium dithionite is not likely to add significant environmental concerns to the anoxic, saline Melhus aquifer.

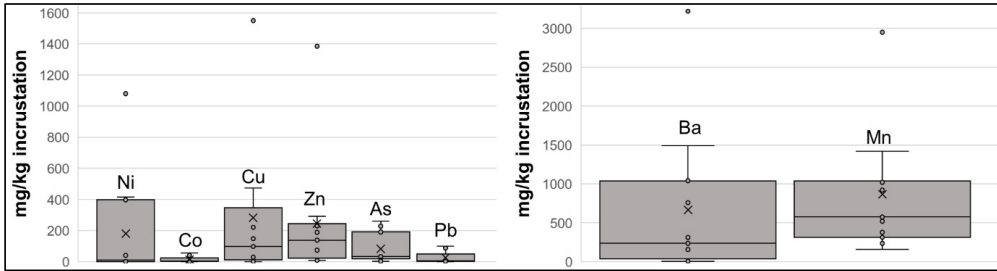


Figure 6.11 Trace element concentration of arsenic (As), nickel (Ni), cobalt (Co, $n = 9$), barium (Ba), copper (Cu, $n = 9$), zinc (Zn), lead (Pb, $n = 9$) and manganese (Mn) in incrustations from GWHP systems in Melhus, Norway ($n = 11$, unless otherwise stated). Data from Stenvik et al. (2022b).

The few environmental concerns with sodium dithionite in the Melhus aquifer (1), its proven effectiveness on mature iron oxide incrustations from Lena terrasse's GWHP (2), its economic competitiveness with thermal rehabilitation (Stenvik, 2022) (3), and iron oxides incrustations high frequency in GWHP systems in Melhus (Figure 6.10) (4), argues for testing $\text{Na}_2\text{S}_2\text{O}_4$ in GWHP wells in Melhus. However, technical competence, including expertise on how to build a gravel washer (Figure 2.7), must probably be acquired from abroad for a safe and effective implementation.

Chemical cleaning of heat exchangers is easier than for wells, and a more mature technology in Norway. Valves and hose connections at the groundwater inlet and outlet of the heat exchangers have facilitated clean-in-place (CIP) rehabilitation in Melhus. The CIP involves circulating a mixture of citric acid and complexing agents at $T = 50^\circ\text{C}$ through the heat exchanger for ~ 1 -2 days. Although the closed circuit allows control on the rinsing chemicals, they are usually disposed to the local stormwater drain. Thus, in practice chemical cleaning of heat exchangers does not differ notably from chemical well cleaning environmentally.

The short-term economic incentives for performing well and heat exchanger cleaning also differ notably. Clogging of the production well will increase the submersible pumping power demand (W_{GP}), while injection well clogging will lead to increasing W_{GP} if the criterion in eq. 6.2 is met. In addition to increasing W_{GP} , clogging of heat exchangers will also decrease the heat transfer coefficient (eq. 2.13). This will decrease the evaporation temperature of the heat pump (Figure 2.5) and increase the heat pump compressor power demand (W_{HP}). Increased power demands will lower the total COP of heating/cooling operation (eq. 2.18). The production well at Lena terrasse and in other GWHPs in Melhus have experienced fewer clogging problems than the heat exchangers and injection wells, see Figure 6.10. Thus, heat exchanger clogging may impede the GHWP system's economy more significantly on short-term, than well clogging.

Figure 6.8 demonstrates a correlation between pumping power and heat exchanger clogging. This is due to the heat exchanger representing the top point of the groundwater circuit, from which water is discharged by gravity down through the injection well. Heat exchanger clogging's effect on the U value has been difficult to assess due to the lack of quality temperature data. Figure 6.12 displays U values from the temperature data which have been deemed acceptable. U varies considerably, even for the same s_{HE} . This is probably due to the two-sided effect of U values, *increasing* with turbulence (1), but *decreasing* with fouling of the heat exchanger plates (2). Both (1) and (2) will increase s_{HE} . The tendency of decreasing U values when $s_{\text{HE}} > 2$ m is probably due to fouling of the heat exchanger plates. This could also explain why the COP values were higher during the 2020/2021 than the 2021/2022 heating season, with the former involving a less clogged heat exchanger (Stenvik et al., 2022d).

Even though injection well clogging will not affect COP significantly on short-term, the maturation of iron oxides and other incrustations will make their removal by rehabilitation harder with time.

Therefore, the author would not recommend ignoring the rehabilitation criteria in Houben and Treskatis (2007), even though they may have been developed for production and not for injection wells.

Apart from the influence on COP, it must also be considered that heat exchanger rehabilitations are less technically complicated and cheaper than injection well rehabilitations. Additionally, heat exchanger flow reversal can supplement, but not completely replace, heat exchanger rehabilitations (Figure 6.8). Altogether, this justifies more frequent heat exchanger than injection maintenance and rehabilitation actions. Still, it encourages developing effective rinsing techniques (e.g., with $\text{Na}_2\text{S}_2\text{O}_4$) for the more infrequent injection well rehabilitations.

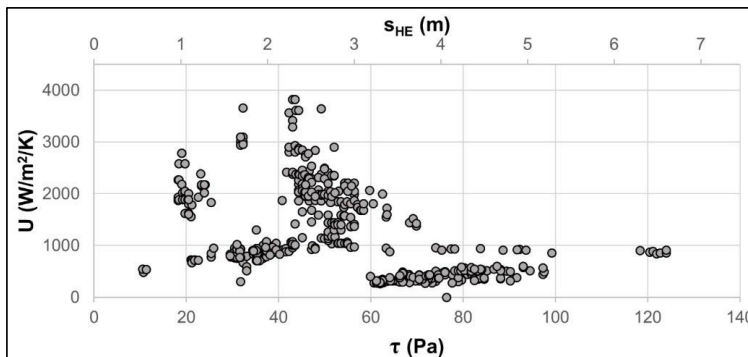


Figure 6.12 Heat exchanger heat transfer coefficient (U ; eq. 2.13) as a function of pressure drop through heat exchanger (s_{HE}) and shear stress on heat exchanger plates' (τ ; eq. 2.17). Data from Stenvik et al. (2022d).

6.1. How to reduce the negative effects of pumping iron and manganese

The conducted research involves certain 'take-home messages' for the location, design, operation, and monitoring of groundwater well systems for water supply (a) and heating/cooling (a-d):

a) Do not expect the initial quality and quantity of extracted groundwater to persist!

Performing qualitative analyses and quantitative monitoring facilitates early detection of alterations and eases troubleshooting. Well owners are there advised to...

- **Analyze hydrochemistry regularly.** Hydrochemistry should be analyzed both by field measurements and water samples. A flow-through cell facilitates precise Eh, DO, and pH measurements in the field over time, which can assist chemical clogging risk assessment.
- **Assess bacteria and suspended solids loading.** Biological activity reaction tests (BARTs) can be used to detect clogging-catalyzing bacteria (e.g., iron-oxidizing bacteria). Suspended solids loading can be analyzed by turbidity measurements in the field (i.e., to avoid chemical precipitation interfering results) or (manual) particle counting. These will aid risk assessment of biological clogging/catalysis of chemical clogging, and mechanical clogging, respectively.
- **Analyze incrustation composition.** First, incrustations should be sampled and characterized mineralogically, since different minerals (e.g., iron sulfides and manganese oxides) may resemble on another visually. Later, visual *in situ* analysis (e.g., by camera inspection) could replace the tedious and expensive laboratory analyses for an already mineralogically described well. Thorough incrustation description will help deciding how to rehabilitate the well.
- **Monitor hydraulics and heat transfer continuously (incl. step-discharge tests).** *Hydraulics* include pressure drawdown through well filters (and heat exchangers for GWHP systems), groundwater flow rate and submersible pump power. GWHP systems should additionally monitor temperatures at the groundwater and secondary circuit fluid in- and outlets of the heat exchanger and heat pump heat production (P). This will aid clogging detection and timing rehabilitation actions. Additionally, it will aid the design/adjustment of a pressure control scheme, and how to operate the groundwater pump to minimize clogging and maximize COP.

- **Assess the risk of manganese sorption fronts** progressing from the recharge area to groundwater works' production well field, especially for bank filtration schemes situated in glaciofluvial aquifers. Monitor water quality regularly in observation wells situated between the riverbank and the extraction wells for early detection of sorption fronts.

b) Involve experts from multiple sciences in GWHP system design and troubleshooting!

The GWHP systems are complex, and their design, operation and maintenance require interdisciplinary expertise. Experts from multiple branches of science should be involved during the GWHP life cycle, including hydrogeologists, hydraulic engineers, heat transfer specialists, chemists and microbiologists.

c) Pressurize the GWHP system, but do not expect it to fix all clogging problems!

Pressurization (including air venting) of groundwater pipes will inhibit gas clogging, and possibly hinder oxygen in-leakage and CO₂ degassing. Experiences from Melhus demonstrate that the latter two will have limited effect on the chemical incrustation risk. Therefore, clogging must still be expected, despite pressurization. Still, low additional operational costs, and flexible design allowing limiting extra investment costs, justifies including pressurization in the GWHP design.

- **Constrict injection pipe(s)** to pressurize the groundwater pipework. This can be realized by adjustable backpressure valves (expensive) or multiple injection pipes with on/off valves (cheap). Both designs will allow adjusting the backpressure to groundwater flow rate (i.e., GWHP heating/cooling demand) and injection well filter clogging status.
- **Install air-release valves at local high points** to allow air venting from the groundwater pipes. Up- and downward bends should be reduced to limit the number of air-release valves (if GWHP is pressurized) and gas pockets increasing the required pumping head (if not pressurized).
- **Install pressure sensor (p^*) at the GWHP pressure minimum.** This is typically in the injection wellhead if the groundwater pipe's maximum elevation is not located significantly higher. The injection pipe(s) constriction should be adjusted from p^* monitoring, to meet but not significantly exceed the chosen overpressure criterion h_c (~0.5 bar).

d) Customize groundwater pumping and rehabilitations for individual GWHP systems!

Clogging issues must be expected for the GWHP system, but groundwater pumping and rehabilitations should seek to extend uninterrupted operational periods and increase the COP of heating/cooling. This underlines a complex optimization, craving hydraulic and thermal monitoring, and water quality and incrustation composition data. Still, some general advice can be provided:

- **Reduce the groundwater pumping rate (Q)**, BUT within the preferred operational range of the heat exchanger (1), without causing vacuum pressures (i.e., if pipework is not pressurized) (2), and without risk of freezing the groundwater or the secondary circuit fluid (3). Advantages of low Q includes reduced submersible pump power input, turbidity (i.e., involving increased sand production and chemical precipitation rate), and nutrients supplied to bacteria. Furthermore, it may delay water quality changes induced by nearby GWHP systems.
- **Consider turning off the groundwater pump** when GWHP heating and cooling demand is low. This presumes a pressurized pipework (i.e., no air in-leakage) and negligible vertical redox mixing in the production well filter, thus not leading to a sped-up oxidation of iron. This will lead to modest pumping cost savings (~3200 kWh/year for Lena terrasse) but will cut off nutrient supply to bacteria and allocate time for camera inspections/rehabilitations/disinfection.
- **Perform heat exchanger flow reversals frequently** (i.e., \geq every 2 months). It is not even necessary to increase Q during the ~2 hours of flow reversal. This can delay clogging and extend periods between, but not fully replace, heat exchanger rehabilitations.
- **Rehabilitate the injection well, although it does not affect the COP on short-term.** The lack of economic incentives calls for more infrequent, but higher efficiency of, injection well than heat exchanger rehabilitations. Therefore, benefits vs. drawbacks of chemical well rehabilitation should be considered (i.e., rinsing efficiency vs. technical and environmental concerns).

7. Conclusions

The conducted research has led to the following conclusions for each of the four research questions:

I) *How do the geochemical signatures of iron and manganese influence groundwater well operation?*

The geochemical differences between iron and manganese become evident during groundwater well operation. The lower required redox potential and faster kinetics of oxidation of iron explains why the anoxic (≤ 0.05 mg/L) GWHP systems in Melhus have been clogged by iron oxides and not manganese oxides. Furthermore, iron sulfides' higher geochemical tendency to occur than manganese sulfides also explain why mainly iron and only trace contents of manganese are found in the sulfide incrustations in Melhus. Redox characteristics also explains why elevated concentrations of manganese, and not iron, have reached the production wells at Ringerike waterworks: The oxygenation around the production wells have probably been sufficient to oxidize and precipitate iron but not manganese in the aquifer formation. Clogging in Ringerike waterworks' production wells was minimal, indicating manganese first was oxidized during water treatment and in the water distribution network. The black manganese oxide particles formed there have necessitated a costly new water treatment system.

The different problems arising from iron and manganese during groundwater extraction have certain implications. Elevated manganese concentrations bring about more problems to drinking water than heating/cooling well systems, since the latter do not have to consider the groundwater's aesthetic/human health aspects. Therefore, GWHP systems can be established in glaciofluvial bank filtration settings like the Kilemoen aquifer, Ringerike with less concerns than for drinking water wells. Groundwater works in similar settings like Ringerike are advised to establish observations wells between the bank filtration area and the production well field for early detection of manganese sorption fronts. The occurrence of both iron oxides and sulfides in GWHP systems in Melhus indicates that clogging problems should be expected in settings with high iron concentrations, regardless of oxygen content.

II) *How important is the microbiology for the GWHP incrustations in Melhus, and which factors control the bacterial activity?*

Iron-oxidizing bacteria (IOB) have been demonstrated to be important contributors to the iron oxide incrustations in Melhus' GWHP systems. The bacteria have been detected semi-quantitatively in the water-phase by biological activity reaction tests (BARTs) and qualitatively in incrustation samples (*Gallionella*, *Sideroxydans*) by DNA analysis. The iron oxide clogging severity, as compared between the different GWHP systems, cannot be explained by purely abiotic factors (Fe^{2+} , Mn^{2+} , O_2 , NO_3^- , pH). This suggests that the preferred growth habitats of iron-oxidizing bacteria influence the oxidation of iron, and that focus should be directed from abiotic to biotic habitats which trigger iron clogging.

Apparently, the IOB thrive at lower salinities. This is evident from iron oxides and iron sulfides encrusting GWHP systems with low and high salinities, respectively. Furthermore, the most strongly iron oxide clogged GWHP system, Lena terrasse, is characterized by lower pH values than the other active GWHP systems. This corresponds well with literature, suggesting that IOBs thrive at lower salinities and neutral to slightly below-neutral pH values.

Both iron oxides and iron sulfides were found during DNA sampling at Lena terrasse's GWHP, although iron oxides previously have been interpreted as the main clogging cause. The DNA analysis demonstrated a microbial environment consisting of genera contributing to nitrogen cycling, iron oxidation, iron reduction, sulfate reduction and sulfur oxidation, among others. This demonstrates the complexity of the microbial community, promoted by hydrochemical conditions on the verge between post-oxic and sulfidic. Probably, the high availability of nutrients at Lena terrasse (i.e., high groundwater flow rate Q and high concentration of sulfate, iron and inorganic carbon) facilitates the complex bacterial community and the extensive iron clogging.

III) *How do vacuum pressures amplify GWHP operational problems, and which design measures are feasible to prevent degassing and gas entrapment?*

Vacuum pressures, together with insufficient Froude numbers (Fr) to carry gas bubbles with the pipe flow, have been demonstrated to cause gas pockets and gas clogging on the injection side of the heat exchanger at Lena terrasse's GWHP. The waterfall flow from the heat exchanger down through the injection pipe leads to additional head losses approximately equal to the elevation difference between the heat exchanger and the injection well water level. Gas clogging of the heat exchanger probably also impedes the heat transfer between the groundwater and the secondary circuit fluid. The influence from oxygen in-leakage into groundwater pipes under vacuum pressure is more uncertain. However, extensive iron oxide incrustations have been demonstrated to occur even without oxygen in-leakage. CO_2 degassing's influence on pH and followingly iron oxidation, has been deemed minimal. Pressurization of the groundwater pipeline is thus expected to restrain gas clogging and improve thermal performance of the heat exchanger but have limited influence on iron oxide incrustations.

Pressurization can be achieved by constricting the injection pipe, either by a backpressure valve or multiple, narrow injection pipes. Due to changing heat demands and injection well filter clogging, the constriction of the injection flow must be varied with time. Therefore, the backpressure valve opening, or alternatively the number of open injection pipes, should be adjustable. The constriction should be regulated by a pressure sensor installed at the pressure minimum of the groundwater circuit (i.e., typically at the injection wellhead), and comply with a chosen overpressure criterion h_c (~ 0.5 bar). The pressurization will only slightly increase groundwater pumping costs, due to only slightly increasing pumping head ($\sim h_c$).

Despite pressurization, gas pockets will remain in the pipeline if the pipe flow velocity (i.e., Fr) is not high enough. Instead of increasing the pumping rate Q , the air should be evacuated by air-release valves installed at local high points (i.e., where gas tends to get entrapped). This also implies that the amount of up- and downward bends should be limited in the GWHP pipeline. By choosing multiple injection pipes for pressurization and limiting the number of up- and downward bends, the added investment costs will be small. Relatively modest additional investment and operational costs related to pressurizing the pipework, and possible benefits with regards to gas clogging, heat transfer and air in-leakage, backs up its implementation in GWHP system design.

IV) *How can groundwater pumping and maintenance procedures be adjusted to reduce clogging risk and improve GWHP system economy?*

The optimization of groundwater pumping is complex, due to its influence on both groundwater pumping and heat pump compressor power input, heat transfer in the heat exchanger and heat pump evaporator, and multiple clogging processes. Therefore, the groundwater pumping scheme should be based on hydraulic and thermal monitoring, and water quality and incrustation composition data. For the Lena terrasse GWHP case, reducing pumping rates in the range 6-12 L/s was suggested.

Particularly GWHP heat exchangers and injection wells have been clogged and necessitated maintenance actions in Melhus. Heat exchanger rehabilitations reduce groundwater pumping (W_{GP}) and heat pump compressor power input (W_{HP}), which justifies their implementation from a short-term economic perspective. Lower W_{HP} is due to increased heat transfer in the heat exchanger, leading to higher evaporation temperature in the heat pump. Frequent reversal of groundwater flow through the heat exchanger has delayed the clogging, but not enough to replace rehabilitations. The waterfall flow down through or adjusted pressurization of the injection pipe(s) means that injection well rehabilitation will first reduce groundwater pumping costs if/when the well filter is severely clogged. Still, maturation of incrustations justifies rehabilitating injection wells before pumping costs are affected. Though, injection well rehabilitations would be more favorable if they proved more efficient. This suggests testing out chemical rinsing chemicals (e.g., $Na_2S_2O_4$ on iron oxide incrustations).

7.1. Further work

During this PhD work many interesting prospects for further investigation had to be deprioritized due to technical, economical and/or time concerns. Some candidates for further work are listed below.

- **Monitor a new bank filtration scheme** in a similar hydrogeological setting as Ringerike waterworks, where geochemical data and advection-reaction modeling predicts the progression of a manganese sorption front. If a sorption front is detected, this would back up the presented explanation for delayed occurrence of elevated manganese concentrations at Ringerike waterworks, and probably provide valuable insight on how future bank filtration schemes should be monitored and operated
- **Analyze the mechanisms controlling dissolved iron concentrations in the Melhus aquifer** and similar aquifers. van Beek et al. (2021) demonstrated how sulfate reduction, sulfide oxidation, and siderite dissolution and precipitation could explain the dissolved iron concentrations in anoxic, Dutch aquifers. It was hypothesized that the same mechanisms governed iron mobility in the Melhus aquifer. However, there were not enough data available to back up this hypothesis, possibly due to very low concentrations of precipitated siderite. Further studies should try to detect siderite coatings on aquifer sediments qualitatively (e.g., by analyzing thin section samples with petrographic microscopy). Knowledge on controlling mechanisms for dissolved iron concentrations would be valuable for choosing GWHP system locations and designs with less risk of iron incrustations.
- **Investigate the microbiology of chemical incrustations** further to describe the microbial community, and analyze how it links with water quality, incrustation build-up and clogging severity. This would be valuable for future incrustation risk assessment.
- **Install a pressure control system** in an existing GWHP system, and assess how it affects the clogging rate (e.g., by avoiding air in-leakage to the pipework). Followingly, the cost vs. benefit of pressurization can be evaluated.
- **Test *in situ* sodium dithionite ($\text{Na}_2\text{S}_2\text{O}_4$) rehabilitation of iron oxide incrustations.** A relevant question is whether the (often-)high hydraulic gradients in Norwegian aquifers affect the cleaning efficiency and spreading of chemicals in the aquifer. It is recommended to first test the chemical in an aquifer which is not used for drinking water supply and where the environmental impact of chemical spills would be limited (e.g., the Melhus aquifer). The results from such testing would be valuable for assessing $\text{Na}_2\text{S}_2\text{O}_4$'s applicability to Norwegian groundwater wells.
- **Model and measure the vertical distribution of flow rates through the injection well.** An uneven vertical distribution of flow rates through the well filter has already been modeled and measured by flowmeter measurements in production wells (Von Hofe and Helweg, 1998, Houben, 2006). The same modeling and measurements should be performed for injection wells. This could have important implications for incrustation build-up and where to place the injection pipe.
- **Perform a sociological study on the knowledge of and possible aversion against GWHP systems** in Melhus and/or town centers with similar hydrogeological settings. What is the public opinion on and knowledge of GWHP systems? Is there aversion against them? And if so, what is the root cause of this? Answering these questions could be vital for the future attractiveness and deployment of this technology.

References

- Appelo, C. A. J., & Postma, D. (2005). *Geochemistry, groundwater and pollution* (2nd ed.). Leiden: Balkema.
- Bakema, G. (2001). *Well and Borehole Failures and Solutions in Underground Thermal Energy Storage* (IF Technology report 2/9805/GW). Arnhem: IF Technology. doi: 10.13140/RG.2.2.10214.98885
- Banks, D. (1992). *Grunnvannsbrønner: Kontroll, vedlikehold, rehabilitering. GiN-veilder nr. 13* [Eng: Groundwater wells: Control, maintenance and rehabilitation. GiN guide no. 13. In Norwegian] (Skrifter 108). Trondheim: NGU.
- Banks, D. (2012). *An Introduction to Thermogeology: Ground Source Heating and Cooling* (2nd ed.). Oxford: Wiley-Blackwell.
- Beckedorf, T., Gräfensteiner, M., & Puronpää-Schäfer, P. (2016). Sustainable rehabilitation strategy of water well gallery on Elbe river bank. *Water Solutions*, (1), 14-16.
- Berner, R. (1981) A New Geochemical Classification of Sedimentary Environments. *Journal Sedimentary Petrology*, 51, 359-365.
- Bloemendal, M., & Hartog, N. (2018). Analysis of the impact of storage conditions on the thermal recovery efficiency of low-temperature ATES systems. *Geothermics*, 71, 306-319. doi:10.1016/j.geothermics.2017.10.009
- Bloemendal, M., Olsthoorn, T., & van de Ven, F. (2015). Combining climatic and geo-hydrological preconditions as a method to determine world potential for aquifer thermal energy storage. *Science of The Total Environment*, 538, 621-633. doi:10.1016/j.scitotenv.2015.07.084
- Breeuwsma, A., Wösten, H., Vleeshouwer, J., Slobbe, A., & Bouma, J. (1986). Derivation of Land Qualities to Assess Environmental Problems from Soil Surveys. *Soil Science Society of America Journal - SSSAJ*, 50 (1), 186-190. doi:10.2136/sssaj1986.03615995005000010035x
- Brugger, M., & Paskert, P. (2020). Groundwater plant with treatment system to remove manganese. *Water Solutions*, (2), 3-6.
- Brøste, H. M. (2017). *Vannkvalitet knyttet til grunnvannsbaserte grunnvarmeanlegg i Melhus og Elverum*. [Eng: Water Quality in Groundwater-Based Heat Pump Systems in Melhus and Elverum] (Master thesis). Trondheim: NTNU.
- Burté, L., Cravotta III, C. A., Bethencourt, L., Farasin, J., Pédrot, M., Dufresne, A., Gerard, M.-F., Baranger, C., Le Borgne, T., & Aquilina, L. (2019). Kinetic study on clogging of a geothermal pumping well triggered by mixing-induced biogeochemical reactions. *Environmental science & technology*, 53(10), 5848-5857. doi:10.1021/acs.est.9b00453
- Bustos Medina, D. A., van den Berg, G. A., van Breukelen, B. M., Juhasz-Holerman, M., & Stuijffzand, P. J. (2013). Iron hydroxide clogging of public supply wells receiving artificial recharge: Near-well and in-well hydrological and hydrochemical observations. *Hydrogeology Journal*, 21 (7), 1393-1412. doi:10.1007/s10040-013-1005-0
- Çengel, Y. A., & Cimbala, J. M. (2010). *Fluid mechanics : fundamentals and applications* (2nd ed.). New York: McGraw-Hill.
- Corcos, G. (2003). *Air in water pipes: A manual for designers of spring-supplied gravity-driven drinking water rural delivery systems*. (2nd ed.). Berkeley: Agua Para La Vida.
- Cullimore, D. R. (2008). *Practical manual of groundwater microbiology* (2nd ed.). Boca Raton: CRC Press.
- Detay, M. (1997). *Water Wells - Implementation, Maintenance and Restoration*. Hoboken: John Wiley and Sons.
- Dimkić, M., Pušić, M., Obradović, V., & Kovačević, S. (2012). The effect of certain biochemical factors on well clogging under suboxic and mildly anoxic conditions. *Water Sci Technol*, 65(12), 2206-2212. doi:10.2166/wst.2012.129
- Driscoll, F. G. (1989). *Groundwater and wells* (2nd ed.). St. Paul: Johnson Division.
- Du, X., Zhang, H., Ye, X., & Lu, Y. (2018). Flow Velocity Effects on Fe(III) Clogging during Managed Aquifer Recharge Using Urban Storm Water. *Water*, 10(4), 1-11. doi:10.3390/w10040358
- Eggen, G., & Vangsnes, G. (2005). Heat pump for district cooling and heating at Oslo airport, Gardermoen. In M. Axell (Ed.), *Proceedings of the 8th IEA Heat Pump Conference, May 30-June 2, 2005, Las Vegas, US* (pp. 1-7). IEA Heat Pump Centre.

- Eggen, O. A., Reimann, C., & Flem, B. (2019). Reliability of geochemical analyses: Deja vu all over again. *Science of The Total Environment*, 670, 138-148. doi:10.1016/j.scitotenv.2019.03.185
- Eggerichs, T., Opel, O., Otte, T., & Ruck, W. (2014). Interdependencies between Biotic and Abiotic Ferrous Iron Oxidation and Influence of pH, Oxygen and Ferric Iron Deposits. *Geomicrobiology Journal*, 31(6), 461-472. doi:10.1080/01490451.2013.870620
- Ellingsen, K. (1992). *Grunnvannskvalitet: Problemer og tiltak. GiN-veilder nr. 12* [Eng: Groundwater quality: Problems and preventiv measures. GiN guide no. 12. In Norwegian] (Skrifter 106). Trondheim: NGU.
- Ellingsen, K., & Finsrud, R. (1990). *Grunnvannsanlegg - eksempler. GiN-veileder nr. 5* [Eng: Groundwater works - examples. GiN-guide no. 5. In Norwegian] (Skrifter 101). Trondheim: NGU.
- Emerson, D., & Moyer, C. (1997). Isolation and characterization of novel iron-oxidizing bacteria that grow at circumneutral pH. *Appl Environ Microbiol*, 63(12), 4784-4792. doi:10.1128/aem.63.12.4784-4792.1997
- Farnsworth, C. E., & Hering, J. G. (2011). Inorganic Geochemistry and Redox Dynamics in Bank Filtration Settings. *Environ. Sci. Technol.*, 45(12), 5079-5087. doi:10.1021/es2001612
- Ford, H. W., & Tucker, D. P. H. (1975). Blockage of drip irrigation filters and emitters by iron-sulfur-bacterial products. *HortScience*, 10, 62-64. doi:10.21273/HORTSCI.10.1.62
- Frengstad, B., Banks, D., Skrede, Å. M., Krog, J.R., Siewers, U., Strand, T. (2002). The hydrochemistry of crystalline bedrock groundwater in Norway. *NGU Bulletin*, 439, 87-97.
- Frengstad, B., & Dagestad, A. (2008). Grunnvann i Norge - om å gå under bekken etter vann [Eng: Groundwater in Norway - a question of looking under the stream for water. In Norwegian]. In T. Slagstad & R. Dahl (Eds.), *Gråsteinen – Geologi for samfunnet i 150 år – arven etter Kjerulf* (pp. 134-141). Trondheim: NGU.
- Garrels, R. M., & Christ, C. L. (1965). *Solutions, minerals and equilibria* (2nd ed.). New York: Harper & Row.
- Gaut, S. (2011). *Beskyttelse av grunnvannsanlegg - en veileder* [Eng: Protection of groundwater works - guidelines. In Norwegian]. Trondheim: NGU.
- Ghiorse, W. C. (1984). Biology of iron- and manganese-depositing bacteria. *Annual Review of Microbiology*, 38(1), 515-550. doi:10.1146/annurev.mi.38.100184.002503
- Gjengedal, S. (2021). *Groundwater heat pump systems: New insights on design and on fluid flow in unconsolidated aquifers* (PhD thesis). Trondheim: NTNU.
- Gjengedal, S., Ramstad, R. K., Hilmo, B. O., & Frengstad, B. S. (2020). Fouling and clogging surveillance in open loop GSHP systems: A systematic procedure for fouling and clogging detection in the whole groundwater circuit. *Bulletin of Engineering Geology and the Environment*, 79(1), 69-82. doi:10.1007/s10064-019-01556-5
- Gjengedal, S., Stenvik, L. A., Ramstad, R. K., Ulfesnes, J. I., Hilmo, B. O., & Frengstad, B. S. (2021). Online remote-controlled and cost-effective fouling and clogging surveillance of a groundwater heat pump system. *Bulletin of Engineering Geology and the Environment*, 80, 1063–1072. doi:10.1007/s10064-020-01963-z
- Gjengedal, S., Stenvik, L. A., Storli, P.-T. S., Ramstad, R. K., Hilmo, B. O., & Frengstad, B. S. (2019). Design of Groundwater Heat Pump Systems. Principles, Tools, and Strategies for Controlling Gas and Precipitation Problems. *Energies*, 12(19), 3657. doi:10.3390/en12193657
- Hallberg, R. O., & Martinell, R. (1976). Vyredox — In Situ Purification of Ground Water. *Groundwater*, 14(2), 88-93. doi:10.1111/j.1745-6584.1976.tb03638.x
- Hanert, H. H. (2006). The Genus Gallionella. In M. Dworkin, S. Falkow, E. Rosenberg, K.-H. Schleifer, & E. Stackebrandt (Eds.), *The Prokaryotes: Volume 7: Proteobacteria: Delta, Epsilon Subclass* (pp. 990-995). New York: Springer. doi:10.1007/0-387-30747-8_46
- Haynes, W. M. (2016). *CRC Handbook of Chemistry and Physics* (97th Ed.). Boca Raton: CRC Press.
- Hellestveit, M. S. (2018). *3D-modellering av grunnvannstrømning og varmetransport i akviferen i Melhus sentrum - En kvartær- og hydrogeologisk tolkning, med vurdering av uttakskapasitet* [Eng: 3D modelling of groundwater flow and heat transport in the aquifer in Central Melhus. In Norwegian] (Master thesis). Trondheim: NTNU.

- Hilmo, B. O. (2007). *Undersøkelsesboringer ved Tjorputten – Oppsummering av resultater og forslag til videre arbeid* [Eng: Test drillings at Tjorputten. In Norwegian] (514555 – Nye brønner til Ringerike vannverk). Asplan Viak AS: Trondheim.
- Hilmo, B. O., & Gurigard, R. (2017). Rehabilitering av filterbrønner – erfaringer fra Norge [Eng: Rehabilitation of groundwater wells - experience from Norway. In Norwegian]. *Grundvattendagarna, November 7-8, 2017, Uppsala, Sweden*.
- Holmström, P., Rudolph-Lund, K., & Sørlic, J. E. (2010). *Korgen vannverk - Hydrogeologisk og vannkjemisk tilstandsvurdering av brønner* [Eng: Korgen waterwork - Hydrogeological and hydrochemical assessment of groundwater wells] (NGI report 20081232-00-1-R). Oslo: Norwegian Geotechnical Institute.
- Holmøy, S. (2020, May 18). *Nytt vannverk* [Eng: New water treatment facility. In Norwegian]. <https://www.lillehammer.kommune.no/nytt-vannverk.6223391-172351.html>
- Houben, G. (2003a). Iron oxide incrustations in wells. Part 1: genesis, mineralogy and geochemistry. *Applied Geochemistry*, 18(6), 927-939. doi:10.1016/S0883-2927(02)00242-1
- Houben, G. (2003b). Iron oxide incrustations in wells. Part 2: chemical dissolution and modeling. *Applied Geochemistry*, 18(6), 941-954. doi:10.1016/S0883-2927(02)00185-3
- Houben, G. (2004). Modeling the Buildup of Iron Oxide Encrustations in Wells. *Groundwater*, 42(1), 78-82. doi:10.1111/j.1745-6584.2004.tb02452.x
- Houben, G., & Sander, J. (2020). Preventing the growth of iron bacteria in water wells by copper and silver coating. *Water supply*, 20(4), 1195-1206. doi:10.2166/ws.2020.033
- Houben, G., & Treskatis, C. (2007). *Water well rehabilitation and reconstruction*. New York: McGraw-Hill.
- Houben, G. J. (2006). The Influence of Well Hydraulics on the Spatial Distribution of Well Incrustations. *Groundwater*, 44(5), 668-675. doi:10.1111/j.1745-6584.2006.00216.x
- Houben, G. J. (2015). Review: Hydraulics of water wells—head losses of individual components. *Hydrogeology Journal*, 23(8), 1659-1675. doi:10.1007/s10040-015-1313-7
- Huisman, L., & Olsthoorn, T. N. (1983). *Artificial Groundwater Recharge*. Ann Arbor: Pitman Advanced Pub. Program.
- Jacob, C. E. (1947). Drawdown Test to Determine Effective Radius of Artesian Well. *Transactions of the American Society of Civil Engineers*, 112(1), 1047-1064. doi:10.1061/TACEAT.0006033
- Kerner, J. (2011). Compact, high-efficiency heat exchangers: Understanding Fouling. *Chemical Engineering*, 118(6), 35-41.
- Kirkhusmo, L. A., & Sønsterud, R. (1988). *Overvåking av grunnvann. Landsomfattende grunnvannsnett (LGN)* [Eng: Groundwater monitoring. National groundwater monitoring network. In Norwegian] (NGU report 88.046). Trondheim: NGU.
- Kløve, B., Kvitsand, H. M. L., Pitkänen, T., Gunnarsdottir, M. J., Gaut, S., Gardarsson, S. M., Rossi, P. M., & Miettinen, I. (2017). Overview of groundwater sources and water-supply systems, and associated microbial pollution, in Finland, Norway and Iceland. *Hydrogeology Journal*, 25(4), 1033-1044. doi:10.1007/s10040-017-1552-x
- Krauskopf, K. B. (1979). *Introduction to geochemistry* (2nd ed.). New York: McGraw-Hill.
- Kruseman, G. P., Ridder, N. A. d., & Verweij, J. M. (1990). *Analysis and evaluation of pumping test data* (2nd ed.). Wageningen: International Institute for Land Reclamation and Improvement.
- Kvitsand, H. M. L., Myrmel, M., Fiksdal, L., & Østerhus, S. W. (2017). Evaluation of bank filtration as a pretreatment method for the provision of hygienically safe drinking water in Norway: results from monitoring at two full-scale sites. *Hydrogeology Journal*, 25(5), 1257-1269. doi:10.1007/s10040-017-1576-2
- Lerm, S., Alawi, M., Miethling-Graff, R., Wolfgramm, M., Rauppach, K., Seibt, A., & Würdemann, H. (2011). Influence of microbial processes on the operation of a cold store in a shallow aquifer: impact on well injectivity and filter lifetime. *Grundwasser*, 16(2), 93-104. doi:10.1007/s00767-011-0165-x
- Lile, A. (2006, January 12). Grumsete vann stengte Leiv Vidar [Eng: Turbid water shut down Leiv Vidar sausage factory. In Norwegian]. *Ringerikes Blad*. <https://www.ringblad.no/nyheter/grumsete-vann-stengte-leiv-vidar/s/1-97-1903261>

- Lindblad-Pässe, A. (1986). *Järnutfällningsproblem i grundvattenvärmesystem* [Eng: Iron incrustation problems in groundwater heating systems. In Swedish] (Report R109:1986). Stockholm: Statens råd för byggnadsforskning.
- Lüders, K., Firmbach, L., Ebert, M., Dahmke, A., Dietrich, P., & Köber, R. (2016). Gas-phase formation during thermal energy storage in near-surface aquifers: experimental and modelling results. *Environmental Earth Sciences*, 75(21), 1-28. doi:10.1007/s12665-016-6181-5
- Lütters-Czekalla, S. (1990). Lithoautotrophic growth of the iron bacterium *Gallionella ferruginea* with thiosulfate or sulfide as energy source. *Archives of Microbiology*, 154(5), 417-421. doi:10.1007/BF00245220
- Mackenzie, R. C. (1970). *Differential Thermal Analyses. Vol. 1: Fundamental Aspects*. Cambridge, US: Academic Press.
- McBeth, J. M., Fleming, E. J., & Emerson, D. (2013). The transition from freshwater to marine iron-oxidizing bacterial lineages along a salinity gradient on the Sheepscot River, Maine, USA. *Environmental Microbiology Reports*, 5(3), 453-463. doi:10.1111/1758-2229.12033
- McLaughlan, R. G. (1992). *Fouling and corrosion of Groundwater Wells in Australia* (PhD thesis). Kensington: University of New South Wales.
- McLaughlan, R. G. (2002). *Managing water well deterioration*. Leiden: Balkema.
- Middtømme, K., Henne, I., Kocbach, J., & Ramstad, R. (2016). Geothermal Energy Use, Country Update for Norway. *Proceedings of European Geothermal Congress 2016, September 19-24, 2016, Strasbourg, France* (pp. 1-10). European Geothermal Energy Council.
- Middtømme, K., Justo Alonso, M., Krafft, C., Kvalsvik, K., Ramstad, R., & Stene, J. (2020). Geothermal Energy Use in Norway, Country Update for 2015-2019. *Proceedings of the World Geothermal Congress 2020+1, October 24-27, 2021, Reykjavik, Iceland* (pp. 1-10). International Geothermal Association.
- Morgan, J. J. (1967). Chemical equilibria and kinetic properties of manganese in natural waters. In S. D. Faust & J. V. Hunter (Eds.), *Principles and Applications of Water Chemistry* (pp. 561-624). Hoboken: Wiley.
- Müller-Steinhagen, H. (2010). C4 Fouling of Heat Exchanger Surfaces. In VDI-Gesellschaft Verfahrenstechnik und Chemieingenieurwesen (Ed.), *VDI Heat Atlas* (2nd ed., pp. 79-104). Berlin: Springer-Verlag. doi:10.1007/978-3-540-77877-6_7
- NGU. (2020, November 5). *Ground sourced energy*. <https://www.ngu.no/en/topic/ground-sourced-energy>
- Norwegian Food Safety Authority. (2021, March 22). *Vannforsyningssystemer til lands* [Eng: Onshore water distribution systems. In Norwegian]. https://www.mattilsynet.no/mat_og_vann/drikkevann/opplysninger_om_vannforsyningssystemer/vannforsyningssystemer_til_lands.36094
- Novak, L. (1981). Fouling in plate heat exchangers and its reduction by proper design. In J. Taborek, G. F. Hewitt, N. Afgan (Eds.), *Advanced Course in Heat Exchangers: Theory and Practice. Proceedings of the 14th ICHMT Symposium on Advances in Heat Exchangers, September 7-12, 1981, Dubrovnik, Yugoslavia* (pp. 871-883). International Centre for Heat and Mass Transfer.
- Novak, L. (1982). Comparison of the Rhine River and the Oresund Sea Water Fouling and Its Removal by Chlorination. *Journal of Heat Transfer*, 104(4), 663-669. doi:10.1115/1.3245183
- Oldmeadow, E., & Marinova, D. (2011). Into geothermal solutions: The sustainability case for Challenge Stadium in Perth, Western Australia. *Environmental Progress & Sustainable Energy*, 30(3), 476-485. doi:10.1002/ep.10476
- Olsthoorn, T. N. (1982). *The clogging rate of recharge wells, main subjects* (KIWA-communications 72). Rijswijk: KIWA.
- Opel, O., Eggerichs, T., Otte, T., & Ruck, W. K. L. (2014). Monitoring of microbially mediated corrosion and scaling processes using redox potential measurements. *Bioelectrochemistry*, 97, 137-144. doi:10.1016/j.bioelechem.2013.11.004
- Oren, O., Gavrieli, I., Burg, A., Guttman, J., & Lazar, B. (2007). Manganese Mobilization and Enrichment during Soil Aquifer Treatment (SAT) of Effluents, the Dan Region Sewage Reclamation Project (Shafdan), Israel. *Environ. Sci. Technol*, 41(3), 766-772. doi:10.1021/es060576+

- Parkhurst, D. L., & Appelo, C. A. J. (2013). *Description of input and examples for PHREEQC version 3—a computer program for speciation, batch-reaction, one-dimensional transport, and inverse geochemical calculations*. Virginia: U.S. Geological Survey.
- Possemiers, M., Huysmans, M., Anibas, C., Batelaan, O., & Steenwinkel, J. (2016). Reactive transport modeling of redox processes to assess Fe(OH)₃ precipitation around aquifer thermal energy storage wells in phreatic aquifers. *Environmental Earth Sciences*, 75:648, 1-17. doi:10.1007/s12665-016-5398-7
- Ramos, E. P., Breede, K., & Falcone, G. (2015). Geothermal heat recovery from abandoned mines: a systematic review of projects implemented worldwide and a methodology for screening new projects. *Environmental Earth Sciences*, 73(11), 6783-6795. doi:10.1007/s12665-015-4285-y
- Ramstad, R. K., Gjengedal, S., Frengstad, B. S., Hilmo, B. O., Riise, M. H., & Holmberg, H. (2020). Groundwater for Heating and Cooling in Melhus and Elverum in Norway – Highlights from the ORMEL-Project with Focus on Infiltration Wells. *Proceedings of the World Geothermal Congress 2020+1, October 24-27, 2021, Reykjavik, Iceland* (pp. 1-7). International Geothermal Association.
- Ramstad, R. K., & Stenvik, L. A. (2020). Norwegian projects and results - Lena terrasse, Melhus. *HPT Annex 52 Short Digital Meeting Series, October 9-December 11 2020* [online]. International Energy Agency – Heat Pumping Technologies.
- Regulation on organic fertilizers. (2003). *Forskrift om gjødselever mv. av organisk opphav* [Eng: Regulation on fertilizers etc. of organic origin] (FOR-2003-07-04-951). Lovdata. <https://lovdata.no/dokument/SF/forskrift/2003-07-04-951>
- Reite, A. J. (1990). *Sør-Trøndelag fylke: kvartærgeologisk kart M 1:250.000 : veiledning til kartet* [Eng: Sør-Trøndelag County: Guide to the Quaternary geological map. In Norwegian] (Skrifter 96). Trondheim: NGU.
- Reite, A. J., Sveian, H., & Eriksen, E. (1999). *Trondheim fra istid til nåtid - landskapshistorie og løsmasser* [Eng: Trondheim from ice age to present - landscape morphology and quaternary geology. In Norwegian] (Gråsteinen 5). Trondheim: NGU.
- Riise, M. H. (2015). *Praktisk guide for grunnvarmeanlegg basert på oppumpet grunnvann* [Eng: Practical Guide for Ground Water Heat Pump Systems] (Master thesis). Trondheim: NTNU.
- Rike, A. G. (2011). *Geovarmeanlegg Oslo lufthavn Gardermoen: Metagenom analyse av bakteriebelegg på pumper og injeksjonsrør* [Eng: Groundwater heat pump system, Oslo airport Gardermoen: Metagenomic analysis of bacteria incrusting pumps and injection pipes] (NGI report 20100413-00-2-R). Oslo: Norwegian Geotechnical Institute.
- Sander, R. (2015). Compilation of Henry's law constants (version 4.0) for water as solvent. *Atmospheric chemistry and physics*, 15(8), 4399-4981. doi:10.5194/acp-15-4399-2015
- Schwertmann, U., & Murad, E. (1983). Effect of pH on the Formation of Goethite and Hematite from Ferrihydrite. *Clays and Clay Minerals*, 31(4), 277-284. doi:10.1346/CCMN.1983.0310405
- Skøien, S. (2000). *Jordlære : teknisk fagskole, linje for naturbruk : fordypningsområde plantedyrking* [Eng: Soil science: technical college, specialization on plant cultivation]. Oslo: GAN.
- Smedley, P. L., & Kinniburgh, D. G. (2002). A review of the source, behaviour and distribution of arsenic in natural waters. *Applied Geochemistry*, 17(5), 517-568. doi:10.1016/s0883-2927(02)00018-5
- Sniegocki, R. T., & Reed, J. E. (1963). *Principles of siphons with respect to the artificial recharge studies in the Grand Prairie region, Arkansas* (Geological Survey Water Supply Paper 1615-D). Washington D.C.: US Government Printing Office.
- Snijders, A. L., & Drijver, B. C. (2016). Open-loop heat pump and thermal energy storage systems. In S. Rees (Ed.), *Advances in Ground-Source Heat Pump Systems* (pp. 247-268). Sawston: Woodhead Publishing. doi:10.1016/B978-0-08-100311-4.00009-1
- Solberg, I.-L., Dagestad, A., & Dalsegg, E. (2014). *2D resistivitetsmålinger ved Brubakken, Melhus sentrum og Skjerdingsstad i Melhus kommun, Sør-Trøndelag. Data og tolkninger* [Eng: 2D resistivity measurements at Brubakken, Melhus town center and Skjerdingsstad in Melhus municipality. Data and interpretations. In Norwegian] (NGU report 2014.022). Trondheim: NGU
- Statistics Norway. (2022). *Population*. Retrieved 1 November 2022 from <https://www.ssb.no/en/befolkning>

- Stene, J. (2001). *Varmepumper : grunnleggende varmepumpeteknikk [Eng: Heat pumps: basics. In Norwegian]* (Report STF84 A97302). Trondheim: SINTEF Energiforskning AS.
- Stenvik, L. A. (2020). Utfellingsproblemer med jern og mangan i norske drikkevannsbrønner [Eng: Iron and manganese incrustations in Norwegian groundwater works. In Norwegian]. *Kommunalteknikk*, 113(4), 44-45.
- Stenvik, L. A. (2022). Laboratorietesting av en kjemikalie som reduserer og løser opp jernoksidutfellinger. Vurdering av anvendbarhet til rensing av grunnvannsbrønner [Eng: Laboratory testing of a chemical which reduces and dissolves iron oxide incrustations. Assessment of applicability to well rehabilitations]. *Vann*, 57(3), 175-184.
- Stenvik, L. A., Gjengedal, S., Ramstad, R. K., & Frengstad, B. S. (2022a). How to avoid gas clogging in groundwater heat pump systems: a case study from the Lena terrasse system in Melhus, Norway. *Bulletin of Engineering Geology and the Environment*, 81(4), 152. doi:10.1007/s10064-022-02652-9
- Stenvik, L. A., Gjengedal, S., Ramstad, R. K., & Frengstad, B. S. (2022b). Hydrochemical and biotic control on iron incrustations in groundwater heat pump systems: Case study from a saline, anoxic aquifer in Melhus, Norway. *Geothermics*, 100, 102349. doi:10.1016/j.geothermics.2022.102349
- Stenvik, L. A., & Hilmo, B. O. (2020). Jern- og manganproblematikk ved grunnvannsutttak med eksempler fra Ringerike og Sunndal vannverk. *Vann*, 55(2), 151-161.
- Stenvik, L. A., Hilmo, B. O., & Frengstad, B. S. (2022c). Elevated manganese concentrations in groundwater wells after longtime abstraction with bank filtration. *Hydrogeology Journal*, 30, 2059-2071. doi:10.1007/s10040-022-02538-w
- Stenvik, L. A., Ramstad, R. K., & Frengstad, B. S. (2022d). Optimizing Submersible Pump Regulation of a Clogging Prone Groundwater Heat Pump System in Melhus, Norway. *Science and Technology for the Built Environment*. doi:10.1080/23744731.2022.2136901
- Storrø, G. (2000). *Grunnvannsundersøkelser i tilknytning til planlagte energibrønner i Lena-området, Melhus sentrum* [Eng: Groundwater investigations ground sourced energy utilization in the Lena area of Melhus town center. In Norwegian] (Report 2000.069). Trondheim: NGU.
- Stuetz, R., & McLaughlan, R. (2004). Impact of localised dissolved iron concentrations on the biofouling of environmental wells. *49(2)*, 107-113. doi:10.2166/wst.2004.0100
- Stumm, W., & Lee, G. F. (1961). Oxygenation of Ferrous Iron. *Industrial & Engineering Chemistry*, 53(2), 143-146. doi:10.1021/ie50614a030
- Stumm, W., & Morgan, J. J. (1996). *Aquatic chemistry : chemical equilibria and rates in natural waters* (3rd ed.). Hoboken: Wiley.
- Stuyfzand, P. (2007). Naar een effectievere diagnose, therapie en preventie van chemische put- en drainverstopping [Eng: Towards a more effective diagnosis, therapy and prevention of chemical clogging of wells and drains. In Dutch]. *H2O*, 8, 44-47.
- Sung, W., & Morgan, J. J. (1980). Kinetics and Product of Ferrous Iron Oxygenation in Aqueous Systems. *Environmental Science and Technology*, 14(5), 561-568. doi:10.1021/es60165a006
- Søgaard, E. G., Medenwaldt, R., & Abraham-Peskir, J. V. (2000). Conditions and rates of biotic and abiotic iron precipitation in selected Danish freshwater plants and microscopic analysis of precipitate morphology. *Water Research*, 34(10), 2675-2682. doi:10.1016/S0043-1354(00)00002-6
- Tamura, H., Goto, K., & Nagayama, M. (1976). The effect of ferric hydroxide on the oxygenation of ferrous ions in neutral solutions. *Corrosion Science*, 16(4), 197-207. doi:10.1016/0010-938X(76)90046-9
- Tassis, G., Gellein, J., & Rønning, J. S. (2016). *Depth to bedrock and bedrock morphology from gravity measurements at Melhus, Melhus Municipality, Sør-Trøndelag* (NGU report 2016.011). Trondheim: NGU.
- United Nations. (2022). *The United Nations World Water Development Report 2022: groundwater: making the invisible visible*. Paris: UNESCO.
- van Beek, C. G. E. M. (1989). Rehabilitation of clogged discharge wells in the Netherlands. *Quarterly journal of engineering geology and hydrogeology*, 22(1), 75-80. doi:10.1144/GSL.QJEG.1989.022.01.06

- van Beek, C. G. E. M., Breedveld, R., & Stuyfzand, P. (2009a). Preventing two types of well clogging. *Journal - American Water Works Association*, 101(4), 125-134. doi:10.1002/j.1551-8833.2009.tb09880.x
- van Beek, C. G. E. M., Breedveld, R. J. M., Juhász-Holterman, M., Oosterhof, A., & Stuyfzand, P. J. (2009b). Cause and prevention of well bore clogging by particles. *Hydrogeology Journal*, 17(8), 1877-1886. doi:10.1007/s10040-009-0537-9
- van Beek, C. G. E. M., Cirkel, D. G., de Jonge, M. J., & Hartog, N. (2021). Concentration of Iron(II) in Fresh Groundwater Controlled by Siderite, Field Evidence. *Aquatic Geochemistry*. doi:10.1007/s10498-020-09390-y
- van Beek, C. G. E. M., & Kooper, W. F. (1980). The Clogging of Shallow Discharge Wells in the Netherlands River Region. *Groundwater*, 18(6), 578-586. doi:10.1111/j.1745-6584.1980.tb03652.x
- Vestland, M. (2010). *Sunnaldsøra groundwater works: Water quality assessments* (Master thesis). Trondheim: NTNU.
- Vestland, M. (2012). *Klausuleringsplan for Ringerike vannverk Kilemoen* [Eng: New wells at Ringerike waterwork Kilemoen] (529119 – Hydrogeologisk rådgivning - Ringerike vannverk). Trondheim: Asplan Viak AS.
- Von Hofe, F., & Helweg, O. J. (1998). Modeling Well Hydrodynamics. *Journal of Hydraulic Engineering*, 124(12), 1198-1202. doi:10.1061/(ASCE)0733-9429(1998)124:12(1198)
- von Langen, P. J., Johnson, K. S., Coale, K. H., & Elrod, V. A. (1997). Oxidation kinetics of manganese (II) in seawater at nanomolar concentrations. *Geochimica et Cosmochimica Acta*, 61(23), 4945-4954. doi:10.1016/S0016-7037(97)00355-4
- Vorren, T. O., & Mangerud, J. (2006). Istider kommer og går. Pleistocen; 2,6 millioner - 11 700 år. [Eng: Ice ages come and go. Pleistocene; 2.6 mill- 11,700 years BP. In Norwegian]. In I. B. Ramberg, I. Bryhni, & A. Nøttvedt (Eds.), *Landet blir til : Norges geologi [Eng: The making of a land : Geology of Norway]*. Trondheim: Norsk geologisk forening.
- Walter, D. A. (1997). *Geochemistry and microbiology of iron-related well-screen encrustation and aquifer biofouling in Suffolk County, Long Island, New York* (Water-Resources Investigations Report 97-4032). Coram: U. S. Geological Survey. doi:10.3133/wri974032
- Weidner, C., Henkel, S., Lorke, S., Råde, T. R., Schüttrumpf, H., & Klauder, W. (2012). Experimental Modelling of Chemical Clogging Processes in Dewatering Wells. *Mine Water and the Environment*, 31(4), 242-251. doi:10.1007/s10230-012-0188-2
- Wolfgramm, M., Rauppach, K., & Puronpää-Schäfer, P. (2010). Berliner Parlamentsbauten – Betrieb, Monitoring und Regenerierungen N2-beaufschlagter Kältespeicherbrunnen [Eng: Geothermal energy storage system at the Parliament buildings in Berlin-Operation, monitoring and rehabilitation of N2-charged groundwater wells. In German]. *EnergieWasserPraxis*, 61(10), 38-45.
- Wood, D. E., & Salzberg, S. L. (2014). Kraken: ultrafast metagenomic sequence classification using exact alignments. *Genome Biol*, 15(3): R46. doi:10.1186/gb-2014-15-3-r46
- Woyessa, A. O. (2012). *Identification of hydrochemical processes in the screen environment in shallow geothermal wells from Gardermoen* (Master thesis). Oslo: University of Oslo.
- Waade, A. (2022). *Sustainability and degradation of chemical deicers in the Gardermoen Aquifer : Iron and manganese redox processes* (Master thesis). Oslo: University of Oslo.
- Zeppenfeld, K. (2005). Untersuchungen über den Einfluss der Strömungsgeschwindigkeit auf die Kalkabscheidung aus calciumhaltigen Wässern [Eng: Studies of the effect of the flow velocity on calcium carbonate precipitation from water containing calcium. In German]. *vom Wasser*, 103(2), 11-19.
- Zhang, J., Lion, L. W., Nelson, Y. M., Shuler, M. L., & Ghiorse, W. C. (2002). Kinetics of Mn(II) oxidation by *Leptothrix discophora* SS1. *Geochimica et Cosmochimica Acta*, 66(5), 773-781. doi:10.1016/S0016-7037(01)00808-0
- Zukoski, E. E. (1966). Influence of viscosity, surface tension, and inclination angle on motion of long bubbles in closed tubes. *J. Fluid Mech*, 25(4), 821-837. doi:10.1017/S0022112066000442

Appendices

Appendix A – Other written and oral scientific contributions

Appendix B – Sources of and measures to reduce uncertainty in data collection

Appendix C – Camera inspections performed in GWHP systems in Melhus

Appendix D – PHREEQC script: Degassing simulation for Lena terrasse's GWHP system

Appendix A – Other written and oral scientific contributions

Other written (professional journal and conference articles) and oral (conference and seminar talks) scientific contributions during employment at NTNU are listed below.

Professional journal articles (not peer reviewed)

- 1) Utfellingsproblemer med jern og mangan i norske drikkevannsbrønner [Eng: A questionnaire on iron and manganese incrustation issues and handling in Norwegian groundwater works. In Norwegian]

Stenvik, L. A.

In *Kommunalteknikk*, (4), 2020. Link: https://issuu.com/kommunalteknikk/docs/6kt_4-20/s/11415728

- 2) Gruveforurensning i det iberiske pyrittbeltet og Norge – et sammenlignende reisebrev [Eng: Acid mine drainage in the Iberian Pyrite Belt and Norway – a comparative travel letter. In Norwegian]

Submitted to *Mineralproduksjon* (in review)

Conference articles (peer reviewed)

- 3) Test of Differential Monitoring of Stability (DMS) Borehole Temperature Data to Map Groundwater Flow in the Unstable Rock Mass at Åknes, Norway

Stenvik, L. A.; Ramstad, R. K.; Kristensen, L.

In *ISRM International Symposium - EUROCK 2020*, physical event not held. Link: <https://onepetro.org/ISRMEUROCK/proceedings/EUROCK20/All-EUROCK20/ISRM-EUROCK-2020-192/447416>

- 4) Diagnosing Encrustation Problems in Open-loop Groundwater Heat Pump Systems in Melhus, Norway

Stenvik, L. A., Frengstad, B. S., Gjengedal, S., & Ramstad, R. K.

In *World Geothermal Congress 2020+1*, 1 March-27 October 2021, Reykjavik, Iceland [online]. Link: https://www.lovegeothermal.org/cpdb/record_detail.php?id=34363

- 5) CO₂-Enhanced Geothermal Systems for Climate Neutral Energy Supply

Sowizdział, Anna; Gładysz, Paweł; Andresen, Trond; Miecznik, Maciej; Frengstad, Bjørn S.; Liszka, Marcin; Chmielowska, Anna; Gawron, Marcel; Løvseth, Sigurd W.; Pająk, Leszek; Stenvik, Lars A.; Tomaszewska, Barbara

In *TCCS-11 – The 11th Trondheim Conference on CO₂ Capture, Transport and Storage*, 21-23 June 2021, Trondheim, Norway. Link: <https://sintef.brage.unit.no/sintef-xmlui/handle/11250/2786085>

- 6) EnerGizerS - Enhanced Geothermal Systems (EGS) using supercritical carbon dioxide as a working medium in Polish and Norwegian conditions

Sowizdział, Anna; Andresen, Trond; Miecznik, Maciej; Frengstad, Bjørn S.; Liszka, Marcin; Gładysz, Paweł; Pająk, Leszek; Chmielowska, Anna; Tomaszewska, Barbara; Løvseth, Sigurd W.; Stenvik, Lars A.; Gawron, Marcel

In *EGC 2022 – European geothermal congress 2022*, 17-21 October 2022, Berlin, Germany. Link: <https://europeangeothermalcongress.eu/abstracts-paper/>

Conference presentations

1) ORMEL 2 – Iron and manganese in ATEs systems

Vinterkonferansen 2019 [Eng: National geological winter conference 2019], 7-9 January 2019 in Bergen, Norway (oral presentation). Abstract: <https://www.geologi.no/konferanser/vinterkonferanser/arkiv/item/984-abstract-vk19>

2) Iron and manganese encrustations in groundwater source heat pump systems

Young Trondhjemites 2019, 22 March 2019, Trondheim, Norway (oral presentation, awarded “Best student presentation”)

3) Application of a flow-through cell to monitor groundwater source heat pump systems in Melhus, Norway

46th International Association of Hydrogeologists (IAH) congress: Groundwater management and governance, 22-29 September 2019 in Málaga, Spain (oral presentation). Abstract: <http://www.iah2019.org/>

4) Elevated concentrations of manganese in some Norwegian groundwater waterworks: a possible explanation

34th Nordic Geological Winter Meeting, 8-10 January 2020 in Oslo, Norway (oral presentation). Abstract: https://geologi.no/images/NGWM20/Abstractvolume_NGWM20.pdf

5) Incrustation monitoring and rehabilitation in Norwegian groundwater works

Vinterkonferansen 2021 [Eng: National geological winter conference 2021], 6-8 January 2021 online (digital oral presentation). Abstract: <https://www.geologi.no/konferanser/vinterkonferanser/item/1108-abstractsvk21>

6) Diagnosing Encrustation Problems in Open-loop Groundwater Heat Pump Systems in Melhus, Norway

World Geothermal Congress 2020+1, March-October 2021 in Reykjavik, Iceland/online (digital oral presentation). Abstract: https://www.lovegeothermal.org/cpdb/record_detail.php?id=34363

7) Biotic Control of Well Incrustations In Groundwater Heat Pump Systems In Melhus, Norway

48th IAH congress: Inspiring Groundwater, 6-10 September 2021 in Brussels, Belgium (oral presentation). Abstract: <https://iah2021belgium.org/programme/abstracts/>

Seminar talks

8) Groundwater as an energy resource: Principles and challenges

1st NTNU Young Researcher Clean Energy Symposium, 8 February 2019 in Trondheim, Norway (oral presentation).

9) «Pumping iron»- fra Gold's Gym, Venice Beach til Melhus, Norge [Eng: «Pumping iron» - from Gold's Gym, Venice Beach to Melhus, Norway. In Norwegian].

IAH-Norway's autumn meeting: Det utfordrende grunnvannet [Eng: Challenging groundwater], 14 November, 2019 in Sandvika, Norway (oral presentation). Presentation: <https://www.ngu.no/nyheter/det-utfordrende-grunnvannet>

10) Lena terrasse, Norway: Long-term performance of GSHP systems for commercial, institutional and multi-family buildings

International Energy Agency Heat Pumping Technologies (IEA HPT) Annex 52 – digital meeting series: Norwegian projects and results, 20 November 2020 online (oral presentation). Program: <https://heatpumpingtechnologies.org/annex52/activities/start-of-hpt-annex-52-short-digital-meeting-series/>

11) Jernutfellinger og brønnrensing [Eng: Iron incrustations and well cleaning, In Norwegian]

Optimal ressursutnyttelse av grunnvann til varme og kjøling i Melhus og Elverum [Eng: Optimized resource utilization of groundwater for heating and cooling in Melhus and Elverum] (ORMEL & ORMEL 2) seminar, 11 November 2021 Trondheim, Norway (oral presentation). Program: <https://www.ngu.no/aktiviteter/seminar-om-grunnvann-til-oppvarming-og-kjoling>

12) Gjentetting av åpne grunnvarmesystemer: Erfaringer fra Melhus, Trøndelag [Eng: Clogging of open-loop ground source heat pump systems: Experience from Melhus, Trøndelag. In Norwegian]

Norconsult's Hydrogeology group meeting at Oscarsborg Fortress, 31 July-1 June 2022 in Drøbak, Norway (oral presentation)

13) Agua subterránea para calefacción y refrigeración: Ventajas y retos [Eng: Groundwater for heating and cooling: Advantages and challenges. In Spanish]

Course 757709311 – Hydrogeology, University of Huelva (guest lecture), 19 October 2022 in Huelva, Spain (oral presentation)

Appendix B – Sources of and measures to reduce uncertainty in data collection

There has been many sources of uncertainty during sampling and analysis of water quality, incrustations and hydraulic/thermal parameters. The most important ones are given below, in addition to measures to reduce their impact on the results.

Hydrochemistry – calibration

The field parameter sensors were calibrated according to the manufacturer’s recommendations. The pH sensor was calibrated with three buffers (pH = 4.0, 7.0, 10.0) at the start of each day of field measurement. The DO sensor’s zero point was calibrated annually with a solution continuously bubbled with N₂ gas for 15 minutes. The 100% DO point was calibrated with a moist sponge. Calibration of the Eh and EC sensors was not advised, and followingly not carried out.

Hydrochemistry – ICP-MS instrument quality control

The influence of changing ICP-MS instrument in February 2020 was assessed by plotting concentration of chloride, sulfate, sodium and iron vs analytical sequence (i.e., date of sampling) (1) and box plots of the same element concentrations vs instrument (2), see Figure A.1. The procedure was inspired by Eggen et al. (2019), and demonstrated that the change of instrument appeared to have limited influence on the results.

Hydrochemistry – incrustation influence on water sampling before/after the heat exchanger

The water samples from the GWHP systems in Melhus were taken both before and after the heat exchanger, depending on where the different systems had installed a water tap. The comparability of water samples taken before vs after the heat exchanger could be hampered by heat exchanger incrustations. Especially, iron concentrations may differ since it is the most abundant element in the incrustations. Lena terrasse’s GWHP has suffered severe clogging from iron incrustations, and has been water sampled from a tap installed after the heat exchanger. This GWHP system will therefore serve as a “worst case scenario” for assessing whether the incrustation induced error in the water sample analyses were acceptably low or not.

Data on the amount of removed incrustations (F_{incrust}) during two heat exchanger rehabilitations (09.10.2019, 21.01.2021) has been collected, plus average pumping rate (Q) and dissolved iron concentrations [Fe^{2+}] from the periods (t_{incrust}) in between and before the first rehabilitation, see Table A.1. Combined, they allow the calculation of the error in dissolved iron concentrations induced by encrustation in the heat exchanger (HE):

$$\text{Error}_{\text{HE}}(\%) = \frac{F_{\text{incrust}}/t_{\text{incrust}}}{Q \cdot [\text{Fe}^{2+}]} \cdot 100\% \quad (\text{A.1})$$

Table A.1: Error in dissolved Fe^{2+} concentrations measured after heat exchanger compared with aquifer concentrations, due to heat exchanger encrustation at Lena terrasse’s GWHP system.

Heat exchanger cleaning		Last cleaning	GWHP operation			Error _{HE}
Date	Fe _{incrust} (g)	Date	t _{incrust} (days)	Q (L/s)	Fe ²⁺ (mg/L)	
09.10.2019	308	01.10.2018 ^a	373	11.1 ^b	3.54 ^b	0.02 %
21.01.2021	673	09.10.2019	470	9.1 ^b	3.51 ^b	0.05 %

^{a)} New heat exchanger installed

^{b)} Average in the actual period

The data in Table A.1 indicate that the induced Error_{HE} is negligible at Lena terrasse. Since Lena terrasse is believed to serve as the “worst case scenario”, water samples taken before/after the heat exchanger are deemed comparable. Also, some GWHP systems which have water taps installed both before and after the heat exchanger (Buen, Gimse) have demonstrated minimal difference in water samples taken before vs after the heat exchanger, to further back up the conclusion.

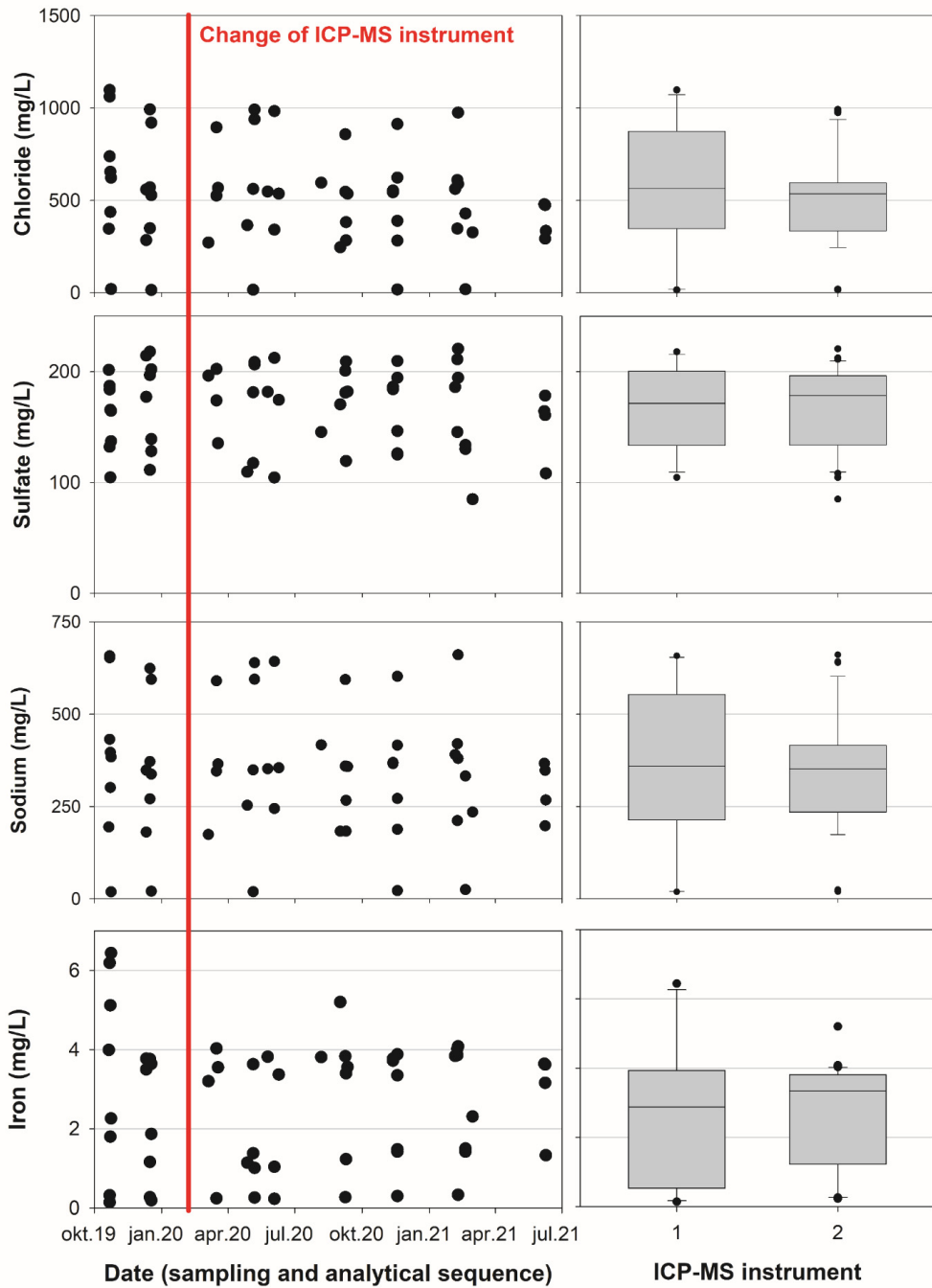


Figure A.1: Quality control of hydrochemistry data from two different ICP-MS instruments: 1 ($n = 16$) and 2 ($n = 39$).

Appendix C – Camera inspections performed in GWHP systems in Melhus

Table A.2: Camera inspections carried out in GWHP system wells in Melhus between 2013 and 2021. All inspections were performed by Gjøvaag AS. “Def.” refers to a well no longer in operation. “-” means same well type today as during inspection.

Date	GWHP	During inspection	Well type
			Today ^a
28.08.2013	Lena terrasse	Production well	Injection well
28.08.2013	Lena terrasse	Injection well (Def.)	-
10.12.2015	Lenavegen 3	Production well (Def.)	-
11.11.2016	Høvdingen	Injection well 1	Injection well 1 (Def.)
11.11.2016	Oterholmgården	Injection well	-
14.11.2016	Thoragården	Production well	-
25.09.2017	Gimse	Production well	-
25.09.2017	Oterholmgården	Injection well	-
18.10.2017	Oterholmgården	Injection well	-
18.10.2017	Thoragården	Injection well (Def.)	-
09.11.2017	Oterholmgården	Injection well	-
15.01.2018	Idegården	Injection well	-
05.02.2018	Buen sykehjem	Production well	Production well (Def.)
05.02.2018	Buen sykehjem	Injection well 1	-
05.02.2018	Buen sykehjem	Injection well 2	Injection well 2 (Def.)
13.02.2018	Idegården	Injection well	-
15.02.2018	Buen sykehjem	Injection well 2	Injection well 2 (Def.)
22.02.2018	Buen sykehjem	Production well	Production well (Def.)
22.02.2018	Buen sykehjem	Injection well 1	-
22.02.2018	Buen sykehjem	Injection well 2	Injection well 2 (Def.)
28.02.2018	Lena terrasse	Injection well	-
02.03.2018	Lena terrasse	Injection well	-
09.05.2018	Idegården	Injection well	-
24.10.2018	Lena terrasse	Injection well	-
14.11.2018	Oterholmgården	Injection well	-
18.01.2019	Thoragården	Injection well 2	-
24.07.2019	Lena terrasse	Injection well	-
11.11.2019	Lenavegen 3	Production well (Def.)	-
20.03.2020	Lena terrasse	Injection well	-
13.05.2020	Lena terrasse	Injection well	-
20.10.2020	Høvdingen	Injection well 2	Injection well 2 (Def.)
14.06.2021	Lena terrasse	Injection well	-
15.12.2021	Lena terrasse	Injection well	-

^{a)} As per December 2021

Appendix D – PHREEQC script: Degassing simulation for Lena terrasse's GWHP system

SOLUTION 1

-units mg/L

-pressure 1.05

Ca 132.30

Cl 280.51

Fe 3.42 pe

Alkalinity 329.5 as HCO3

K 10.48

Mg 24.94

Mn 0.64 pe

Na 179.44

S 180 pe

TEMP 4.6

O(0) 0.05

ph 7.35 CO2(g) -1.84 #-1.94 (pco2 = 0.0115; ptot = 1 atm), -1,84 (pco2 = 0.0146; ptot = 1.41 atm)

pe 2.44

Ntg 1 Ntg(g) 0.15 10 #-0.01 (pN2 = 0.9772; ptot = 1 atm), 0.15 (pN2 = 1.4; ptot = 1.41 atm)

Oxg 1 Oxg(g) -99 10 #-1.91 (pO2 = 0.0123; ptot = 1 atm), - (p02 = 0; ptot = 1.41 atm)

END

GAS_PHASE 1 Fixed-pressure gas phase

-fixed_pressure

-temperature 4.6

-volume 1 #Vg / Vw = 0 for initially water-filled pipes, Vg / Vw = 1 for 50/50% water-/gas-filled pipes initially

CO2(g) 0.0146

Ntg(g) 1.4

Oxg(g) 0.0

END

USE solution 1

USE gas_phase 1

REACTION_PRESSURE

0.1 1.4 in 27 steps

SELECTED_OUTPUT

-file gas_1dot41atm_50%gasfilled.xls

-ph

-gas CO2(g) Ntg(g) OXg(g)

-si CO2(g) Ntg(g) OXg(g)

USER_GRAPH 1

-headings pressure pH CO2(g) Ntg(g) OXg(g) Volume_gas

-axis_titles "Pipe pressure (atm)" "Partial pressure (atm), Gas volume (litres per litre water)"
"pH"

-axis_scale y_axis 0.00001 100 auto auto log

-axis_scale sy_axis 7.3 7.37 0.01 0.01

-axis_scale x_axis 0.0 1.2 0.2 0

-initial_solutions false

-connect_simulations true

-plot_concentration_vs x

-start

10 GRAPH_X pressure

20 GRAPH_SY -LA("H+")

30 moles = (GAS("CO2(g)") + GAS("Ntg(g)") + GAS("OXg(g)"))

40 vol = gas_vm * moles

50 GRAPH_Y PR_P("CO2(g)", PR_P("Ntg(g)", PR_P("OXg(g)", vol

-end

-active true

END

Paper I

Jern- og manganproblematikk ved grunnvannsuttak med eksempler fra Ringerike og Sunndal vannverk

Av Lars Aaberg Stenvik og Bernt Olav Hilmo

Lars Aaberg Stenvik er stipendiat ved Institutt for geovitenskap og petroleum, NTNU.

Bernt Olav Hilmo er dr.ing. og hydrogeolog i Asplan Viak AS.

Summary

Iron and manganese in groundwaterworks – review of problems and case studies from Ringerike and Sunndal. Iron and manganese are redox sensitive elements that precipitate as (hydr)oxides in oxic and dissolve in anoxic environments respectively. These elements represent risks in groundwater extraction due to precipitation and clogging in the wells and pipelines, and coloring and bad taste of the drinking water. Iron precipitation is generally a larger problem than manganese precipitation, as manganese is less abundant and has slower oxidation kinetics. Sunndal waterworks have for a long time experienced problems with iron incrustations. Mechanical rehabilitations have been unsuccessful to remove all incrustations and fully restore the well capacities. The lack of success can be explained by maturing of iron (hydr)oxides to harder and less soluble minerals with time. Rehabilitation should thus be carried out early, possibly combined with chemical additives increasing the oxide solubility. Ringerike waterworks have experienced an increase in manganese concentrations after 19 years of operation. Problems with high concentrations of manganese with time can be explained by slow oxidation rates and sorption retarding the manganese transport. Redox parameters and specific yield should be measured regularly to reveal problem (type).

Sammendrag

Jern og mangan er redoks-sensitive elementer som oksideres og felles ut som (hydr)oksider i oksygenrikt miljø, og reduseres og løses i vann ved oksygenfattige forhold. Høye elementkonsentrasjoner ved grunnvannsuttak gir problemer med utfellinger som tetter brønnfiltre og ledningsnett, samt uønsket farge og smak på drikkevannet. Utfelling av jern gir vanligvis større driftsproblemer enn utfelling av mangan, grunnet større tilgjengelighet i naturmiljøet og raskere utfellingskinetikk, mens mangan representerer en større utfordring i vannbehandlingsammenheng. Sunndal vannverk har hatt store utfordringer med høyt innhold av jern og jernutfellinger siden etableringen. Brønnrehabiliteringer har ikke klart å gjenopprette kapasiteten, noe som kan skyldes modning av utfellingene til mindre løselige jernminerale over tid. Rehabiliteringer, eventuelt inkludert kjemiske metoder for å øke løseligheten, bør derfor gjennomføres på et tidlig stadie. Problem med høye konsentrasjoner av mangan etter lengre tid kan skyldes treg utfellingskinetikk og sorpsjon som sinker mangantransporten i grunnvannsmagasinet. Dette kan forklare forhøyede mangankonsentrasjoner etter 19 års drift ved Ringerike vannverk. For å avdekke problem(type) bør redoksparametere og spesifikk brønncapacitet måles jevnlig.

Introduksjon

Høye konsentrasjoner av løst jern og mangan i forbindelse med grunnvannsutttak har lenge vært et kjent problem internasjonalt og nasjonalt, både for drikkevannskvaliteten (Ellingsen, 1992) og driften av grunnvannsbrønner (Banks, 1992). De negative sidene ved jern og mangan i et drikkevannsperspektiv er først og fremst knyttet til farge og smak, og ikke til helsemessige konsekvenser (World Health Organization, 2017). Drikkevannsforskriften (2017) angir grenseverdier på 0,2 mg/l for jern og 0,05 mg/l for mangan. I brønndriftssammenheng vil høye konsentrasjoner av stoffene føre til risiko for utfelling av jern- og manganforbindelser som tetter igjen brønnefiltere og -rør, og gir lavere uttakskapasitet (Banks, 1992).

Flere av de store grunnvannsanleggene i Norge har problemer med for høyt innhold av jern og/eller mangan. For eksempel har løsmassebrønner som forsyner vannverkene i Lillehammer, Ringerike og Sunndal opplevd problemer med høye konsentrasjoner av mangan eller jern som har medført etablering av nye brønner og kostbare vannbehandlingsanlegg. Særlig kostbart har dette vært for Lillehammer og Ringerike hvor det henholdsvis er planlagt og etablert vannbehandlingsanlegg for manganfjerning. Anlegget til Ringerike vannverk kom i drift fra februar 2018 og kostet 120 millioner kr (Ramsrud, 2018), mens anbefalt løsning i Lillehammer vil koste drøyt 250 millioner kr (Holmøy, 2019). Årsak(e) til problemene med økning i mangan-konsentrasjoner over tid er likevel ikke fullt ut forstått.

Vi skal her se nærmere på Ringerike vannverk og Sunndal vannverk. Begge anleggene er basert på *indusert elveinfiltrasjon* for mating av akviferen (grunnvannsmagasinet). Dette er en naturlig effekt av grunnvannsutttak fra en akvifer i kontakt med et vassdrag, der elvevann infiltreres inn i akviferen når grunnvannsnivået senkes under elvas nivå. Denne endringen i strømningsmønster medfører også endring i akviferens geokjemiske prosesser som påvirker mobiliteten til jern og mangan (Farnsworth & Hering, 2011).

Videre gjennomgås jern- og manganproblematikk i grunnvannsbrønner, basert både på de geokjemiske prosessene ved indusert elveinfiltrasjon og strømning i og rundt grunnvannsbrønner, med eksempler fra Ringerike og Sunndal vannverk.

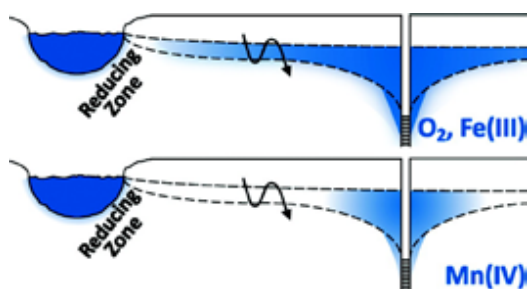
Jern- og manganproblematikk ved grunnvannsutttak

Jern og mangan er to grunnstoffer med relativt lik oppførsel i naturmiljøet. Begge opptrer med forskjellige oksidasjonstall avhengig av reduksjons-oksidasjonsforhold. Under oksiderende forhold vil stoffene gi fra seg elektroner, typisk til oksygen, og opptre med høyt oksidasjonstall, lav løselighet og danne (hydr)oksid-mineraler som felles ut fra vannfasen. Ved reduserende forhold uten tilgang på oksygen vil jern og mangan være mer løselig, og opptre som løste ioner i vannfasen. I tillegg vil lavere pH-verdier føre til økt løselighet av stoffene. Hvorvidt jern og mangan foreligger som løste stoffer i vannfasen eller som faste stoffer er derfor avhengig av redoksmiljøet og pH (Garrels & Christ, 1965).

Det er også noen viktige forskjeller mellom de to stoffene. Mangan krever mer energi, i.e. høyere oksygenkonsentrasjoner, for å oksidere. I tillegg er manganoksidasjon generelt tregere enn jernoksidasjon (Stumm & Morgan, 1996). For øvrig finnes det normalt mer jern enn mangan i jorda (jordskorpa består av mye mer jern enn mangan), noe som ofte gjenspeiles i høyere konsentrasjoner av jern enn mangan i grunnvannet (Houben & Treskatis, 2007).

Jern og mangans oppførsel ved indusert elveinfiltrasjon har blitt studert av Farnsworth & Hering (2011) (se Figur 1). De viser at det typisk dannes en reduserende sone ved elvebanken. Dette skyldes at oksygenet i elvevannet forbrukes ved nedbryting av organisk materiale i akviferen eller infiltrert elvevann, som fører til reduserende forhold og oppløsning av jern og mangan. Elvevann har typisk lavere pH enn grunnvann, noen som vil kunne føre til oppløsning av jern- og mangankarbonater, og ytterligere økning i jern- og mangankonsentrasjon i grunnvannet.

Avhengig av akviferens sorpsjonskapasitet vil en gitt mengde løst jern og mangan adsorberes til akviferematerialet, noe som vil bremse jern- og mangantransporten mot brønnen. Rundt produksjonsbrønnen vil også hyppige svingninger i grunnvannsnivået føre til oksygenering av grunnvannet ved at gassbobler «fanges» inn i porer i akviferen, som igjen vil føre til oksiderende forhold for jern og mangan (blå sone i Figur 1). Ettersom mangan krever mer oksygen for å oksidere enn jern, er manganoksidasjon begrenset til et mindre område rundt produksjonsbrønnen enn jernoksidasjon.



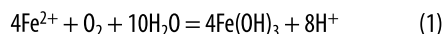
Figur 1. Indikasjon av redokstilstand for jern (Fe) og mangan (Mn) ved elveindusert grunnvannsuttak: Oksidert, uløst (blå sone) og redusert («Reducing zone»), løst (hvit sone) (Farnsworth & Hering, 2011).

Mangans relativt trege oksidasjonskinetikk kan også føre til at mangan ikke rekker å oksideres og felles ut før det når brønnen (Bourg & Richard-Raymond, 1994). I så fall vil det eneste som hindrer det løste manganet i å nå brønnen være sorpsjon av mangan til akvifersedimenter. Finkornet materiale med stor(t) overflateareal og -ladning, som silt, leire, organisk materiale og oksider vil være effektive adsorbenter (Appelo & Postma, 2005). Sorpsjon vil likevel ved lengre tids elveinfiltrasjon ikke være tilstrekkelig til å «rense» vannet for mangan, ettersom sorpsjonsplassene i akvifersedimentene til slutt brukes opp (Farnsworth & Hering, 2011). Dette kan føre til at en *sorpsjonsfront* med høy konsentrasjon av mangan i sedimentene og grunnvannet når produksjonsbrønnen etter lengre tids drift. Et eksempel på denne effekten er vist ved et renseanlegg i Israel, der avløpsvann infiltreres gjennom et basseng i umettet sone. Først etter 8-12 års drift viste observasjons-

brønner 500 meter nedstrøms infiltrasjonsbassenget økning i mangankonsentrasjoner (Oren et al, 2007).

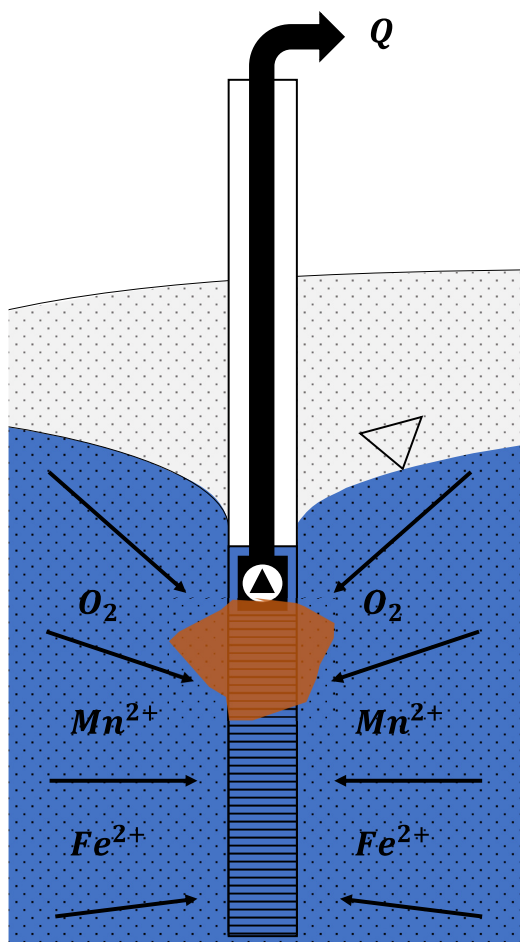
Eventuelt kan lokalt høye konsentrasjoner av mangan skyldes nærhet til leirlinser eller annet finkornet materiale, som medfører lengre oppholdstider og mindre oksygentilførsel, og legger til rette for trege redoksreaksjoner (Bourg & Richard-Raymond, 1994).

Redoksmiljøet vil også endres vertikalt i en akvifer, med en oksisk sone øverst i kontakt med atmosfæren som gradvis blir mer reduserende mot dypet etter hvert som oksygen brukes opp i redoksreaksjoner. Det forventes derfor å finne høyere konsentrasjoner av først mangan og senere jern mot dypet, som følge av at mangan reduseres ved høyere redokspotensiale. En brønn vil ofte trekke vann fra både den grunne, oksiderte sonen, og den dypere, reduserte sonen, se Figur 2. Brønnen vil da fungere som en «redokskortslutning», der oksygen- og jernrikt vann blandes (eng: «mixing»). Dette vil føre til jernoksidasjon, som beskrevet med likevektsligningen (Houben & Treskatis, 2007)



der Fe^{2+} er redusert, løst jern, O_2 er løst oksygen, H_2O er vann, $\text{Fe}(\text{OH})_3$ er jernhydroksid som utfelles, og H^+ er løst hydrogenion. Forholdet mellom akviferens selv- og elvemating vil avgjøre forholdet mellom lateral og vertikal endring i redoksmiljø.

Området i og rundt en grunnvannsbrønn er et meget dynamisk system. Kjemisk likevekt under blanding av grunnvann med ulike redokstilstand kan derfor ikke antas. Kinetiske betraktninger bør derfor inngå i forståelsen av de kjemiske prosessene. Rundt nøytral pH styres utfellingskinetikken til jernhydroksider av jernoksidationsraten, som er lineært proporsjonal med jern- og oksygeninnhold, og proporsjonal i andre potens med pH (Stumm & Lee, 1961). Videre vil jern oksidere raskere når det er adsorbent til jern(hydr)oksider (Tamura et al., 1976), noe som medfører at oksidasjonsraten vil øke med økende jernoksiddannelse på akviferemateriale



Figur 2. Blanding av grunt, oksygenrikt vann og dypt, jernrikt vann rundt produksjonsbrønn under pumping. Indikasjon av filtersone som typisk har mest utfelling (oransje) (etter Houben & Treskatis (2007)).

og i brønnene. I tillegg til denne selv-katalyserende effekten vil også jernoksidende bakterier som tilegner seg energi fra jernoksidasjon kunne katalysere utfelling av jern (Houben & Treskatis, 2007).

Manganutfellinger er sjeldnere enn jernutfellinger i brønner ettersom mangan er mindre tilgjengelig enn jern i jordskorpa og oksidasjonskinetikken til mangan er tregere enn for jern. For øvrig er det sjelden jern- og manganutfellinger finnes i samme del av en brønn, ettersom de dannes ved forskjellige redoksbetingelser (Houben & Treskatis, 2007).

Mengden utfelt materiale i og rundt brønnen henger tett sammen med dens uttakskapasitet, ettersom utfellingene minsker strømningsarealet og øker friksjonen i porerommene i akviferen og filterslissene i brønnfilteret. Dette, sammen med utfellingenes selv-katalytiske effekt, forklarer hvorfor spesifikk kapasitet avtar raskere med tiden i brønner der jernoksid utfeller (Houben, 2004).

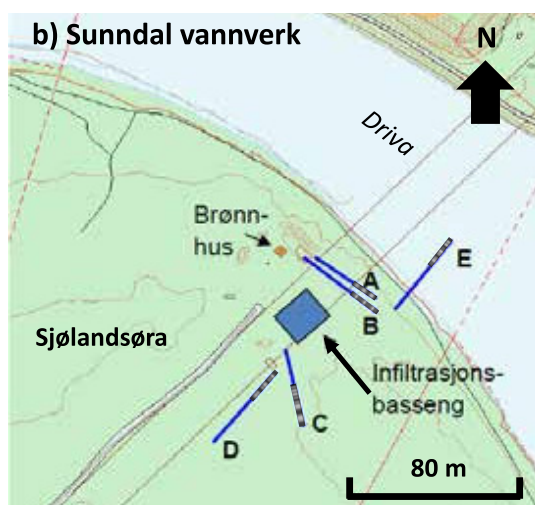
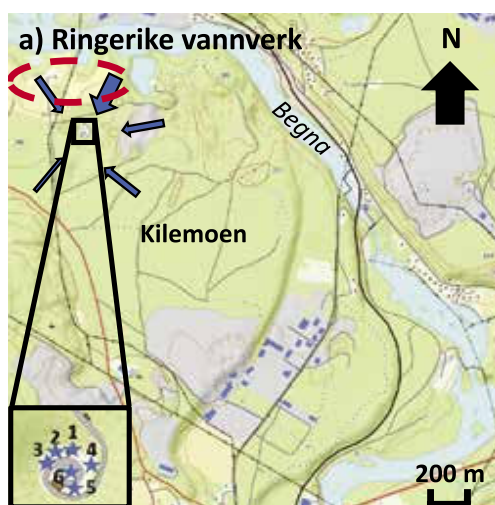
Jernhydroksid-utfellingene vil til å begynne med være amorf, finkornede krystaller med stort overflateareal. Disse krystallene er ikke stabile, og vil med tiden omformes til større minealkorn, med mindre overflateareal og lavere løselighet. De «modnede» jernoksidene vil med sin økte stabilitet være vanskeligere å fjerne ved brønnrehabilitering (Houben & Treskatis, 2007). Tidshorisonten for denne omvandlingen er fra dager til år, og er blant annet avhengig av pH, der høyere pH medfører raskere modning av mineralene (Schwertmann & Murad, 1983).

Det er dermed på forhånd ikke mulig å sette noen klar tidsgrense for når brønner bør rehabiliteres uten kjennskap til det enkelte problem. I litteraturen nevnes ulike tiltaksgrenser tilknyttet spesifikk kapasitet Q/s , der Q er pumperate og s er senkning av vannnivå i brønn fra naturlig nivå. Erfaring fra Tyskland tilsier at brønner bør rehabiliteres før de har mistet 20 % kapasitet (Houben & Treskatis, 2007). Driscoll (1986) og McLauhglan (2002, i Houben & Treskatis, 2007) anbefaler derimot rehabilitering ved henholdsvis 25 % og 10 % redusert kapasitet. I Norge har anbefalingen vært å rehabiliteres ved 30 % kapasitetsnedgang, en anbefaling som ofte ikke følges grunnet mangelfull overvåking av den spesifikke kapasiteten til produksjonsbrønnene (Hilmo & Gurigard, 2017).

Når grunnvannspumpa er plassert over brønnfilteret, og filteret ikke penetrerer hele akviferen, vil mesteparten av innstrømningen til brønnen foregå i øverste del av brønnfilteret. Erfaringsmessig er dette også sonen med mest jernutfellinger (se Figur 2). Økende utfellingsrate med strømningshastighet mistenkes for jernoksid (Houben, 2006), slik som allerede er bevist for kalsitt (Zeppenfeld, 2005). Ettersom jernutfellinger først tetter toppen av filteret vil

Tabell 1. Generell informasjon om grunnvannsverkene på Ringerike og i Sunndal. Informasjon er innhentet fra Vestland^a (2012), Hilmo & Møller^b (2012), Hilmo^c (2018), data fra vannverket i Ringerike^d og Hilmo^e (2017). Mut = meter under terrengoverflaten.

	Ringerike	Sunddal
Midlere uttak (l/s)	80-90 ^a	50 ^b
Abonnenter	23500 ^a	5500 ^b
Brønner (antall)	6 (+ 2 i reserve) ^a	5 ^c
Brønntype	Vertikale ^a	Skråstilte (6,6-20,5 ^o) ^c
Brønndybde (m)	27-47 ^d	6,6-15 ^{c, e}
Filtertopp (mut)	16-27 ^d	5-10 ^{c, e}
Filterlengde (m)	10-20 ^d	10-20 ^{c, e}
Brønnetablering (år)	1987 (Brønn 1, 2, 3) ^d 2007 (Brønn 4 og 5) ^d 2009 (Brønn 6) ^d	1992 (Brønn A, B, C) ^b 2009 (Brønn D) ^b 2011 (Brønn E) ^b
Pumpeplassering (mut)	Ca. 15 ^d	Sugepumper i brønnekum (plassert under grunnvannsnivå) ^b
Grunnvannsspeil (mut)	3-4 ^d	3-4 ^{c, e}



Figur 3. Plassering av produksjonsbrønner (blå stjerner), grunnvannsstrømning ved uttak (blå piler; størrelse indikerer strømningshastighet) og leirlag (rød stiptet ellipse) på Ringerike (a) (modifisert etter NGU (u.å.) og Hilmo (2008)). Plassering av skrå produksjonsbrønner ved Sunndal vannverk med indikert filterplassering (b) (modifisert etter Hilmo & Møller (2012)).

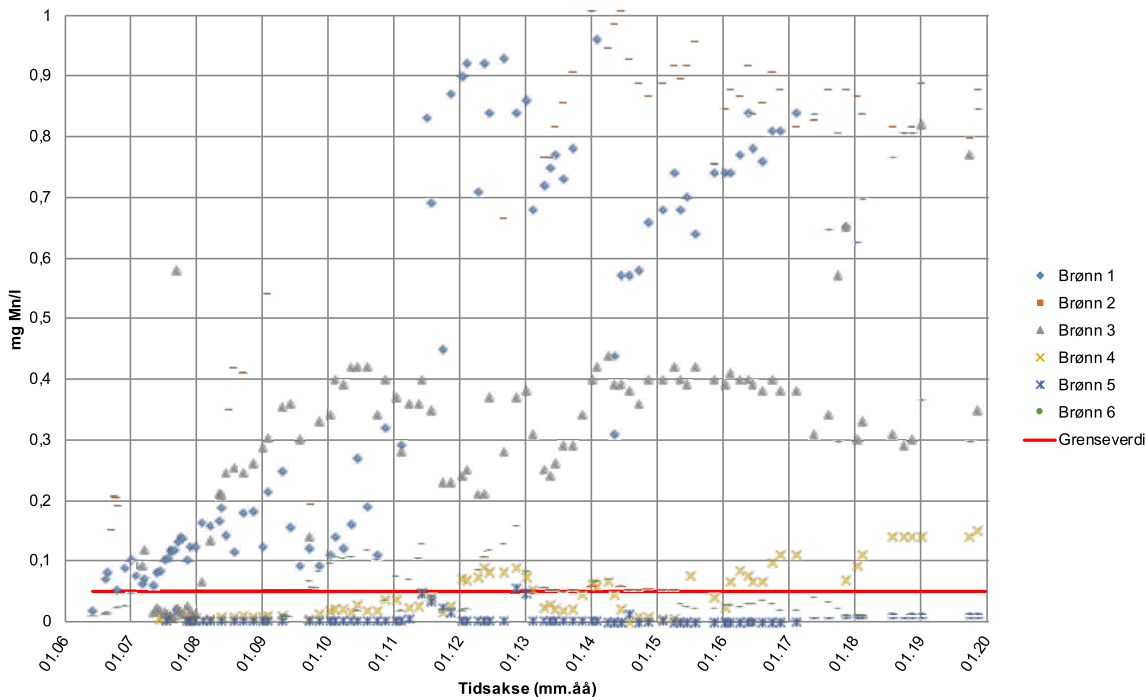
sonen med høyest innstrømningshastighet gradvis flyttes nedover, noe som medfører gradvis mer utfellinger mot bunnen av filteret over tid. Dette kan være med på å endre kvaliteten på det utpumpede grunnvannet, med gradvis høyere jerninnhold i råvannet etter hvert som jernutfellinger tetter brønnen fra toppen og nedover (Houben & Treskatis, 2007). Dette er nok et argument for å gjøre brønnrehabilitering tidlig.

Eksempler fra Ringerike og Sunndal vannverk

I Tabell 1 er grunnleggende informasjon tilknyttet grunnvannsverkene på Ringerike og i Sunndal gjengitt, mens plassering av produksjonsbrønnene er vist på kart i Figur 3a og b.

Videre gis en innføring i problemene som har oppstått ved Ringerike og Sunndal vannverk. Dersom ikke annet er oppgitt, er vann-

Mangan-konsentrasjon - Ringerike vannverk



Figur 4. Mangan-konsentrasjoner i produksjonsbrønner ved Ringerike vannverk (modifisert etter data fra teknisk avdeling i Ringerike kommune).

verksdataene innhentet av og tilsendt fra kommunenes vann og avløpsavdelinger.

Ringerike

Ringerike vannverk startet driften med tre brønner (1, 2 og 3) fra en dødsgrop på Kilemoen i 1987. Akviferen mates fra elva Begna, primært nordfra, men også fra sør og øst, se Figur 3a (Vestland, 2012). Mellom brønnområdet og matingsområdet i nord finnes det marine leiravsetninger, silt og finsand med opptil 10-15 meters tykkelse over grunnvannsmagasinet (NGU, u.å.; Skarphagen, 1982; Klemetsrud, 1986; Vestland, 2012). Problemene med høye verdier av mangan i råvannet oppstod først etter 19 års drift i 2006 (Svingerud, 2006) (se Figur 4). I et forsøk på å løse problemene ble det etablert grunnere brønner sør for de opprinnelige brønnene, brønn 4 og 5 i 2007 og brønn 6 i 2009. De tre sistnevnte brønnene har opplevd mindre problemer med høye manganverdier,

selv om både brønn 4 og 6 også tidvis har ligget over grenseverdien, se Figur 4. Brønn 5 er den grunneste brønnen. Påvist økning i manganninnhold kan ikke relateres til større endringer i vannuttaket som i gjennomsnitt har ligget på 80-90 l/s siden driftsstart i 1987.

De høye mangankonsentrasjonene har ført til at brønner midlertidig er tatt ut av produksjon. Videre har driften av grunnvannspumpene blitt frekvensstyrt etter at problemene oppstod. I tillegg er det utført brønnrehabiliteringer, i form av børsting og luft- og vannspyling, selv om utfelling ikke er et stort problem i brønnene. Hverken endret pumpedrift eller rehabiliteringer har stoppet manganproblemet. Det ble dermed besluttet å anlegge et nytt vannbehandlingsanlegg for manganfjerning. Dette stod klart i 2018 (Ramsrud, 2018).

Jernkonsentrasjonene i råvannet er lavere enn mangankonsentrasjonene, og relativt stabile over tid. Relevante vannkjemiske data for råvan-

Tabell 2. Råvannsdata fra Ringerike og Sunndal vannverk hentet fra tekniske avdelinger i kommunene ^a, Hilmo & Møller ^b (2012), og Hilmo ^c (2018). Spennet i verdier representerer forskjell mellom brønner og variasjon over tid. OBS! Basert på relativt få målinger av nitrat og sulfat.

	Ringerike	Sunndal (Brønn A, B og C)
Jern (mg/l)	<0,01 ^a	0,01 – 0,73 ^{b,c}
Mangan (mg/l)	0 – 1 ^a	0,002 – 0,06 ^{b,c}
Nitrat (mg N/l)	0,01 – 0,3 ^a (Brønn 1 og 3)	0,24 – 0,27 ^c
Sulfat (mg SO ₄ /l)	5 – 7,5 ^a (Brønn 1 og 2)	3 – 5 ^c
pH	7 – 7,3 ^a (Brønn 1, 2 og 3)	6,3 – 6,7 ^{b,c}
Løst oksygen	Ukjent	Ukjent
Redokspotensiale	Ukjent	Ukjent

net er oppsummert i Tabell 2. Lave konsentrasjoner av løst organisk karbon i grunnvannet (Vestland, 2012) indikerer at Kilemoen-avsetningen inneholder lite organisk materiale. Det foreligger ikke mineralogiske analyser av løsmassene som kan bekrefte dette.

Sunndal

Testpumping av undersøkelsesbrønner i elvesedimenter i Sunndal viste økende jernkonsentrasjoner mot dypet. Det var også store variasjoner i organisk innhold i elvesedimentene, samt soner med silt/leire og varierende hydraulisk kontakt med elva. Sunndal vannverk har følgelig hatt betydelige utfordringer med høyt jerninnhold helt siden vannverket på elvesletta på Sjølandsøra ble tatt i bruk i 1988. Den svenske *in situ* jernutfellingsmetoden *Vyredox* ble brukt fra 1988 til 1992, men med dårlig resultat, sannsynligvis pga. høyt innhold av organisk materiale i akviferen. Som en alternativ løsning på de høye jernverdiene ble det besluttet å bore grunnere skrårønner i et område nærmere elva Driva, se Figur 3b. Det nye anlegget, bestående av brønn A, B og C, stod klart i 1992 (Klemetsrud, 1992).

Det har likevel fortsatt vært problemer med høyt jerninnhold i enkelte brønner etter 1992. Det ble derfor anlagt et infiltrasjonsbasseng med marmorfilter på elvesletta i 1997, se Figur 3b. Det er ikke mulig å vurdere effekten av vanninfiltrasjonen på jerninnholdet ettersom det ikke foreligger vannanalyser av jerninnhold fra

tiden før infiltrasjonsbassenget. En tilnærmet uendret pH etter at bassenget ble etablert tyder likevel på en begrenset effekt på jernproblemet (Hilmo & Møller, 2012).

To skråstilte brønner D og E ble satt i drift fra 2014 (se Figur 3b) for å øke kapasiteten på anlegget, og erstatte den dypeste mest jernholdige brønnen (B) (Hilmo & Møller, 2012). Høsten 2017 ble nytt vannbehandlingsanlegg satt i drift og det ble registrert problemer med jernholdig suspendert materiale i vannet (Hilmo, 2018). Det er antatt at dette skyldes løsnede utfellinger fra ledningsnett eller utfellinger katalysert av blanding av vann fra brønner med henholdsvis høyt jern- og oksygeninnhold.

Brønnene A, B og C har vært midlertidig satt ut av drift etter etablering av vannbehandlingsanlegget, delvis pga. høyt jerninnhold. Brønn D og E ble rehabilitert med steaming og seksjonsvis filtertrekking i april 2017, mens brønn A, B og C ble rehabilitert ved jetspyling i januar 2018. Brønnrehabiliteringene var effektive, men klarte ikke å gjenopprette den opprinnelige spesifikke kapasiteten til brønnene, se Tabell 3. Det må her nevnes at opprinnelig brønnkapasitet ble målt mens kun brønnen som skulle testes var i drift, mens målinger før og etter rehabilitering ble målt mens alle brønnene var i drift. Tallene før og etter rehabilitering er derfor trolig for lave sammenlignet med opprinnelig kapasitet.

Etter rehabiliteringene i 2018 har alle brønnene vært i drift. Det er for øvrig ingen signifikant forskjell mellom jerninnholdet i råvannet før og

Tabell 3. Spesifikk kapasitet (Q/s) rett etter brønnetablering, rett før brønnrehabilitering og rett etter rehabilitering i prosent av opprinnelig kapasitet. Modifisert etter Hilmo (2018) for brønn A, B og C, og modifisert etter Hilmo (2017) for brønn D og E.

Spesifikk kapasitet (% Q/s)	Brønn				
	A	B	C	D	E
Etter boring (%)	100 %	100 %	100 %	100 %	100 %
Før rehabilitering (%)	30 %	?	36 %	41 %	52 %
Etter rehabilitering (%)	43 %	70 %	55 %	52 %	83 %

etter rehabilitering av brønn A, B og C (Hilmo, 2018). Mangan har ikke vært et stort problem ved Sunndal vannverk, selv om også mangannivået har ligget over grenseverdien ($>0,05$ mg/l). Se Tabell 2 for relevante vannkjemiske data.

Diskusjon

Økningen i manganinnhold i produksjonsbrønner ved Ringerike vannverk på Kilemoen etter nærmere 20 års drift kan tyde på at en sorpsjonsfront, som beskrevet i Oren et al (2007) og Farnsworth & Hering (2011), er utviklet fra innmatingsområdet i nord og sørover mot brønnfeltet. Brønnrehabiliteringens manglende effekt på mangankonsentrasjonen er med på å underbygge at økningen skyldes endringer i selve akviferen og ikke kjemiske prosesser lokalt rundt brønnene. Det må likevel nevnes at Oren et al (2007) studie var av infiltrasjon av avløpsvann rikt på organisk materiale, svært ulik infiltrasjon av rent elvevann. Det antas likevel at konseptet har en viss overføringsverdi.

Det marine leirlaget nord for Kilemoen antas å fungere som en «reduksjons-hotspot» der lang oppholdstid og mindre kontakt med atmosfæren gir opphav til reduserende forhold og mobilisering av mangan, som beskrevet i Bourg & Richard-Raymond (1994). Ut fra vannanalysene ser det også ut til at mangankonsentrasjonene stabiliseres etter en viss tids økning, se Figur 4. Dette tyder på at sorpsjonskapasiteten til akviferen har blitt brukt opp, og at redoks-forholdene i akviferen er stabile. Den faktiske sorpsjonskapasiteten ved Kilemoen er vanskelig å bestemme uten mineralogiske analyser av løsmassene (Appelo & Postma, 2005). Et begrenset innhold av organisk materiale og leire indikerer lav sorp-

sjonskapasitet i akviferen. Det er likevel mulig utfelling av oksider og det finkornede laget over akviferen bidrar til å øke sorpsjonsevnen.

Det kan også se ut til å være en vertikal endring i redoksmiljø med mest oksygen tilgjengelig i de grunnere delene av akviferen ettersom manganproblemet er størst i de dypeste brønnene. Brønnene med lavest manganinnhold (4, 5 og 6) er også de som trolig tilføres mest vann fra områdene sør og øst for brønnfeltet (se Figur 3a). Fra sør og øst har grunnvannet lengre strømningsvei fra elva og strømmer gjennom løsmasser bestående av mindre leire (NGU, u.å.). Lengre strømningsvei og mindre leire tilrettelegger for henholdsvis større sorpsjonskapasitet og mindre manganreduksjon, som begge vil bidra til mindre mangan i vannet som når brønnområdet.

Ved Sunndal vannverk er problemet både at råvannskvaliteten tidvis (2017) ikke tilfredsstillende drikkevannsforskriften og at brønnfiltrene tettes igjen av jernutfellinger. Dette kan forklares med at jernoksidasjon er raskere kinetisk og krever mindre oksygen enn manganoksidasjon (Stumm & Morgan, 1996). Det er derfor som forventet at brønnene på Ringerike har mindre problemer med gjentetting av filtre enn Sunndalsøra. Økning i jerninnhold med brønnfilterdybde tyder på at utfellingene skyldes blanding av grunt oksygenrikt med dypere jernrikt grunnvann. Økning i jerninnhold med avstand fra elva indikerer at jernreduksjon ikke er begrenset til sonen nærmest elvebanken som Figur 1 indikerer. Påvisning av høyt innhold av organisk materiale i akviferen underbygger sistnevnte tolkning.

Brønnrehabilitering ved Sunndal vannverk ble utført etter at den spesifikke brønnkapasiteten

hadde sunket til rundt 50 % av opprinnelig kapasitet og lavere, se Tabell 3. Dette er langt lavere enn anbefalt rehabilitering ved 10-30 % kapasitetsnedgang (Driscoll, 1986; McLauhglan, 2002, i Houben & Treskatis, 2007; Houben & Treskatis, 2007; Hilmo & Gurigard, 2017). Den mekaniske brønnrehabiliteringen klarer dermed ikke å gjenopprette opprinnelig kapasitet. Poenget understrekes av at brønnene som har mistet minst prosentvis kapasitet også har best effekt av rehabiliteringen, se Tabell 3.

Etter hvert som utfellingene tetter brønnfilteret fra toppen og nedover vil dypere grunnvann trekkes inn i brønnene, og kunne føre til endret råvannskvalitet (Houben & Treskatis, 2007). Mangel på signifikante endringer i råvannets jernkonsentrasjon før og etter rehabiliteringen av brønn A, B og C kan skyldes at brønnene ikke var i kontinuerlig drift i perioden før rehabilitering. Flere prøver av hver brønn isolert før og etter rehabilitering ville gjort det lettere å vurdere om utfellingene har hatt effekt på råvannskvaliteten.

Det er for øvrig en tendens til at brønnrehabilitering av løsmassebrønner i Norge kun omfatter mekaniske metoder, jfr. vannverkene i/på Lom, Kvam, Røros, Trandum, Årdal, Rena (Banks, 1992), Ringerike og Lillehammer (Marie Fossum, ved Vannverk og renseanlegg, Lillehammer kommune (e-post, 5. juli 2019)). Ifølge Houben & Treskatis (2007) oppnås best effekt når brønnrensingen omfatter en kjemisk rehabiliteringsmetode kombinert med mekanisk rensing før og etter kjemisk behandling. Erfaringer har vist at det reduserende middelet *natrium-thiosulfat* effektivt oppløser og mobiliserer harde og modnede jernhydroksider (Houben, 2003). Som et alternativ til kjemiske tilsetningsstoffer har "steaming" kombinert med seksjonsvis filtertrekking vist seg å være en effektiv rensemetode i Norge. Denne metoden har også den fordelen at nærliggende brønner kan produsere under rehabiliteringen uten fare for kjemikalieforurensning (Hilmo & Gurigard, 2017). Ettersom jernutfelling har en selvkatalyserende effekt er det et viktig poeng å få fjernet alle jernutfellingene fra brønnfilter og formasjonen rundt brønnen. Hvis ikke kan rensprosessen virke som en

katalysator for mer utfelling ettersom jernutfellingene får større overflateareal til sorpsjon og oksidasjon av løst jern.

Høyere konsentrasjoner av jern indikerer et mer reduserende grunnvannsmiljø ved Sunndalen enn ved Ringerike (se Tabell 2). Riktignok påvirker også pH løselighet av stoffene, og i størst grad for jern(hydr)oksider (Garrels & Christ, 1965), noe som kan forklare høyere jernverdier ved Sunndal der pH er lavest. Redoks-sensitive stoffer, som løst oksygen, nitrat, sulfat og organisk materiale, og redokspotensiale, måles sjelden eller aldri ved vannverkene. Jevnlig måling av disse parameterne ville gitt en bedre oversikt over potensielle endringer i redoksmiljøet i brønnene og akviferen. En enkel tolkning av aktive redoksprosesser kan fås ved å benytte aktuelle vannanalyser som inngangsparametere i et Excel-program utviklet ved United States Geological Survey (Jurgens et al, 2009).

Jevnlig måling av redoks-sensitive parametere kan også være med på å avdekke årsakene til problemene. En gradvis mer reduserende råvannskvalitet kan tyde på at brønnen trekker inn dypere vann, som følge av at utfelling tetter brønnen og som medfører at gradvis mer jernholdig dypere vann trekkes inn i brønnen. Endring tilbake mot opprinnelig redoksmiljø etter brønnrehabilitering vil styrke mistanken ytterligere. Hvis problemet derimot er utvikling av en sorpsjonsfront vil ikke brønnrehabilitering ha noen effekt på råvannskvaliteten, og endringen i redoksforhold vil trolig også stabilisere seg etter hvert som sorpsjonskapasiteten er brukt opp. Tilførselen av organisk materiale ved elveinfiltrasjon vil også over tid kunne føre til utviklingen av en *redoksfront* med gradvis mer reduserende forhold nærmere og nærmere brønnområdet.

Mens problemer med lavere uttakskapasitet og endret vannkvalitet som følge av utfelling kan begrenses ved å rehabilitere brønnen i tide, er økning i mangan som følge av oppbrukt sorpsjonskapasitet i akviferen et vanskeligere problem å løse. Jevnlig prøvetaking av observasjonsbrønner mellom infiltrasjons- og uttaksområdet kan avdekke eventuelle sorpsjonsfronter

før de påvirker grunnvannsutttaket, og dermed gi bedre tid til å planlegge tiltak som for eksempel vannbehandling, flytting av brønnområdet eller ny vannkilde.

Oren et al (2007) hevder at brønner tilstrekkelig langt unna infiltrasjons- og reduksjonsområdet vil unngå problemer med høye manganverdier, ettersom manganet da rekker å blandes med oksygenrikt vann og oksidere. Dette er i liten grad erfart ved norske grunnvannsanlegg på elvesletter. Det er heller lavere manganinnhold i brønner nær elva enn i brønner lenger unna, ettersom norske elvesletter gjerne består av fluvial sand og grus iblandet noe organisk materiale. Nedbryting av dette organiske materiale forbraker oksygen og gir dermed økt løselighet av jern og mangan. Oren et al (2007) hypotese kan likevel stemme for Kilemoen der grunnvannet strømmer gjennom en mektig breelavsetning med lite organisk innhold.

Et viktig poeng angående norske grunnvannsforkomster i et internasjonalt perspektiv er at de ofte er små og inhomogene, noe som gjør det vanskelig å generalisere problemer og tiltak tilknyttet jern og mangan. Teori og erfaringer viser også at jern og mangan til dels har forskjellige egenskaper og oppreden ved grunnvannsutttak, noe som er med på å forklare forskjellene i problemene ved Ringerike og Sunndal vannverk. Disse forskjellene er viktig å være klar over når en utreder mulige problemer med jern og mangan ved grunnvannsutttak.

Konklusjon og anbefalinger

Ut fra studier av jern- og manganproblematikk ved grunnvannsutttak generelt, og på Ringerike og i Sunndal spesielt, gis følgende konklusjoner:

- Jern og mangan har mange like egenskaper, men også en del ulike som gjør at de i forbindelse med grunnvannsutttak gir opphav til forskjellige problemer.
- Ringerike vannverks manganproblemer tolkes til å være forårsaket av en sorpsjonsfront fra elva i nord mot brønnområdet i sør, mens Sunndals jernproblemer ser ut til å forårsakes av blanding av grunt oksygenrikt vann med dypere jernrikt vann.

- Eksempelene fra Ringerike og Sunndal viser viktigheten av å gjøre gode hydrogeologiske undersøkelser både før etablering og under drift av grunnvannsanlegg. Dette omfatter kartlegging av grunnvannsmagasin, -strømning, -nydannelse og -kjemi som grunnlag for plassering og dimensjonering av brønner. For tidlig å kunne avdekke problem(ty)er bør redoks-sensitive stoffer som løst oksygen, nitrat, jern, mangan og sulfat i tillegg til redokspotensiale måles jevnlig, både i produksjons- og nærliggende observasjonsbrønner.
- Effektiv fjerning av jernutfellinger fra brønner oppnås ved å foreta rens før jern(hydr)oksidene har modnet til mindre løselige mineraler. Ettersom jernutfellinger har en selv-katalytisk effekt bør alt jern fjernes. For å oppnå dette bør en kombinasjon av ulike mekaniske og kjemiske rehabiliteringsteknikker benyttes.

Takksigelser

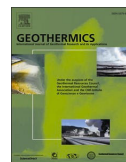
Vi vil rette en stor takk til alle som har bidratt med data og diskusjon rundt disse ved vannverkene. Dette gjelder Marie Fossum ved Vannverk og renseanlegg i Lillehammer kommune, Grete Marie Trædal ved Kommunalteknisk tjeneste i Sunndal kommune og Tormod Tobiassen ved Vann og avløp i Ringerike kommune. Takk også til professor Bjørn Frengstad ved Institutt for geovitenskap og petroleum, NTNU for sparring og korrekturlesing. For øvrig vil vi takke Midt-norsk Forskningsråd og NTNU for finansiering av forskningen.

Referanser

- Appelo, C.A.J. & Postma, D. (2005) *Geochemistry, groundwater and pollution*. Leiden, Nederland: Balkema.
- Banks, D. (1992) *Grunnvannsbrønner: Kontroll, vedlikehold, rehabilitering*. GiN-veileder nr. 13 (Skrifter 108). Trondheim: Norges geologiske undersøkelse (NGU).
- Drikkevannsforskriften. (2017) Forskrift om vannforsyning og drikkevann (FOR-2016-12-22-1868). Hentet fra <https://lovdata.no/dokument/SF/forskrift/2016-12-22-1868>

- Driscoll, F.G. (1986) *Groundwater and Wells* (2. utg.). St. Paul, MN: Johnson.
- Ellingsen, K. (1992) *Grunnvannskvalitet: Problemer og tiltak*. GiN-veileder nr. 12 (Skrifter 106). Trondheim: NGU.
- Farnsworth, C.E. & Hering, J.G. (2011) Inorganic geochemistry and redox dynamics in bank filtration settings. *Environmental Science & Technology*, 45(12), 5079-5087. doi:10.1021/es2001612
- Garrels, R.M. & Christ, C. L. (1965). *Solutions, minerals and equilibria* (2. utg.). New York: Harper & Row.
- Hilmo, B.O. (2008) *Endringer i klausuleringsplan for Ringerike vannverk*. Trondheim: Asplan Viak AS.
- Hilmo, B.O. (2017) *Rehabilitering av brønn D og E ved Sunndal vannverk*. Trondheim: Asplan Viak AS.
- Hilmo, B.O. (2018) *Rehabilitering av brønn A, B og C ved Sunndal vannverk*. Trondheim: Asplan Viak AS.
- Hilmo, B.O. & Gurigard, R. (2017) Rehabilitering av filterbrønner – erfaringer fra Norge. *Grundvattendagarna*, 7.-8. november 2017. Uppsala, Sverige: Sveriges geologiska undersökning.
- Hilmo, B.O. & Møller, B.S. (2012) *Sunndal vannverk – Forprosjekt vannforsyning*. Trondheim: Asplan Viak AS.
- Holmøy, S. (2019, 22. mai) Behov for nytt vannverk i Lillehammer kommune. *Gudbrandsdølen Dagingen*. Hentet fra <https://www.gd.no>
- Houben, G.J. (2003) Iron oxide incrustations in wells. Part 2: chemical dissolution and modeling. *Applied Geochemistry*, 18, 941-954. doi:10.1016/S0883-2927(02)00185-3
- Houben, G.J. (2006) The Influence of Well Hydraulics on the Spatial Distribution of Well Incrustations. *Groundwater*, 44(5), 668-675. doi:10.1111/j.1745-6584.2006.00216.x
- Houben, G.J. & Treskatis, C. (2007) *Water Well: Rehabilitation and Reconstruction*. New York: McGraw-Hill.
- Jurgens, B.C., McMahon, P.B., Chapelle, F.H., & Eberts, S.M. (2009) *An Excel® Workbook for Identifying Redox Processes in Ground Water* (National Water-Quality Assessment Program, Open-File Report 2009-1004). Reston, Virginia: United States Geological Survey.
- Klemetsrud, T. (1986) *Ringerike vannverk – Kilemoen: Pilotboringer i grop 8, ved Tjorputten* (NGU-rapport 86.009). Oslo: NGU.
- Klemetsrud, T. (1992) *Grunnvannsforsyning til Sunndalsøra fra Sjølandsøra i Sunndal kommune* (NGU-rapport 92.266). Trondheim: NGU.
- McLauhglan, R.G. (2002) *Managing Water Well Deterioration* (International Contributions to Hydrogeology 22). Lisse, Nederland: Balkema.
- NGU. (u.å.) GRANADA – Nasjonal grunnvannsdatabase. Hentet fra: <http://geo.ngu.no/kart/granada/>
- Oren, O., Gavrielli, I., Burg, A., Guttman, J., & Lazar, B. (2007) Manganese Mobilization and Enrichment during Soil Aquifer Treatment (SAT) of Effluents, the Dan Region Sewage Reclamation Project (Shafdan), Israel. *Environmental Science & Technology*, 41, 766-772. doi: 10.1021/es060576
- Ramsrud, K.A. (2018, 18. februar) Mandag får du vann fra helt nytt vannverk. *Ringerikes blad*. Hentet fra <https://www.ringblad.no>
- Schwertmann, U. & Murad, E. (1983) Effect of pH on the formation of goethite and hematite from ferrihydrite. *Clays and Clay Minerals*, 31(4), 277-284. doi:10.1346/CCMN.1983.0310405
- Skarphagen, H. (1982) *Grunnvannsanlegg Kilemoen. Vedrørende undersøkelsesboringer i forbindelse med plassering av infiltrasjonsbrønner ved Tjorputten* (NGU-rapport 82.055). Oslo: NGU.
- Stumm, W. & Lee, G.F. (1961). Oxygenation of Ferrous Iron. *Industrial & Engineering Chemistry*, 53(2), 143-146. doi:10.1021/ie50614a030
- Stumm, W. & Morgan, J.J. (1996) *Aquatic chemistry: chemical equilibria and rates in natural waters* (3. utg.). New York: Wiley.
- Svingerud, J.K. (2006) *Ringerike vannverk – Kilemoen*. Ringerike: Ringerike vannverk.
- Tamura, H., Goto, K., & Nagayama, M. (1976) The effect of ferric hydroxide on the oxygenation of ferrous ions in neutral solutions. *Corrosion Science*, 16(4), 197-207. doi:10.1016/0010-938X(76)90046-9
- Vestland, M. (2012) *Klausuleringsplan for Ringerike vannverk Kilemoen*. Trondheim: Asplan Viak AS.
- World Health Organization. (2017) *Guidelines for drinking-water quality: fourth edition incorporating the first addendum*. Geneva, Switzerland: World Health Organization.
- Zeppenfeld, K. (2005) Untersuchungen über den Einfluss der Strömungsgeschwindigkeit auf die Kalkabscheidung aus calciumhaltigen Wässern [Studies of the Effect of the Flow Velocity on Calcium Carbonate Precipitation from Water Containing Calcium]. *Vom Wasser*, 103(2), 3-34.

Paper II



Hydrochemical and biotic control on iron incrustations in groundwater heat pump systems: Case study from a saline, anoxic aquifer in Melhus, Norway

Lars A. Stenvik^{a,*}, Sondre Gjengedal^b, Randi K. Ramstad^{a,c}, Bjørn S. Frengstad^a

^a Norwegian University of Science and Technology, S. P. Andersens vei 15A, Trondheim N-7491, Norway

^b Norwegian Geotechnical Institute, P.O. Box 5687 Torgarden, Trondheim N-7485, Norway

^c Asplan Viak AS, Hotellgata 2, Stjørdal N-7500, Norway

ARTICLE INFO

Keywords:

Groundwater heat pump
Incrustation
Iron oxide
Iron sulfide
Clogging
Iron-oxidizing bacteria

ABSTRACT

Clogging by incrustations of nine groundwater heat pump (GWHP) systems in Melhus, Norway have been investigated by field and laboratory methods for water quality and incrustation composition. Iron oxides incrust systems extracting relatively shallow, low-saline groundwater, while iron sulfides are associated with deeper, more saline groundwater. Hydrochemical conditions in iron oxide clogged GWHP systems are favorable for the growth of iron-oxidizing bacteria. Also, sediment deposits clog the well systems. The variety of incrustation problems detected in Melhus emphasizes that clogging must be expected and dealt with, instead of solely attempted avoided through system design or re-location.

1. Introduction

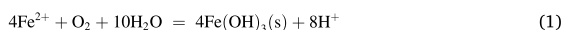
Shallow aquifers function as storages for solar heat. This can be utilized for heating and cooling of buildings by means of a groundwater heat pump (GWHP) system. An aquifer thermal energy storage (ATES) system additionally comprises seasonal storage and extraction of excess building heat to/from the aquifer. Both these open-loop ground source heat pump systems essentially comprise two groundwater wells, one for extraction and one for injection. The extracted groundwater undergoes heat exchange to/from a heat pump coupled to a building heat distribution system before injection. The technologies reduce the electricity demand compared to conventional electrical heating. However, their operation is impeded by dissolved and suspended material of inorganic and/or organic origin in the groundwater which may precipitate or deposit to form incrustations. Incrustations have been observed to clog vital parts of GWHP and ATES systems such as well screens and filters, pumps, pipes and heat exchangers (Bakema, 2001; Eggen and Vangsnes, 2005; Lerm et al., 2011; Possemiers et al., 2016; Burté et al., 2019; Gjengedal et al., 2020). Clogging impels costly rehabilitations or even reconstructions, with the remedy depending on incrustation type and

extent (Mansuy, 1998; Bakema, 2001; Houben and Treskatis, 2007). This underlines the importance of properly identifying and characterizing incrustations in GWHP and ATES systems in time.

This article presents water chemical and incrustation investigations of nine GWHP systems in Melhus, Norway which have experienced clogging, and aims to unravel incrustation composition and genesis.

1.1. Incrustations in groundwater wells

Incrustations are categorized as either chemical, biotic or mechanical, but the processes are often concomitant. The most common chemical incrustations in groundwater wells are iron oxides/hydroxides (both termed iron oxides in this article) (Houben and Treskatis, 2007). Iron oxides form when dissolved oxygen (O₂) oxidizes dissolved ferrous iron (Fe²⁺) to practically insoluble ferric iron (Fe³⁺) which precipitates as solid iron oxide (Fe(OH)₃(s)). The reaction proceeds according to (Stumm and Morgan, 1996):



Oxidation of ferrous iron is the rate-controlling step of the iron oxide

Abbreviations: BART, Biological activity reaction test; GWHP, Groundwater heat pump; ICP-MS, Inductively coupled plasma mass spectrometry; IOB, Iron-oxidizing bacteria; LOI, Loss on ignition, weight-loss of incrustation samples ignited at 400 °C; Q, Volumetric groundwater pumping rate; SLYM, Slime-forming bacteria; SRB, Sulfate-reducing bacteria; XRD, X-ray diffraction.

* Corresponding author.

E-mail address: lars.a.stenvik@ntnu.no (L.A. Stenvik).

<https://doi.org/10.1016/j.geothermics.2022.102349>

Received 25 October 2021; Received in revised form 20 December 2021; Accepted 8 January 2022

Available online 16 January 2022

0375-6505/© 2022 The Authors. Published by Elsevier Ltd. This is an open access article under the CC BY license (<http://creativecommons.org/licenses/by/4.0/>).

precipitation at circumneutral pH. The homogenous (i.e., in the water phase) kinetic rate of iron oxidation can be described by the equation (Stumm and Lee, 1961)

$$\frac{d[\text{Fe}^{2+}]}{dt} = k[\text{Fe}^{2+}][\text{O}_2][\text{H}^+]^{-2} \quad (2)$$

where k is the homogenous rate constant and parentheses indicate concentrations. The rate constant k generally decreases with increasing ionic strength, but an exact value is difficult to determine since numerous hydrochemical parameters inhibit or catalyze the reaction (Sung and Morgan, 1980). It is evident from Eq. (1) and ((2) that higher pH and oxygen concentrations accelerate iron oxidation. Typically, there is a vertical zonation of redox environments in soils, with oxic conditions close to the surface which gradually become more anoxic with depth as oxygen is depleted through redox reactions. In anoxic environments, iron is found as reduced and dissolved Fe^{2+} ions. Production wells may extract water from different redox zones, causing them to mix and trigger ferrous iron oxidation by oxygen (van Beek, 1989). Furthermore, oxygen in-leakage through improperly sealed parts of the groundwater pipeline also poses risk of iron-oxygen reactions (Bakema, 2001). The amorphous, unstable ferrihydrite ($\text{Fe}(\text{OH})_3$) that usually first forms will recrystallize to the more stable goethite (FeOOH) with time. Manganese oxides can also incrust well systems but are less frequent than iron oxides. This is due to manganese's lower earth crust abundance, higher oxygen demands for oxidation and slower reaction kinetics (Stumm and Morgan, 1996; Houben and Treskatis, 2007).

Eq. (2) does not consider the effect of heterogenous iron oxidation which occurs on surfaces. The presence of oxidized iron (Fe^{3+}) on solid surfaces will sorb dissolved ferrous iron and catalyze oxidation. This causes an autocatalytic effect, described by the combined homogenous and heterogenous rate equation (Tamura et al., 1976)

$$\frac{d[\text{Fe}^{2+}]}{dt} = (k[\text{O}_2][\text{H}^+]^{-2} + k'K[\text{O}_2][\text{H}^+]^{-1}[\text{Fe}^{3+}])[\text{Fe}^{2+}] \quad (3)$$

where k' is the heterogenous rate constant, K is the adsorption constant for ferrous iron onto iron oxides. The heterogenous reaction's first order dependence on pH compared with the second order dependence of homogenous oxidation, suggest that the heterogenous effect is most pronounced at lower pH levels. Iron-oxidizing bacteria (IOB) which gain energy from iron oxidation (e.g., *Gallionella* and *Leptothrix*) thrive on solid surfaces and may further catalyze iron oxidation. Different genera have different hydrochemical preferences, for instance with regards to dissolved oxygen and iron concentrations, pH, and salinity (Houben and Treskatis, 2007; McBeth et al., 2013; Eggerichs et al., 2014). Thus, the apparent increase in iron oxidation with pH and oxygen from Eq. (2) and ((3) may be disturbed indirectly by hydrochemical conditions which dictate the IOB genera's growth conditions and influence on the rate constant k' .

Oxygen depleted, iron-rich conditions facilitate iron sulfide mackinawite (FeS) and/or iron carbonate siderite (FeCO_3) incrustations, if dissolved sulfur and/or carbonate are present, respectively. Reducing, sulfur-rich environments are characterized by the smell of rotten eggs (i.e., H_2S gas). Sulfide precipitation is accelerated by the presence of sulfate-reducing bacteria (SRB), which nurture from sulfate (SO_4^{2-}) reduction (Houben and Treskatis, 2007). SRB also facilitate corrosion of metallic iron, together with high oxygen contents, low pH, and high salinity. Corrosion will also produce iron oxides (rust) and sulfide incrustations. Rust possesses magnetic properties, unlike iron oxides of non-corrosion origin (Houben and Treskatis, 2007).

Biotic incrustations, or biofouling, are caused by microorganisms and other biotic material building up fluffy and slimy biofilms. The group of microorganisms responsible for the formation of biofilms are therefore often termed slime-forming bacteria (SLYM). Their build-up around production and injection wells is facilitated by the constant nutrient supply from locally elevated groundwater flow rates. The SLYM

and IOB bacteria categories partly overlap. Thus, biofouling and iron oxides incrustations are commonly found in the same wells (Mansuy, 1998).

Mechanical incrustations comprise aquifer or well filter pack materials which have entered and deposited in the well system. This is typically caused by improper well screen and/or filter design or development, or too high inflow velocities in and around the well screen (Bakema, 2001). The latter could be triggered, for example, by iron oxide incrustations gradually decreasing the available inflow cross-section (Mansuy, 1998).

1.2. Study area

Nine GWHP systems have been established in the town center of Melhus, Mid-Norway in the period 1999–2015, see Fig. 1. The GWHP systems supply heating and cooling to the 6,686 inhabitants' (Statistics Norway, 2020) apartments, nursing homes, schools, grocery stores and offices, by extracting water from the same aquifer. The Melhus aquifer consists of coarse unconsolidated glaciofluvial sediments hydraulically connected to the river Gaula (Hellestveit, 2018), and covered by a marine clay layer. The aquifer has both unconfined and confined characteristics, depending on location, due to inclination and variable thickness of the marine clay layer. The natural groundwater table is located ~10–20 m below ground level. The area's marine history with isostatic uplift in Holocene (Reite, 1990) has left the aquifer with a salinized groundwater quality, with salinity increasing with the thickness of the overlying clay layer (Brøste, 2017).

All GWHP systems in Melhus comprise a production well with a submersible pump installed above the well screen. The pumped water is then led to a heat exchanger, where the ~6–8 °C groundwater temperature is reduced/increased ~3 °C. Then, the water is either re-infiltrated to the aquifer through an injection well (6 out of 9 systems) or lead to the local sewage system (3 out of 9 systems), see Fig. 1. All well filters are naturally developed (i.e., not gravel packed), and with continuously slotted well screens. Seven systems operate at a constant groundwater pumping rate, while two operate with variable speed drive according to the heat demand, see Fig. 1. The pumping rates range between 4 and 17 l/s (Gjengedal et al., 2020), see Table 1.

Previous investigations have revealed incrustation problems in all nine GWHP systems. The first incrustation review by Riise (2015) suggested iron oxides as the main incrustation problem. The problems have been further studied in the national research projects ORMEL and ORMEL 2 ("Optimal utilization of heating and cooling in Melhus (and Elverum)") (Brøste, 2017; Gjengedal et al., 2018, 2019, 2020). The water chemistry, incrustation mineralogy and camera inspections of wells have been studied previously (Riise 2015; Brøste, 2017; Gjengedal et al., 2018). However, new hydrochemical measurements have been deemed necessary since the former ones did not include air-tight flow-through cell measurements of parameters such as pH, dissolved oxygen and redox potentials. Supplemental analysis of incrustation mineralogy, microbiology and camera inspections were also considered favorable to assess the link between water quality and incrustation genesis.

2. Methods

2.1. Water quality

The water chemistry was investigated by a combination of laboratory analysis of water samples and field measurements between May 2019–June 2021. Each GWHP was sampled and measured up to eight times from taps located right before and after the heat exchangers, see Fig. 1. The Oterholmgården GWHP was only sampled once due to lack of water sampling tap until spring 2021. The water chemistry of the abandoned production well at Lenavegen 3 was also investigated while performing biological activity reaction tests (see description below). Water samples

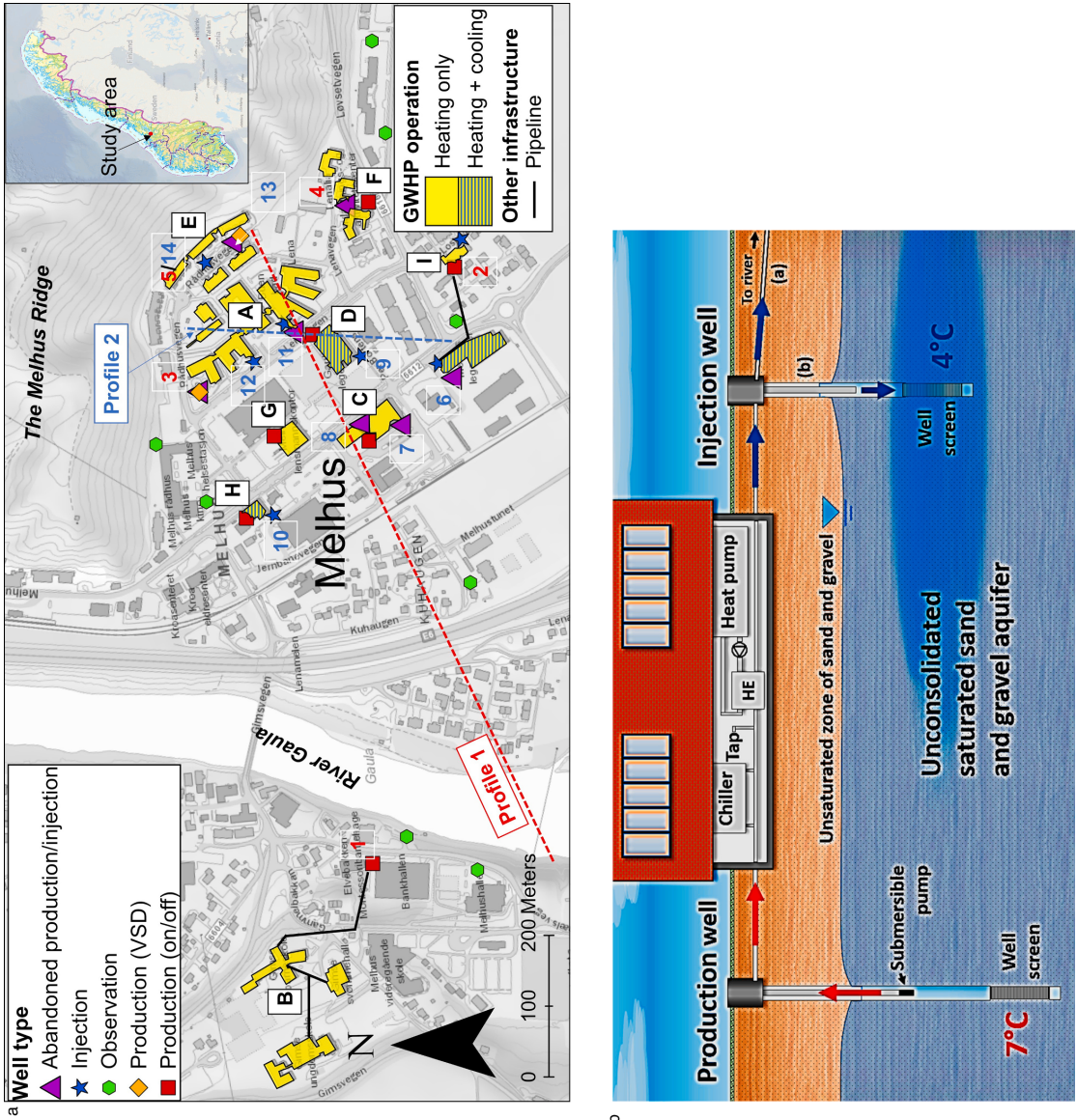


Fig. 1. Top: Map of study area. Location of GWHP systems that re-inject groundwater to the river Gaula (B, F, G) in the town center of Melhus is indicated. Name of systems (A-I) are given in Table 1. Profile 1 (production well 1–5) and 2 (injection wells 6–14) are presented in Fig. 5. VSD = pump operates with variable speed drive. On/off = pump operates at one single speed. Bottom: Groundwater heat pump (GWHP) system design in Melhus, Norway. Two designs exist with (a) discharge to river and (b) infiltration through an injection well (Gjengedal et al., 2019).

Table 1.

Basic information about the GWHP systems in Melhus, see Fig. 1. Q = groundwater pumping rate. bgl = below ground level. Pumping rate data is partly retrieved from Røise (2015).

GWHP system(Start of operation)	Production well screen (meters bgl)	Q(l/s)	Injection well(s)	Clogging measures ^c (#)	
				Rehabilitations	Reconstructions
A) Buen (2013-)	36–44 (29.5–32.5 ^b)	8–9 ^b	2	1	2
B) Gimse (2009-)	19–34	6–7	–	2	0
C) Høvdingen (2015–2020)	66–69 (65–68 ^b)	7.5	2	0	2
D) Idegården (2008-)	46–60	6.5	1	2	0
E) Lena terrasse (2003–2006, 2015-)	30–36 (27–37 ^b)	7–12 ^b	1	8	3
F) Lenavegen 3 (1999–2013, 2014-)	39.5–43 (17.5–23.5 ^b)	15–16	–	0	2
G) Melhuset (1999-)	24.5–34.5	4	–	1	0
H) Oterholmgården (2010-)	36–38	5.5	1	2	0
I) Thoragården (2013-)	73–78 (79.5–83 ^b)	4–5	2	0	1

(a) Defect/replaced production wells. bgl = below ground level.

(b) Variable speed drive (VSD) groundwater pump.

(c) Clogging measures in wells, heat exchangers or submersible pumps per September (2021).

were filtered with a 0.45 μm membrane filter in the field and conserved with 0.1 M HNO_3 acid. All sample batches were analyzed by inductively coupled plasma mass spectrometry (ICP-MS) (Element 2 - ICP-HR-MS, ICP-MS Agilent 8800) at the Department of Chemistry, NTNU. The ICP-MS instruments could detect chloride (Cl^-) and sulfur (S). The latter could be recalculated as sulfate (SO_4^{2-}), assuming sulfate was the prevailing sulfur species. Earlier investigations have revealed low nitrate concentrations (NO_3^-) (Brøste, 2017). Therefore, ion chromatography analyses of anions were left out of this study. Only analyzes displaying charge balance $\leq \pm 5\%$ between major cations and anions were included in this study to exclude analytical errors.

Alkalinity, pH, electrical conductivity (EC), oxidation–reduction potential (ORP), dissolved oxygen (DO) and temperature were measured in situ. Alkalinity was measured by “Gran titration” (Stumm and Morgan, 1996) with Merck MColorrest, while temperature, pH (WTW SensoIyt 900-P), EC (WTW TetraCon 925/C), ORP (SensoIyt ORP 900-P) and DO (WTW FDO 925) were measured by electrodes connected to a WTW Multi 3630 IDS digital meter. The ORP values were later converted to the redox potential with respect to the normal hydrogen electrode (Eh). The electrodes were submerged in a custom-made flow-through cell, to which water was lead from the same taps where water samples were taken, at 0.1–0.2 l/s flow rate. The sensors were continuously measuring every 30 s for as long as two hours, due to sluggish Eh stabilization.

Biological activity reaction tests (BART) (Hach) were used to identify microbiological activity in the GWHP systems. Tests for iron-oxidizing bacteria (IOB), sulfate-reducing bacteria (SRB) and slime-forming bacteria (SLYM) were carried out for all GWHP systems except Oterholmgården during continuous pumping. Furthermore, the Idegården, Lena terrasse and Oterholmgården GWHP and the old, abandoned production well at Lenavegen 3 were BART sampled after shut-off periods ranging from 2 h to 5 years. Longer shut-off periods are expected to increase the number of bacteria present in the water-phase (Cullimore, 2008). Thus, the BART samples taken after 2 hour and 5 years were not necessarily comparable. The BART test procedure comprised of adding water sampled from the GWHP system/well to an incubator in the laboratory. Type and semi-quantitative count of bacteria could be determined based on time until and type of reaction in the BART incubators.

2.2. Laboratory incrustation analysis

Thirteen incrustation samples were brought to the laboratory for x-ray diffraction (XRD), ICP-MS, loss on ignition (LOI) and magnetic analyses, see Table 2. XRD on single grains and bulk samples and ICP-MS of dissolved incrustations were used to analyze mineralogical and chemical composition, respectively. LOI was used to assess the incrustations' organic content. Observing the incrustation materials' attraction to a magnet was used to assess the presence of magnetic minerals (e.g., metallic

Table 2.

Summary of laboratory and field incrustation analyses in the Melhus GWHP systems. Abbreviations: HE = heat exchanger, pipe = abandoned pipe, pipe filter = filter in groundwater pipes right before heat exchanger, cell = deposits in flow-through cell after water chemical field measurements, inj. = from injection well during rehabilitation.

No.	GWHP system	Sampling site (year)	Sample appearance	Analyses ^a		
				XRD	ICP-MS	LOI
1	Buen	Pipe filter (2019)	Black, hard	+	+	+
2	Gimse	Pipe (2020) ^a	Orange, brittle	+	+	+
3	Høvdingen	Pipe filter (2019)	Orange, brittle	+ ^b	+	+
4	Idegården	Pipe filter (2020)	Black, hard, magnetic	+	N/A	+ ^c
5	Lena terrasse	HE (2018)	Orange, gray, brittle	+	+	+
6	Lena terrasse	HE (2019)	Orange (rinsing fluid)	N/A	+	N/A
7	Lena terrasse	Inj. (2020)	Sediments, orange	+ ^b	+	+
8	Lena terrasse	HE (2021)	Orange (rinsing fluid)	N/A	+	N/A
9	Lenavegen 3	Pipe (old) ^d	Rusty red, brittle	+ ^e	+	+
10	Lenavegen 3	Cell (2020) (new) ^d	Sand, gravel	+	N/A	+
11	Melhuset	Pipe (2019) ^a	Orange, layered	+	+	+
12	Oterholmgården	HE (2021)	Light yellow (rinsing fluid)	N/A	+	N/A
13	Thoragården	Cell (2020)	Black, flaky, magnetic	+ ^b	+	N/A

^aXRD, LOI and ICP-MS of used rinsing fluids were carried out continuously (i.e., shortly after sampling), while ICP-MS analysis of nitric acid dissolved incrustations were carried out in May 2020.

(a) Two (Gimse, Lenavegen 3) and five (Melhuset) years storage under atmospheric conditions prior to sampling.

(b) XRD analysis of single grain.

(c) Ignited at 450°C (all others at 400°C).

(d) Samples from old, abandoned production well and new, currently operating GWHP system.

(e) Data from Brøste (2017).

iron). Houben and Treskatis (2007) recommend sampling fresh incrustation material to avoid maturation and contamination. It was difficult to obtain fresh samples from the GWHP systems. Consequently, incrustations which had been stored up to five years under atmospheric conditions prior to sampling were included in the sampling program.

The samples analyzed by XRD (Bruker D8 Advance) and for LOI (Nabertherm B180) were mortared and dried at 35/65°C (XRD) and

105°C (LOI) prior to analysis. The LOI, measured as % weight loss after 4 h of ignition at 400°C, was assumed to equal the incrustation sample's organic content, as suggested by McLaughlan (1992). This temperature is conservative compared with the custom 550°C, but reduces the risk of igniting carbonates. ICP-MS analyses were performed both on (1) solid incrustations dissolved in nitric acid (HNO₃) and filtered in the mineralogy lab at the Department of Geoscience and Petroleum, NTNU (Perkin Elmer ELAN DRC II), and (2) rinsing fluid samples containing both dissolved incrustations and rehabilitation chemicals in the chemistry lab at the Department of Chemistry, NTNU (Element 2 - ICP-HR-MS, Agilent 8800). All other analyses were carried out in the mineralogical lab at the Department of Geoscience and Petroleum, NTNU.

2.3. Camera inspection and other field observations

Well camera inspections have been carried out in eight out of nine GWHP system in Melhus, see Table 1, to assess incrustation type and extent, and evaluate well rehabilitation success. The inspections were carried out from 2013 onwards by local water and wastewater entrepreneur Gjøvaag AS. Some of the inspections have already been described by Riise (2015) and Gjengedal et al. (2018; 2020).

Field observations of water quality were performed, including observation of suspended solid deposition in the flow-through cell and H₂S gas odor. Furthermore, mud color registered during drilling of the observation wells, see Fig. 1, was used to assess redox conditions. The depth where the color changed from orange/red to clear/gray was interpreted as the transition depth from oxic to anoxic iron conditions. This was based on the characteristic rusty color of iron oxides which forms under oxic conditions.

3. Results

3.1. Water quality

The GWHP systems' key hydrochemical data are summarized in Table 3. The coexistence of different water types in the Melhus aquifer is evident from the range of total dissolved solids. Most GWHP systems extract a typical seawater Na-Cl water quality, while a mixed Ca-HCO₃/

Cl water type is found at Gimse and Lena terrasse. The groundwater is neutral-basic and alkaline. Dissolved oxygen, iron and manganese concentrations correspond to an anoxic, iron-reducing redox regime, while measured redox potentials (Eh) indicate iron oxidation as the dominant redox process (Stumm and Morgan, 1996).

None of the BART tests from the first batch (i.e., taken after longer periods of continuous pumping of the GWHP system) had reacted after 9 days in the incubator. This indicated "non-aggressive" activity of IOB, SRB and SLYM. For the second batch of BART testers (i.e., taken after pump shut-off periods), the Lenavegen 3 (abandoned production well), Lena terrasse and Oterholmgården IOB incubators yielded brown clouds and rings after 3–8 days. This indicated "moderate" (5–8 days to reaction) to "aggressive" (0–4 days to reaction) bacteria activities, see Fig. 2. "Non-aggressive" IOB activity (≥ 9 days to reaction) was detected at Idegården even after pump shut-off. Some of the IOB samples reacted to form bubbles and blackened liquids. This is indicative of anaerobic and SLYM bacteria (Cullimore, 2008), respectively. The long reaction times of the SLYM and SRB incubators imply "non-aggressive" growth of these bacteria groups, see Fig. 2.

3.2. Laboratory incrustation analysis

The laboratory incrustation analyzes are summarized in Fig. 3. Goethite (FeOOH), mackinawite (FeS), quartz (SiO₂) and other silicates were the main phases detected during XRD analysis. However, the XRD analysis only yielded information about the crystalline part of the incrustation samples, which was generally low. Iron was the main element detected during ICP-MS of dissolved incrustations, with smaller amounts of calcium, sodium, and sulfur. The iron oxide dominated incrustations' ferrihydrite (Fe(OH)₃) weight percentages were estimated from the incrustations' iron concentration (from ICP-MS). The calculations assumed that all dissolved iron stemmed from ferrihydrite. Iron sulfide weight percentage was not estimated for the sulfide dominated Buen incrustation sample, since the nitric acid was ineffective dissolving this sample. The incrustations which contained iron oxides displayed a higher loss on ignition than those primarily consisting of iron sulfides and/or silicates. Most incrustation samples displayed a low degree of magnetism. The exceptions were the Thoragården and Idegården

Table 3.

Summary of key water chemical parameters measured in the GWHP systems, represented as mean \pm two standard deviations (SD). See Table 1 for explanation for GWHP system abbreviations.

GWHP	Water samples (ICP-MS)					Field measurements				
	Fe ²⁺ (mg/l)	Mn ²⁺ (mg/l)	Ca ²⁺ (mg/l)	Cl ⁻ (mg/l)	SO ₄ ²⁻ (mg/l)	TDS (g/l)	Alk (mM)	pH	Eh (mV)	DO (mg/l)
A) Buen	4.03 \pm 1.97	0.63 \pm 0.06	99 \pm 9	552 \pm 81	176 \pm 19	1.53 \pm 0.12	4.9 \pm 0.2	7.46 \pm 0.07	42 \pm 28	0.03 \pm 0.01
B) Gim.	1.70 \pm 0.73	0.17 \pm 0.02	87 \pm 9	17 \pm 4	130 \pm 17	0.50 \pm 0.05	3.5 \pm 0.6	7.40 \pm 0.21	47 \pm 58	0.04 \pm 0.00
C) Høv.	0.21 (0.14-1.01) ^a	0.07 \pm 0.02	47 \pm 5	998 \pm 147	203 \pm 22	2.24 \pm 0.18	4.5 \pm 0.2	8.13 \pm 0.12	75 \pm 48	0.7 (0.3-2.4) ^a
D) Ide.	3.97 \pm 1.00	0.61 \pm 0.06	107 \pm 16	556 \pm 103	180 \pm 24	1.56 \pm 0.15	5.0 \pm 0.5	7.47 \pm 0.05	40 \pm 41	0.03 (0.03-0.19) ^a
E) Len.t.	3.49 \pm 0.63	0.60 \pm 0.09	138 \pm 14	301 \pm 64	201 \pm 25	1.20 \pm 0.12	5.4 \pm 0.4	7.31 \pm 0.11	107 \pm 33	0.04 \pm 0.01
F1) Len. 3 (old)	5.20 \pm 0.21	0.58 \pm 0.02	119 \pm 5	246 \pm 32	170 \pm 10	1.24 \pm 0.05	7.8 \pm 0.5	7.13 \pm 0.02	49 \pm 65	0.03 \pm 0.01
F2) Len. 3 (new)	4.18 \pm 1.99	0.52 \pm 0.05	69 \pm 5	610 \pm 142	139 \pm 16	1.55 \pm 0.22	4.5 \pm 0.2	7.45 \pm 0.09	8 \pm 29	0.03 \pm 0.01
G) Mel.	1.32 \pm 0.47	0.27 \pm 0.04	51 \pm 8	378 \pm 77	115 \pm 21	1.10 \pm 0.16	4.0 \pm 0.3	7.92 \pm 0.12	11 \pm 10	0.03 \pm 0.00
H) Oter.	2.31 \pm 0.10	0.37 \pm 0.01	52 \pm 1	326 \pm 11	85 \pm 2	1.00 \pm 0.02	4.3 \pm 0.1	7.71 \pm 0.02	15 \pm 41	0.04 \pm 0.01
I) Thor.	0.28 \pm 0.07	0.05 \pm 0.01	49 \pm 3	948 \pm 137	206 \pm 24	2.21 \pm 0.19	5.0 \pm 0.3	8.11 \pm 0.14	-19 \pm 37	0.03 \pm 0.00

GWHP system (number of samplings): A ($n = 8$), B ($n = 5$ water samples (ws) + alkalinity (alk), $n = 6$ for other field measurements (fm)), C ($n = 4$ ws + alk, $n = 3$ fm), D ($n = 8$), E ($n = 7$ ws + alk, $n = 8$ fm), F1 ($n = 1$), F2 ($n = 6$ ws + alk, $n = 7$ fm), G ($n = 8$), H ($n = 1$), I ($n = 7$ ws + alk, $n = 8$ fm). Where $n = 1$, analytical mean and error is displayed.

^(a) Measured values vary considerably, thus median and range of values is displayed instead of mean \pm 2SD.

GWHP	Lenavegen 3 (old)				Idegården		Lena terrasse		Oterholmgården	
Date(s)	03.09.20				02.12.20		02.12.20	22.01.21	17.03.21	
Shut-off period	5 years				2 hours		2 hours	2 days	1 day	
Q (l/s)	1.0				6.5		8.1	12.1	5.5	
Sampling time (min)	10	60	120	240	2	90	10	120	30	120
IOB rx. time (days)	3	4	5	5	-	-	5	7	6	6
BART-IOB incubator (time after sampling)										
	3 days	4 days	5 days	5 days	9 days	9 days	5 days	7 days	6 days	6 days
SLYM rx. time (days)	7	7	7	7	-	-	7	9	8	8
SRB rx. time (days)	-	-	-	-	-	-	N/A	-	-	-

Fig. 2.. Results from biological activity reaction tests (BART) taken after pump shut-off periods. Sampling time refers to time after re-start of pumping. Old = abandoned, defect production well, see Fig. 1. Rx. = reaction. “-“ means reaction after > 9 days. Color refers to bacteria activity: red = aggressive, yellow = moderate, green = non-aggressive. N/A = not sampled.

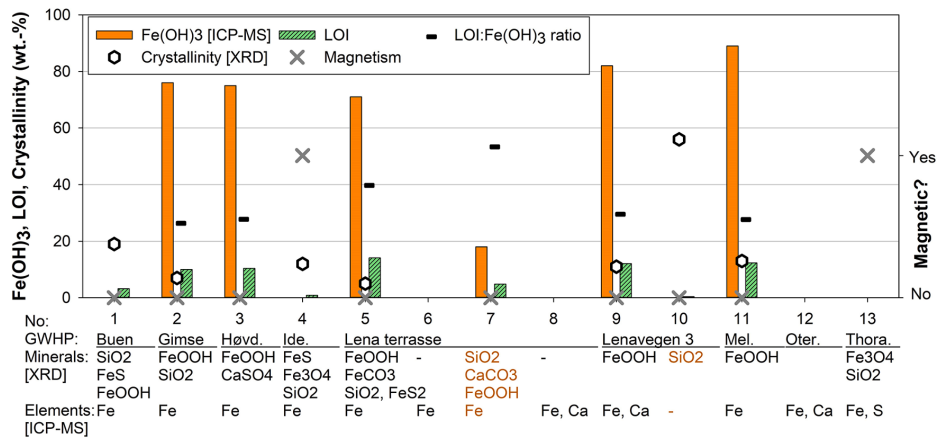


Fig. 3.. Summary of incrustation analyses. Plot of weight-percentage (wt.-%) of Fe(OH)₃ (calculated from ICP-MS analysis), loss on ignition (LOI) and crystallinity (from XRD analysis). Also calculated LOI: Fe(OH)₃ ratio and magnetism (yes/no) is plotted. “Elements [ICP-MS]” refer to elements with weight concentration ≥ 2%. XRD analyzed samples not displaying crystallinity (3, 7, 13) were performed on single grains (small sample). Mineral and element formulas: SiO₂ = quartz (refers to quartz and other silicate minerals), FeS = mackinawite, FeOOH = goethite, CaSO₄ = gypsum, NaCl = halite, Fe₃O₄ = magnetite, FeCO₃ = siderite, FeS₂ = pyrite, CaCO₃ = calcite, Fe = iron, Ca = calcium, S = sulfur.

incrustations, which contained the magnetic mineral magnetite (Fe₃O₄) (from XRD).

3.3. Camera inspection and other field observations

Observations from camera inspections and drilling logs are shown in Fig. 4 and plotted versus location in Fig. 5, where observations are simplified to one single point representative for each incrustation type.

Camera inspection and laboratory incrustation analyses pointed to iron oxides and iron sulfides as the main chemical incrustation minerals.

Observations during camera inspections were interpreted based on laboratory incrustations analyzes (XRD, ICP-MS) and the authors’ experience with incrustation appearance (color, structure). Orange incrustations were interpreted as iron oxides. Black, hard incrustations were interpreted as iron sulfide incrustations. The latter were first wrongly interpreted as manganese oxides due to their similar visual appearance. Followingly, it could be distinguished that Gimse, Høvdingen, Lena terrasse, Lenavegen 3 (abandoned well), Melhuset and Oterholmgården suffered from iron oxide incrustations, while Buen, Idegården and Thoragården suffered from iron sulfides. Both iron oxide

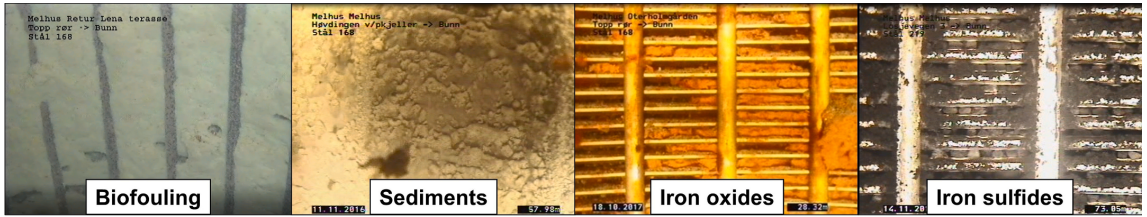


Fig. 4.. Photos from camera inspections: Lena terrasse's injection well screen in 2018 (left), Høvdingen's injection well screen in 2016 (middle left), Oterholmgården's injection well screen in 2017 (middle right), and the production well screen at Thoragården in 2016 (right).

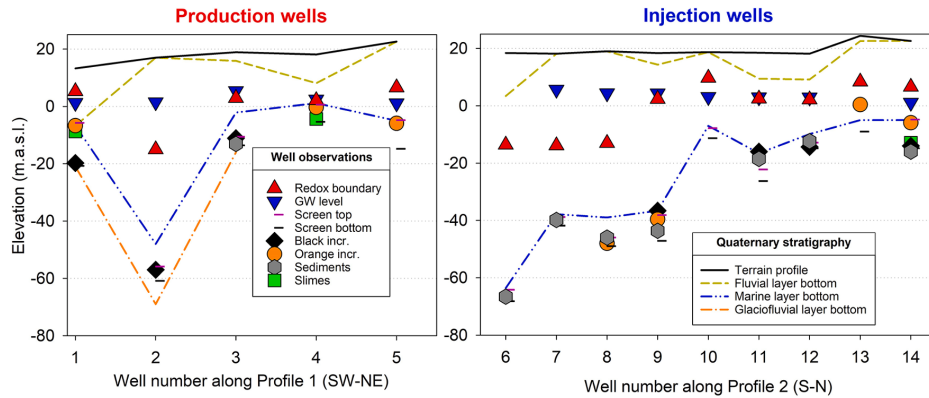


Fig. 5.. Camera inspections and drilling logs. Observations during camera inspections of production (left) and injection wells (right). X-axis not to scale. "Redox boundary" refers to transition from oxic to iron-reducing conditions, and is interpreted from visual observations during well drilling. GW = groundwater. The glaciofluvial layer bottom could not be indicated entirely along the profiles since drilling was often stopped before reaching bottom of the layer.

and sulfide incrustations were accompanied with varying levels of sediments (silicates), most likely stemming from the aquifer formation or well filter pack (i.e., mechanical incrustation). The new Lenavegen 3 GWHP production well has not been camera inspected, but deposition of gravel sized (> 2 mm) sediments in the flow-through cell have been observed several times during hydrochemical measurements.

4. Discussion

Kinetic calculations show that the water residence times (on the scale of minutes) of GWHP systems incrustated by iron oxides are well below the homogenous iron oxidation half-times (on the scale of hours to days). Half-times were calculated by modifying Eq. (2), and assuming a rate constant k around 1.4×10^{-12} mol/min (Houben, 2004). The discrepancies between reaction half- and residence time indicate that abiotic, homogenous iron oxidation is not intense enough to clog the systems alone. Severe iron oxide clogging has been detected under similar redox conditions as in the Melhus aquifer, in water supply wells in Belgrade, Serbia (Barbić et al., 1974; Dimkić et al., 2012) and an ATEs system in Berlin, Germany (Lerm et al., 2011; Eggerichs et al., 2014). The activity of iron-oxidizing bacteria was identified to control the clogging at the latter two sites (Barbić et al., 1974; Lerm et al., 2011). These results suggest heterogenous, biotic catalysis should be considered for the GWHP systems in Melhus as well.

Microbes prefer to inhabit solid surfaces if nutrients are continuously supplied (e.g., around a production well screen during continuous pumping), but will start to move out in the liquid phase under more stagnant conditions (Cullimore, 2008). Thus, BART samples taken during continuous pumping is likely to reflect the background microbiological activity in the aquifer, while samples after pump shut-off periods

probably reflect microbes in and around the well screen incrustations. Iron-oxidizing bacteria (IOB) and slime-forming bacteria (SLYM) incubators taken after pump shut-off periods reacted much faster than the ones taken during continuous pumping in iron oxide incrustated systems (Lena terrasse, Lenavegen 3 (old), Oterholmgården), while long reaction times were observed in the iron sulfide incrustated system (Idegård), see Fig. 2. This implies good growth conditions for IOB and SLYM bacteria in iron oxide incrustated GWHP systems.

There also seems to be a link between chemical incrustation type and hydrochemistry, see Fig. 6. Most strikingly, iron oxides seem to incrust systems extracting water of lower salinity (TDS). On the other hand, there is no distinct relation between concentration of the redox sensitive species dissolved oxygen, nitrate (Riise, 2015; Brøste, 2017; Solberg et al., 2014), iron, manganese and sulfate, and incrustation type. One exception is the Høvdingen GWHP system which measured considerably higher dissolved oxygen levels than the other systems, probably due to oxygen in-leakage through a sediment filter installed in the groundwater pipes just before the heat exchanger. The rest of the systems extract water with similar redox conditions.

The salinity's apparent effect on incrustation type could also be indirect, by its influence on the microbial community. The two most common iron-oxidizing bacteria *Gallionella* and *Leptothrix* have been observed to prefer lower salinities (McBeth et al., 2013; Eggerichs et al., 2014). This is in correspondence with the observed iron oxide incrustations and activity of iron-oxidizing bacteria in Melhus, see Fig. 6. The higher loss on ignition (i.e., a proxy for organic matter content) in the low-saline, iron oxide incrustated GWHP systems indicate that bacteria thrive more in these systems.

The GWHP system which has suffered the most clogging issues (i.e., the iron oxide incrustated Lena terrasse (Table 1)) is furthermore

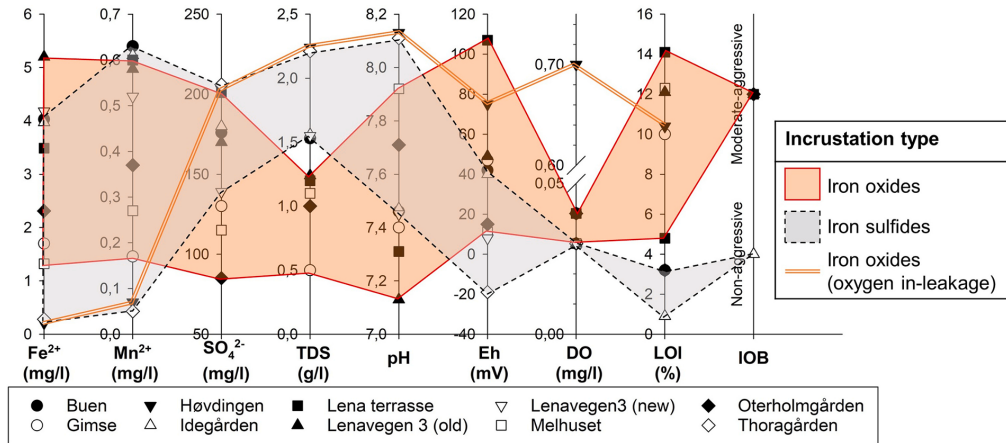


Fig. 6.. Relation between hydrochemistry (average and median values from Table 3) and major chemical incrustation type for groundwater heat pump (GWHP) systems in Melhus, Norway. TDS = total dissolved solids, DO = dissolved oxygen, LOI = loss on ignition, IOB = iron-oxidizing bacteria.

characterized by relatively high iron concentrations (> 3 mg/l) and a circumneutral pH (7.2–7.4), see Fig. 6. These pH conditions are favorable for the neutrophilic (i.e. thrive at circumneutral pH) *Gallionella* and *Leptothrix* genera (Eggerichs et al., 2014), while higher iron concentrations at least are favorable for the *Gallionella* bacteria. The Lena terrasse GWHP also display the highest measured redox potentials (Fig. 6), which indicates that iron oxidation is most active in this system.

From a purely abiotic point of view, a lower pH imposes slower homogenous and heterogenous iron oxidation rates, see Eqs. (2) and (3). Thus, the hydrochemistry of the iron oxide incrustated Oterholmgården and Lena terrasse suggest faster iron oxide clogging at Oterholmgården than Lena terrasse. Using mean/median values from Table 3 inserted in Eqs. (2) and (3), suggest 60–310% faster iron oxidation at Oterholmgården than Lena terrasse, depending on whether homogenous or heterogenous oxidation is rate controlling. This assumes the same rate constants for both systems, due to comparable salinities in the two GWHP systems (Sung and Morgan, 1980). More clogging related rehabilitations and reconstructions (Table 1) and higher redox potentials measured at Lena terrasse than Oterholmgården, rejects the hypothesis of a purely abiotic cause of iron oxide clogging. This further highlights the microbes' importance on iron oxidation and incrustation.

Odor of H_2S gas has been documented in the GWHP systems in Melhus, which together with high ferrous iron concentrations facilitates iron sulfide precipitation. Measured redox potentials (Fig. 6) suggest sulfate reduction is not a governing redox process. This indicates that the iron sulfide formation at Buen, Idegården and Thoragården could be a pure precipitation reaction. Limited sulfate reduction around the well systems also may explain the low sulfate reducing bacteria (SRB) activity deduced from BART tests, see Fig. 2. Possibly, the mechanical incrustations often found together with the iron sulfides (Fig. 5) may be the major clogging process in these well systems.

The hydrochemistry at Lenavegen 3 resembles that of Idegården and Buen, see Fig. 6. Iron sulfides are thus expected to incrust this production well as well. Furthermore, the gravel size (> 2 mm) sediment deposits found in the flow-through cell during measurement at Lenavegen 3 is indicative of serious abrasion/corrosion of the 1 mm production well screen slots. This could possibly have been mediated by incrustations blocking the formation filter and/or well screen.

The magnetism of the incrustation samples from Idegården and Thoragården indicates that these GWHP systems suffer from corrosion. Holes detected in a steel valve in the groundwater pipeline at Idegården in December 2020 further confirms the corrosion problems. The "non-

aggressive" SRB activity at Idegården from BART tests is thus surprising, since these bacteria often form essential parts of corrosion processes (Houben and Treskatis, 2007). However, more detailed investigations of the microbiology must be conducted to disprove the presence of SRBs.

The camera inspections show that iron oxides incrust shallower while iron sulfides incrust deeper production wells, see Fig. 5. This corresponds with proximity to the oxic to iron-reducing redox boundary. Still redox species concentrations and measured redox potentials are comparable in the shallow and deep systems. The depth tendency for iron oxide formation also correlates with changing salinity and pH with depth, which could influence microbial activity, as mentioned above.

Some exceptions to the trend of shallow iron oxide and deep iron sulfide incrustations are also found. What resembles iron sulfides have been observed in the bottom part of the relatively long well screens at the Gimse production well (15 m) and the Lena terrasse injection well (10 m). Non-uniform flow through well screens may lead to stagnant zones in the bottom part of the well screens which promotes anoxic conditions (Mansuy, 1998). This could explain the observations at Gimse and Lena terrasse. On the other hand, iron oxides are found in some deep injection wells at Idegården and Høvdingen, which is probably caused by oxygen in-leakage through the surface part of the groundwater pipes. Relatively high oxygen concentrations (> 0.1 mg/l) have been detected in both these GWHP systems, see Table 3. The corrosion holes at Idegården and a leaky sediment filter at Høvdingen are probably responsible for these oxygen levels.

Mechanical incrustations (i.e., sediment deposits) seem to be a bigger problem for injection than production wells. This can be explained by injection wells functioning as a sink for sediments mobilized in the production well. The cementation of mechanical incrustation with iron oxides or sulfides may explain why injection wells suffer more from deteriorating clogging problems. Mobilization in the production well can both be caused by improper well development or filter design, or incrustations blocking the inflow cross-section and causing turbulent flow (Mansuy, 1998; Bakema, 2001). It is noteworthy that the GWHP systems which have suffered the most from mechanical incrustations have (1) relatively short production well filters (3.0–3.5 m) (Buen, Høvdingen, Lenavegen 3, Thoragården) and/or high pumping rates (Lenavegen 3, Lena terrasse), see Table 1. Longer well filter designs and lower pumping rates thus may be a viable measure against mechanical clogging problems in Melhus.

Some uncertainties are associated with the field water quality and the laboratory incrustation analyses. Redox potentials did not stabilize

during the two-hour measurement period in any of the GWHP systems. Still, consistent redox levels prevail for each GWHP system over the two-year sampling period. The two-hour reading was thus believed to be indicative of the relative Eh level between the nine GWHP systems. Furthermore, measured oxygen levels are lower than the zero-point of the oxygen sensor. Still, correlations between temperature and oxygen even below the zero-point are observed, which indicates that at least some oxygen is present in the pumped-up groundwater. Lastly, the long storage time of incrustation samples made them vulnerable to oxidation of sulfides and organic matter, and maturation of amorphous iron oxides. Few samples displayed a partition between sulfides and oxides, neither analytically nor visually between core and surface, as would have been expected for partial oxidation of sulfide samples. Organic matter contents (LOI) of iron oxide samples were comparable to those found by [McLaughlan \(1992\)](#) despite long storage periods. This is interpreted as a sign of modest organic matter decomposition with time, and backs up the reliability of the analytical method. The crystallinity of iron oxide incrustation samples detected during XRD analysis were generally low, and thus rule out substantial maturation to have occurred. Consequently, the results and analysis presented here are concluded to be valid.

4.1. Practical implications

Both iron oxides and sulfides incrust the GWHP systems, although most systems extract anoxic water from well below the iron redox boundary. Thus, vertical mixing of water from different redox zones in the production well is probably not triggering the iron oxide precipitation. Furthermore, iron sulfide incrustations are also found. This means locating the production well screen deep beneath the iron redox boundary, as suggested by [Possemiers et al. \(2016\)](#), will probably not prevent incrustation problems in Melhus. The well owners should rather focus on regular maintenance with appropriate rehabilitation methods. Still, this study reveals which conditions are favorable for oxide and sulfide formation, meaning the well designers could to some extent pick their problems from well location and dimensioning.

The range of deteriorating problems detected in the GWHP systems in Melhus justifies proper monitoring and analysis of the incrustation problems. System performance monitoring of pressure, temperature and flow rate, as described in [Gjengedal et al. \(2020\)](#), is a prerequisite for early clogging detection, but does not necessarily provide implications for further actions. This can be illustrated by the difference between iron oxides and sulfides: While iron oxides are best dissolved by the reducing agent sodium dithionite ($\text{Na}_2\text{S}_2\text{O}_4$) under pH neutral conditions ([Houben, 2003](#)), this measure will not dissolve iron sulfide incrustations, which are best dissolved by inorganic acids (e.g., hydrochloric acid (HCl) ([Houben and Treskatis, 2007](#))), or an oxidizing agent (e.g., sodium hypochlorite (NaClO) ([van Beek and Kooper, 1980](#))).

Incrustation samples can be hard to obtain but will help to interpret the observations during camera inspections. The GWHP system design should thus facilitate easy access for water and incrustation sampling and camera inspections, as already suggested by [Gjengedal et al. \(2018\)](#). The combination of flow-through cell measurements and BART tests have proven to yield valuable information on biochemical incrustation potential. Both methods are therefore advised to be included for GWHP clogging risk assessment.

5. Conclusions

The investigations presented in this article show that:

- Iron oxides and iron sulfides, together with aquifer sediments, incrust groundwater heat pump (GWHP) systems extracting water from the same saline (total dissolved solids = 0.4–2.4 g/l), anoxic (dissolved oxygen ≤ 0.05 mg/l), and iron-rich (dissolved ferrous iron = 0.14–6.44 mg/l) aquifer in Melhus.
- Water quality seems to dictate problem type, with sulfides incrusting systems extracting deeper, more saline groundwater, while shallower systems extracting fresher groundwater suffer from iron oxide incrustations. The identification of iron-oxidizing bacteria (IOB) from biological activity reaction tests (BART) solely in iron oxide incrustated GWHP systems, also point to biotic influence on incrustations
- The most frequent clogging problems were detected in the Lena terrasse GWHP system which is clogged by iron oxides and sediments. This GWHP system displays the highest redox potential, high organic matter (LOI) to iron oxide ratios in the incrustations, IOBs present (BART), relatively high groundwater pumping rates and high iron concentrations. This combination of hydrochemical, biotic and hydraulic conditions seems to facilitate severe clogging
- Though type and severity of iron incrustations to some extent could be controlled by location and design of the systems, these clogging issues must be expected in groundwater heat pump systems. Thus, more focus should be directed towards tailored and timed rehabilitations. Detailed water quality and incrustation investigations should be compulsory prior to and during operation to customize cost-effective rehabilitation techniques.

Funding

This work was supported by the Regional Research Funds in Mid-Norway [grant number 284965]; the Norwegian University of Science and Technology (including St. Olav's Hospital - Trondheim University Hospital). The funding sources were not involved in the study design, writing of the report; nor in the decision to submit the article for publication.

Availability of data and material

The authors approve that all data and materials support their published claims and comply with field standards. The authors agree to share their research data.

Ethics approval

The authors approve that they have followed the rules of good scientific practice.

CRediT authorship contribution statement

Lars A. Stenvik: Conceptualization, Data curation, Formal analysis, Investigation, Methodology, Project administration, Software, Visualization, Writing – original draft. **Sondre Gjengedal:** Conceptualization, Data curation, Formal analysis, Investigation, Methodology, Supervision, Visualization, Writing – review & editing. **Randi K. Ramstad:** Conceptualization, Data curation, Formal analysis, Funding acquisition, Investigation, Project administration, Resources, Supervision, Writing – review & editing. **Bjørn S. Frengstad:** Conceptualization, Formal analysis, Funding acquisition, Methodology, Project administration, Resources, Supervision, Validation, Writing – review & editing.

Declaration of Competing Interest

The authors declare that they have no known competing financial interests or personal relationships that could have appeared to influence the work reported in this paper.

Acknowledgements

This study is part of the research project Optimal Utilization of Groundwater for Heating and Cooling in Melhus 2 (ORMEL 2). This is a cooperation between Melhus municipality, the Norwegian University of

Science and Technology, Asplan Viak AS, the Geological Survey of Norway and Gjøvaag AS, receiving funding from the Regional Research Funds in Mid-Norway. We would like to thank all the involved institutions and persons for cooperation and financial support, and all the helpful janitors at the GWHP plants in Melhus. We would also like to thank senior engineers Torill Sørør and Laurentius Tjihuis at the mineralogical lab for help with XRD, ICP-MS and LOI analysis and discussions, and to staff engineer Håkon Myhren at the mechanical lab who designed, built, and rehabilitated the flow-through cell (all three at the Department of Geoscience and Petroleum, NTNU). Furthermore, many thanks to Dr. Georg J. Houben at the Federal Institute for Geosciences and Natural Resources (BGR) in Hannover, Germany for helpful input on iron bacteria, and to Dr. Clara Sena at the University of Oslo for discussions and input on data interpretation and presentation. Finally, the authors would like to thank the two reviewers for their constructive comments and feedback.

Supplementary materials

Supplementary material associated with this article can be found, in the online version, at doi:[10.1016/j.geothermics.2022.102349](https://doi.org/10.1016/j.geothermics.2022.102349).


References

- Bakema, G., 2001. Well and Borehole Failures and Solutions in Underground Thermal Energy Storage. IF Technology, Arnhem. <https://doi.org/10.13140/RG.2.2.10214.98885>. IF Technology report 2/9805/GW.
- Barbić, F.F., Bracilović, D.M., Djindjić, M.V., Djorelijevski, S.M., Živković, J.S., Krajinčanić, B.V., 1974. Iron and manganese bacteria in Ranney wells. *Water Res.* 8 (11), 895–898. [https://doi.org/10.1016/0043-1354\(74\)90103-1](https://doi.org/10.1016/0043-1354(74)90103-1).
- Broste, H.M., 2017. Vannkvalitet knyttet til Grunnvannsbaserte grunnvarmeanlegg i Melhus og Elverum [Eng: Water Quality in Groundwater-Based Heat Pump Systems in Melhus and Elverum. NTNU, Trondheim. In Norwegian] (Master thesis).
- Burté, L., Cravotta III, C.A., Bethencourt, L., Farasin, J., Pédrot, M., Dufresne, A., Gerard, M.F., Baranger, C., Le Borgne, T., Aquilina, L., 2019. Kinetic study on clogging of a geothermal pumping well triggered by mixing-induced biogeochemical reactions. *Environ. Sci. Technol.* 53 (10), 5848–5857. <https://doi.org/10.1021/acs.est.9b00453>.
- Cullimore, D.R., 2008. *Practical Manual of Groundwater Microbiology*, 2nd ed. CRC Press, Boca Raton.
- Dimkić, M., Pušić, M., Obradović, V., Kovačević, S., 2012. The effect of certain biochemical factors on well clogging under suboxic and mildly anoxic conditions. *Water Science and Technology* 65 (12), 2206–2212. <https://doi.org/10.2166/wst.2012.129>.
- Eggen, G., Vangnes, G., 2005. Heat pump for district cooling and heating at Oslo airport, Gardermoen. In: Axell, M. (Ed.), 8th IEA Heat Pump Conference. Las Vegas, USA. Borås, Ed. IEA Heat Pump Centre.
- Eggerichs, T., Opel, O., Otte, T., Ruck, W., 2014. Interdependencies between biotic and abiotic ferrous iron oxidation and influence of pH, Oxygen and Ferric Iron Deposits. *Geomicrobiol. J.* 31 (6), 461–472. <https://doi.org/10.1080/01490451.2013.870620>.
- Gjengedal, S., Ramstad, R.K., Hilmo, B.O., Frenstad, B.S., 2018. Video inspection of wells in open loop ground source heat pump systems in Norway. IGSHPA Research Track, Stockholm. Oklahoma State University, Sweden. Stillwater. <https://doi.org/10.22488/okstate.18.000025>.
- Gjengedal, S., Stenvik, L.A., Storli, P.T.S., Ramstad, R.K., Hilmo, B.O., Frenstad, B.S., 2019. Design of Groundwater Heat Pump Systems. Principles, Tools, and Strategies for Controlling Gas and Precipitation Problems. *Energies* 12 (19), 3657. <https://doi.org/10.3390/en12193657>.
- Gjengedal, S., Ramstad, R.K., Hilmo, B.O., Frenstad, B.S., 2020. Fouling and clogging surveillance in open loop GSHP systems. *Bull. Eng. Geol. Environ.* 79, 69–82. <https://doi.org/10.1007/s10064-019-01556-5>.
- Hellestveit, M.S., 2018. 3D-Modellering av Grunnvannstrømning og Varmetransport i Akviferen i Melhus sentrum [Eng: 3D Modelling of Groundwater Flow and Heat Transport in the Aquifer in Central Melhus. NTNU, Trondheim. In Norwegian] (Master thesis).
- Houben, G.J., 2003. Iron oxide encrustations in wells. Part 2: chemical dissolution and modeling. *Appl. Geochem.* 18 (6), 941–954. [https://doi.org/10.1016/S0883-2927\(02\)00185-3](https://doi.org/10.1016/S0883-2927(02)00185-3).
- Houben, G.J., 2004. Modeling the Buildup of Iron Oxide Encrustations in Wells. *Groundwater* 42 (1), 78–82. <https://doi.org/10.1111/j.1745-6584.2004.tb02452.x>.
- Houben, G.J., Treskatis, C., 2007. *Water Well Rehabilitation and Reconstruction*. McGraw-Hill, New York.
- Lerm, S., Alawi, M., Miethling-Graff, R., Wolfram, M., Rauppach, K., Seibt, A., Würdemann, H., 2011. Influence of microbial processes on the operation of a cold store in a shallow aquifer: impact on well injectivity and filter lifetime. *Grundwasser* 16 (2), 93–104. <https://doi.org/10.1007/s00767-011-0165-x>.
- Mansuy, N., 1998. *Water Well Rehabilitation: A Practical Guide to Understanding Well Problems and Solutions*. CRC Press, Boca Raton.
- McBeth, J.M., Fleming, E.J., Emerson, D., 2013. The transition from freshwater to marine iron-oxidizing bacterial lineages along a salinity gradient on the Sheepsfoot River. *Environ. Microbiol. Rep.* 5 (3), 453–463. <https://doi.org/10.1111/1758-2229.12033>.
- McLaughlan, R.G., 1992. *Fouling and Corrosion of Groundwater Wells in Australia*. University of New South Wales, Kensington. Ph.D. thesis.
- Possemiers, M., Huysmans, M., Anibas, C., Batelaan, O., Van Steenwinkel, J., 2016. Reactive transport modeling of redox processes to assess Fe(OH)₃ precipitation around aquifer thermal energy storage wells in phreatic aquifers. *Environ. Earth Sci.* 75, 648. <https://doi.org/10.1007/s12665-016-5398-7>.
- Reite, A.J., 1990. Sør-Trøndelag fylke: Kvartærgeologisk Kart M 1:250.000: Veiledning Til Kartet [Eng: Sør-Trøndelag county: Quaternary geology Map M 1:250.000 : Guidance to the map. In Norwegian]. Skriftr 96. Geological Survey of Norway, Trondheim.
- Riise, M.H., 2015. Praktisk guide for grunnvarmeanlegg basert på oppumpet grunnvann: Hydrogeologiske undersøkelser, etablering, drift og oppfølging med utgangspunkt i erfaringer fra etablerte anlegg i Melhus sentrum [Eng: Practical Guide for Ground Water Heat Pump Systems. NTNU, Trondheim. In Norwegian] (Master thesis).
- Solberg, L.L., Dagestad, A., Dalsegg, E., 2014. 2D resistivitetsmålinger ved Brubakken, Melhus sentrum og Skjerdingsstad i Melhus kommun, Sør-Trøndelag. Data og tolkninger [Eng: 2D resistivity measurements at Brubakken, Melhus town center and Skjerdingsstad in Melhus municipality. Data and interpretations. Geological Survey of Norway, Trondheim. In Norwegian] NGU report 2014.022.
- Statistics Norway. (2020). Population and land area in urban settlements. <https://www.ssb.no/en/befolkning/folketall/statistikk/tettsteders-befolkning-og-areal>. Accessed 30 August 2021.
- Stumm, W., Lee, G.F., 1961. Oxygenation of Ferrous Iron. *Ind. Eng. Chem.* 53 (2), 143–146. <https://doi.org/10.1021/ie50614a030>.
- Stumm, W., Morgan, J.J., 1996. *Aquatic chemistry: Chemical Equilibria and Rates in Natural Waters*, 3rd ed. John Wiley & Sons Inc, Hoboken.
- Sung, W., Morgan, J.J., 1980. Kinetics and product of ferrous iron oxygenation in aqueous systems. *Environ. Sci. Technol.* 14 (5), 561–568. <https://doi.org/10.1021/es60165a006>.
- Tamura, H., Goto, K., Nagayama, M., 1976. The effect of ferric hydroxide on the oxygenation of ferrous ions in neutral solutions. *Corrosion Sci.* 16 (4), 197–207. [https://doi.org/10.1016/0010-938X\(76\)90046-9](https://doi.org/10.1016/0010-938X(76)90046-9).
- van Beek, C.G.E.M., 1989. Rehabilitation of clogged discharge wells in the Netherlands. *Q. J. Eng. Geol. Hydrogeol.* 22, 75–80. <https://doi.org/10.1144/GSL.QJEG.1989.022.01.06>.
- van Beek, C.G.E.M., Kooper, W.F., 1980. The clogging of shallow discharge wells in the Netherlands river region. *Groundwater* 18 (6), 578–586. <https://doi.org/10.1111/j.1745-6584.1980.tb03652.x-0537-9>.

Paper III

Article

Design of Groundwater Heat Pump Systems. Principles, Tools, and Strategies for Controlling Gas and Precipitation Problems

Sondre Gjengedal ^{1,*} , Lars A. Stenvik ¹, Pål-Tore S. Storli ², Randi K. Ramstad ¹, Bernt O. Hilmo ³ and Bjørn S. Frengstad ¹

¹ Department of Geoscience and Petroleum, Norwegian University of Science and Technology, 7034 Trondheim, Norway; lars.a.stenvik@ntnu.no (L.A.S.); randi.kalskin.ramstad@ntnu.no (R.K.R.); bjorn.frengstad@ntnu.no (B.S.F.)

² Department of Energy and Process Engineering, Norwegian University of Science and Technology, 7034 Trondheim, Norway; pal-tore.storli@ntnu.no

³ Asplan Viak AS, 7030 Trondheim, Norway; berntolav.hilmo@asplanviak.no

* Correspondence: sondre.gjengedal@ntnu.no

Received: 30 July 2019; Accepted: 23 September 2019; Published: 25 September 2019



Abstract: The utilization of groundwater heat pump systems is increasing in Norway, which are currently widely employed for heating and cooling applications in the town center of Melhus. The investigations of the Melhus installations are detecting gas exsolution as a possible trigger for precipitation reaction that causes incrustation of iron and manganese compounds in the systems. This paper discusses risks associated with gas exsolution and considers gas exsolution triggers in a typical Norwegian groundwater heat pump (GWHP) system configuration. The concept of the solubility grade line (SGL) is developed and suggested as a tool for optimizing the design. Based on SGL analysis and the intention of avoiding gas exsolution during heat production, an alternative system design in the same aquifer is presented and compared. The analyses show that the traditional system design is predisposed to gas clogging risks and prone to vacuum pressures in parts of the system. The alternative design mediates the risks by adjusting the well and piping configuration and by applying a backpressure technique. The results demonstrate how the groundwater heat pump system design can be customized according to local aquifer conditions to avoid gas exsolution during operation. It is recommended that the presented method of analysis should be utilized in dimensioning of systems and included in the monitoring scheme of the systems.

Keywords: groundwater; groundwater heat pump (GWHP) systems; aquifer; design and control principles; dissolved gases; temperature; pressure; hydraulic grade line; solubility grade line

1. Introduction

Ground source heat pump (GSHP) systems have become increasingly popular in Norway during the recent decades. Similar trends are also seen worldwide, and recent studies indicate a large potential for the technology [1]. Among a wide range of GSHP concepts, groundwater heat pump (GWHP) systems, also known as open loop GSHP systems, are unique because they extract thermal energy directly from groundwater rather than via heat collectors in soil or bedrock formations. These systems are less common than closed loop GSHP systems, but GWHP systems provide an efficient and cost-effective alternative in areas where the local hydrogeological conditions are favorable, especially for medium to large facilities (>100 kW heating capacity systems) and for facilities with large annual cooling demands.

These systems extract groundwater from an aquifer. In Norway, GWHP technology is typically applied in areas with large Quaternary deposits of saturated sand and gravel material. Many aspects of system performance are governed by the local and the over-all aquifer conditions. An aquifer formation beneath the town center of Melhus (Norway) is currently utilized as a heat source by nine individual GWHP systems. The first installation started production in 1999 and is still in operation today. A range of clogging and fouling problems has occurred in the different systems over the years, leading to the recent investigations [2–5].

The problems typically distinguish into three main categories: (1) Suspension and deposition of sediments in the system, (2) bacterial growth in the groundwater—biofouling, (3) chemical fouling, typically by iron and/or manganese compounds. These problems are identical to problems reported in many similar GWHP systems [6–13]. However, these references also emphasize several clogging issues caused by or catalyzed by a fourth problem category: (4) Exsolution of gases dissolved in groundwater. The exsolution and escape of specific gases, e.g., CO₂, can facilitate chemical imbalances in the groundwater and cause precipitation reactions. Nordell et al. [12] describe findings of iron precipitation caused by exsolution of CO₂ in borehole bedrock wells in the Emmaboda borehole thermal energy storage system. Gas exsolution also represents a direct risk of clogging by gas bubbles in, e.g., the well screen upon re-injection, which is a reported problem by many others e.g., [6,9,10]. Observations and investigations in Melhus by Brøste [3] have revealed gas bubbles in the groundwater during groundwater sampling, similar to some of the observations of Yon-Gyung et al. [14] in a CO₂ storage site in Korea. This arguably points towards gas exsolution as a possible cause for some of the clogging and fouling problems found in Melhus. This is currently being investigated.

This paper deals with the topic of GWHP design solutions and their influence on pressure- and temperature-induced gas exsolution within the systems. The traditional Norwegian design does not consider in-situ pressures and temperatures as key design parameters to avoid clogging problems, and the design thus enforces alterations to the in-situ groundwater conditions during operation. As examples of a typical gas exsolution triggers, pressure and temperature changes within a typical Norwegian GWHP system configuration are analyzed and presented. The analysis shows how the design affects the gas solubility in groundwater. An alternative design strategy introduces the solubility grade line (SGL) as a design tool for optimizing the system configuration. The new strategy provides an alternative approach to the traditional Norwegian GWHP design methodology and focuses on preventing or limiting the risk of gas exsolution.

1.1. Current Investigations in Melhus

There are two typical GWHP system design concepts employed in Melhus, i.e., with or without reinjection of groundwater to the aquifer (Figure 1). The heat pump system connects to the aquifer through a production well with slotted screens. Groundwater is pumped from the production well through a groundwater heat exchanger (HE), where thermal energy is extracted from or injected into the water. The water temperature is typically reduced or increased by 3–4 °C, respectively. The Melhus aquifer receives sufficient groundwater recharge and the systems can discharge the heat-exchanged groundwater through the local drainage system (Figure 1a). However, the more common system solution is designed to re-inject the heat-exchanged groundwater back into the aquifer in an injection well (Figure 1b). Re-injection is deemed favorable because it helps maintain the water level in the aquifer and the contractors do not have to apply for extraction permits from the regulating authorities. Groundwater from different depths are extracted depending on the location of the different installations. The shallowest installation utilizes water from a depth of 5–20 m and the deepest installation utilizes water from a depth of 60–70 m with respect to the water table.

The nine GSHP systems are cost-effective, but all of them have experienced a variety of different clogging and fouling issues. The major issues are related to clogging of the injection wells and the surrounding aquifer formation. All of the seven re-injection systems have experienced clogging of the injection well screen [5]. The clogging material is often a mixture of sediments and precipitated

hydroxides [3,4]. Inspections of the systems have shown that re-injection of groundwater is done without a backpressure technique, and vacuum pressures have been observed in the re-injection pipeline in several installations. Banks [10] (p.226) discusses this issue and suggests that >0.5 bar over-pressure should be achieved everywhere within the groundwater circuit to mediate this problem. Similarly, gas-related problems in deep Australian groundwater systems (>500 m depth) have led their industrial standard to recommend fully pressurized GWHP systems, typically with 1–4 bar over-pressure [11].

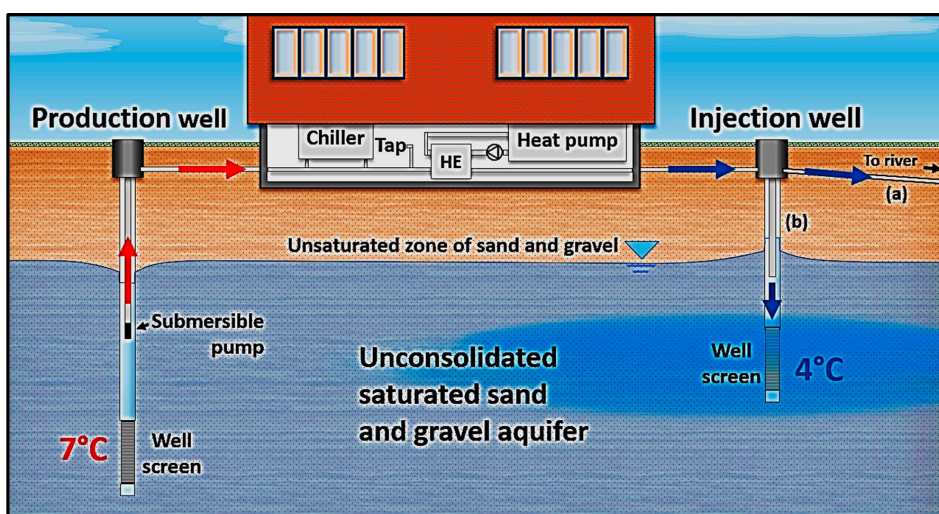


Figure 1. Types of groundwater heat pump (GWHP) systems in Melhus. (a) Design solution with run-off to nearby river through the local drainage system. (b) Most common design with re-injection of groundwater. A tap in the machinery room allows for water quality sampling.

Vacuum pressures have also been observed in the pipeline leading into the basement of the building on several occasions, sometimes as far back as the groundwater heat exchanger. Seven of the Melhus systems have experienced fouling of the groundwater heat exchanger (Figure 2a), but whether this is triggered by vacuum pressures or not is unclear. Mixing of different groundwater qualities in the system, or alteration of the groundwater temperature, are typically emphasized to explain why such fouling has occurred [6,9,10,15]. Water quality sampling of the aquifer [2,3], in different installations and observation wells, has revealed large spatial variations in both ion concentrations and dissolved oxygen levels in the aquifer. For instance, dissolved iron and manganese ions were found to vary from 0.05–5.78 mg/L and 0.01–0.68 mg/L respectively, depending on the location and depth of the different wells in the aquifer formation. The issue of chemical precipitation is thus a complex matter, probably with multiple triggering factors. In Melhus, the loss of in-situ pressure in the pipeline is now perceived to be a part of the problem.

Inspection of a particular production well in 2017 suggests that loss of pressure might be relevant for the observed fouling problems. The production wells in Melhus are seldom affected by clogging issues [4], but in this particular well, the pump was installed in the screened section of the well (Figure 2b). During a routine maintenance check of the 15-m-long screen, a video-inspection of the well revealed a minor issue where precipitated iron hydroxides were found highly localized in the screen area at the location of the suction inlet section of the submersible pump, 10–11 m below the water table. Houben [15] reports that similar observations are typical for water wells in general, and emphasizes that the rate of fouling deposition is enhanced in areas of high flow velocities. He states that this is likely caused by the mixing of different groundwater qualities, but this explanation seems

insufficient considering the small area of affected screen (20 cm in diameter) after eight years of continuous operation. The suction inlet section of the pump is often associated with high entrance velocities that cause relatively large losses of hydrostatic pressure around the pump entrance. If these pressure losses contribute to exsolution of dissolved gases that in turn affect the chemical balance of the groundwater, it might provide an explanation for the observed fouling. In this case, the problem can be easily avoided by correcting the system design. The physical–chemical relations concerning gas solubility and chemical precipitation are thus relevant for GWHP designers.

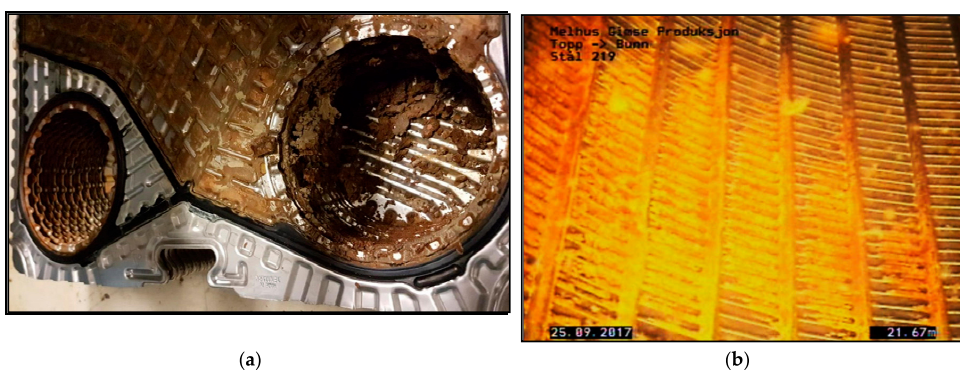


Figure 2. Clogging issues in Melhus. (a) Iron compounds and sediment inside a groundwater plate heat exchanger. (b) Local iron precipitation in the well screen surrounding the water inlet of a submersible pump in a production well. Affected area is approximately 20 cm in diameter and is probably caused by loss of hydrostatic pressure and gas exsolution during production.

1.2. Relevance of Gas Solubility and Chemical Precipitation in GWHP Design

To broaden the relevance of gas solubility in GWHP systems, it is appropriate to recount the relations of some gases to that of chemical precipitation. Numerous physical–chemical relations concern the topic of dissolved gases and their possible influence on precipitation reactions. Oxygen (O_2) and carbon dioxide (CO_2) are often considered the most relevant gases because they affect the chemical equilibrium of many compounds [16]. Most of the clogging problems in Melhus are connected to precipitation of iron and manganese compounds specifically. The following section therefore focuses on these two elements in relation to oxygen (O_2) and carbon dioxide (CO_2) gases. Some possible gas-related precipitation triggers are highlighted. Microbial activity that catalyzes precipitation reactions is not within the scope of this paper.

The dissolution and precipitation of iron and manganese is governed by the solvent’s redox potential (Eh) and pH [16,17]. Assuming chemical equilibria, the stability fields of various iron species can be visualized in Eh–pH diagrams. Higher Eh and pH levels in groundwater would, for most elements, tend to favor insoluble species. In the case of iron and manganese (Figure 3), it is evident that the soluble species of Fe^{2+} and Mn^{2+} are favored below $pH \approx 6$ with decreasing solubility with higher Eh levels, conditions that are commonly found in many aquifer formations. However, numerous factors control Eh and pH, thus making the dissolution–precipitation process more complex.

Eh is controlled by the oxidant availability. High Eh values indicate a large abundance of oxidants, leading to higher oxidation states of the reductants, i.e., electron donors. Oxygen (O_2) is the thermodynamically preferred oxidant. Oxygen depletion, so called anoxic conditions, make nitrate (NO_3^-), manganese (Mn^{4+}), iron (Fe^{3+}), sulphate (SO_4^{2-}), and carbon dioxide (CO_2) in sequence the thermodynamically preferred oxidants [18]. Anoxic conditions are usually found in deeper parts of water bodies, as oxygen supply is lower there [16]. Mixing anoxic groundwater with oxygen-rich groundwater, or mixing with oxygen in the air, are typical precipitation triggers because this alters the preferred iron or manganese species from soluble species, e.g., Fe^{2+} , to insoluble species that are

unable to stay in solution, e.g., Fe_2O_3 (Figure 3). Groundwater quality mixing and leakages of air into the system should thus be avoided. This forms the basis for much of the prevailing emphasis on groundwater quality issues within the GWHP design [10].

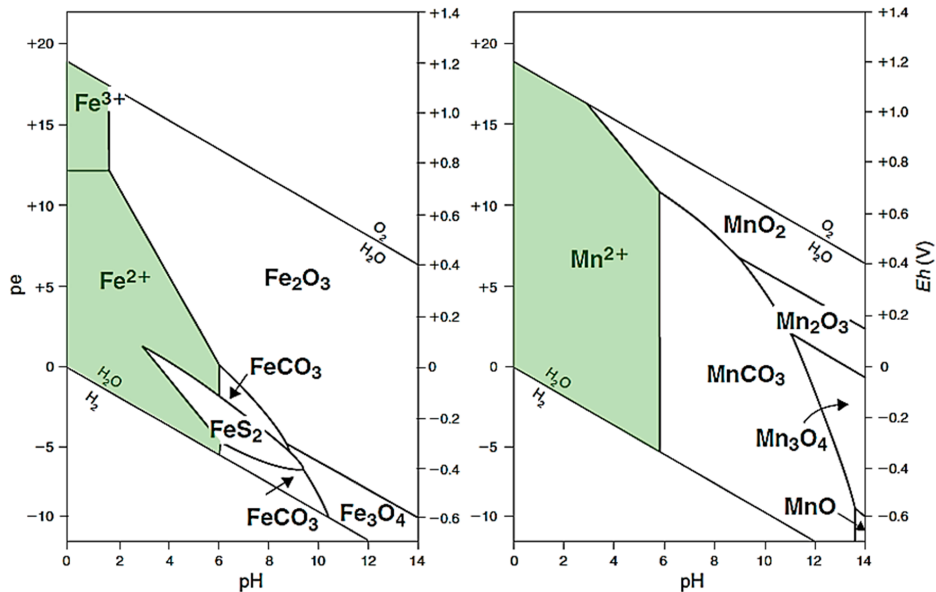


Figure 3. Relations for iron and manganese at 25 °C and 1.0 bar total pressure. Solubility contours are plotted at activities = 10^{-6} . Total dissolved sulfur = 10^{-6} mol/l. Total dissolved inorganic carbon activity = 10^0 mol/l. Soluble species are highlighted in green, while insoluble species are shown in white (modified after [18] and [19]).

The Eh–pH diagram represents an equilibrium approach and characterizes a steady state situation where the reactions have had sufficient time to stabilize. Aquifers in general, and especially aquifers utilized in GWHP systems, never achieve equilibrium, making kinetic considerations necessary for evaluating chemical relations. The reactions involved in iron and manganese dissolution and precipitation display various rates and rate controlling factors. For the oxidation of ferrous iron, the following rate equation is relevant and exemplifies some interesting relations [20]:

$$-\frac{d[\text{Fe}^{2+}]}{dt} = k[\text{Fe}^{2+}] \cdot p_{\text{O}_2} \cdot [\text{OH}^-]^2 \quad (1)$$

where k is a temperature-dependent rate constant, $[\text{Fe}^{2+}]$ is the ferrous iron concentration, $p(\text{O}_2)$ is the partial pressure of oxygen, and $[\text{OH}^-]$ is the hydroxide concentration. Catalytic effects of other ions in solution and complex formation affects the reaction rate, which often makes the practical utilization of Equation (1) difficult. Even in ideal conditions, Equation (1) is only rate controlling up to $\text{pH} \approx 7$. When $\text{pH} > 8$, the pH component of Equation (1) is so large that the amount of available O_2 and the diffusion of O_2 becomes rate controlling in practice [20]. Temperature effects have a minor and often negligible influence on the rate reaction constant (k). This is because the magnitude of temperature change is often small in GWHP systems, as discussed by, e.g., [21]. Without emphasizing the practical usefulness of Equation (1), the equation shows how the kinetics are more sensitive to alterations of pH than to Eh if $\text{pH} > 5$, due to the second order term of $[\text{OH}^-]$ and the single order term of $p(\text{O}_2)$, respectively. The works of, e.g., [15,22,23] demonstrate that the severity of precipitation problems in

groundwater wells often cannot be explained by oxygenation ($p(O_2)$) or large concentration of dissolved iron ions alone ($[Fe^{2+}]$), and pH alteration mechanisms have been identified as major contributors to the problems. Accounting for pH controlling physical–chemical relations in the GWHP system design is thus relevant.

Carbon dioxide is the major pH-controlling component in groundwater [18]. This is due to the dissolution and chemical reactions CO_2 undergoes in contact with water. A relatively small proportion of the total dissolved CO_2 hydrates, forming carbonic acid (H_2CO_3). This diprotic acid affects the pH level of the groundwater and lowers the pH if the water does not have sufficient buffering capacity. The magnitude of pH change depends on the water quality in question and the amount of alteration of dissolved carbon dioxide in the water [16]. Other gases are also relevant, e.g., the sulfur system may contribute to the acidity of natural waters [24,25], but this will not be elaborated upon here.

Physical properties that control the amount of dissolved carbon dioxide in the groundwater can have an indirect influence on the pH level of the water. Gas solubility (in water) is dependent on pressure, concentration, and temperature, as stated in Henry's law [26]. Figure 4 shows data provided by Colt [27] and exemplifies the relations of Henry's law in a water body supplied with CO_2 from an atmosphere with 0.039% atm $p(CO_2)$. The figure shows that higher partial pressures and lower water temperatures facilitate more gas dissolution. For groundwater with a given chemical signature, this implies that CO_2 is more soluble at low water temperatures and higher partial pressures of $p(CO_2)$, corresponding to greater aquifer depths.

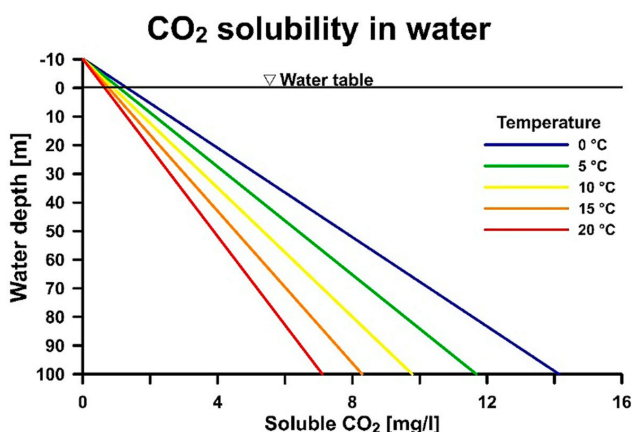


Figure 4. CO_2 solubility as a function of water depth (m) and temperature ($^{\circ}C$). Derived from a fixed concentration of CO_2 gas of 0.039% atm $p(CO_2)$. Based on data from [27–29], found in [27].

This has practical relevance for GWHP systems, because extracting water from a water body at a given depth below the water table triggers a loss of pressure, leading to CO_2 oversaturation. The exsolution of CO_2 triggers a chemical imbalance in the groundwater. This results in a rise of pH, and subsequently causes precipitation reactions [16,18]. This phenomenon is stressed by Garcia-Gil et al. [23], who demonstrate a direct risk for precipitation in groundwater systems in Zaragoza (Spain) if the water is allowed to interact with the atmosphere before re-injection. This is both because oxygen can dissolve into the water, and also because carbon dioxide can escape the system.

The water might also be oversaturated with gas if the temperature is increased. In this way, even though the temperature effects are often negligible, e.g., on the rate reaction of Equation (1) directly (k), the temperature can have an indirect influence on the pH. Accordingly, temperature indirectly poses an important role in the kinetics. The utilization of groundwater for cooling purposes in a GWHP system is thus more at risk than a system that utilizes groundwater for heating applications.

The concentration of ions and gases in the groundwater is defined by the local geological conditions in an aquifer system, and there is typically no intention for the GWHP system to alter the chemical composition of the groundwater during production [10]. However, altering the pressure and temperature conditions of the groundwater do enforce changes to the in-situ groundwater conditions. To evaluate the pressure and temperature conditions in the whole GWHP system is necessary to properly assess the risks of gas clogging caused by gas exsolution and its possible relevance for other fouling issues.

2. Method of Analysis

To properly assess the risks of gas exsolution in a system, one must investigate the influence of the system design on the groundwater pressure and temperature during operation. GWHP systems and aquifer thermal energy storage (ATES) systems are highly fluctuating pressure and temperature systems. Pressure changes through a system can be visualized in diagrams via the hydraulic grade line (HGL); a method frequently applied in fluid mechanics [30]. The HGL describes the magnitude of hydrostatic pressure head and elevation head at any given location through the entire length of a system. The method requires a detailed description of each system component. Effects caused by size, length, and roughness of the piping system need to be considered, in addition to their elevation with respect to a common reference datum. Energy losses caused by flow through the aquifer, pump, heat exchanger, pipes, and pipefittings (valves, bends, filters, etc.) must also be considered. All these effects are dependent on the groundwater flow rate. These effects are expressed in terms of hydraulic heads (m) in the form of the steady-flow energy equation (rearranged after equation 5.77 in [30]):

$$\frac{p_2}{\rho g} = \frac{p_1}{\rho g} + \alpha_1 \frac{V_1^2}{2g} - \alpha_2 \frac{V_2^2}{2g} + (z_1 - z_2) + h_{pump} - h_{losses} - h_{turbine} \quad (2)$$

where p denotes the hydrostatic pressure (Pa), V the mean groundwater flow velocity (m/s), g the acceleration due to gravity (m/s^2), ρ the density of groundwater (kg/m^3), z the elevation (m) in relation to a reference plane, and α is a correction factor for turbulence in pipes, usually $\alpha = 1.05$ [30]. The subscripts 1 and 2 denote two arbitrary locations in the system. The terms $p/\rho g$ are the pressure heads (m), $V^2/2g$ are the velocity heads (m), and z are the elevation heads (m) for the two points along the system. Hydraulic head supplied by the submersible pump is included in the term h_{pump} (m). The sum of all frictional and inertial losses is included in the term h_{losses} (m). The term $h_{turbine}$ (m) is usually not relevant, but signifies that regeneration of energy is possible in some system. The reader is encouraged to read [30] for more information on this topic and for examples on how to estimate these parameters in piping systems. For estimation of aquifer pressure losses, the reader is encouraged to read [31].

Equation (2) states that parts of the hydrostatic pressure are converted to kinetic energy, especially in regions of high flow velocities, e.g., at the pump entrance or through narrow channels, e.g., within a plate heat exchanger. Pressure is also converted into potential energy if the water is relocated to a point of higher elevation relative to the reference elevation. When considering their effects on gas solubility, alterations of energy forms must be considered as losses of pressure, in a similar fashion as to that of the frictional pressure losses induced by fluid flow through the system. For this reason, Equation (2) is rearranged in this paper for pressure head to give a modified form of the HGL, termed the gauge pressure head grade line (GPHGL). The assumption made is: Point 1 can be chosen to be at the water table in the aquifer and at a sufficient distance away from the inlet of the pump. The velocity squared of the water at this point is thus negligible. The reference elevation is said to be at this elevation, thereby $z_1 = 0$. The pressure here is, by definition, the atmospheric pressure, and substituting into Equation (2) the gauge pressure at an arbitrary point can be calculated by Equation (3):

$$\frac{p_{gauge}}{\rho g} = h_{pump} - z_2 - h_{losses} - h_{turbine} - \alpha \frac{Q^2}{2gA^2} \quad (3)$$

The term h_{pump} and h_{losses} are the heads corresponding to energy added by the pump and lost to friction, respectively, to the flow up to a given point. Inside the pipe, the mean velocity is conveniently calculated as Q/A , where Q is the flow (m^3/s) and A is the cross-sectional area of the pipe (m^2). The pump being a component at a fixed location means that, for a point in front of the pump, h_{pump} should not be present in Equation (3). The sum of all the head losses are met by the submersible pump, which must supply an amount of hydraulic head equal to the losses to maintain the balance of Equation (3) at the designed rate of flow. The argument for this is understood if the arbitrary point is at the water table a significant distance away from the injection well; here, the elevation is zero, the velocity squared is negligible, the gauge pressure is zero—making h_{pump} and h_{losses} equal. The equation thus also describes the power needed, P (W), to circulate the groundwater:

$$P = \frac{\rho \cdot g \cdot Q \cdot h_{pump}}{\eta} \quad (4)$$

where η is the coefficient of mechanical and hydraulic efficiency of the pump, typically ranging from 0.5–0.75 or less for submersible pumps depending on pump size and motor speed [32]. In this sense, the GPHGL also visualizes the energy needed for groundwater circulation at the specific mode of operation.

The GPHGL analysis is constructed by Equation (3) along a line (A–I) that describes the pressure exerted on the water traveling along the line through the system during operation. Along the line, the water is assigned properties with respect to the water table and the flow velocity at each point along the line. The GPHGL is a visualization of the bulk pressure exerted on the water at different segments in the GWHP system. This pressure directly controls gas solubility in the water. As the pressure varies through the system, the solubility of gases is altered according to Henry's law. The GPHGL therefore describes the general risk of gas exsolution in the system.

However, alterations of temperature in the groundwater heat exchanger renders the GPHGL and Equation (3) unable to adequately describe the system's influence on gas solubility. Combining Equation (3) with the temperature solubility relations for, e.g., CO_2 in water, the GPHGL is modified further to provide a solubility grade line (SGL) for the system in relation to CO_2 specifically. In this study, this is done for water with 0.039% atm. $p(CO_2)$, corresponding to atmospheric concentrations. This data is readily available for a wide range of temperatures and pressures in Colt [27]. The behavioral trends are seen in Figure 4, and the variable pressure and temperature components result in different solubilities for the water along the line (A–I). The reader is referred to [27] for the specific details regarding the solubility relations that constitute Figure 4. Solubility of other gases are not considered in the SGL.

For simplicity, the SGL analysis in this paper does not consider the thermal energy provided by cooling of the submersible pump motor or the thermal energy provided by frictional losses through the system, as these thermal contributions are estimated to be small in relation to the heat exchanged in the groundwater heat exchanger. Considering the GWHP system presented in Figure 1, it is apparent that several components can cause considerable alterations to the gas solubility as the groundwater travels through the system. The application of the GPHGL and the SGL will be presented in the following section for two different fictional GWHP systems with 0.039% atm. $p(CO_2)$ -saturated groundwater conditions.

3. Example of Gas Exsolution Triggers and Application of the SGL

The examples presented in the following sections are theoretical and are not actual systems in Melhus. The first example presents a design that follows the traditional Norwegian GWHP concept. Numerous risk areas of this design are presented. The second example is a new design approach that eliminates all of the risk areas by relocating the system components in the aquifer. The components are otherwise identical in both examples. These two systems demonstrate that the design and location of the wells and piping system can have a profound effect on gas solubility during groundwater circulation.

For simplicity, the example cases assume that the groundwater is saturated with CO_2 at the location of the production well screen and injection well screen depths, corresponding to the solubility relations provided by Colt [27]. This situation would resemble an unconfined aquifer with limited or no organic material in the soil formation. This situation serves as an example of how gas clogging risks in an aquifer can be managed through design and system control.

The water table is, per definition, the location of the atmospheric pressure in the aquifer. The GPHGL analysis in the presented examples refers to the water table as the reference datum for gauge pressure calculations, $Z_{\text{water table}} = 0$. It should be noted that the water table might have seasonal fluctuations in natural groundwater systems and that the presented examples must be viewed as steady state situations. Only the aquifer, piping (3" ID), and heat exchanger pressure losses are included in the analysis and the components are equal for the two cases, with the exception of the piping length and well depths. The cases are thus simplified versions of actual systems, but they are intended to demonstrate the concepts, not to present a specific system in Melhus.

3.1. The Traditional Norwegian GWHP Design Concept

The traditional Norwegian open loop well design follows the same dimensioning principles utilized in wells constructed for drinking water purposes. The main purpose of the design is to provide the GWHP system with sufficient groundwater circulation (Q (m^3/s)) and, thus, thermal energy. In practice, these principles involve minimizing the investment cost by limiting the well size and depth (z (m)) and, thus, reduce the drilling costs. In a homogeneous and isotropic aquifer, where impermeable sediments in the aquifer are not an issue, this principle can typically lead to the GWHP system configuration in Figure 5. Here, the injection well screen (H) is located at a shallow depth ($\Delta z > 0$ (m)) compared to the production well screen (B).

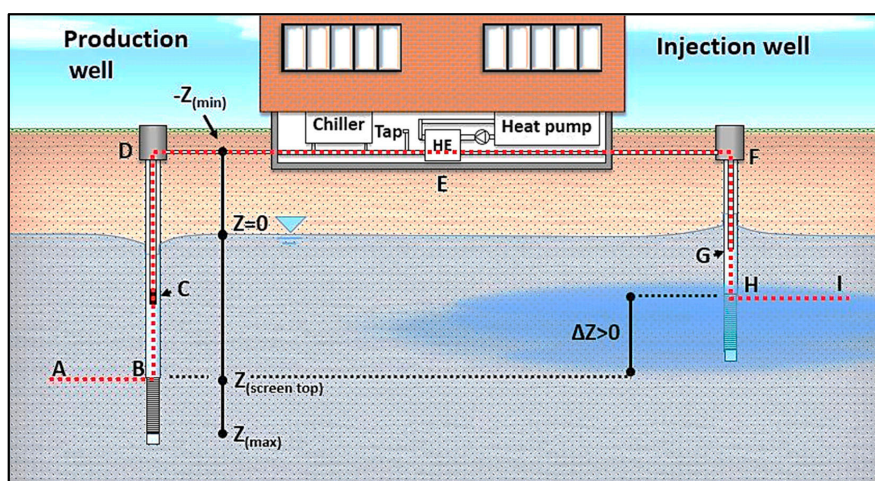


Figure 5. Traditional Norwegian GWHP design methodology can typically result in this system configuration. Different key components (A–I) are installed at various depths (z) in relation to the water level of the aquifer, $Z_{\text{water table}} = 0$ m.

The exact placement of the submersible pump in the production well (C) and the outlet pipe in the injection well (G) are selected based on evaluations of operational risks. The submersible pump must be installed sufficiently deep to prevent excessive drawdown of the well water level at the designed maximum flow rate. This often leads to a pump placement directly above the well screen, consequently maximizing the available drawdown potential of the well. However, if the well is sufficiently deep and the risks of excessive drawdown are small, the pump can typically be located as seen in Figure 5

to save costs on raiser pipe length and electrical cable. Similarly, the injection pipe outlet (G) must be submerged below the water table to limit the risk of mixing with the air in the well bore before injection. The injection pipe is rarely located deeper than a few meters below the well water table.

Before injection, the thermal energy is extracted in the groundwater heat exchanger in the basement of the building, which is located a certain elevation above the water table in the aquifer ($-Z_{\min}$ (m)). The location of the heat exchanger is often close to the heat pump unit, contributing to an as short as possible indirect loop of secondary fluid, yielding lower costs associated with the indirect loop and the circulation of secondary fluid. This might be convenient in many installations, but if the distance from the wells to the building is great, the length of the groundwater loop can sometimes be several hundred meters more than the shortest distance between the wells themselves.

The system design presented in Figure 5 imposes a number of pressure changes to the groundwater as it travels through the system. As a simplified example, we can consider the following situation where the production well screen is installed at B = 20–25 m depth and the injection well screen at H = 10–15 m depth. The submersible pump is installed at C = 10 m depth and the injection pipe exit at G = 3 m depth. Figure 6 presents these key design components in view of their effects on CO₂ solubility in groundwater. In addition, the groundwater temperature is altered depending on the energy demand in the building. If there exists a cooling demand, the groundwater temperature is re-injected into the aquifer with a higher temperature than the original temperature, e.g., an increase from 5–10 °C.

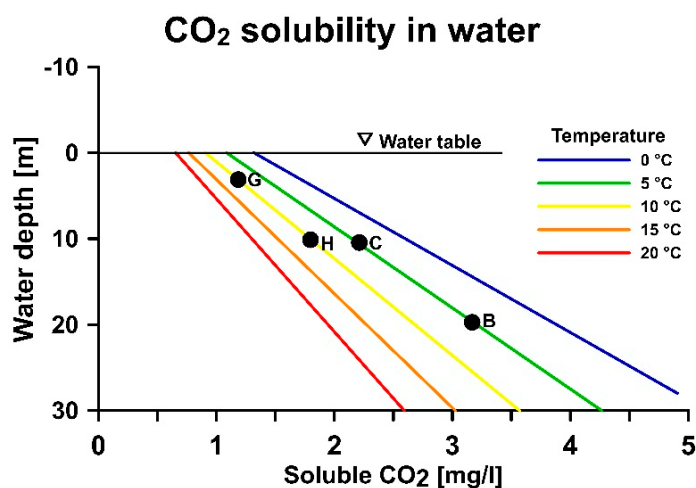


Figure 6. Degassing of CO₂ in the production well and the injection well associated with the traditional Norwegian GWHP design. The location of the screens (B,H), pump (C), and injection pipe (G) are plotted in the solubility regions for CO₂, ref. Figure 4. Here, the GWHP system operates in a 5 °C cooling mode.

The location of the pump at 10 m above the production well screen triggers a pressure drop of 1.0 bar and the solubility of CO₂ decreases (Figure 6B,C). The initial groundwater is saturated with CO₂, the gas is exsolved out of the water phase, and chemical reactions are triggered. These reactions increase the pH level of the water, which in turn can trigger precipitation reactions.

The shallow placement of the injection pipe (G) in the injection well, combined with the increased temperature caused by the cooling of the building, further decreases the solubility of gases and increases the gas exsolution (Figure 6C vs. Figure 6G). The groundwater is further depleted with CO₂ and the chemical reactions are accelerated and allowed to continue. The shallow injection screen depth prevents the CO₂ bubbles from dissolving, and the bubbles effectively clog the well screen and aquifer formation near the well (Figure 6G,H).

The GPHGL analysis of the pressure reveals the dynamic pressure changes through the piping system. The GPHGL analysis along the dotted line A–I in Figure 5 shows that the traditional system configuration is predisposed to losses of pressure after the groundwater has entered through the production well screen (Figure 7). Frictional losses in this aquifer only cause minor drawdown losses before entry through the screen (A–B). This is typical for highly permeable aquifers. The length of the well screen allows for mixing of groundwater from 20–25 m depth before the entry to the pump. The groundwater entering at the bottom of the screen is thus subjected to larger losses of pressure and corresponding changes in gas solubility.

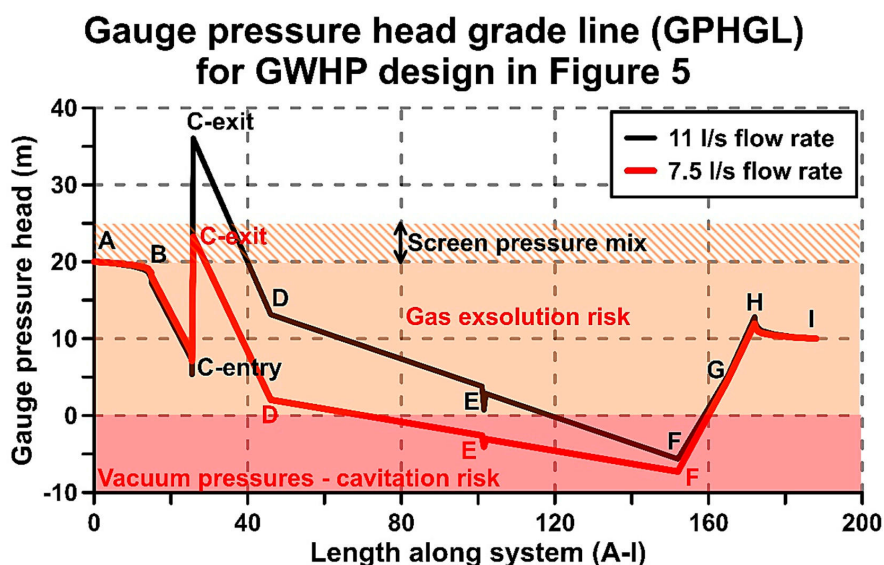


Figure 7. Pressure grade line (GPHGL) for the groundwater flow line A–I in Figure 5. The GPHGL is estimated based on Equation (3). The groundwater is saturated with gas at the depth of the well screens. The gas exsolution risk area is relevant for all types of gases, and these gases form bubbles in the highlighted area.

In addition to the 1.0 bar pressure loss before the pump (B–C), the actual pressure loss at the pump entry can be higher because of the relatively high speed of the water when entering into the pump impellers (7.5 l/s vs. 11 l/s of C-entry in Figure 7). The abrupt pressure increase displayed at C represents the additional pressure, h_{pump} , that is supplied by the submersible pump. The input power is equal to the frictional and elevation losses in the system. The input power and the supplied pressure is thus smaller for the 7.5 l/s vs. 11 l/s mode of operation. After pump exit (C-exit), the additional pressure supplied by the pump is quickly dissipated by the elevation rise towards the top well fitting (C-exit towards D).

The length D–F represents the pipe length from the production well to the injection well which, in this case, is 105 m. Since the heat exchanger is located in the basement of the building, the distance D–F is often unnecessarily long and filled with bends, valves, and filters. These components are not included in this analysis, but can contribute to local low-pressure zones along the D–F line that might enter the vacuum region of the GPHGL diagram. This is exemplified by the slight dip within the heat exchanger (E). The risk associated with vacuum is, e.g., severe gas exsolution caused by significant loss of gas solubility (Figure 4). In the worst case, the water starts to boil, and the onset of cavitation might occur. The severity of the vacuum and size of the vacuum region depends on the flow rate and the

specific location of different components in the system. For this system, the heat exchanger (E) enters the vacuum region if the flow rate is reduced from 11 to 7.5 l/s (Figure 7).

The injection pipe (G) is submerged beneath the water table and the risk of entering the vacuum region is largely controlled by the elevation difference from water table within the well and the injection well top fitting (F). The elevation difference from F to the well water table causes a suction within the pipe, and the magnitude of suction is proportional to the elevation distance of F above the well water table. The re-injection of groundwater into the aquifer (I) requires an increase in the hydraulic gradient (H–I). This leads to an artificially high water level within the injection well. The magnitude of suction in the system is thus a function of the injection well characteristics and the mode of operation. For instance, the suction is larger at lower rates of flow, as seen in Figure 7.

The GPHGL analysis shows that the location of the injection well screen at a shallower depth causes a permanent loss of pressure (I vs. A). The traditional system design is unable to avoid gas clogging issues if the groundwater is saturated with gas.

3.2. New Design Principle and Proposed Alternative Design Concept

The new design alternative incorporates considerations of pressure and temperature, in addition to the traditional design principles. The design should provide the building with sufficient thermal energy without allowing gas exsolution to occur. This can be avoided by imposing a consistent rise in pressure within the system, instead of allowing pressure to drop. This means that the whole system must be designed in relation to the location of the production well screen relative to the aquifer water table (Figure 8). Solubility relations also depend on the temperature, meaning the magnitude of temperature alteration during operation must be considered in relation to the corresponding pressures needed to avoid gas exsolution.

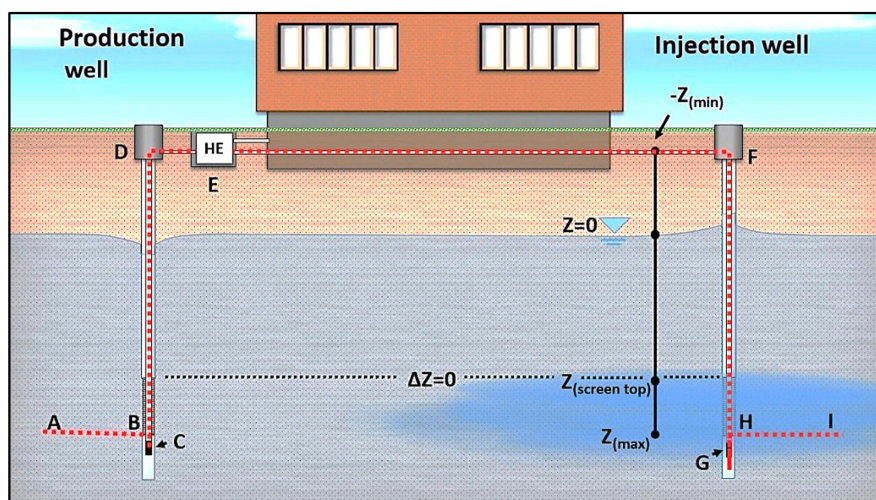


Figure 8. GWHP design concept. The heat exchanger is located outside the building in separate housing close to the production well. The slightly longer indirect loop of secondary fluid connects the heat pump to the groundwater. The depths of both well screens are equal.

The location and length of the production well screen enables extraction of groundwater with a fixed pressure range relative to the groundwater table (20–25 m). The highest pressures are found in the deepest part of the well, at the lower end of the screen. The installed depth of the screen bottom thus forms the baseline for the design (B = 25 m). The location of the pump below the screen bottom ensures that the pressure level is preserved until the water has entered the pump impellers

($C > 25$ m). Similarly, the re-injection pipe in the injection well must be installed beneath the injection well screen to ensure over-pressure upon re-entry to the well ($G > H$). Without considering alterations to the groundwater temperature yet, it is evident that the injection well screen (H) must be installed at minimum the same depth as the production well screen to avoid a permanent loss of pressure after the groundwater has left the GWHP system.

The GPHGL analysis shows that these minor design adjustments ensure a pressure level that reduces the risk of gas exsolution in the production well and the injection well (Figure 9). The pressure drop in the aquifer around the production well (A–B) cannot be avoided, but the magnitude of drawdown can be controlled by adjusting the pumping rate through the system.

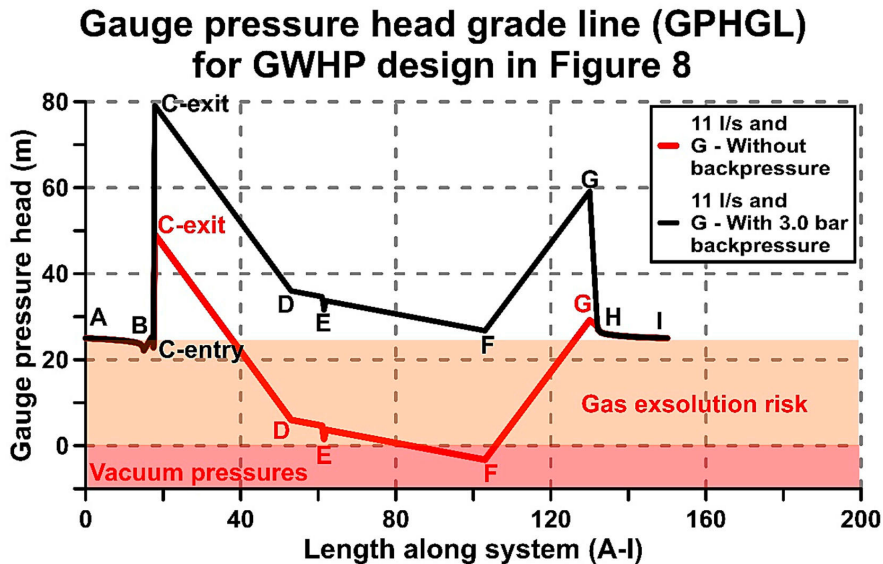


Figure 9. Pressure grade line (GPHGL) for the groundwater flow line A–I in Figure 8. Groundwater flow rate is 11 l/s for both cases. Backpressure valve is 3.0 bar (30 m) and is installed at the injection pipe exit (G).

The pressure within the groundwater pipeline (C–G) is still not sufficiently controlled. Sufficient over-pressure is only achieved by installing a backpressure device (G). The magnitude of backpressure required is a function of the reference pressure in the production well (2.5 bar), the required elevation lift above the water table (1.0 bar), and the groundwater flow rate in the system. For instance, for the pressure to be 2.5 bar at F at zero flow, the additional backpressure at G must be 3.5 bar to simulate a 25-m-high “water column” above F. During groundwater circulation, the friction in the injection pipe and the water level increase in the injection well provide some of this backpressure. The additional backpressure needed is correspondingly less. If the flow rate is set to, e.g., 11 l/s, the GPHGL analysis of this system shows that the pipeline pressure is sufficient if the backpressure valve is 3.0 bar (Figure 9). The main drawback with the backpressure technique is the substantial amount of additional pumping power required for groundwater circulation. This is seen in the 30-m-higher C–exit point for the black GPHGL (Figure 9).

The precise location of the injection well screen and the magnitude of backpressure required is a function of the mode of system operation. The system is typically operated in heating mode or cooling mode, or a combination of these two modes, depending on the demand in the building. Since the solubility of the dissolved gases is affected by temperature, the risk of gas exsolution is affected by the mode of operation. The SGL of the black GPHGL (Figure 9) is shown in Figure 10. The SGL

shows that the GWHP system in heating mode reduces the risks of gas exsolution after heat extraction. Operating the system in cooling mode forces the solubility line below the initial solubility limit and CO₂ exsolution occur (Figure 10). The backpressure valve of 3.0 bar is not sufficient to prevent CO₂ exsolution during cooling mode. Furthermore, the installed injection screen depth needs to be deeper in cooling mode to avoid gas exsolution in the injection well and aquifer formation. This is not necessary in heating mode, where a shallower depth would suffice for the colder water.

The location of the heat exchanger in the new design is moved to separate housing close to the production well (Figure 8). The distance D–F is reduced to 50 m in this case. This is done to exemplify the strategic benefit of controlling where in the system the temperature change should occur (Figure 10). Early heat exchange provides additional gas solubility in heating mode, and vice versa in cooling mode. The optimum location of the heat exchanger is not necessarily at the same location for both modes and installing the heat exchanger close to the production well helps to avoid vacuum pressures in the heat exchanger.

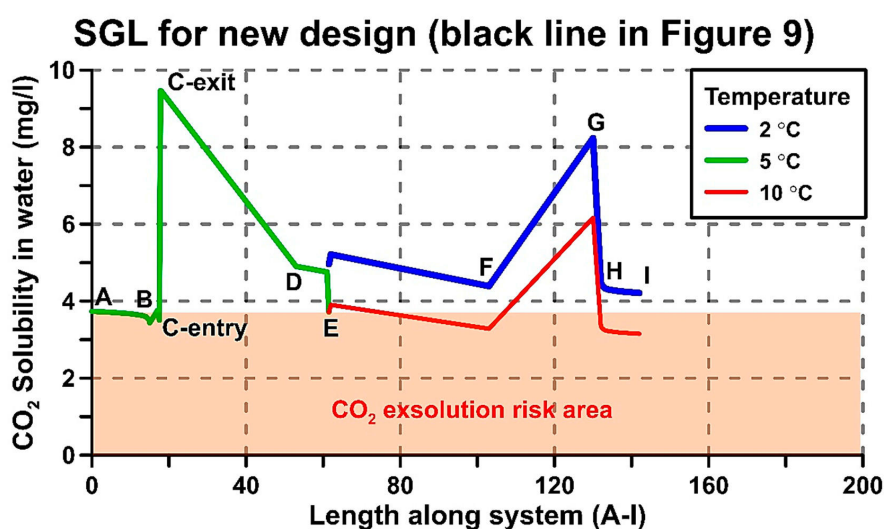


Figure 10. Solubility grade line (SGL) for the groundwater flow line A–I in Figure 8. The SGL is calculated from the black GPHGL (Figure 9) and the solubility of CO₂ in water (Figure 4). The backpressure valve is set to 3.0 bar. Return temperature after heat exchange is 2 °C for heating mode (blue) and 10 °C for cooling mode (red).

4. Discussion and Comparison of Design and Design Tools

Two different GWHP system designs have been presented in an attempt to highlight the risks of gas exsolution in such systems. GPHGL analysis is a useful tool for system analysis because it can display the effect of each system component on the hydrostatic pressure. The analysis presented in this paper only shows a simplified representation of actual systems, but demonstrates how the GPHGL can be applied for dimensioning of GWHP systems. For dimensioning of actual systems, a detailed description that includes all relevant components should be analyzed. Alternatively, an existing GWHP system can be installed with pressure sensors and the values from these sensors can be plotted in a similar fashion. This would represent the actual GPHGL of the system. It is recommended to install pressure sensors in both well water tables (B and H), on both well housings (D and F), and on both sides of the groundwater heat exchanger (E) to ensure the proper visualization of the most basic GPHGL. Some systems might require more sensors depending on the complexity of the design.

The GPHGL analysis of the traditional Norwegian GWHP system configuration shows that the system configurations are predisposed to gas exsolution risks. To some degree, these risks are unavoidable, particularly in view of the production well and its influence on the aquifer. Extraction of groundwater from an aquifer always induces loss of pressure around the well, and these losses can presumably be enough to trigger exsolution of dissolved gases if the groundwater is saturated with gas. Pre-investigation of the aquifer formation with appropriate techniques is necessary for establishing the limits of the system. The current state-of-the-art techniques applied in Norway do not consider levels of dissolved gas in the pre-investigation phase of projects [2], but this should be included in the portfolio of water quality sampling. These limits can function as the baseline for the dimensioning GPHGL analysis.

The only design parameters that can influence aquifer pressure loss are the rate of groundwater extraction or the size and length of the well screen. In this regard, it is recommended that due consideration is given to reducing the required flow rate, rather than increasing the well screen length. The length of the well screen essentially limits the range of pressures that can be extracted from the aquifer; longer screens enable groundwater with larger pressure variability and, thereby, gas solubility to enter the well bore. The screen length thus determines the risk of “groundwater quality mixing” and “pressure mixing” before groundwater extraction, as exemplified in Figure 7. Reducing the extraction rate would limit the pressure loss, but also reduce the required screen length of the well, which seems doubly beneficial if chemical stability is a concern for the system.

The GPHGL analysis shows that the installation depth of the submersible pump is a key feature in the system design. The location of the pump high above the production well screen is a possible gas exsolution trigger. The current well design is not able to prevent gas bubbles from escaping the well bore [4]. If these gases are pH-regulating, e.g., CO₂, the design might facilitate alterations of the groundwater chemistry and trigger precipitation reactions. Installing the pump below the screen bottom helps negate the risks of gas exsolution in the production well but triggers a range of other operational consequences that increase the investment cost of the production well. For instance, a flow sleeve that forces water past the motor is necessary to ensure appropriate cooling of the pump. The flow sleeve increases the width of pump and the size of the well must increase slightly to meet the space requirements. The well must also be slightly deeper to account for the installation space needed by the pump. Furthermore, a sensor that regulates the speed of the pump motor is necessary to ensure and control that excessive drawdown is prevented. The risk of sediments entering the pump is higher when the pump is installed below the screen, and appropriate screen design should be given high priority.

The highest risks are linked to the onset of the vacuum in the system, and the GPHGL analysis identifies the injection well configuration as a particularly high-risk vacuum area in the system. If the vacuum region in the system is left unchecked, it might extend backwards to the groundwater heat exchanger. Observed vacuum conditions in some of the injection wells and systems in Melhus confirm this effect. The vacuum poses a problem even if the groundwater is not fully saturated with gas, because the vacuum causes severe flashing conditions for dissolved gases and might cause the water to boil. Alternatively, if the groundwater piping system is insufficiently sealed, the vacuum can also cause invasion of air into the system through leaky components. These leakages would not be visible on the outside of, e.g., a pipe, which makes these types of faults particularly difficult to discover. This means that the traditional system design is also predisposed to air-mixing risks if components are not airtight. The onset of the vacuum can be prevented by installing a backpressure device at the injection pipeline exit, but the magnitude of backpressure required is dependent on several factors. These factors will be highlighted in the subsequent discussion.

The GPHGL analysis shows similar results to that of the installation depth of the pump in the production well for the installation depth of the pipeline in the injection well. The location of the pipeline exit at a shallow depth, high above the injection well screen, is a possible gas exsolution trigger. A sudden drop in flow speed after the pipeline exit aids the escape of gas bubbles up the well bore,

possibly triggering precipitation reactions. Installing the pipe exit below the injection well screen can negate the risks of gas exsolution in the injection well, but only if the injection well screen is installed at a depth that yields satisfactory solubility conditions. This depth is not directly revealed by the GPHGL analysis. As a general rule of thumb, this would be the same depth as the production well screen, but might be deeper or shallower depending on the mode of GSHP operation and the initial level of dissolved gas in the groundwater. There would be considerable risks associated with installing the injection pipeline below the screen if the screen is not installed sufficiently deep in the aquifer. Gas bubbles can then enter the well screen with ease and clog the well and aquifer formation.

The new design concept incorporates the solubility grade line (SGL) analysis as a tool for deciding on the specific location of the injection well screen depth. The added benefit of the SGL compared to the GPHGL is the possibility to analyze the system for groundwater qualities that are under-saturated with respect to gas. The actual gas solubility in an aquifer, discovered through pre-investigative measures, can function as a limit in the SGL (Figure 10), and the injection depth and the operational temperatures must be selected according to the limit. In the presented case (Figure 10), the groundwater is saturated with CO₂ and the injection depth should be deeper than the extraction depth if the water is used for the cooling of the building. If the water is utilized for heating purposes, the injection depth can be shallower than the extraction depth.

Operating the GSHP system in heating mode provides additional gas solubility in the groundwater and reduces the risk of gas exsolution. The strategic benefit of achieving heat exchange early in the system is apparent. This means that the groundwater heat exchanger should be installed as close as possible to the production well in systems with a predominant annual heating demand (Figure 8), and not necessarily in the basement of the building (Figure 5). The SGL also shows that the magnitude of temperature alteration in the heat exchanger can be used strategically, depending on the mode of operation. For instance, if the groundwater quality is sensitive to increased temperatures, the increase should be kept small, i.e., $\Delta T = 2\text{--}3\text{ }^{\circ}\text{C}$. Thus, most of the thermal energy could be supplied by circulating larger quantities of groundwater. Alternatively, the groundwater flow rate can be kept low and most of the thermal energy extracted by means of a larger temperature alteration, e.g., $\Delta T = 5\text{--}6\text{ }^{\circ}\text{C}$, increasing gas solubility before re-injection. Before determining the optimal mode of operation, these alternatives should be reviewed in light of their influence on the heat pump system's seasonal coefficient of performance (SCOP). Increasing the ΔT means that a heat pump would receive lower suction pressures to the compressor, which reduces the SCOP and the heating capacity of the system [33].

A major disadvantage of the alternative design strategy (Figure 8) is the large increase of work required for the groundwater circulation. A backpressure device (G) supplies additional losses. Assuming the efficiency of a submersible pump in Figure 9 is 0.6, the added power consumption for a 3.0 bar backpressure valve is approximately 5.4 kW if the circulation rate is maintained at 11 l/s (Equation (4)). Assuming that reducing the flow rate by half would reduce the efficiency of the pump to 0.5 and the required backpressure would increase to 3.25 bar, the additional pumping power required would reduce to 3.2 kW. If this backpressure is supplied by a passive flow valve device, e.g., a ball valve, spring valve, or a constriction at the pipe ending, this added loss leads to large amounts of "wasted" energy in the process of water circulation. These losses can presumably be too high in some cases, especially for small installations where even a slight alteration of system SCOP can disturb the financial benefit of the GWHP installation.

Passive backpressure devices also provide pressures that are flow rate-dependent, and the required backpressures could be difficult to achieve for a range of flow rates with a single device. For instance, avoiding gas exsolution when the system is shut-off would be difficult if the backpressure is supplied by a constriction of the injection pipe. Minimizing the total amount of frictional losses, and thereby the required pumping power, is a possible solution to the problem. This could be done by increasing the pipe diameter and reducing the length of the pipeline and number of fittings, bends, valves, etc.

(D–F), or by selecting a mode of operation that requires a low rate of flow, e.g., higher ΔT through the heat exchanger.

An alternative and favorable approach would be to supply the necessary backpressure by installing a turbine that can regenerate the losses into electrical energy. A turbine can essentially be a pump working in reverse and can be preprogrammed to follow a predefined algorithm that accounts for flow rate variations in the system and only provides the backpressure needed. The turbine would also be able to retain the backpressure when the system is shut-off. Installing a turbine in GWHP systems also provides a range of benefits in regard to simplifying certain maintenance routines of the system. For instance, it enables the operator to alter the flow direction through the loop, which is useful when cleaning the system. The turbine can also function as a backup solution if the production well pump suffers unforeseen problems and must be taken out of service. A turbine seems beneficial for ATEs systems in particular. ATEs systems have well doublets with submersible pumps in both the production well and the injection well, irrespective of the groundwater quality. Utilizing these pumps as turbines seems beneficial, regardless of gas-related groundwater quality issues.

Another problem with the alternative design can occur if groundwater is extracted from deep aquifers with high native pressure levels. A typical example can be the Challenge Stadium installation in Perth, Australia, where the production well is located at 750 m depth [11]. Maintaining the same pressure level throughout the loop would result in more than 75.0 bar over-pressure at the surface. Some system components, the plate heat exchanger in particular, have problems with operating at such high-pressure loads. Piping materials also have pressure limitation and it is reasonable to assume that avoiding gas exsolution in deep aquifers can lead to increased investment costs if “high-grade” materials are needed in the design. On the other hand, deep aquifers have higher gas solubility and can dissolve more gas than shallow aquifers, and the alternative design might be the best solution nonetheless.

The alternative design solution offers a range of design and control strategies that arguably benefit GWHP and ATEs systems in gas-saturated aquifer conditions. Some of the solutions have both benefits and drawbacks, which proposes that deriving a single optimal solution for all aquifer conditions is difficult. The added effort of avoiding gas-related issues should outweigh the downside of allowing gas exsolution to occur. The additional investment and operational costs should be lower than the clogging maintenance cost of a system built in the traditional manner. Alternatively, the additional costs must provide a more stable system with less unforeseen faults. GWHP systems that function relatively well, even though they allow vacuum conditions in the loop exist. Aquifers with low concentrations of dissolved iron and manganese ions presumably pose less risk than aquifers with high dissolved ion concentrations. In Norway, aquifers utilized for domestic water purposes have to satisfy certain national guidelines to qualify as a source of potable water. Similar guidelines should be developed for GWHP systems, where risks associated with different levels of ion concentrations and gas concentrations are explained. The guideline should preferably relate levels of ion concentrations and gas concentrations to the risks of clogging in a fashion that allows designers to select the best system configurations for particular conditions. Applying the SGL methodology to the gas solubility data allows such water quality data and guidelines to be integrated in the monitoring scheme of the plant. The data can be presented as a figure in the control unit display that is easily understood by the operator, e.g., similar to that of Figure 10. The operator would then be able to see the situation live on a monitor and assess whether the current mode of operation is within the safety limits of the aquifer.

Often in groundwater quality studies, e.g., [21–23], the effects of a GWHP system on the groundwater quality is simplified to models that investigate the production wells, injection wells, or the aquifer conditions alone. The influence of the whole system design on the pressure, temperature, and quality alterations are not necessarily accounted for. The presented examples demonstrate that, e.g., the pressure conditions within the system piping layout can provide worse gas solubility conditions in the groundwater than can be identified in the wells or aquifer itself, particularly in view of vacuum conditions. At any given GWHP aquifer, it is thus relevant to incorporate the influence of the actual

system design on the development of the local groundwater quality. It is often the intension of the system designer to not alter the groundwater chemistry, but the presented results show that a given system must be customized to the particular water quality situation in question for this to be a genuine objective. Both Bakema [7] and Banks [10] emphasize the lack of input from a hydrogeologist as one of the major shortcomings in the design of groundwater GSHP systems. By simplifying the design of the piping system, it would be easier for the hydrogeologist to customize the heat source system in agreement with the challenges given by the aquifer. The application of the GPHGL and the SGL would then be easy to construct in the planning and dimensioning phase of new projects.

5. Conclusions

Problems caused by dissolved gases are closely linked to that of chemical precipitation in GWHP and ATES systems. Exsolution of dissolved gases from groundwater can be induced by alterations of in-situ pressure, concentration, and temperature conditions, and exsolution of some gases, e.g., CO₂, can catalyze precipitation reactions of dissolved ions. The design and control strategy of GWHP systems must include considerations regarding pressure and temperature alterations to mediate these risks. The gauge pressure head grade line (GPHGL) is an adequate design tool for evaluating pressure-related risks, while the solubility grade line (SGL) is a new design tool that directly evaluates and identifies gas exsolution risk zones in the entire system configuration with respect to specific gases. For this reason, the SGL should be included in the design strategy of GWHP and ATES systems.

Avoiding gas exsolution is possible through correct system design. The conditions at the production well screen depth function as the baseline of the design, and the other components must be selected based on the in-situ gas solubility in the aquifer at this location. The findings from the SGL analysis presented in this paper can be summarized as follows:

- The traditional Norwegian GWHP design is predisposed to clogging risks in gas-saturated groundwater conditions. Installing the injection well at a shallow depth compared to the production well is unfavorable. The traditional injection well configuration is a particularly high-risk component in the design because it can trigger vacuum pressures in the piping system. The injection well must utilize a backpressure device to avoid vacuum conditions if the elevation lift from the water table is too high.
- The new design methodology can prevent gas exsolution. The new design utilizes the depth of the production well as a baseline for the design of all other components. The analysis shows that installing the pump and injection pipe below the well screens and utilizing a turbine to supply parts of the necessary backpressure in the system are necessary to avoid gas exsolution.

The new system design configuration requires higher investment costs than the traditional solution. Optimizing the design through strategic heat exchange, reducing the groundwater pipeline length, and reducing the groundwater flow rate can help decrease the cost of the new system design. However, if viewed in a broader picture, the new design might allow utilization of challenging aquifers as heat sources that would otherwise be too risky for the traditional design configuration.

Further work is being conducted that investigates the correlation of vacuum, gas exsolution, and precipitation in the affected GWHP systems in Melhus. The solubility grade line method and the alternative design methodology can then be tested and verified when designing new systems and configurations. Similar investigations in a variety of groundwater conditions should be conducted to help develop and verify the methods.

Author Contributions: Conceptualization, S.G.; methodology, S.G., L.A.S., and P.-T.S.S.; formal analysis, S.G. and L.A.S.; field investigation, S.G., L.A.S., R.K.R., B.O.H., and B.S.F.; data curation, S.G. and L.A.S.; writing—original draft preparation, S.G., L.A.S., and P.-T.S.S.; writing—review and editing, S.G., L.A.S., P.-T.S.S., R.K.R., B.O.H., and B.S.F.; visualization, S.G. and L.A.S.; Supervision, R.K.R., B.O.H., and B.S.F.; Project administration, R.K.R. and B.S.F.; Funding acquisition, R.K.R. and B.S.F.

Funding: The Regional Research Funds in Mid-Norway (grant number 209074) funded this research. The Norwegian University of Science and Technology funded the APC.

Acknowledgments: This work was conducted as part of the research project “Optimal Utilization of Groundwater for Heating and Cooling in Melhus and Elverum (ORMEL)”. The project is a cooperation between the municipalities of Melhus and Elverum, the Norwegian University of Science and Technology, Asplan Viak AS, and the Geological Survey of Norway. We would like to thank all the involved institutions and persons for cooperation and financial contributions.

Conflicts of Interest: The funders had no role in the design of the study; in the collection, analyses, or interpretation of data; in the writing of the manuscript; or in the decision to publish the results.

References

1. Bloemendal, M.; Olsthoorn, T.; van de Ven, F. Combining climatic and geo-hydrological preconditions as a method to determine world potential for aquifer thermal energy storage. *Sci. Total Environ.* **2015**, *538*, 621–633. [[CrossRef](#)] [[PubMed](#)]
2. RIISE, M.H. Praktisk Guide for Grunnvarmeanlegg Basert på Oppumpet Grunnvann—Hydrogeologiske Forundersøkelser, Etablering, Drift og Oppfølging med Utgangspunkt i Erfaringer fra Etablerte Anlegg i Melhus Sentrum [eng: Guide to the Open Loop GSHP Systems in Melhus]. Master’s Thesis, NTNU, Trondheim, Norway, 2015.
3. Brøste, H.M. Vannkvalitet Knyttet til Grunnvannsbaserte Grunnvarmeanlegg i Melhus og Elverum [eng: Water Quality with Respect to Open Loop GSHP Systems in Melhus and Elverum. In Norwegian]. Master’s Thesis, NTNU, Trondheim, Norway, 2017.
4. Gjengedal, S.; Ramstad, R.K.; Hilmo, B.O.; Frengstad, B.S. Video inspection of wells in open loop ground source heat pump systems in Norway. In Proceedings of the IGSHPA Conference, Stockholm, Sweden, 18–20 September 2018. [[CrossRef](#)]
5. Gjengedal, S.; Ramstad, R.K.; Hilmo, B.O.; Frengstad, B.S. Fouling and clogging surveillance in open loop GSHP systems. A systematic procedure for fouling and clogging detection in the whole groundwater circuit. *Bull. Eng. Geol. Environ.* **2019**. [[CrossRef](#)]
6. Jenne, E.A.; Andersson, O.; Willemsen, A. Well, hydrology, and geochemistry problems encountered in ATEs systems and their solutions. In Proceedings of the Aquifer Thermal Energy Storage, San Diego, CA, USA, 2–7 August 1992. [[CrossRef](#)]
7. Bakema, G. *Well and Borehole Failures in UTESS: State of the Art 2000 (Second Draft)*; IF Technology Report 2/9805/GW; 2001; Unpublished work.
8. Banks, D.; Pumar, A.F.; Watson, I. The operational performance of Scottish minewater-based ground source heat pump systems. *Q. J. Eng. Geol. Hydrogeol.* **2009**, *42*, 347–357. [[CrossRef](#)]
9. Oldmeadow, E.; Marinova, D. Into Geothermal Solutions: The Sustainability Case for Challenge Stadium in Perth, Western Australia. *Environ. Prog. Sustain. Energy* **2010**, *30*, 476–485. [[CrossRef](#)]
10. Banks, D. *An Introduction to Thermogeology: Ground Source Heating and Cooling*, 2nd ed.; Wiley-Blackwell: Chichester, UK, 2012; pp. 1–526.
11. Pujol, M.; Richard, L.P.; Bolton, G. 20 years of exploitation of the Yarragadee aquifer in the Perth Basin of Western Australia for direct-use of geothermal heat. *Geothermics* **2015**, *57*, 39–55. [[CrossRef](#)]
12. Nordell, B.; Scorpo, A.L.; Andersson, O.; Rydell, L.; Carlsson, B. *Long-Term Evaluation of Operation and Design of Emmaboda BTES: Operation and Experiences 2010–2015*; Research Report; LTU: Luleå, Sweden, 2015; ISBN 978-91-7583-530-3.
13. Snijders, A.L.; Drijver, B.C. Open-loop heat pump and thermal energy storage systems. In *Advances in Ground-Source Heat Pump Systems*, 1st ed.; Rees, S., Ed.; Woodhead Publishing: Amsterdam, The Netherlands, 2016; pp. 247–268. [[CrossRef](#)]
14. Yon-Gyung, R.; Hyun-Kwon, D.; Kyoung-Ho, K.; Seong-Teak, Y. Vertical Hydrochemical Stratification of Groundwater in a Monitoring Well: Implications for Groundwater Monitoring on CO₂ Leakage in Geologic Storage Sites. *Energy Procedia* **2017**, *114*, 3863–3869. [[CrossRef](#)]
15. Houben, G.J. Iron oxide incrustations in wells. Part 1: Genesis, mineralogy, and geochemistry. *Appl. Geochem.* **2003**, *18*, 927–938. [[CrossRef](#)]
16. Stumm, W.; Morgan, J.J. *Aquatic Chemistry: Chemical Equilibria and Rates in Natural Waters*, 3rd ed.; Wiley: New York, NY, USA, 1996.
17. Garrels, R.M.; Christ, C.L. *Solutions, Minerals and Equilibria*, 2nd ed.; Harper & Row: New York, NY, USA, 1965.

18. Appelo, C.A.J.; Postma, D. *Geochemistry, Groundwater and Pollution*, 2nd ed.; CRC Press: Leiden, The Netherlands, 2005.
19. Krauskopf, K.B. *Introduction to Geochemistry*, 2nd ed.; McGraw-Hill: New York, NY, USA, 1979.
20. Stumm, W.; Lee, G.F. Oxygenation of Ferrous Iron. *Ind. Eng. Chem.* **1961**, *53*, 143–146. [[CrossRef](#)]
21. Possemiers, M.; Huysmans, M.; Batelaan, O. Influence of Aquifer Thermal Energy Storage on groundwater quality: A review illustrated by seven case studies from Belgium. *J. Hydrol. Reg. Stud.* **2014**, *2*, 20–34. [[CrossRef](#)]
22. Larroque, F.; Franceschi, M. Impact of chemical clogging on de-watering well productivity: Numerical assessment. *Environ. Earth Sci.* **2011**, *64*, 119–131. [[CrossRef](#)]
23. García-Gil, A.; Epting, J.; Ayora, C.; Garrido, E.; Vázquez-Suñé, E.; Huggenberger, P.; Gimenez, A.C. A reactive transport model for the quantification of risks induced by groundwater heat pump systems in urban aquifers. *J. Hydrol.* **2016**, *542*, 719–730. [[CrossRef](#)]
24. Brown, K.A. Sulphur in the environment: A review. *Environ. Pollut. Ser. B Chem. Phys.* **1982**, *3*, 47–80. [[CrossRef](#)]
25. Brookins, D.G. *Eh-pH Diagrams for Geochemistry*, 1st ed.; Springer: Berlin, Germany, 1988; ISBN 3540184856.
26. Henry, W., III. Experiments on the quantities of gases absorbed by water, at different temperatures, and under different pressures. *Philos. Trans. R. Soc. Lond.* **1803**, *93*, 29–273.
27. Colt, J. *Dissolved Gas Concentration in Water: Computation as Functions of Temperature, Salinity and Pressure*, 2nd ed.; Elsevier: Amsterdam, The Netherlands, 2012.
28. Weiss, R.F. Carbon dioxide in water and seawater: The solubility of a non-ideal gas. *Mar. Chem.* **1974**, *2*, 203–215. [[CrossRef](#)]
29. Millero, F.J.; Poisson, A. International one-atmosphere equation of state of seawater. *Deep Sea Res. Part A Oceanogr. Res. Pap.* **1981**, *28*, 625–629. [[CrossRef](#)]
30. Çengel, Y.A.; Cimbala, J.M. *Fluid Mechanics: Fundamentals and Applications*, 2nd ed.; McGraw-Hill: Boston, MA, USA, 2014.
31. Kruseman, G.P.; Ridder, N.A.D.; Verweij, J.M. *Analysis and Evaluation of Pumping Test Data*, 2nd ed.; International Institute for Land Reclamation and Improvement: Wageningen, The Netherlands, 1990.
32. Grundfos A/S. Grundfos Data Booklet. SP A, SP Submersible Pumps, Motors and Accessories. ECM: 116286. Denmark. Grundfos a/s. 2017. Available online: <http://www.grundfos.com> (accessed on 9 April 2019).
33. Stene, J. *Varmepumper: Grunnleggende Varmepumpeteknikk [eng: Heat Pumps: Basics]*; SINTEF Energi, Klima-og Kuldeteknikk: Trondheim, Norway, 2001.



Paper IV



Online remote-controlled and cost-effective fouling and clogging surveillance of a groundwater heat pump system

A case study from Lena Terrace in Melhus, Norway.

Sondre Gjengedal¹ · Lars A. Stenvik¹ · Randi K. Ramstad¹ · Jan I. Ulfesnes² · Bernt O. Hilmo³ · Bjørn S. Fregstad¹

Received: 4 December 2019 / Accepted: 25 August 2020 / Published online: 10 September 2020
© The Author(s) 2020

Abstract

Fouling and clogging of groundwater wells and heat exchangers are among the major operational challenges for groundwater heat pump (GWHP) and aquifer thermal energy storage (ATES) systems. This article presents the application of a step-test surveillance procedure developed for early detection of clogging in distinct parts of the GWHP system, tested at Lena Terrace in Melhus Norway. Three versions of the test procedure are presented and demonstrate that the test can be performed with a minimum of four steps, each of 15-min duration, while the GWHP system is actively producing heat. The results prove that the surveillance test can detect changes in the hydraulic resistance of the groundwater circuit and locate clogging problems within all of the relevant system components in the groundwater circuit simultaneously. At the Lena Terrace GWHP system, these tests indicate a gradual increase of hydraulic resistance with time, which verify that clogging issues are continuously developing in the injection well, in the production well, and in the groundwater heat exchanger. Cleaning of the heat exchanger was then performed. This increased the pumping capacity by 8.3% points, but continuous clogging of the injection well and the production well necessitates further maintenance to ensure a reliable operation. It is demonstrated that multidisciplinary competence and experience with GWHP-systems, aquifers, and groundwater wells are needed for the evaluation of the results. These results can therefore serve as a reference for other GWHP systems with similar design configurations.

Keywords Groundwater · Step-test · Clogging · Surveillance · Hydrogeology · Heat pumps

Introduction

Ground water heat pump (GWHP) systems have become increasingly popular in Norway during the latest decades. Recent studies indicate a large potential for this technology, and similar trends are also seen worldwide (Bloemendal et al. 2015). One of the largest consumers of GWHP heating and cooling in Norway is the municipality of Melhus. An aquifer beneath the town center of Melhus is currently utilized as a heat source by ten individual GWHP systems. The first installation started

production already in 1999 and is still in operation today. All of these GWHP systems use a Quaternary deposit of saturated sand and gravel material as their heat source.

Many aspects of the system performance are governed by the local and the overall hydrogeological conditions within this deposit. The groundwater quality is an important factor in all types of GWHP installations (Bakema 2001; Banks 2012; Snijders and Drijver 2016). Problems caused by chemical reactions, suspended soil particles, or microbial growth in the water are a well-known and widespread issues for these systems, and clogging and fouling of system components is a common problem in Melhus (Riise 2015; Brøste 2017; Gjengedal et al. 2018; Gjengedal et al. 2019a; Gjengedal et al. 2019b). These problems typically involve clogging of the groundwater heat exchanger, the well screens, the pipeline, and the aquifer formation, also causing increased fatigue and erosion of the submersible pump. Usually, the heat pump performance and overall cost of the operation are affected by reduced heat production capacities and efficiencies. In severe

✉ Sondre Gjengedal
sondre.gjengedal@ntnu.no

¹ Norwegian University of Science and Technology, Trondheim, Norway

² Optiview AS, Vihals, Norway

³ Asplan Viak AS, Trondheim, Norway

cases, the complications can lead to complete system failure. Fouling and clogging of groundwater wells and heat exchangers therefore put the long-term reliability and sustainability of GWHP and, similarly, aquifer thermal energy storage (ATES) systems at risk. Consequently, groundwater source systems require a higher level of surveillance and maintenance than other ground source heat pump systems (Banks 2012; Snijders and Drijver 2016; Gehlin and Andersson 2019).

Monitoring and surveillance of GWHP systems is typically carried out by recording and analyzing pressure, temperature, and volume flow rate data (Gjengedal et al. 2019a). This type of monitoring is common in many heat pump applications (Stene 2001; Rees 2016) and is also standard for many industrial heating and cooling applications. District heating applications and the oil & gas industries are some examples (Müller-Steinhagen 2000; Melo et al. 1988). However, a variety of clogging and fouling issues in GWHP systems can cause similar symptoms and data responses, hence making it challenging to evaluate the data correctly.

A surveillance procedure for early detection of clogging and fouling in GWHP systems has previously been developed for GWHP systems in particular (Gjengedal et al. 2019a). Gjengedal et al. (2019a) demonstrate that the dynamic behavior of GWHP systems requires the pressure, temperature, and volume flow rate data to be evaluated with a specific procedure to enable proper interpretation of the data. The suggested procedure allows for testing and evaluation of all of the individual system components in the GWHP system simultaneously. The procedure has now been applied regularly in one of the installations in Melhus during routine maintenance of the system. This paper presents the experiences with the surveillance method and demonstrates the usefulness of the method for performance monitoring.

Site description and system specification

The town of Melhus is located in the Gauldal valley in Mid-Norway, approximately 20 km south of the city of Trondheim (Fig. 1). The town is located on a floodplain next to the river Gaula. Immediately to the north of the populated area, the landscape is dominated by Melhusryggen, a forested terminal moraine that stretches halfway across the valley, from the mountain of Vassfjellet in the east to the eastern embankment of the river Gaula. This glaciofluvial ridge marks the upper part of the Quaternary sand and gravel deposit known as the Melhus aquifer, an aquifer that in part extends beneath the town center south of the ridge. The river Gaula intersects the town center and separates both the town center and the aquifer into a western and eastern part.

Today, this aquifer supplies ten individual building complexes with heat and three building complexes with both heating and cooling. The Lena Terrace apartment complex

was built in 2003. It is located at the foot of the Melhusryggen ridge and is highlighted as the case study site in Fig. 1. The apartment complex' GWHP system is designed as a reinjection type system (Fig. 2). The local sediments are dominated by unconsolidated sand and gravel of glaciofluvial origin, and the groundwater water table is located approximately 20–21 m below the terrain level. At this depth and location within the aquifer, the groundwater temperature is found to be stable all year round at ~ 7 °C. The “natural” groundwater level, which imply the water level unaffected by the local GWHP activity, fluctuates approximately ± 1.0 m throughout the year (Hellestveit 2018). The aquifer is accessed by the GWHP system through two groundwater wells, one production well, and the other an injection well. The permeability of the aquifer formation is high, and this is reflected in the design of the wells.

The production well design is customized to the local soil conditions. The original design was a larger 219 mm OD well size, but due to drilling problems, the well size was reduced during construction. The finalized well design is 36.4-m deep and has a steel casing width of 168–158 mm (ODxID). The water is extracted from the well by a 10.8 kW Grundfos SP 60-5-MS6000 (50 Hz) submersible pump, which is installed at 28 m depth, immediately above the well screen. The well screen is the perforated section of the well and is installed from 29.4 to 35.4 m depth, providing 6 m of screened well length. The screen is a 161–150 mm ODxID con-slot screen, with 1.0 mm slot openings and a 31.3% perforation ratio. This screen design was selected based on grain size analysis of the soil, which are dominated by medium to coarse sand and gravel particles.

This production well design was originally selected to ensure proper operating conditions for the submersible pump. The Grundfos SP 60-5 pump generally requires 4–5 m of net pressure suction head (NPSH) during production (NPSH required depends on the motor speed). When the pump is inactive, the water table in the well is typically 6.0–7.0 m above the submersible pump. The available drawdown is thus limited to 2–3 m, leaving limited margin for potential clogging issues. There is however a 0.5-m sump pipe installed beneath the screen to accommodate potential sediment suffusion during operation.

The injection well is 36.5-m deep and has an identical design, but the screened segment of the well is installed from 23.5 to 33.5 m depth, which provide 10 m of screened well length. The return pipe is installed at 27.5 m depth, in the middle of the screened section of the well. There is a 3-m-long sump pipe beneath the screen to accommodate potential sediment suffusion during operation. The natural water table is typically 18.0–19.0 m below the well top during the heating season. This large elevation drop towards the well water level generates a suction in the groundwater piping system during production, causing vacuum pressures to develop in the pipe and in parts of the surface installation.

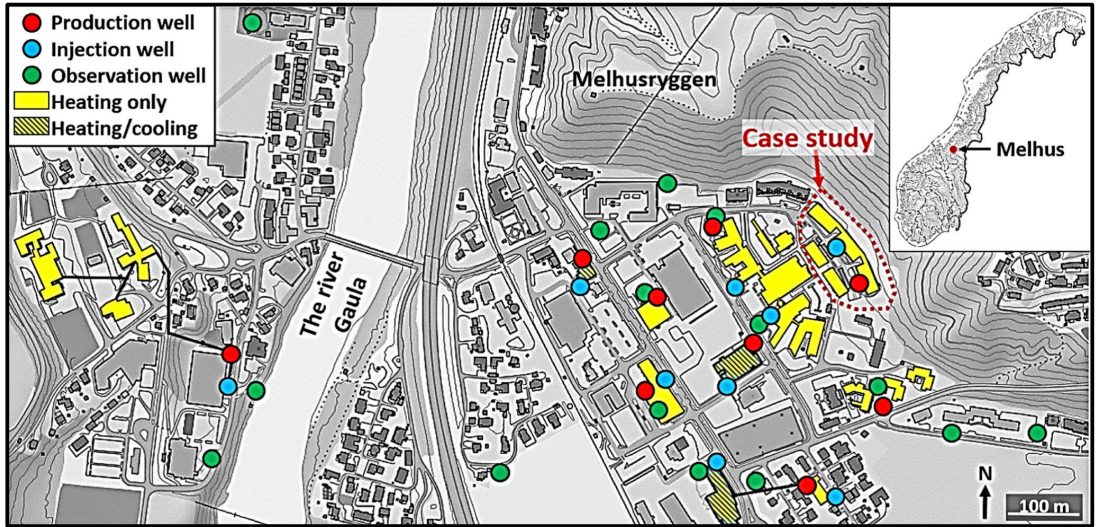


Fig. 1 Overview of the town center of Melhus with the ten GWHP installations (yellow buildings) and the corresponding groundwater wells indicated. There are 34 groundwater wells in the area, of which

18 are used for heating and cooling purposes. The location of the Lena Terrace building complex is highlighted as the case study site. Details of the Lena Terrace GWHP system are provided in Fig. 2 and Fig. 3

The groundwater circuit part of the surface installation is visualized in Fig. 3. The system consists of approximately 100 m of 160 mm ID HDPE pipes that connect the two wells to the groundwater heat exchanger situated in the basement of the building. The groundwater heat exchanger is a 260-kW gasket plate heat exchanger with a total of 72 m² plate surface

area (1.3 fouling factor). The total peak heating demand of 350 kW is provided by two custom Chiller Oy heat pump units (R134a). The heat pumps are coupled in parallel to a secondary loop circuit with 20% ethylene glycol antifreeze fluid. The secondary loop is connected to a plate heat exchanger for heat transfer with the groundwater loop.

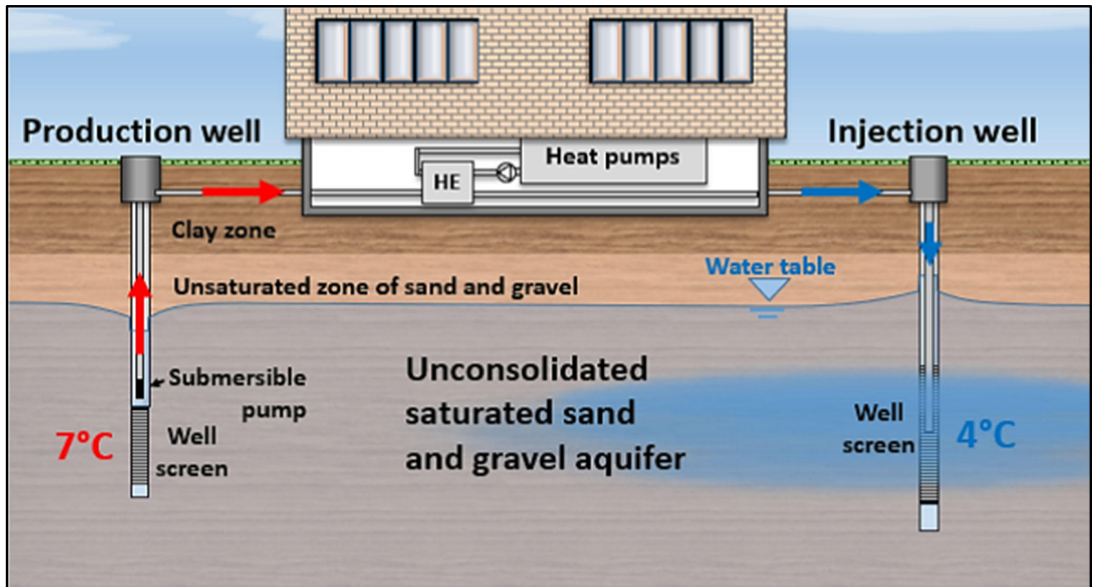


Fig. 2 Schematic sketch of the soil conditions and the reinjection type GWHP system employed at Lena Terrace in Melhus, Norway (the sketch is not to scale)

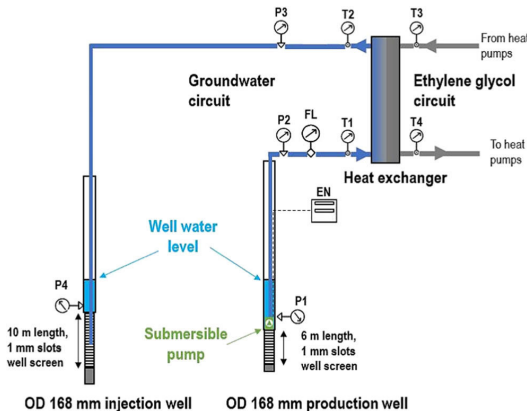


Fig. 3 Schematic sketch of the GWHP system at Lena Terrace, including real time monitoring of operational parameters. The groundwater pipe segment is approximately 100 m long. The relative location of the pressure transducer (P1–4), the flow meter (FL), the energy meter (and frequency converter) of the submersible pump (EN), and the temperature sensors (T1–4) are shown. The sketch is based on the online OPTIVIEW® interface

The designed efficiency point for the whole system is a coefficient of performance of 3 at maximum heating capacity ($COP = 3$). The groundwater system is designed to supply approximately 18 l/s of groundwater to accommodate the thermal demand during peak load conditions in the winter months. It assumed a groundwater temperature reduction from 7 °C to 4 °C ($\Delta T = 3$ K) at these conditions. During part load conditions, in the autumn and spring, the amount of groundwater circulation is reduced. This is controlled by adjusting the operating point of the submersible pump, between 60 and 100% of the maximum pump motor frequency (30–50 Hz).

Since its construction in 2003 the Lena Terrace GWHP plant has been affected by a variety of clogging and fouling issues. These are recurring problems, where fouling of iron precipitates affects the heat exchanger, while soil particles clog the injection well. The heat exchanger was most recently replaced in 2018 because of insufficient heat transfer capacity. The injection well is cleaned annually, most recently in 2018 and 2019, in an effort to maintain the reinjection capacity. Following the latest rehabilitation measures in 2018, the installation was re-equipped with new sensory equipment to improve the monitoring. These sensors are visualized in Fig. 3. The implementation of an automated control system now allows for remote control of the installation through an online TOSIBOX® system.

It is planned to clean the heat exchanger annually with an organic acid treatment before each heating season to mediate the iron precipitation fouling problem. The step-test method data presented here was applied in a period before and after the cleaning treatment on the 8th–9th of October 2019, to evaluate the need and the effect of the acid treatment. Three

of these step-tests are presented in this paper. The two first tests were conducted before the fouling treatment of the heat exchanger, while the third test was performed after the treatment.

Methodology

The surveillance procedure employed in this study involves conducting a series of incremental adjustments to the motor speed of the submersible pump, a so-called step-test. This is done by remote control through the online TOSIBOX® system, where the motor speed is controlled between 60 and 100% of its pumping capacity. The hydraulic and thermal performance of the system is then simultaneously measured at each speed, and the data is evaluated with least square regression analysis. The data response is evaluated with regard to potential clogging and fouling issues that affect the performance of the system in distinct ways, depending on their location within the system, as described in Gjengedal et al. (2019a).

The control system's integrated monitoring and control instrumentation are used for the data acquisition. The instrumentation and their relative location in the relevant part of the system control interface are shown in Fig. 3. The sensors used in the instrumentation are further described in Table 1. The temperature (T1–T4), pressure (P1–4), flow rate (FL), and the pumping power (EN) at the various speeds were recorded at each step of the test. All sensory data was automatically recorded by the monitoring system each minute and stored. The input data for the least square regression analysis and calculations are average values of the last eight measurements of each step of the tests, where steady-state conditions were assured.

The step-test procedure follows the methodology described in detail in Gjengedal et al. (2019a). Three variants of the procedure were tested to evaluate the applicability of the method (Table 2). The first test was performed with the minimum three steps required for the method, each of the steps having a duration of 1 h. Traditionally, each step of the tests is recommended to be between 0.5 and 2 h (Kruseman and de Ridder 1994), but the time can be reduced if the pressure response reaches steady state earlier. The purpose of test 1 was to evaluate the timeframe needed to achieve steady-state flow and pressure responses in the wells and the piping system. The pressures response stabilized within the first 1–3 min for each step, indicating a highly permeable aquifer formation. The duration of each step could therefore be reduced to 15 min for the two consecutive tests to investigate the possibility of reducing the timeframe of future tests.

The second test was performed with 19 individual steps to see if more steps would provide higher accuracy and possibly improve the usefulness of the surveillance data. The third test was an intermediate version with six steps. For tests 1 and 2,

Table 1 Instrumentation relevant for the step-test surveillance procedure

Location in Fig. 3	Instrument type	Accuracy
P1	Pressure transducer, Siemens SITRANS LH100	± 0.0015 bar
P2, P3	Pressure transducer, Danfoss MBS 4010 0–6 BAR ABS	± 0.03 bar
P4	Pressure transducer, Kacise GXPS430	± 0.015 bar
FL	Flow meter, Badger ModMAG M1000	± 0.04 l/s
EN	Energy meter, Grundfos CUE 3X380-500 V IP55 15KW 32A/2	–
T1–T4	Temperature probes, PT1000	± 0.3 °C

See Fig.3 for the relative location of the instruments in the GWHP system

the system was shut off before the tests to measure the unaffected pressure responses. Test 3 was performed without a shutoff period before the test, due to the continuous heat demand in the building. The unaffected groundwater level was then estimated via inverse calculation, using tests 1 and 2 as a reference for the expected water level draw-down at 60% pump capacity.

The procedure for test 2 is demonstrated in Fig. 4 and visualizes the progression of the test procedure. The test is performed with a pyramid-shaped speed increment adjustment. The first and the last step have the same speed (60%), while incremental adjustments were distributed evenly and mirrored around the 100% speed, producing the pyramid-shaped power curve. This mirroring of the test provided a mean of control during the test and confirmed that the behavior of the system is unchanged throughout the test procedure. Similar performance “pyramids” were observed in the data response in the control instrumentation.

Results

The four temperature sensors (T1–T4 in Fig.3) are installed on the four heat exchanger pipe segments to measure the temperature development of both fluids through the heat exchanger. In ideal conditions, the temperature data should be included in the analysis, but these temperature sensors were found to be incorrectly calibrated and could not be used to determine the efficiency of the heat exchanger. Thus, primarily the hydraulic

performance of the system, with the pressure, energy meter, and flow meter data, is used in the performance analysis.

The pyramid shape of the test 2 procedure (Fig. 4) is reflected in the pressure response that is presented in Fig. 5 for the heat exchanger. The differential pressure between the two sensors describes the hydraulic losses through the heat exchanger, which is used in the regression analysis. The data also demonstrate that the groundwater heat exchanger is subjected to vacuum pressures if the groundwater flow rate is reduced below a given threshold value (red shaded area in Fig. 5). This is observed in the P3 sensor when the groundwater flow rate is lower than 10.0 l/s, which corresponds to the 80% step in Fig. 4. At the lowest step (the 60% step), a – 7 kPa gauge pressure is observed in the P3 sensor. When the pump is turned off, the vacuum extends to the whole surface installation and stabilizes at approximately – 70 kPa gauge pressure in both P2 and P3.

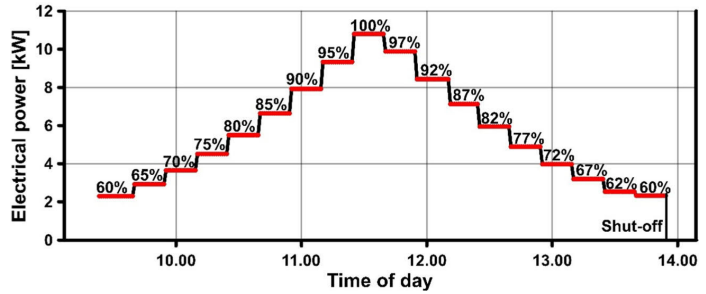
The results of the regression analyses of the three step-tests are presented in Table 3 and visualized in Fig. 6. The test results show that the electrical power consumption of the groundwater pump is equal for each corresponding step for each test, but the corresponding flow rates vary. A reduction in the pumping capacity signifies that the pump produces less water at a given motor speed. This can be observed by comparing the 100% speed flow rate of each test in Fig. 6d. In test 1, the flow rate is 16.2 l/s, which is 10% reduction from the initial 18.0 l/s capacity of the system. For test 2, the maximum capacity has reduced to 15.7 l/s, corresponding to a further 3.0% point reduction in pumping capacity over a 41-day

Table 2 The step-test specification for each of the three tests

Test no.	Date	Test time [h]	No. steps	Time per step [min]	Start point [% of 50 Hz]	Increment [% points]	Shutoff
1	28.08.2019 (Reference test)	4	3	60	0%	20	Yes
2	08.10.2019 (41 days later)	5.5	19	15	0%	2–3	Yes
3	16.10.2019 (55 days later)	1.5	6	15	60%	10	No

The various steps were distributed evenly through the 60–100% speed intervals, 60% (30 Hz) is the minimum speed and 100% (50 Hz) is the maximum speed of the pump. All measurements were automatically recorded each 1 min by the monitoring system

Fig. 4 Step-test procedure of test 2 at Lena Terrace GWHP system. The test involves 19 steps of incremental pumping speed adjustments between 60 and 100% of the pump power capacity. The first and final step are at the 60% speed. Each step lasts for 15 min. The test is completed with a shutoff sequence at the end



period. After the cleaning treatment, Test 3 shows a consistent increase in pumping capacity at all speeds and the pump provides 17.2 l/s with the same power consumption of 10.8 kW, a recovery of 8,3%-point compared with the initial 18.0 l/s capacity.

The variable pump performance implies that the hydraulic resistance of the system is different for each of the three tests. This is confirmed in the three differential pressure responses, which show both vertical and horizontal shifts of the pressure graphs in the data of the injection well, the production well, and of the groundwater heat exchanger (Fig. 6A-C). However, different types of performance changes are observed in these three components, which implies that the hydraulic resistance might have been altered differently in different parts of the system.

Since the sensors and the instrumentation were installed after the heat exchanger was replaced in the autumn of 2018 there are no initial on-site measurements of the heat exchangers hydraulic performance. However, the manufacturer provides a differential pressure of 2.64 m at 20.6 l/s pumping rate, which can serve as a reference for the tests. Plate heat exchangers are typically designed to operate within turbulent flow conditions, and this is observed for this installation as well where the groundwater heat exchanger pressure response is non-linear with respect to the flow rate (Fig. 6C). During Test 1 the pressure builds up to a maximum of 6.9 m of hydraulic head at 16.2 l/s flow rate, which is a substantial increase of hydraulic resistance compared with the data

specified by the manufacturer. This has further increased in Test 2 to a maximum pressure head of 8.0 m, even with a 0.5 l/s lower flow rate, indicative of clogging development. After the cleaning treatment, test 3 shows a consistent decrease in pressure head for all pumping speeds. By comparing the regression results in Table 3, it is seen that both the linear and the non-linear data response have changed after the cleaning. The acid cleaning treatment has reduced the hydraulic resistance of the heat exchanger significantly.

Unlike the heat exchanger, a properly designed groundwater well should ideally have a fully linear pressure relation with respect to the pumping rate. This occurs in the injection well where the pressure increases linearly with the flow rate for all three tests. However, a consistent increase of magnitude of overpressure is observed between tests 1, 2, and 3, respectively. The linear regression results indicate that the hydraulic resistance in the injection well has increased by 65% from test 1 in August to test 3 in October. This is indicative of clogging development. Approximately half of the increased hydraulic resistance occurs after test 2, which indicates that the rate of clogging deposition is accelerating.

For the production well, the drawdown increases non-linearly with respect to the flow rate and the non-linear component dominates the pressure response (Fig. 6b). A consistent increase of water level drawdown is also observed between test 1 and 2, while the data points of test 3 plots almost equal to those of test 2. The peak drawdown was 0.3 m larger for test 3 at the 100% speed, but this corresponds to the

Fig. 5 Test 2 performance pyramid for the P2 and P3 pressure sensor. See Fig. 4 for test increments. At the 60% pumping speed, the pressures correspond to -7 kPa pressure in the P3 sensor. After the pump is shut off, the vacuum extends to the P2 sensor, and a -70 kPa vacuum is observed in the whole groundwater pipeline (outside the y-axis)

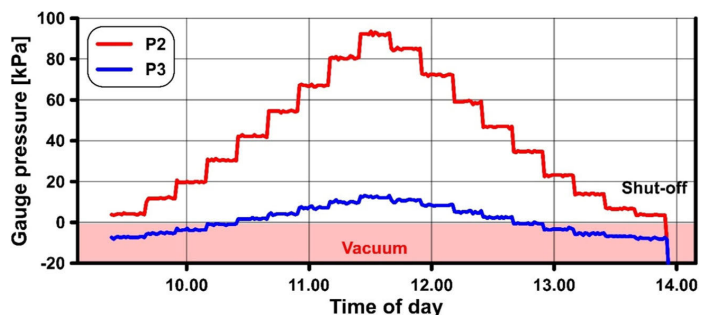


Table 3 The step-test regression results. ΔP [m] denotes the pressure differential and Q [l/s] denotes the variable flow rate. All regression curve fits are within $R^2 > 0.99$. The curves are visualized in Fig. 6

Test no.	Date	Injection well	Production well	Heat exchanger
1	28.08.2019 (Reference test)	$\Delta P = 0.068 \cdot Q$	$\Delta P = 0.018 \cdot Q + 0.010 \cdot Q^2$	$\Delta P = 0.064 \cdot Q + 0.022 \cdot Q^2$
2	08.10.2019 (41 days later)	$\Delta P = 0.094 \cdot Q$	$\Delta P = 0.030 \cdot Q + 0.011 \cdot Q^2$	$\Delta P = 0.056 \cdot Q + 0.029 \cdot Q^2$
3	16.10.2019 (55 days later)	$\Delta P = 0.112 \cdot Q$	$\Delta P = 0.039 \cdot Q + 0.010 \cdot Q^2$	$\Delta P = 0.016 \cdot Q + 0.011 \cdot Q^2$

increased pumping rate capacity of the submersible pump after the cleaning treatment. By comparing the regression results in Table 3, it is seen that it is primarily the linear data response that have changed, while the non-linear data response is virtually unchanged. The linear part of the regression results have increased by 116% from test 1 in August to test 3 in October. Approximately half of the increased hydraulic resistance occurs after test 2, similar to that of the injection well.

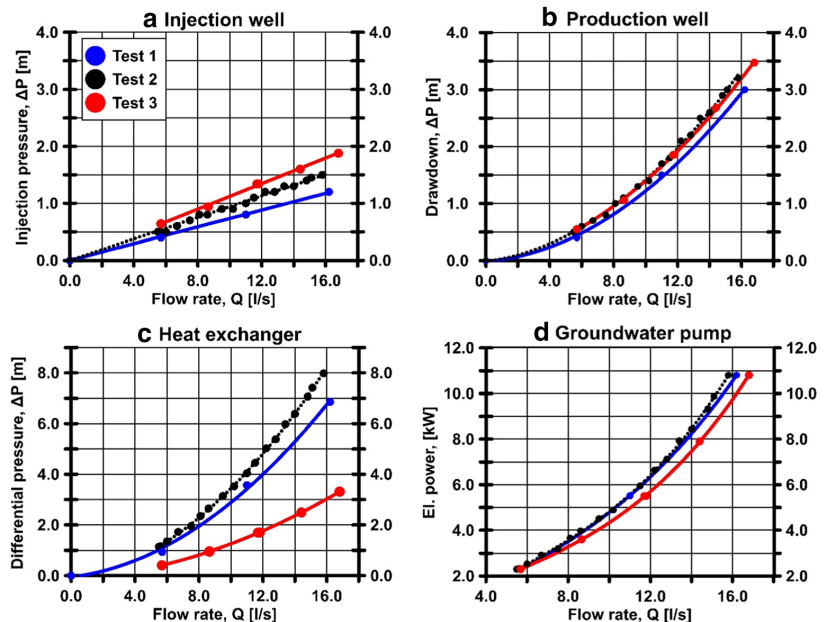
Discussion

The presented step-test data demonstrate how the performance of the heat source system at Lena Terrace can be monitored with the applied surveillance procedure. The integrated sensory equipment is able to detect changes in the hydraulic performance of the submersible pump, the groundwater heat exchanger, the production well, and the injection well. The results from the three different step-test procedures show that a

variety of test configurations can be applied, but a minimum number of steps are preferable when the test is applied in practice. It is shown that test 1, with only three steps, describes the trends of the wells and the heat exchanger performances properly. The potential benefit of including more steps is not reflected in the added detail of the data of test 2 as it is possible to describe the same trend with only three of the data points. The surveillance procedure therefore only needs three steps to work in practice. This does however require a shutoff period before the test, which might not be acceptable if the building needs heating, e.g., during the winter months. As described in Gjengedal et al. (2019a), the benefit of the test 3 procedure is the possibility to perform the test without disrupting the heat production of the heating system. A step-test with four steps is thus recommended.

The step-test must be able to locate problems in the system in order to work as a surveillance tool. It is here demonstrated that the tests detect variability in the pump performance, which indicates that the hydraulic resistance of the system

Fig. 6 The injection pressure (ΔP) responses for the injection well (a), the drawdown (ΔP) of the production well (b), the differential pressure response (ΔP) of the heat exchanger (c), and the electrical power supplied to the pump (d) as a function of the flow rate (Q) for the three step-test in the Lena Terrace GWHP system. Tests 1 and 2 are performed before the maintenance of the groundwater heat exchanger in October. Test 3 is performed after the cleaning



has changed. The first two tests show a reduction of production capacity for the whole groundwater system prior to the treatment of the groundwater heat exchanger. This increased hydraulic resistance indicates that clogging problems are developing in the entire system, especially in the production well, the injection well, and in the groundwater heat exchanger. Multidisciplinary competence and experience with GWHP-systems, aquifers, and groundwater wells are therefore needed to properly evaluate and interpret the results. The tests do not reveal what type of clogging material that impedes the system, but Bakema (2001) and Olsthoorn (1982) argue that monitoring over a longer timeframe can reveal different trends that are associated with various types of clogging, e.g., gas intrusion, chemical incrustations, or sediment suffusion. In this case, the test results can be interpreted and evaluated based on the system design and previous experience with faults found in the system. The tests can thus serve as a reference for other similar GWHP systems.

It was known beforehand that the groundwater heat exchanger is affected by fouling issues, typically by iron precipitates and fine soil particles clogging the heat exchanger plates. In these three tests, it is shown how this affects the hydraulic resistance of the heat exchanger. An increase in differential pressure, which is observed in tests 1 and 2, indicates that clogging and fouling development is in progress. The cleaning treatment reduced the hydraulic resistance, and test 3 demonstrates how the effects of the cleaning treatment yields a significant reduction in hydraulic resistance. The main benefit of the cleaning was presumably the improved heat transfer properties of the heat exchanger, but this could not be estimated accurately with the uncalibrated temperature sensors. The actual improvement to the thermal performance can therefore not be evaluated. However, the test shows that an increase in pumping capacity, by 1.5 l/s at maximum motor speed, is achieved after the cleaning. The test thus reveals how the lower hydraulic losses through the groundwater heat exchanger also affect the other parts of the system, e.g., through increasing the maximum drawdown in the production well at 100% pumping rate. Cleaning of the heat exchanger thus affects all parts of the system in the hydraulic sense, because the overall pumping capacity is affected.

An important benefit of the cleaning is that the pump is able to supply the necessary amount of groundwater at lower motor speeds. This reduces the electrical power consumption of the pump and the pumping cost for the installation. Some of the costs of annual cleaning of the heat exchanger are thus saved through improving the performance of the groundwater system. In the future, the performance of the heat exchanger should be monitored with calibrated temperature sensors. The heat-conducting properties of the heat exchanger are more sensitive to fouling than the hydraulic resistance. Monitoring the heat flux is thus expected to provide a more sensitive tool for

fault detection in the heat exchanger (Gjengedal et al. 2019a).

The clogging material that was removed during the injection well cleaning operations and rehabilitations in 2018 and 2019 showed that the injection well was filled with a mixture of soil sediments and particles. These sediments were found to have been derived from suffusion through the production well screen. This has likely occurred this time as well. The increased hydraulic resistance observed in the injection well pressure response is a clear indication that clogging development is in progress. Similar pressure responses are described by Olsthoorn (1982) for injection well clogging in general. The data display a gradual buildup of the pressure response over the 55-day period, and the regression results (Table 3) show that the rate of clogging deposition is accelerating. In order to ensure continuous and reliable operation of the GWHP system, it is therefore necessary to perform additional maintenance on the injection well screen but also the production well to stop the suffusion of particles.

Suffusion of soil particles through the production well screen is known to affect the production well performance in a distinct manner (Olsthoorn 1982; Van Beek 2007). The presented tests demonstrate that the drawdown in the production well react non-linearly to the flow rate (Fig. 6b), deviating from the anticipated fully linear drawdown curve expected from a properly design groundwater well. The question is whether this excessive drawdown is a sign of clogging of the production well screen or not. By comparing the pressure response of tests 2 and 3, relative to test 1, it is observed that there is an increased hydraulic resistance in the well. However, the relative increase in drawdown originates from an increase of the linear pressure responses, while the non-linear pressure response is virtually unaffected. The majority of linear head losses originate from aquifer losses and/or well screen losses (Houben 2015a). This increase of linear head losses is therefore a likely sign of clogging of the well screen and/or the aquifer.

The lack of change in the non-linear component indicates that the cause of these losses has not been altered throughout the test period. Non-linear drawdown losses are associated with inertial losses that occur at high velocities (e.g., convective acceleration or turbulence). The fully linear response of the injection well reveals that the local soil conditions do not induce non-linear losses in the flow for the pumping rates tested. The production well has similar soil conditions, but compared with the injection well, it has slightly higher flow velocities through the well screen because of the shorter screen length. Assuming an even distribution of the flow along the entire well screen, the average maximum flow velocity (17.2 l/s flow rate at 100% Hz) through the production well screen is 1.81 cm/s, while it is 1.09 cm/s through the injection well screen. The 1.81 cm/s velocity is perhaps high enough to induce some non-linear losses in the aquifer

(Houben 2015a), but not to the degree that is measured here. The difference in screen flow velocity does therefore not explain the dominant non-linear component of the production well pressure response.

The most likely cause to these non-linear losses is the relatively large contraction and expansion of the flow channel in the well-bore segment around the submersible pump motor. Houben (2015b) states that the upwards flow velocity in a well should be kept below 1.5 m/s to maintain well losses at an acceptable level. This is ensured in the well-bore itself, but not in the section around the pump. The SP60-5-MS6000 submersible pump (Grundfos 2019) has a motor diameter of 139.5 mm. The internal well diameter of 158.0 mm then provides a 9.25-mm annular channel opening past the pump motor, which is very narrow for the 17.2 l/s flow rate. The average flow velocity past the 0.6 m long motor will then be approximately 3.9 m/s, indicating highly turbulent flow conditions. This channel opening is unchanged from test 1–test 3, and it is therefore reasonable that the non-linear component is unchanged as well. The non-linear behavior is thus not likely caused by clogging, but by a faulty well design with a too narrow well diameter.

Apart from the clogging issues that are detected, the tests reveal that the production well water level drawdown is too large to ensure that the pump operates reliably. The submersible pump requires 5 m of overpressure (NPSH) to operate reliably at 100% Hz motor speed (Grundfos 2019). With 3.5 m of drawdown, the pump operates with 2.9 m of overpressure, and the pump is thus subjected to increased risks of, e.g., flow separation and vacuum pressures at the suction inlet and internal cavitation at the pump impellers (Mackay 2004). To ensure continuous and reliable operation of the GWHP system, it is necessary to perform additional maintenance on the production well screen or to limit the pumping rate to 80% of the maximum capacity where 4 m of NPSH is sufficient.

The tests also reveal that parts of the groundwater pipeline operate with vacuum pressures. Vacuum pressure can potentially trigger exsolution of gases that are dissolved in the groundwater (Banks 2012; Snijders and Drijver 2016; Gjøngedal et al. 2019b). The tests thus indicate that the system has an unfavorable design configuration with respect to the local groundwater conditions, which can potentially be the underlying reason for the clogging issues that has troubled this installation since 2003.

Conclusions

The performance of the Lena Terrace groundwater heat pump system has been monitored with a step-test surveillance procedure. Results from three versions of the test demonstrate that the test can be performed with a minimum of four steps, each of 15-min duration, while the GWHP system is active

and producing heat. The results demonstrate that the surveillance test can detect changes in the hydraulic resistance of the groundwater circuit and locate clogging problems within all of the relevant system components in the groundwater circuit simultaneously. At the Lena Terrace GWHP system, these tests indicate a gradual increase of hydraulic resistance with time, which verify that clogging issues are continuously developing in the injection well, the production well, and in the groundwater heat exchanger. Cleaning of the heat exchanger has increased the pumping capacity by 8.3% points, but continuous clogging of the injection well and the production well necessitates further maintenance to ensure a reliable operation. These results can function as a reference for other GWHP systems with similar design configurations.

Acknowledgments Open Access funding provided by Norwegian University of Science and Technology (incl St. Olavs Hospital - Trondheim University Hospital). This work was conducted as a part of the research project Optimal Resource Utilization of Groundwater for Heating and Cooling in Melhus and Elverum (ORMEL). The project is a cooperation between the municipalities of Melhus and Elverum, the Norwegian University of Science and Technology, Asplan Viak AS, and the Geological Survey of Norway. We would like to thank all the involved institutions and persons for cooperation and financial contributions.

Funding The Regional Research Funds in Mid-Norway (grant number 209074) funded this research.

Compliance with ethical standards

Conflict of interest The authors declare that they have no conflict of interest.

Open Access This article is licensed under a Creative Commons Attribution 4.0 International License, which permits use, sharing, adaptation, distribution and reproduction in any medium or format, as long as you give appropriate credit to the original author(s) and the source, provide a link to the Creative Commons licence, and indicate if changes were made. The images or other third party material in this article are included in the article's Creative Commons licence, unless indicated otherwise in a credit line to the material. If material is not included in the article's Creative Commons licence and your intended use is not permitted by statutory regulation or exceeds the permitted use, you will need to obtain permission directly from the copyright holder. To view a copy of this licence, visit <http://creativecommons.org/licenses/by/4.0/>.

References

- Bakema G (2001) Well and borehole failures in UTESS. State of the art 2000, 2nd edn. IF Technology BV, Arnhem
- Banks D (2012) An introduction to Thermogeology: ground source heating and cooling, 2nd edn. Wiley-Blackwell, Chichester
- Bloemendal M, Olsthoorn T, van de Ven F (2015) Combining climatic and geo-hydrological preconditions as a method to determine world potential for aquifer thermal energy storage. *Sci Total Environ* 538: 621–633. <https://doi.org/10.1016/j.scitotenv.2015.07.084>

- Brøste HM (2017) Vannkvalitet knyttet til grunnvannsbaserte grunnvarmeanlegg i Melhus og Elverum [eng: Water quality with respect to open loop GSHP systems in Melhus and Elverum]. Master thesis, Norwegian University of Science and Technology Trondheim (NTNU Trondheim) (in Norwegian)
- Gehlin S, Andersson O (2019) Geothermal energy use, country update for Sweden. Proceedings of the European Geothermal Congress, Den Haag, The Netherlands, 11–14 June
- Gjengedal S, Ramstad RK, Hilmo BO, Frengstad BS (2018) Video inspection of wells in open loop ground source heat pump systems in Norway. Editor: prof. Jeffrey D. Spitzer. International ground source heat pump association, Oklahoma. In IGSHA conference proceedings 2018. <https://doi.org/10.22488/okstate.18.000025>
- Gjengedal S, Ramstad RK, Hilmo BO, Frengstad BS (2019a) Fouling and clogging surveillance in open loop GSHP systems. A systematic procedure for fouling and clogging detection in the whole ground-water circuit. *Bull Eng Geol Environ*. <https://doi.org/10.1007/s10064-019-01556-5>
- Gjengedal S, Stenvik LA, Storli PT, Ramstad RK, Hilmo BO, Frengstad BS (2019b) Design of groundwater heat pump systems. Principles, tools and strategies for controlling gas and precipitation problems. *Energies* 12:3657. <https://doi.org/10.3390/en12193657>
- Grundfos (2019) Grundfos data booklet. SP engineering manual <https://nogrundfoscom/campaigns/download-sp-engineering-manual.html> Accessed on: 29 November 2019
- Hellestveit MS (2018) 3D-modellering av grunnvannstrømning og varmetransport i akviferen i Melhus sentrum - en kvartær- og hydrogeologisk tolkning, med vurdering av uttakskapasitet. [eng: 3D modeling of groundwater flow and thermal development in the Melhus aquifer – an evaluation of quaternary and hydrogeological conditions and exploitation limitations] master thesis. Trondheim. NTNU. (in Norwegian)
- Houben GJ (2015a) Review: hydraulics of wells – the flow laws and influence of geometry. *Hydrogeol J* 23:1633–1657. <https://doi.org/10.1007/s10040-015-1312-8>
- Houben GJ (2015b) Review: hydraulics of water wells—head losses of individual components. *Hydrogeol J* 23:1659–1675. <https://doi.org/10.1007/s10040-015-1313-7>
- Kruseman GP, de Ridder NA (1994) Analysis and evaluation of pumping test data, 2nd edn. Wageningen, International Institute for Land Reclamation and Improvement
- Mackay R (2004) The practical pumping handbook. Elsevier, Oxford
- Melo LF, Bernardo CA, Bott TR (1988) Fouling science and technology. Kluwer, Dordrecht
- Müller-Steinhagen H (2000) Heat exchanger fouling: mitigation and cleaning technologies: handbook. Publico Publications, Essen
- Olsthoorn TN (1982) The clogging of recharge wells, technical report. The Netherlands Waterworks' testing and research institute KIWA, Rijswijk
- Rees S (2016) Advances in ground-source heat pump systems. Woodhead Publishing, Amsterdam
- Riise MH (2015) Praktisk guide for grunnvarmeanlegg basert på oppumpet grunnvann - Hydrogeologiske forundersøkelser, etablering, drift og oppfølging med utgangspunkt i erfaringer fra etablerte anlegg i Melhus sentrum [eng: Guide to a better design and operation of groundwater heat pump systems – with examples from Melhus]. Master thesis, NTNU Trondheim (in Norwegian)
- Snijders AL, Drijver BC (2016) Open-loop heat pump and thermal energy storage systems. In: Rees S (ed) Advances in ground-source heat pump systems, 1st edn. Woodhead Publishing, Amsterdam, pp 247–268
- Stene J (2001) Varmepumper: grunnleggende varmepumpeteknikk [in English: Heat pumps: basics] Trondheim, SINTEF Energi
- Van Beek C (2007) Cause and prevention of clogging of wells. Abstracting groundwater from unconsolidated aquifers. PhD Thesis, Vrije University, Amsterdam

Paper **V**



How to avoid gas clogging in groundwater heat pump systems: a case study from the Lena terrasse system in Melhus, Norway

Lars A. Stenvik¹ · Sondre Gjengedal² · Randi K. Ramstad^{1,3} · Bjørn S. Frengstad¹

Received: 14 July 2021 / Accepted: 9 March 2022 / Published online: 17 March 2022
© The Author(s) 2022

Abstract

Vacuum pressures are unfavorable in water pipes since they pose a risk to degassing dissolved gases from the water and air in-leakage. If the water flow rate through the pipeline is too low, gas bubbles will rise to local high points and create stagnant gas pockets. Gas pockets may clog both directly by obstructing the flow cross-section and indirectly by disturbing chemical equilibria. Gas clogging in the Lena terrasse groundwater heat pump system (GWHP) in Melhus, Norway, has been investigated by pressure, temperature, groundwater flow rate, and pump power consumption monitoring data. The GWHP extracts groundwater through a production well, leads it to a heat exchanger at the terrain level, and then re-injects the water through an injection well. It thus operates as a siphon which is prone to vacuum pressures. Analytical tools adapted from hydraulic engineering have been used to identify vacuum pressures and insufficient pipe flow rates to remove gas pockets in the Lena terrasse GWHP. Monitoring data shows that incrustation induced pressure build-up in the injection well filter does not impact the pump production capacity. This indicates gravity driven *waterfall flow* from the heat exchanger to the injection well, caused by stagnant gas pockets. It is recommended to install a backpressure valve at the end of the injection pipe or multiple narrow injection pipes inside the injection well, and air release valves at the local high points, to ensure the system is kept pressurized and water-filled. The extra required pumping head will approximately equal the overpressure criterion (e.g., 0.5 bar) set at the pressure minimum in the groundwater circuit, which introduces quite modest extra pumping costs per year.

Keywords Gas · Clogging · Ground source heat pump · Groundwater · Well test · Pipe flow

Introduction

Groundwater heat pump (GWHP) systems utilize groundwater as a heat source and/or a heat sink for temperature regulation purposes in buildings. GWHPs usually comprise pumping up groundwater from a production well to a heat exchanger, and re-injecting the heat exchanged water into the aquifer through an injection well; see Fig. 1. This technology can reduce the electricity demand by ~60–70% compared to conventional electric heating. However, the economic and environmental benefits of GWHPs are hampered by various

clogging mechanisms which obstruct the groundwater flow in well filters, groundwater pumps, heat exchangers, pipes, etc. (Jenne et al. 1992; Bakema 2001; Possemiers et al. 2016; Snijders and Drijver 2016; Gjengedal et al. 2020).

A groundwater heat pump system resembles a *siphon*; an inverted U-shaped tube that moves liquid up from one reservoir and down to another one under the influence of gravity and cohesive forces (Çengel and Cimbala 2010). This creates vacuum pressures on the top side of the GWHP, which initially lowers the required pumping head from the submersible pump in the production well. However, the vacuum pressures induce gas formation which will clog the system and increase the required pumping head through the pipeline. The siphon effect thus leads to unstable operating conditions for the submersible pump. Designers of GWHPs and other systems containing injection wells are therefore advised to keep the pipes *pressurized* (i.e., with pressure higher than the atmospheric) (Sniegocki and Reed 1963; Olsthoorn 1982; Andersson 1988; Jenne et al. 1992; Banks 2012; Snijders and Drijver 2016; Guttman et al. 2017; Gjengedal et al. 2019).

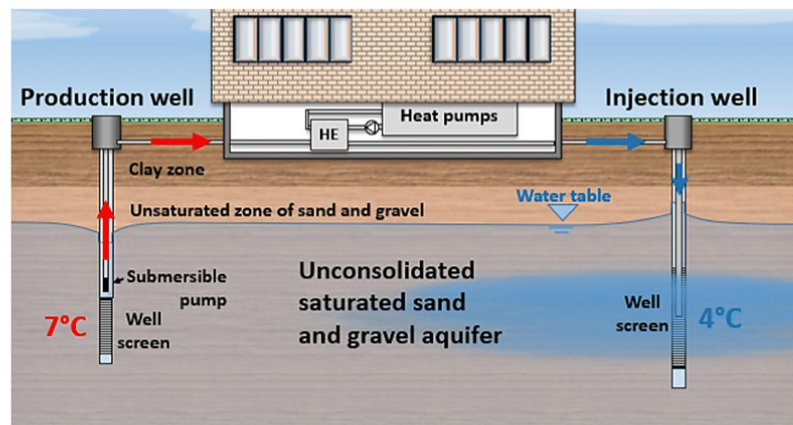
✉ Lars A. Stenvik
lars.a.stenvik@ntnu.no

¹ Department of Geoscience and Petroleum, Norwegian University of Science and Technology, 7491 Trondheim, Norway

² Norwegian Geotechnical Institute, Torgarden, PO Box 5687, 7485 Trondheim, Norway

³ Asplan Viak AS, Hotellgata 2, 7500 Stjørdal, Norway

Fig. 1 Sketch of a typical groundwater heat pump system (GWHP) design in Melhus, Norway (Gjengedal et al. 2021)



Limited literature exists on the cost–benefit of pressurizing versus gas clogging and how to design and dimension gas control measures. This knowledge gap is sought tightened in this article by presenting analytical tools from hydraulic engineering applied to gas clogging problems in GWHP systems. Additionally, practical advice on how to mitigate gas clogging is presented and discussed.

The case study focuses on the Lena terrasse GWHP plant in Melhus, Norway, which currently operates without dedicated measures to pressurize its groundwater pipes. This work is a continuation of a theoretical analysis of gas clogging in GWHP systems (Gjengedal et al. 2019) and an article concerning the instrumentation and monitoring of the same GWHP system as in this study (Gjengedal et al. 2021). Two years of monitoring have provided data for testing and modifying the conclusions in Gjengedal et al. (2019, 2021) and facilitated new insights into troubleshooting and solving gas clogging problems.

Gas in water pipes

Gas can form in pipes either by degassing of dissolved gases in the water or in-leakage through improperly sealed pipes. For dilute solutions, Henry's law states that the solubility c_A of gas A is proportional to the gas' partial pressure p_A in contact with the solvent liquid (Stumm and Morgan 1996):

$$p_A = K_{H,A} c_A \quad (1)$$

where the solubility constant $K_{H,A}$ typically increases with temperature. Since Eq. 1 is valid for all gases, the total amount of gas dissolved in water c_{gas} is proportional to the total gas pressure p_{gas} . Thus, if the liquid pressure p falls below p_{gas} , or the temperature increases, gas will escape the liquid phase (i.e., degas). In a review of gas-phase formation during

thermal energy storage in near-surface aquifers by Lüders et al. (2016), 95% of the groundwaters were found to be in contact with $p_{gas} \leq 1.41$ atm, with a median $p_{gas} = 1.02$ atm. Pressure drops below atmospheric pressure ($p_{atm} = 1$ atm) creates a pressure gradient from outside towards the interior of the pipe. This may facilitate air in-leakage through improperly sealed parts of the pipeline (Bakema 2001). Vacuum pressures thus expose the pipeline to risk of gas formation both from in situ degassing and air in-leakage.

Flowing water is exposed to pressure drops when the elevation and/or the velocity increases and due to frictional losses to its surroundings (Çengel and Cimbala 2010). Thus, if groundwater is extracted from an aquifer near gas saturation pressures, the pressure drop resulting from locally elevated water flow around the well filter may lead to degassing. Surface tension between the gas bubbles and porous media then may obstruct (i.e., clog) the water flow and increase the pressure drawdown in the extraction well. Water flow through the GWHP system will result in pressure drops from frictional losses and higher elevations (i.e., the siphon effect). This makes the injection well prone to vacuum pressures. Thus, gas bubbles moving with the flow can also clog the injection well filter and the surrounding aquifer formation, before eventually becoming dissolved if sufficient overpressure ($p > p_{gas}$) is applied to the bubbles in the aquifer. According to Bakema (2001), gas clogging is a bigger problem in injection well filters than in extraction well filters. Furthermore, degassing and air in-leakage may indirectly increase the precipitation potential for typical incrustation minerals such as oxides and carbonates; oxygen in-leakage will trigger oxidation of iron, while CO_2 degassing decreases oxide/carbonate solubility by increasing the pH.

Gas does not necessarily accumulate where it first forms but tends to rise to the highest point in the pipes due to buoyancy forces. The drag exerted by the flow on a gas bubble

opposes this effect by pushing the bubble in the flow direction. The balance between these two effects can be expressed by the Froude number Fr (Çengel and Cimbala 2010)

$$Fr = \frac{q}{\sqrt{gL_c}} \tag{2}$$

where q is the flow rate Q divided by flow cross section A , g is gravitational acceleration, and L_c is a characteristic length (i.e., the pipe diameter in a circular pipe). Extensive theoretical and experimental research has been conducted to find a critical Froude number Fr_c ; the minimum Froude number which causes gas bubbles to be carried with the liquid flow. Some of the relevant results for this case study are listed in Table 1. The results show that Fr_c depends on the pipe inclination. For upward oriented pipes, the gas will move in the flow direction. For horizontal and downward facing pipes, experimental results indicate that Fr_c is lowest in vertical, higher in horizontal, and highest in inclined pipes (30–45°).

The actual Froude number Fr must therefore exceed the maximum Fr_c for inclined pipes to remove gas from downward bends between horizontal and vertical pipe sections. If not, gas will accumulate in pockets at local high points and on the downward side of bends, where the flow velocity is unable to exceed the critical Fr_c number; see Fig. 2. This also means that an initially empty (i.e., a gas-filled GWHP system) must start operation at $Fr > Fr_c$ to remove the gas and become water-filled. Conversely, a system where $Fr < Fr_c$ will remain at least partly gas-filled during operation.

Gas pockets will lead to higher head losses in the pipeline (i.e., clogging) by inducing open channel or gravity driven flow. This is known as *waterfall flow* among pipe engineers. The gas phase has lower density than water, meaning that the pipe pressure at the top and bottom of a gas pocket will be approximately the same. The gas pocket then causes a head loss h_{gas} equal to the elevation drop from top to bottom of the gas pocket (Corcos 2003); see Fig. 2. Thus, vacuum

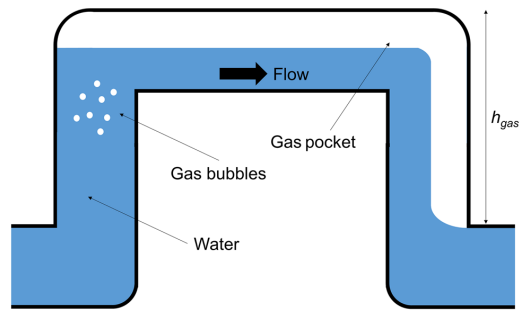


Fig. 2 Gas pocket entrapped around a local high point of a pipe. The extra head loss caused by the gas pocket h_{gas} is shown

pressures and subcritical Froude numbers are sought avoided in pipe networks.

Site description

Ten groundwater heat pump systems operate within a radius of 500 m in the town center of Melhus, Norway (Fig. 3). All systems extract groundwater from the Melhus aquifer: a coarse unconsolidated ice marginal deposit from Younger Dryas, with the Melhus Ridge as its most prominent feature. The aquifer is hydraulically connected with River Gaula which controls the water table, some ~10–20 m below terrain level (Hellestveit 2018). A marine clay layer on top of the ice marginal deposit has left the aquifer with semi-confined characteristics and a saline, reducing water quality (Riise 2015).

The Lena terrasse GWHP supplies 350 kW heating to 119 apartments; see the area marked with “Case study” in Fig. 3. The groundwater part of the system comprises a production well with a submersible pump, water pipes, a heat exchanger, and an injection well; see Fig. 4. The production well is 36.4 m deep, with a screen of 6 m, and a 1-m sump pipe below the screen. A Grundfos SP 60–5 pump is installed right above the well screen, operating at variable speed drive between 6 and 16 l/s. The injection well is 36.5 m deep, with 10 m of screen, and 3 m of sump pipe in the bottom. Both wells are made up of 158/168 mm ID/OD stainless steel casing and 150/161 mm ID/OD screens with 1 mm continuous slots. The gasket plate heat exchanger conducts heat from the groundwater to a secondary circuit of ethylene glycol with a capacity of 260 kW. The temperature of the produced groundwater is reduced 3–5 K in the heat exchanger. For an in-depth description of the system and heating operation at Lena terrasse, see Gjengedal et al. (2021).

The Lena terrasse GWHP system has suffered from major incrustation problems caused by iron oxides and sediments, especially in the heat exchanger and the injection well (Riise

Table 1 Review of critical Froude numbers Fr_c for air bubble transport in water pipes of different inclinations and diameters

Pipe inclination	Fr_c (-)	Pipe diameter (mm)	Reference
Horizontal	0.48	178	Zukoski (1966)
	0.60	45–200	Mosevoll (1976)
	0.60	150	Escarameia (2007)
Vertical (downward)	0.32	76	Viana et al. (2003)
	0.34	178	Zukoski (1966)
	0.35	79	Davies and Taylor (1950)
Inclined (30–45° downward)	0.64	178	Zukoski (1966)
	0.77	45–200	Mosevoll (1976)
	0.90	150	Escarameia (2007)

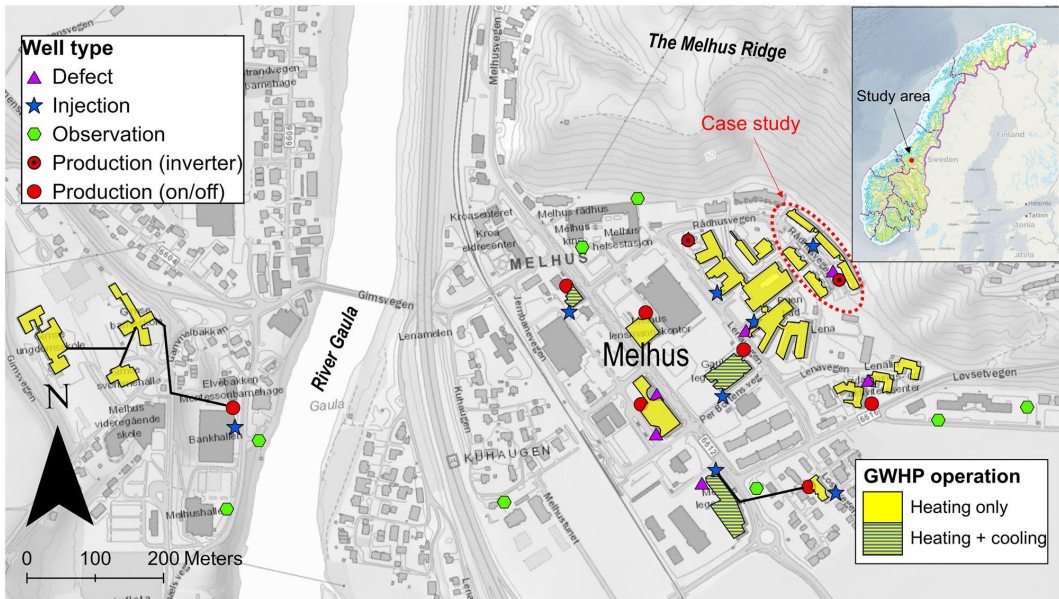


Fig. 3 Map of Melhus town center with the Lena terrasse GWHP location (*Case study*) indicated. Location of study area is also shown in the map inset in the upper right corner, where the highlighted area is Norway

2015; Gjengedal et al. 2020). This has motivated the authors to examine measures to improve the GWHP’s operational conditions. The piping part of the GWHP (Table 2), from

the submersible pump inlet in the production well to the end of the injection pipe inside the injection well, has been the focus during the present work.

Fig. 4 Conceptual model and monitoring scheme of the Lena terrasse groundwater heat pump system (GWHP), including monitoring of p =pressure, T =temperature, Q =groundwater flow rate, and P =power demand of the pump. Modified from Gjengedal et al. (2021)

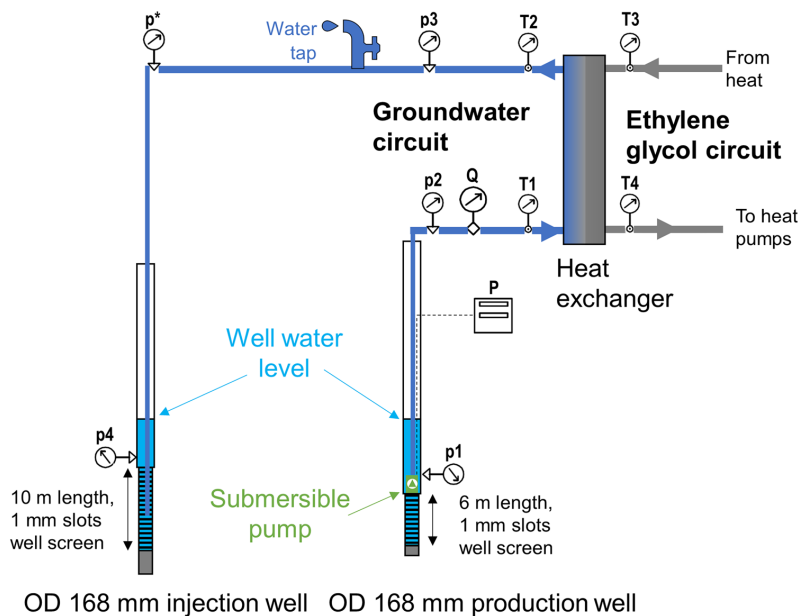


Table 2 Pipeline structure from submersible pump to the end of the injection line. Data partly from Gjengedal et al. (2021)

Unit	From-to length (m)	Inner diameter (mm)	Δz (m)	Material
Production riser pipe	0–27	90	27.0	PE SDR11
Pipe (before HE)	27–82	160	-3.6	HDPE
HE	82–83.5	-	1.5	Stainless steel
Pipe (after HE)	83.5–130	160	-0.6	HDPE
Injection pipe	130–160	76	-30.0	Polyurethane (flexible hose)

Methods and materials

Pressure, temperature, flow rate, and pump power demand have been continuously monitored at Lena terrasse since April 2019; see Table 3. Two years of monitoring data, from May 2019 to May 2021, are presented in this article. The pressure sensors p1 and p4 are located inside the wells, but outside the submersible pump inlet and injection pipe outlet, respectively. Step–discharge tests of the system have been performed semi-monthly according to a procedure developed by Gjengedal et al. (2020). One test carried out on 11 March 2021 is analyzed in this article. The test comprised operating the pump stepwise at four different frequencies (ω), 60, 70, 80, and 90% of the maximum, which yielded flow rates Q of 5.7, 8.5, 11.1, and 13.6 l/s, respectively. Meanwhile, pressures ($p1$ – $p4$) and pump power consumption (P) were continuously measured. Each step lasted until the pressure measurements stabilized (i.e., 5–10 min). Additionally, a manual manometer (p^*) was temporarily installed at the top of the injection well (see Fig. 4) and read off during each of the four steps. This location was expected to represent the minimum pressure in the groundwater circuit (Gjengedal et al. 2019) and thus of special interest with regard to gas clogging. Additionally, gas-related field observations were noted during visits to the GWHP plant.

Pressures and pump power measurements during the step–discharge test of 11 March 2021 were used to produce four hydraulic grade lines (HGL), one for each step. A HGL visualizes the sum of pressure and elevation head of a fluid versus the pipe profile. Intersection between the hydraulic

grade lines and the pipe profile indicates atmospheric pressure conditions ($p = 1$ atm). Hydraulic grade lines below or above the pipe profile indicate $p < 1$ atm and $p > 1$ atm, respectively (Çengel and Cimbala 2010). The hydraulic grade lines were drawn as straight lines between six points; five based on pressure measurements ($p1$ – $p4$, p^*); and one from calculation of the pumping head (h_p) (Çengel and Cimbala 2010):

$$h_p = \frac{P\eta}{\rho g Q} \tag{3}$$

where P is pump power consumption, η is the pump efficiency including the motor and frequency converter, ρ is water density, g is gravitational acceleration, and Q is volumetric flow rate. Grundfos (n.d.) provided η values of 43.1, 51.2, 55.6, and 57.5% for pump frequencies 60, 70, 80, and 90%, respectively. GPS measured elevation data of the wells were retrieved from Riise (2015). No internal pipe friction loss calculations were conducted. Lines where $p = 1.41$ atm and $p = 0$ atm were also drawn, representing the 95-percentile of groundwater gas pressures (Lüders et al. 2016) and the absolute vapor pressure, respectively.

Equation 2 was modified by using the definition of flow velocity $q = Q/A$ for a water-filled circular pipe with cross-sectional area $A = \pi d^2/4$. Based on critical Froude numbers Fr_c from Table 1 and diameters d from Table 2, critical flow rate Q_c ranges could be calculated for each pipe segment:

$$Q_{c,i} = \frac{\pi\sqrt{g}}{4} Fr_{c,i} d^{5/2} \tag{4}$$

Table 3 Monitoring equipment and accuracy. Data partly from Gjengedal et al. (2021). See Fig. 4 for location of instruments

Abbreviation	Instrument type, model	Accuracy	Measurement type
$p1$	Pressure transducer, Siemens SITRANS LH100	± 0.0015 bar	Continuous
$p2, p3$	Pressure transducer, Danfoss MBS 4010 0–6 BAR ABS	± 0.03 bar	Continuous
$p4$	Pressure transducer, Kacise GXPS430	± 0.015 bar	Continuous
p^*	Pressure transducer, Hasvold manometer	± 0.064 bar	Manual (discontinuous)
Q	Flow meter, Badger ModMAG M1000	± 0.04 l/s	Continuous
P	Energy meter, Grundfos CUE 3X380-500 V IP55 15KW 32A/2	-	Continuous
$T1$ – $T4$	Temperature probes, PT1000	± 0.3 °C	Continuous

where $i = \min, \max$ corresponding to the minimum and maximum empirical Fr_c values in Table 1. Measured Q was plotted versus the critical flow rates along the pipeline. This was used to assess the likelihood of gas entrapment: $Q \geq Q_{c, \max}$ was interpreted as *unlikely*, $Q_{c, \min} \leq Q < Q_{c, \max}$ was interpreted as *possible*, while $Q < Q_{c, \min}$ was interpreted as *likely*.

Results

Figure 5 displays 2 years of monitoring data from the Lena terrasse GWHP system. The pressure right after the heat exchanger ($p3$), pump power consumption (P), and pumping rate (Q) remains relatively stable during large portions of this period, despite the injection pressure ($p4$) increasing 10–15 m; see Fig. 5. The pressure build-up is due to well filter incrustations. This is evident from $p4$ which is lower after injection well rehabilitations. Thus, the increase in incrustation resistance in the injection well filter does not impact the head loss or pump power consumption between the heat exchanger and the end of the injection pipeline.

The P and Q is not perfectly correlated, as would be expected for a pump operating with a fixed resistance. For instance, in May–July 2020 Q first increases and later decreases, while P remains stable. This can be explained by the yearly snowmelt flood which leads to a peak discharge in River Gaula and a corresponding increase in recharge to the Melhus aquifer. This has been confirmed by water table fluctuations in nearby observation wells (Geological Survey of Norway (NGU) 2021).

Some gas-related field observations have also been noted. Large amounts of gas have released from the pipeline through a water tap located after the heat exchanger (Fig. 4) during water chemical sampling with a flow-through cell. *Trickling* or *stream sounds* have been heard from the groundwater pipes in the machinery room and the injection well drain, especially at low pumping rates.

Data from the step–discharge test of 11 March 2021 (purple star in Fig. 5) are presented in Fig. 6, in a format suitable to assess risk of gas formation (a) and gas entrapment (b) in the pipeline from the production well via heat exchanger to the injection well. Figure 6a displays hydraulic grade lines for pumping frequencies 60–90%. The plot shows that vacuum pressures occur at $\omega = 60$ –80%. At $\omega = 90\%$, the flow is pressurized ($p > 1$ atm) throughout the entire pipe circuit, but partly below the $p = 1.41$ atm-line. The lowest pressures are found on the injection side of the GWHP system. This is due to frictional losses as the water flows through the pipeline. It is evident from the HGLs' inclinations that the frictional losses increase with pumping rate in the production pipe. Meanwhile, the head losses decrease as the pumping rate increases in the injection pipe. This indicates different flow regimes in the production and injection pipeline. The pressure in the injection well ($p4$) increases considerably, while the production well pressure ($p1$) stays relatively stable, as the flow rate increases. This indicates that clogging is more intense in the injection than in the production well filter.

Figure 6b shows measured and critical flow rates plotted versus length along the pipeline at different pump frequencies, ω . The Q_c values vary little throughout the system. Exceptions are found in the downward bends (stars),

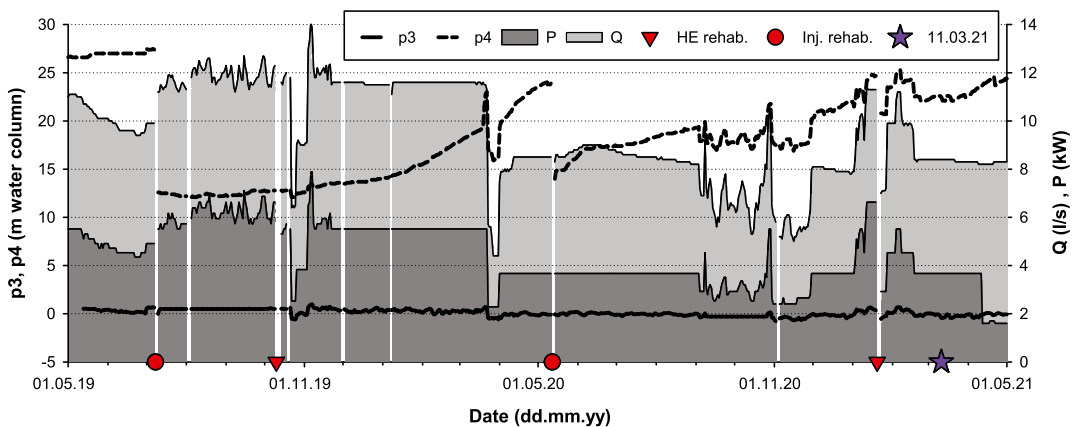
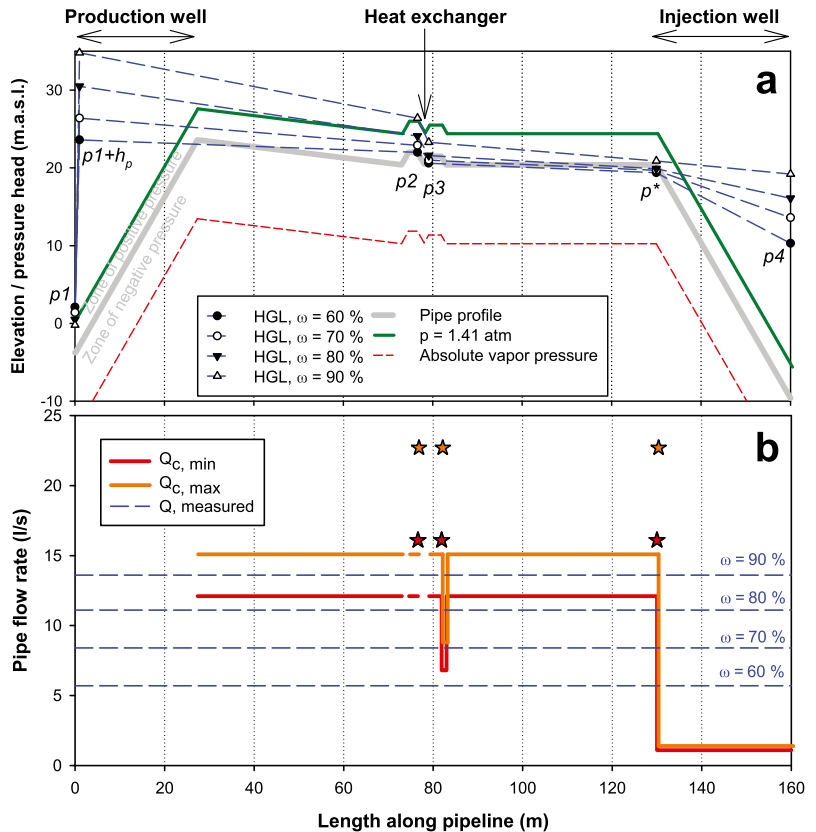


Fig. 5 Two years of monitoring data (daily median) of groundwater flow rate (Q) pressure after heat exchanger ($p3$), pressure inside injection well ($p4$), and power consumption of the submersible ground-

water pump (P). *HE rehab.* = heat exchanger rehabilitation, *Inj. rehab.* = injection well rehabilitation. 11.03.21 (purple star) indicates the time when the analyzed step–discharge test was conducted

Fig. 6 Plots used to assess risk of gas formation (a) and gas entrapment (b) in the pipeline from the production well via heat exchanger to the injection well. Results from a step discharge test at the Lena terrasse GWHP plotted as (a) hydraulic grade lines (HGLs) based on pressure measurements ($p1-4$, p^*) and pumping head (h_p ; see Eq. 3) at pump frequencies (ω) between 60 and 90% vs. pipe profile, $p=1.41$ atm, and absolute vapor pressure ($p=0$ atm) lines and (b) critical flow rates ($Q_{c, min}$, $Q_{c, max}$) for gas entrapment plotted versus measured flow rates (Q) in horizontal and downward inclined pipes. Stars represent downward bends (i.e., where Q_c values are highest)



downward vertical pipe segments, and the injection well where pipe diameter is smaller; see Table 2. $Q < Q_{c, min}$ at $\omega = 60-80\%$ and $Q_{c, min} < Q < Q_{c, max}$ at $\omega = 90\%$ in the surface part of the pipeline (i.e., between the top of the production and the top of the injection well). However, the $Q_{c, min}$ is higher than all measured Q values in the downward bends. The measured pumping rates exceed the critical flow rates in the injection well.

Discussion

The results presented in Fig. 5 indicate a *waterfall flow* between the heat exchanger and the injection well during typical operating conditions (i.e., $\omega = 60-80\%$). This is evident from the parameters $p3$, Q , and P being independent of pressure in the injection well $p4$. This indicates that the submersible pump only lifts the water to the heat exchanger. The water then discharges by gravity down through the injection well (i.e., “waterfall flow”). The inverse correlation between head loss from p^* to $p4$

and pumping rate Q at $\omega = 60-80\%$ (Fig. 6a) further supports the assumption of a gravity-driven flow in the injection well. The opposite would be expected for a pressurized pipe flow (Çengel and Cimbala 2010), as observed between the groundwater pump in the production well ($p1+h_p$) and the heat exchanger ($p2$).

Vacuum pressures occur between the heat exchanger ($p3$) and the top of the injection well (p^*) at pumping speeds between 60 and 80% (see Fig. 6a). This involves risk of gas formation in this part of the system. At the same pumping speeds, $Q < Q_{c, min}$ indicates risk of gas entrapment (i.e., pipes will remain partly gas-filled). This is confirmed by observation of gas release from the water tap in Fig. 4. The entrapped gas causes the gravity-driven waterfall flow down through the injection pipe. This is probably what is causing the *trickling stream* sounds heard in the machinery room and the injection well drain. The head loss then equals the elevation difference between the heat exchanger and the water table in the injection well, as shown in Fig. 2.

At 90% pumping frequency, the frictional losses in the pipeline and the injection well filter are high enough to keep the flow pressurized throughout the entire groundwater circuit. This means there is less risk of gas formation, although at high gas pressures ($p_{gas} > 1.1$ atm) degassing could occur. It should be noted that the HGL in Fig. 6a represents intense injection well filter clogging conditions (i.e., elevated p_4 values), which adds backpressure to the flow. As the head difference $p_1 - p_4$ increases, the flow situation progressively resembles pumping from a lower to a higher reservoir rather than a siphon. Consequently, the potential for vacuum conditions and gravity-driven waterfall flow down through the injection well decreases. However, vacuum conditions could occur at higher pumping frequencies than shown in this study after injection well rehabilitation. This illustrates that vacuum conditions and waterfall flow are dynamic phenomena.

The flow rate is in the range $Q_{c, min} < Q < Q_{c, max}$ when $\omega = 90\%$, meaning gas entrapment is possible but not definitely occurring. This indicates that flushing the system at 90% could be enough to push out some of the stagnant gas pockets, but not from the local high points. Particularly, gas entrapment risk is associated with downward bends marked with stars in Fig. 6b. At these points, the submersible pump will not be able to remove the gas (i.e., fill the pipeline with water) even at max pumping. This implies that if the GWHP system is filled with air upon start-up, the system will never become completely water-filled, but remain partly gas-filled.

There is a risk that gas bubbles are carried with the flow and clog the injection well filter and aquifer formation, because the flow rates are higher than the critical one in the injection pipe (Fig. 6b). Gas clogging would lead to a rapid pressure build-up (i.e., within seconds–minutes) in the injection well (Bakema 2001). The injection well clogging at Lena terrasse is a much slower process (i.e., on the scale of weeks–months) and is attributed to sediments and iron oxide incrustations. The negligible injection well filter gas clogging could be explained by sufficient overpressure at the end of the injection pipe ($p > 2$ atm (Fig. 6a)) to dissolve the gas before injection into the aquifer.

The risk of gas formation and entrapment at all pumping rates, although lower at $\omega \geq 90\%$, suggests that measures against gas clogging should be considered for the Lena terrasse GWHP.

How to avoid gas clogging

The easiest way to keep the Lena terrasse GWHP pressurized and to hinder gas entrapment would be to run the system continuously at larger pumping rates; see Fig. 6. However, this would also involve numerous disadvantages. Firstly, it would mean larger pumping costs and less

flexibility to adjust pumping rate to the heating demand during part load conditions. Secondly, higher flow rates also mean more turbulence, which is known to trigger erosion in the well filter and consequently sand production (Bakema 2001; Snijders and Drijver 2016). Lastly, laboratory experiments have shown that reaction kinetics of calcite (Zeppenfeld 2005) and iron hydroxides (Du et al. 2018) precipitation increase with increasing turbulence. Thus, increasing the pumping rate does not seem to be an appropriate solution to gas clogging in GWHP systems.

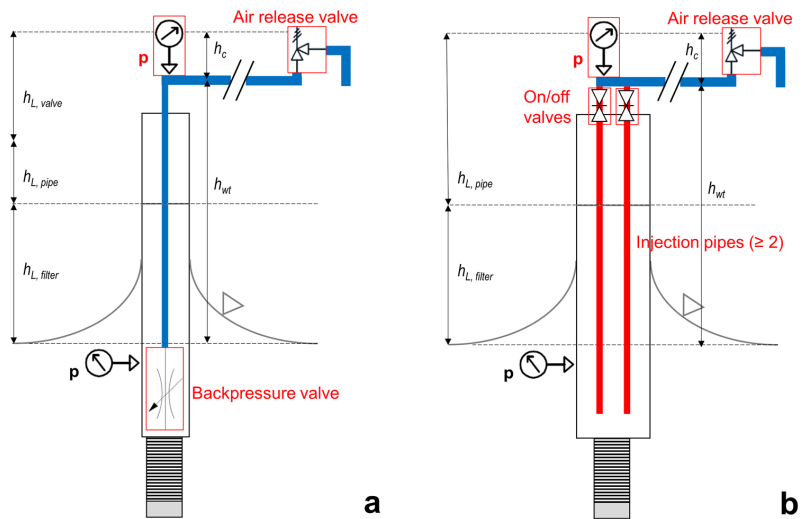
Alternatively, the pressure in the groundwater circuit could be increased without increasing the pumping rate. To achieve this, the pipe network must be modified to increase the frictional losses on the injection side of the system. This can be done either by installing a narrower injection pipe (Olsthoorn 1982; Corcos 2003) or a constant or adjustable orifice at the end of the injection line (Sniegocki and Reed 1963; Olsthoorn 1982; Andersson 1988; Guttman et al. 2017). Solutions which allow adjusting the frictional losses are preferred since the groundwater pumping rate in GWHP systems typically is regulated by the heat demand. An automated *backpressure valve* offers the desired flexibility (Snijders and Drijver 2016). The valve should be installed at the end of the injection pipe: (1) below the natural groundwater table to avoid water cascading and (2) above the well screen to allow gas bubbles to rise to the top of the injection well instead of clogging the well filter (Guttman et al. 2017). However, the technical complexity of these valves makes them expensive. A simpler, but still adjustable measure to pressurize the injection flow was chosen at Arlanda airport's *aquifer thermal energy storage* (ATES, i.e., a GWHP also comprising seasonal storage of heat) system in Stockholm, Sweden. Multiple narrow injection pipes were installed inside the same injection well with on/off valves in the top part. This facilitates stepwise adjustment to the frictional flow resistance by adjusting the number of open injection pipes (O. Andersson, personal communication, 13 January 2022). On the downside, this solution may necessitate larger well diameters (i.e., higher drilling costs).

Figure 7 displays two suggested system designs and instrumentations to avoid gas clogging. The designs include the following:

- A *backpressure valve* at the end of the injection pipe (a) or *multiple narrow injection pipes* (b)
- *Pressure monitoring* on top of the injection well
- *Air release valve(s)* at the local high point(s) where gas tends to get trapped

The frictional resistance that must be added by the backpressure valve h_{valve} and injection pipe h_{pipe} must obey the equation:

Fig. 7 Two proposed injection well designs and instrumentations to mitigate gas clogging. Red color indicates components which are currently not custom to the GWHP design in Melhus, Norway. The h_L 's correspond to flow head losses through various components: $h_{L, valve}$ through the backpressure valve, $h_{L, pipe}$ through the injection pipe, and $h_{L, filter}$ through the well screen and filter. h_{wt} represents the head difference from top of the injection well to the natural water table, and h_c is the chosen critical head at the top of the injection well. The p 's represent pressure measurements



$$h_{valve} + h_{pipe} = h_c + h_{wt} - h_{filter} \tag{5}$$

where h_c is the critical overpressure necessary to avoid degassing, h_{wt} is the height from the top of the injection well down to the natural water table, and h_{filter} are the frictional losses in the injection well filter; see Fig. 7. h_{wt} and h_{filter} can be measured in the field when the system is turned off and on, respectively, while h_{pipe} can be estimated from typical friction coefficients for internal flow (Çengel and Cimbala 2010). Conversely, if $h_{valve} + h_{pipe} < h_{wt} - h_{filter}$, then the injection pipe will not be pressurized. This was observed at the Lena terrasse GWHP when an insufficiently narrow constriction was installed at the end of the injection pipe in Spring 2020. As a result, the system remained unpressurized.

The h_c must be chosen, either based on direct gas measurements of the aquifer or typical values with some factor of safety. Since direct gas measurements are expensive and therefore seldom carried out, the 95-percentile for gas pressures at 1.41 atm from Lüders et al. (2016) could be used as a design baseline. A $h_c = 0.5 \text{ bar} \approx 5 \text{ m}$ of water column was chosen for the Fladie GWHP in Sweden (Andersson 1988). This corresponds with Lüders et al. (2016) p_{gas} value multiplied by a ~ 1.25 overpressure safety factor, and thus seems like a reasonable h_c value.

The extra pumping head required (Δh_p) at the Lena terrasse GWHP would approximately equal the h_c value. This is due to the present waterfall flow which comprises injection well head losses equal to h_{wt} ; see Fig. 7. Using Eq. 3 and assuming an average yearly pumping rate $Q = 10 \text{ l/s}$ (i.e., $\omega \sim 75\%$) at Lena terrasse, $\Delta h_p = 5 \text{ m}$, $g = 9.81 \text{ m/s}^2$, $\rho = 1000 \text{ kg/m}^3$, $\eta = 50\%$, yields an extra pump power consumption $\sim 8600 \text{ kWh/year}$. This introduces relatively

small extra operational costs to the system, which had and average power input $\sim 300\,000 \text{ kWh/year}$ to the heat pump and submersible pump in 2019–2020. Still, it discourages supplying more backpressure h_{valve} than needed to satisfy Eq. 5, as this would increase the pumping costs. A pressure sensor is recommended at the top of the injection well to make sure the right resistance $h_{valve} + h_{pipe}$ is supplied to maintain $p = h_c$ at the top of the injection well. Both the h_{pipe} and h_{filter} head losses depend on the flow rate, while the latter is also strongly dependent on well filter incrustation extent. Accordingly, $h_{valve} + h_{pipe}$ must be regulated, with less constriction of the flow at higher flow rates and as the injection well filter clogs.

Independent of the pressure being pumped up to a level above h_c , the flow rate will still not be sufficient to remove entrapped gas. The system would then benefit from air release valves at the local high points to release entrapped gas from the pipes (Corcos 2003; Pozos et al. 2010). Double orifice air valves are typically used for this purpose (Chadwick et al. 2013). The designer should make sure that $p > 1 \text{ atm}$ where the air release valves are located, to avoid gas in-leakage through the valves. The need for air release on local high points also stipulates that the number of bends and local high points should be kept to a minimum. During startup of an initially gas-filled system, the air release valves will let out entrapped gas and make sure the system gets filled with water. At Lena terrasse, four local high points where air release valves should be installed are identified: at the top of the production, at the top of the injection well, and before and after the heat exchanger; see Fig. 6b.

Backpressure valve or multiple injection pipes, pressure sensors, and air release valve(s) introduce extra investment

costs for GWHP systems, but cause relatively modest extra operational costs. The potential benefits from pressure control, although not quantified here, justifies considering these measures for the Lena terrasse GWHP and during the design phase of new systems.

Conclusions

Monitoring data and field observations show that the groundwater pipes at the Lena terrasse groundwater heat pump (GWHP) system are partly gas-filled during operation. This is caused by vacuum pressures and the associated risk of gas formation, and groundwater flow rates which are insufficient to remove gas from the pipeline. The risk of both gas formation and gas entrapment is higher at lower pumping rates and on the injection side of the heat exchanger. The gas leads to a gravity-driven *waterfall flow* from the heat exchanger down through the injection well, where the head loss equals the elevation drop.

Attention should be directed towards pressurizing ($p > 1$ atm) the system to mitigate gas clogging. The overpressure should be adjustable, to accommodate changing pumping rates and injection well clogging conditions. This can be achieved either by (1) installing a backpressure valve at the end of the injection pipe or (2) multiple injection pipes regulated by on/off valves inside the same injection well. The valve or pipes should be designed and regulated to maintain an overpressure $h_c \geq 5$ m water column. The pressure minimum is typically found at the top of the injection well. A pressure sensor should be installed at this point to document that the system is kept sufficiently pressurized. Local high points are especially prone to gas entrapment. Air release valves should be installed at these locations to release entrapped gas and make sure the system is kept water-filled.

The extra required pumping head from the backpressure valve or multiple injection pipes would approximately equal the chosen critical overpressure h_c . This introduces quite modest extra operational costs to the GWHP.

Acknowledgements The research presented is part of the research project ORMEL 2 (Optimal Utilization of Groundwater for Heating and Cooling in Melhus 2). This is a cooperation between Melhus municipality, the Norwegian University of Science and Technology, Asplan Viak AS, the Geological Survey of Norway, and Gjøvaag AS. We would like to thank all the involved institutions and persons for cooperation and financial support. We would also like to thank associate professor Pål-Tore Selbo Storli, at the Department of Energy and Process Engineering, NTNU, for input on the hydraulic grade line framework. Lastly, thank you to the two reviewers, whose comments and remarks contributed to improve the manuscript.

Author contribution Conceptualization: Lars A. Stenvik, Sondre Gjengedal, Randi K. Ramstad, Bjørn S. Frengstad. Methodology: Lars A. Stenvik, Sondre Gjengedal, Randi K. Ramstad, Bjørn S. Frengstad. Formal analysis and investigation: Lars A. Stenvik, Sondre Gjengedal.

Writing — original draft preparation: Lars A. Stenvik. Writing — review and editing: Sondre Gjengedal, Randi K. Ramstad, Bjørn S. Frengstad. Funding acquisition: Randi K. Ramstad, Bjørn S. Frengstad. Resources: Sondre Gjengedal, Randi K. Ramstad. Supervision: Sondre Gjengedal, Randi K. Ramstad, Bjørn S. Frengstad.

Funding Open access funding provided by NTNU Norwegian University of Science and Technology (incl St. Olavs Hospital - Trondheim University Hospital). The presented research has received funding (grant number 284965) from the Regional Research Funds in Mid-Norway.

Availability of data and material The authors approve that all data and materials support their published claims and comply with field standards.

Code availability Not applicable.

Declarations

Ethics approval The authors approve that they have followed the rules of good scientific practice.

Consent to participate Not applicable.

Consent to publication Not applicable.

Conflict of interest The authors declare no competing interests.

Open Access This article is licensed under a Creative Commons Attribution 4.0 International License, which permits use, sharing, adaptation, distribution and reproduction in any medium or format, as long as you give appropriate credit to the original author(s) and the source, provide a link to the Creative Commons licence, and indicate if changes were made. The images or other third party material in this article are included in the article's Creative Commons licence, unless indicated otherwise in a credit line to the material. If material is not included in the article's Creative Commons licence and your intended use is not permitted by statutory regulation or exceeds the permitted use, you will need to obtain permission directly from the copyright holder. To view a copy of this licence, visit <http://creativecommons.org/licenses/by/4.0/>.

References

- Andersson O (1988) The Fladie groundwater heat pump plant: experiences from the first years of operation. D9:1988. Swedish Council for Building Research, Stockholm
- Bakema G (2001) Well and borehole failures and solutions in underground thermal energy storage, 2/9805/GW. IF Technology, Arnhem
- Banks D (2012) An introduction to thermogeology: ground source heating and cooling. Wiley-Blackwell, Oxford
- Çengel YA, Cimbala JM (2010) Fluid mechanics: fundamentals and applications, 2nd edn. McGraw-Hill, Boston
- Chadwick A, Borthwick M, Morfett JC (2013) Hydraulics in civil and environmental engineering, 5th edn. CRC Press, Boca Raton
- Corcos G (2003) Air in water pipes: a manual for designers of spring-supplied gravity-driven drinking water rural delivery systems, 2nd edn. Agua para la vida, Berkeley
- Davies RM, Taylor GI (1950) The mechanics of large bubbles rising through extended liquids and through liquids in tubes. Proc R Soc

- Lond A *Math Phys Sci* 200(1062):375–390. <https://doi.org/10.1098/rspa.1950.0023>
- Du X, Zhang H, Ye X, Lu Y (2018) Flow velocity effects on Fe(III) clogging during managed aquifer recharge using urban storm water. *Water* 10(4):358. <https://doi.org/10.3390/w10040358>
- Escarameia M (2007) Investigating hydraulic removal of air from water pipelines. *Proc Inst Civ Eng Water Manage* 160(1):25–34. <https://doi.org/10.1680/wama.2007.160.1.25>
- Gjengedal S, Stenvik LA, Storli PTS, Ramstad RK, Hilmo BO, Frengstad BS (2019) Design of groundwater heat pump systems. Principles, tools, and strategies for controlling gas and precipitation problems. *Energies* 12(19):3657. <https://doi.org/10.3390/en12193657>
- Gjengedal S, Ramstad RK, Hilmo BO, Frengstad BS (2020) Fouling and clogging surveillance in open loop GSHP systems: a systematic procedure for fouling and clogging detection in the whole groundwater circuit. *Bull Eng Geol Env* 79(1):69–82. <https://doi.org/10.1007/s10064-019-01556-5>
- Gjengedal S, Stenvik LA, Ramstad RK, Ulfnesn JI, Hilmo BO, Frengstad BS (2021) Online remote-controlled and cost-effective fouling and clogging surveillance of a groundwater heat pump system. *Bull Eng Geol Env* 80:1063–1072. <https://doi.org/10.1007/s10064-020-01963-z>
- Grundfos (n.d.) SP 60–5. <https://product-selection.grundfos.com/products/sp-sp-g/sp-sp-60-5-14A30005?productnumber=14A30005&tab=variant-specifications&pumpssystemid=1282389125>. Accessed 15 April 2021
- Guttman J, Negev I, Rubin G (2017) Design and testing of recharge wells in a coastal aquifer: summary of field scale pilot tests. *Water* 9(1):53. <https://doi.org/10.3390/w9010053>
- Hellestveit MS (2018) 3D-modellering av grunnvannstrømning og varmetransport i akviferen i Melhus sentrum - En kvartær- og hydrogeologisk tolkning, med vurdering av uttakskapasitet (3D modellering of groundwater flow and heat transport in the aquifer in Central Melhus). Master Thesis, NTNU, Trondheim
- Jenne EA, Andersson O, Willemsen A (1992) Well, hydrology, and geochemistry problems encountered in ATEs systems and their solutions. SAE Technical Paper. <https://doi.org/10.4271/929153>
- Lüders K, Firmbach L, Ebert M, Dahmke A, Dietrich P, Köber R (2016) Gas-phase formation during thermal energy storage in near-surface aquifers: experimental and modelling results. *Environ Earth Sci* 75(21):1–28. <https://doi.org/10.1007/s12665-016-6181-5>
- Mosevoll G (1976) Luft i utslippsledninger (Air in outfall sewers). PRA 8. Prosjektkomiteén for rensing av avløpsvann, Oslo
- NGU (2021) GRANADA: Nasjonal grunnvannsdatabase (GRANADA: National groundwater database), http://geo.ngu.no/kart/granada_mobil/. Accessed 23 June 2021
- Olsthoorn TN (1982) The clogging rate of recharge wells, main subjects. KIWA-communications 72. KIWA, Rijswijk
- Possemiers M, Huysmans M, Anibas C, Batelaan O, Steenwinkel J (2016) Reactive transport modeling of redox processes to assess Fe(OH)₃ precipitation around aquifer thermal energy storage wells in phreatic aquifers. *Environ Earth Sci* 75:648. <https://doi.org/10.1007/s12665-016-5398-7>
- Pozos O, Gonzalez CA, Giesecke J, Marx W, Rodal EA (2010) Air entrapped in gravity pipeline systems. *J Hydraul Res* 48(3):338–347. <https://doi.org/10.1080/00221686.2010.481839>
- Riise MH (2015) Praktisk guide for grunnvarmeanlegg basert på oppumpet grunnvann (practical guide for ground water heat pump systems). Master Thesis, NTNU, Trondheim
- Sniegocki RT, Reed JE (1963) Principles of siphons with respect to the artificial recharge studies in the Grand Prairie region, Arkansas. Water Supply Paper 1615-D. U.S. Geological Survey, Washington
- Snijders AL, Drijver BC (2016) Open-loop heat pump and thermal energy storage systems. In: Rees S (ed) *Advances in Ground-Source Heat Pump Systems*. Woodhead Publishing, Amsterdam, pp 247–268
- Stumm W, Morgan JJ (1996) *Aquatic chemistry: chemical equilibria and rates in natural waters*, 3rd edn. Wiley, New York
- Viana F, Pardo R, Yáñez R, Trallero JL, Joseph DD (2003) Universal correlation for the rise velocity of long gas bubbles in round pipes. *J Fluid Mech* 494:379–398. <https://doi.org/10.1017/S0022112003006165>
- Zeppenfeld K (2005) Untersuchungen über den Einfluss der Strömungsgeschwindigkeit auf die Kalkabscheidung aus calciumhaltigen Wässern (studies of the effect of the flow velocity on calcium carbonate precipitation from water containing calcium). *vom Wasser* 103(2):11–19.
- Zukoski EE (1966) Influence of viscosity, surface tension, and inclination angle on motion of long bubbles in closed tubes. *J Fluid Mech* 25(4):821–837. <https://doi.org/10.1017/S0022112066000442>

Paper VI

Optimizing submersible pump regulation of a clogging prone groundwater heat pump system in Melhus, Norway

LARS A. STENVIK^{1*} , RANDI K. RAMSTAD^{1,2} , AND BJØRN S. FRENGSTAD¹

¹Department of Geoscience and Petroleum, Norwegian University of Science and Technology, Trondheim, Norway

²Infrastructure north/central Asplan Viak AS, Trondheim, Norway

The groundwater heat pump (GWHP) system at Lena terrasse in Melhus, Norway has suffered from clogging by iron oxide incrustations, sediment deposits, organic slimes and gas entrapment. This has necessitated annual rehabilitations of the injection well and heat exchanger, and questioned how the submersible pump should be regulated to maximize the seasonal performance factor (SPF = heat output/power input) and reduce the clogging risk. The submersible pump operates with variable speed drive to yield groundwater pumping rates (Q) between 4 and 16 l/s. The GWHP system has been continuously monitored by pressure, temperature, flowmeter and energy meter sensors for 2.5 years, and with semimonthly step-discharge tests. During three step-discharge tests hydrochemistry and suspended solids content were also measured. Monitoring data show that the monthly performance factor (SPF_M) is negatively correlated with Q . At $Q > 12$ -13 l/s, suspended solids concentrations increase. Heat exchanger clogging rates increase at $Q < 6$ l/s. Hydrochemistry is stable, regardless of pumping rate. All clogging rates appear to be independent of pumping rate in the range 6-12 l/s. Therefore, pumping rates are advised to be kept between 6-12 l/s, and minimized but adjusted to the heating demand to avoid freezing of the groundwater.

Introduction

Groundwater heat pump (GWHP) systems use aquifers as their heat sources and/or sinks. The aquifer loop includes extraction, heat exchange and re-injection of groundwater, see Figure 1. GWHP systems utilize convection of heat stored in the groundwater, which is more effective than the predominantly conductive heat transfer of conventional closed-loop ground source heat pump *energy wells*. This makes GWHP systems favorable in areas with permeable aquifers of sufficient size and temperature to cover the design heating and/or cooling load (Banks 2012). In Norway, this is typically found in unconsolidated, (glacio)-fluvial sand and gravel aquifers (Gaut and Ellingsen 1992).

On the downside, groundwater contains dissolved and suspended substances of both organic and inorganic origin that may precipitate, deposit or degas to clog GWHP systems. Clogging occurs in well screens, pump inlets, heat

exchangers etc., and increases the pumping costs and reduces the heat transfer capacity of the system. Costly rehabilitations or even reconstruction measures are required to remediate the clogging issues. This impedes the systems' economical profitability (Jenne, Andersson, and Willemsen 1992; Bakema 2001; Eggen and Vangsnes 2005; Banks 2012; Gjengedal et al. 2020).

The operation of the submersible groundwater pump is a key aspect with respect to the heat performance and clogging risk, both influencing the system economy. Firstly, pumping power consumption (W_{GP}) and costs, increase with groundwater pumping rate (Q) (as quoted in Çengel and Cimbala 2010)

$$W_{GP} = \frac{\rho \cdot g \cdot Q \cdot h_p}{\eta} \quad (1)$$

where ρ is the water density, g is the gravitational acceleration, h_p is pumping head and η is the submersible pump efficiency. Q also influences the groundwater temperature change ΔT_{gw} in the heat exchanger for a set heat exchange rate P_{HE} (as quoted in Banks 2012):

$$P_{HE} = Q \cdot c_p \cdot \Delta T_{gw} \quad (2)$$

where c_p is the specific heat capacity of water (= 4182 J/kg/°C). In heating mode, a too low Q may reduce the groundwater temperature below water's freezing point, which would be detrimental to the GWHP system. Conversely, a higher pumping rate Q will lower ΔT_{gw} , and

Received June 18, 2022; accepted October 12, 2022

Lars A. Stenvik, M.Sc, is a PhD candidate. Randi K. Ramstad, PhD, is an Associate Professor II. Bjørn S. Frengstad, PhD, is a Professor.

*Corresponding author e-mail: lars.a.stenvik@ntnu.no

This is an Open Access article distributed under the terms of the Creative Commons Attribution License (<http://creativecommons.org/licenses/by/4.0/>), which permits unrestricted use, distribution, and reproduction in any medium, provided the original work is properly cited.

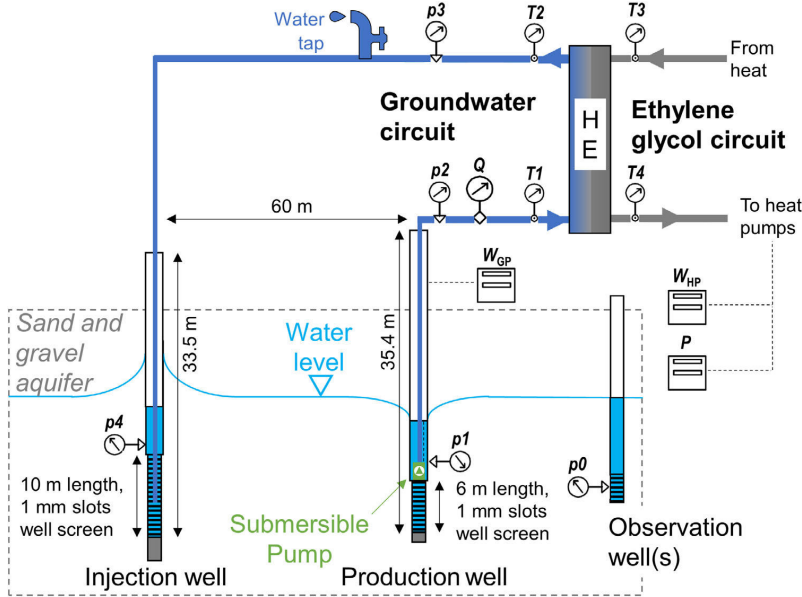


Fig. 1. Conceptual groundwater heat pump (GWHP) system design in Melhus, Norway. HE = heat exchanger. System monitoring of p = pressure, T = temperature, P = heat output, W = power input, Q = groundwater pumping rate is displayed (modified from Gjengedal et al. 2021).

increase the evaporation temperature of the heat pump. This means the required compressor power consumption (W_{HP}), which is needed to lift the temperature of the heat pump's working fluid to the level required by the heat distribution system, will be reduced. W_{HP} will be converted to heat (P_{HP}) which can be utilized by the heat distribution system (Stene 2001). The groundwater pumping rate Q is therefore a fit parameter to maximize the seasonal performance factor SPF. SPF is the time integrated GWHP coefficient of performance (COP_{GWHP}) over a period $\Delta t = t_2 - t_1$ (modified from equation as quoted in Banks 2012):

$$SPF = \frac{\int_{t_1}^{t_2} P dt}{\int_{t_1}^{t_2} W dt} = \frac{\int_{t_1}^{t_2} (P_{HE} + P_{HP}) dt}{\int_{t_1}^{t_2} (W_{HP} + W_{GP} + W_{SC}) dt} \quad (3)$$

where Δt is typically one year and W_{SC} is the pump power consumption of the secondary circuit fluid between the heat exchanger and the heat pump (i.e., the ethylene glycol circuit in Figure 1).

Optimum submersible pump operation to avoid clogging depends on the clogging type (Pérez-Paricio and Carrera 1998; Bakema 2001; Houben and Treskatis 2007; Kerner 2011; Martin 2013; Stuyfzand and Osma 2019; Banks and Birks 2020):

High groundwater flow rates in and around the GWHP system increase the nutrient supply rate (Huisman and Olsthoorn 1983 as quoted in Houben and Treskatis 2007) and erosion of sediments in the aquifer formation outside the well screen (Bakema 2001). This facilitates biological (i.e., biofilms) and mechanical clogging (i.e., sediment deposits), respectively. The eroded and transported sediments may deposit and clog production wells (van Beek,

Breedveld, and Stuyfzand 2009), heat exchangers (Kerner 2011) and injection wells (Olsthoorn 1982). Filter pack erosion is sought avoided by not exceeding a critical entrance velocity through the production well screen v_{crit} ($= Q/A_{eff}$, where A_{eff} is the perforated screen area). The v_{crit} is much debated, with typical empirical guideline values ranging from 3 cm/s (Driscoll 1986) to 0.6-1.2 m/s (Williams 1985).

Chemical clogging by iron oxide incrustations are typically triggered by *mixing* of shallow, oxygen-rich and deep, iron-rich groundwater in production wells (van Beek 1989). The mixing can be amplified by frequently switching on and off the pump. Therefore, iron oxide clogged well systems are advised to operate at constant pumping rates to reduce the mixing effect (van Beek, Breedveld, and Stuyfzand 2009). The increasing turbulence from higher flow rates (i.e., higher Reynolds numbers) have been shown to kinetically accelerate the precipitation of calcite (Zeppenfeld 2005) and iron oxide (Du et al. 2018) in laboratory experiments. This may explain why production well filters have been observed to be more heavily incrustated in sections of higher inflow velocities (Houben 2006).

Low pumping rates could be problematic for the heat exchanger. The wall shear stress (τ) of a plate heat exchanger is advised to be high, to avoid sedimentation of fine particles and biofilms (Novak 1982, 1983; Kerner 2011):

$$\tau = \frac{\Delta p_{HE} \cdot d_h}{4L} \quad (4)$$

where Δp_{HE} is the heat exchanger pressure drop, d_h is the hydraulic mean diameter of the heat exchanger channels and

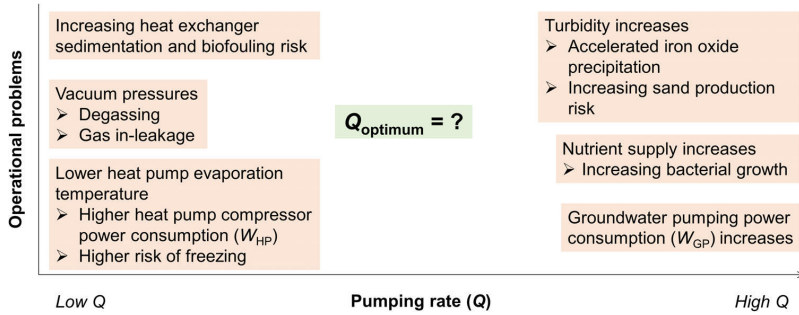


Fig. 2. Operational problems of GWHP systems related to low and high groundwater pumping rates (Q).

L is the effective plate length. Δp_{HE} increases with Q . Thus, the wall shear stress criterion can be met by increasing the pumping rate Q .

Low pressures, especially vacuum pressures, may induce gas in-leakage through improperly sealed pipes or degassing of dissolved gases (i.e., gas clogging). Therefore, vacuum pressures are sought avoided in groundwater well systems. Pipe overpressure is achieved by either (1) narrowing or constricting the end of the injection pipe or (2) increasing the flow rate (Olsthoorn 1982).

The pros and cons of high vs. low groundwater pumping rates are summarized in Figure 2.

The Lena terrasse GWHP system, located in a glaciofluvial aquifer in Melhus, Mid-Norway, is one of the most thoroughly investigated and monitored GWHP systems in Norway (Riise 2015; Gjengedal et al. 2021; Stenvik et al. 2022a; Stenvik et al. 2022b). The current GWHP system started its operation in 2015, and supplies floor heating and hot water to 119 apartments at a capacity of 350 kW. Lena terrasse's submersible pump is regulated with variable speed drive (VSD) capable to deliver 4-16 l/s of groundwater. The current regulation strategy seeks to lower the pumping rate, but limit freezing and the risk of vacuum pressures. The groundwater temperature is reduced from 6-7°C (natural aquifer temperature) to 2-5°C in the heat exchanger, with temperature reduction depending on the heat demand. The GWHP system has been demonstrated to suffer from various clogging issues, including iron oxides, sediments, biofouling, and gas entrapment, especially in the heat exchanger and injection well (Riise 2015; Stenvik et al. 2022a, 2022b).

System monitoring and water quality data retrieved from the Lena terrasse GWHP system facilitates optimizing the submersible groundwater pump regulation with regards to clogging prevention and SPF maximization (eq. 3).

Materials and methods

The monitoring scheme at Lena terrasse's GWHP system includes flowmeter measurements of groundwater flow rate (Q), pressure measurements in the production well ($p1$), before ($p2$) and after ($p3$) the heat exchanger, and in the injection well ($p4$), power consumption of the submersible

groundwater pump (W_{GP}) and heat pump compressor (W_{HP}), and heat delivered from the heat pump to the heat distribution system (P), see Figure 1. This facilitated calculation of the monthly performance factor (SPF_M) (eq. 3), assuming W_{SC} was negligible, and analyzing how it links with groundwater pumping rate (Q) and the delivered heat (P).

Clogging increases the flow resistance. Therefore, *step-discharge tests* were used to assess the hydraulic performance of the production well, injection well, heat exchanger and submersible pump at different pumping rates Q . The tests were carried out semimonthly in the period August 2019-April 2022, according to a procedure described in detail in Gjengedal et al. (2021). The procedure comprised operating the submersible pump at four or more speeds (i.e., steps) in set time intervals, while system performance parameters ($p1-4$, Q , W_{GP}) were monitored. Typically, each step lasted 15 minutes (i.e., until steady state conditions were reached). The measured pressure and Q data were fitted to the equation (Jacob 1947 as quoted in Kruseman, de Ridder, and Verweij 1990)

$$\Delta p_i = B_i Q + C_i Q^2 \quad (5)$$

where Δp_i is the pressure drop or drawdown over i = production well filter ($p1-p0$), injection well filter ($p4-p0$) or heat exchanger ($p3-p2$), and B_i and C_i are the linear and non-linear loss coefficients, respectively. Higher B_i and C_i values correspond to more hydraulic resistance (i.e., clogging). Water level measurements from nearby observation wells were used as proxies for the natural water level ($p0$) in the production and injection wells (i.e., when $Q=0$), see Figure 1. Generally, good fits between data and eq. 5 were achieved for the production well, injection well and heat exchanger ($R^2 > 0.99$).

Combining eq. 1 with eq. 5 for the whole GWHP system, and defining pumping head h_p as the sum of all dynamic (Δp) and static losses (Δh) (i.e., due to elevation differences), yields

$$W_{GP} = \frac{\rho \cdot g}{\eta} (\Delta h Q + B_{tot} Q^2 + C_{tot} Q^3) \quad (6)$$

where B_{tot} and C_{tot} are the cumulative linear and non-linear loss coefficients for the whole GWHP system, respectively. W_{GP} and Q data measured during step-discharge tests

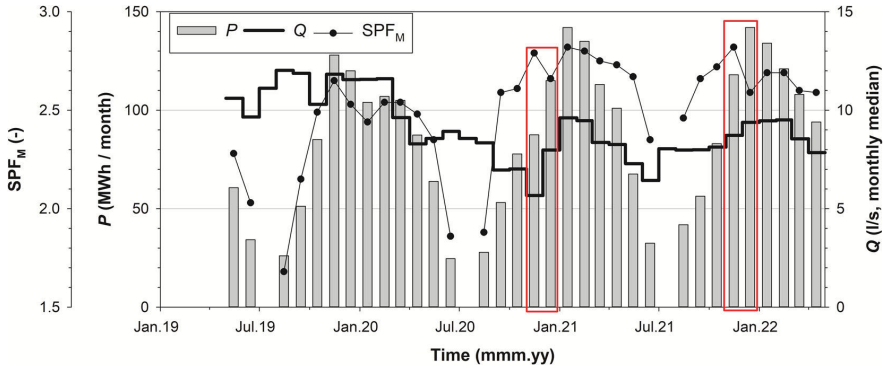


Fig. 3. Heat performance data from Lena terrasse GWHP system between May 2019 and April 2022. Red outline = data periods when changes in SPF_M do not positively correlate with delivered heat. P = delivered heat from heat pump, SPF_M = monthly performance factor (eq. 3), Q = average groundwater pumping rate.

were fitted to eq. 6. After each step-discharge analysis, Δp_i (eq. 5) and W_{GP} (eq. 6) were calculated for $Q = 8 \text{ l/s}$, to keep a Q -referenced clogging record with time. $Q = 8 \text{ l/s}$ approximately represents the average pumping rate during the last two years of measurement.

During the measurement period, there were several rehabilitation actions in the heat exchanger and injection well. The injection well filter was rehabilitated by a combined hydraulic and thermal technique, developed by Hilmo and Gurigard (2017). The technique comprised pouring hot water ($\sim 100^\circ\text{C}$, 30 l/min) into the well for ≥ 12 hours, before performing sectional filter cleaning with an airlift aerator. The heat exchanger was “cleaned in place” (CIP) by Øwre-Johnsen AS with their own mixture of citric acid and a complexing agent (“Bio Gen Active”). The rehabilitation chemicals were circulated through the heat exchanger at elevated temperature ($\sim 50^\circ\text{C}$). Additionally, flow reversal through the heat exchanger were carried out three times during autumn-winter 2021/2022 for preventive maintenance. The flow reversal comprised reversing the flow through the heat exchanger and discharging it to the local stormwater system for ~ 2 hours, without increasing the Q .

The correlation between pumping rate Q and clogging risk, was further assessed by measuring how the groundwater quality changed during step-discharge tests. The measurements were facilitated through a water tap installed right after the heat exchanger in the groundwater circuit, see Figure 1.

Hydrochemistry was measured during one step-discharge test by a combination of field measurements and water samples, according to a procedure described in Stenvik et al. (2022b). Field measurements comprised continuous measurements with electrodes (e.g., dissolved oxygen (WTW FDO 925) and electric conductivity (WTW TetraCon 925/C) sensors) submerged in a flow-through cell leading water from the above-mentioned water tap. Water samples were filtered ($0.45 \mu\text{m}$) and acidified ($65\% \text{ HNO}_3$) in the field, and analyzed for major cations by ICP-MS (Thermo Scientific Element 2 - ICP-HR-MS) in the

laboratory at the Department of Chemistry, NTNU, Trondheim, Norway.

The suspended solids concentration of the abstracted groundwater was measured during two step-discharge tests. The procedure comprised sampling groundwater three times during each step of the step-discharge test, and analyzing the water samples in the laboratory with a turbidity meter (WTW Turb® 430 T) and by manual particle counting. The turbidity analyses were carried out the same day as the sampling, to reduce the influence of chemical reactions (e.g., oxidation of iron) on turbidity. Particle counting of suspended solids which had settled in the water sample containers was carried out manually by visual inspection after the turbidity measurements.

Results

Heat performance data

Heat performance data are presented in Figure 3. The system SPF_M correlates well with the delivered heat (P). Exceptions are found in the periods when the groundwater pumping rate Q does not positively correlate with P (delimited with red lines). In these periods the SPF_M decreases with increasing Q . This trend is further confirmed when comparing the winter season 2019/2020 with the winters 2020/2021 and 2021/2022. The SPF_M was much higher during the last two winters when the pumping rates Q generally were lower than during the winter season 2019/2020. This shows that the effect of increasing submersible pump work is more pronounced than the effect of decreasing heat pump compressor work, as the groundwater pumping rate and heat pump evaporation temperature increases concurrently.

Step-discharge tests

Summary of the step-discharge tests between August 2019 and April 2022 are displayed in Figure 4. Results represent pressure drop or drawdown Δp_i (in meter water column at

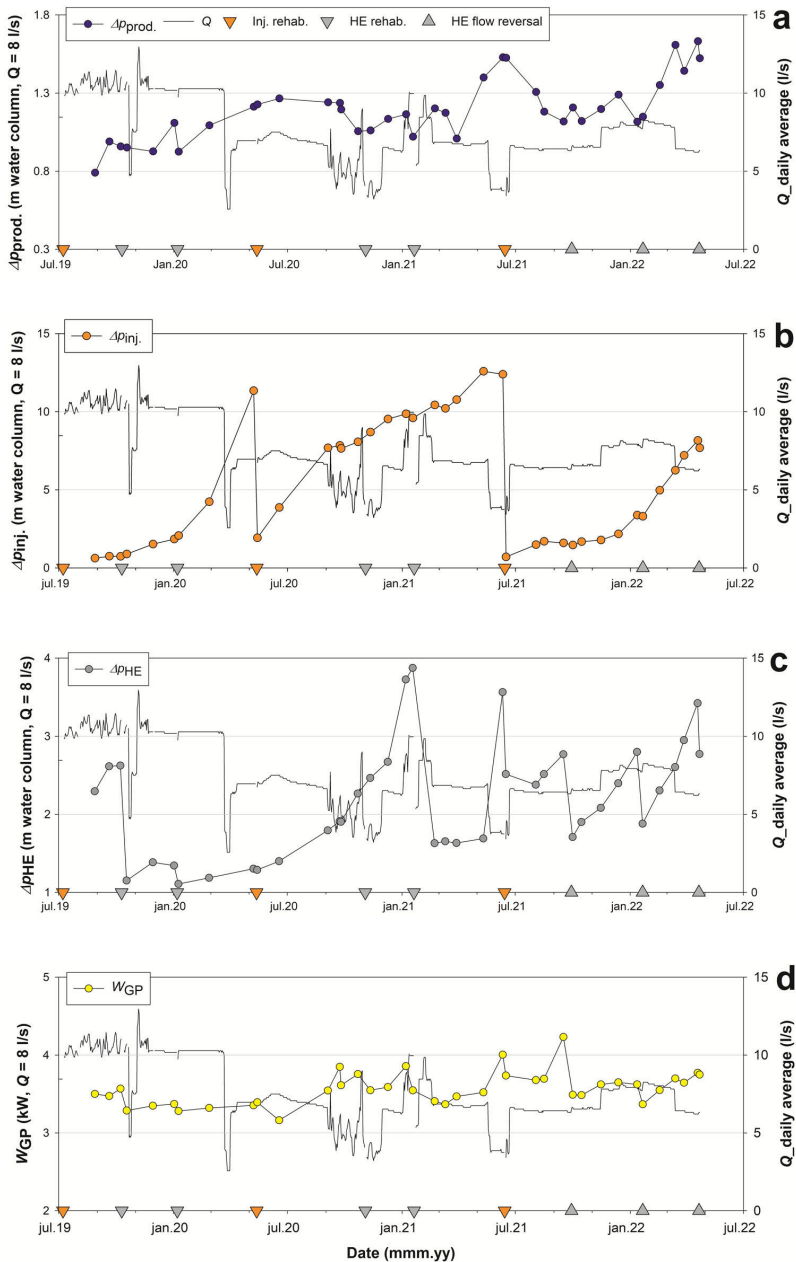


Fig. 4. Hydraulic performance of production well (a), injection well (b), heat exchanger (c) and submersible groundwater pump (d) between August 2019 and April 2022. Data points are calculated from step-discharge test results (B_i - and C_i -values) to the reference groundwater pumping rate $Q = 8$ l/s (eq. 5 and 6). Δp_i = pressure drop/drawdown, W_{GP} = submersible pump power consumption, rehab. = rehabilitation.

$Q = 8$ l/s) in extraction and injection well filters and heat exchanger, and pumping power demand (in kW at $Q = 8$ l/s) of the submersible pump.

Different clogging trends are observed for the production and injection well, heat exchanger and submersible pump. The production well drawdown was relatively stable during

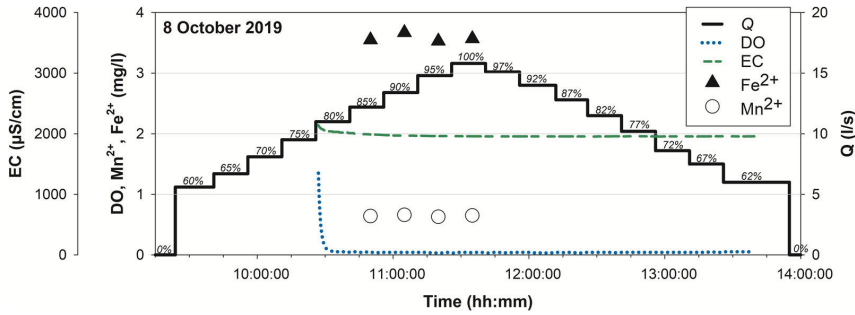


Fig. 5. Hydrochemistry measurements during a prolonged step-discharge test 8 October 2019. Q = groundwater pumping rate, DO = dissolved oxygen, EC = electrical conductivity, Fe^{2+} = dissolved iron, Mn^{2+} = dissolved manganese. Percentages refer to pumping frequency relative to the maximum.

the measurement period, indicating little or no clogging (Figure 4a). The heat exchanger and injection well suffer from severe clogging problems, necessitating semiannual rehabilitations (Figure 4b and c). The pressure build-up accelerated some time after the rehabilitations for both the heat exchanger and the injection well. The pumping power demand (W_{GP}) was relatively stable, indicating sparse clogging of the pump inlet, and correlated with the heat exchanger clogging (Figure 4c and d). This is because the pump only lifts the water up to the heat exchanger, from which it is “cascaded” down through the injection well (Stenvik et al. 2022a).

The rehabilitation and maintenance actions in the heat exchanger and injection well achieved varying degrees of success. For instance, the injection well rehabilitation in May 2020 was less efficient than the ones in 2019 and 2021. The pressure also increased more rapidly after the well cleaning in 2020, although well rehabilitations were needed within approximately one year after the more successful cleanings in 2019 and 2021. The varying degree of success of heat exchanger rehabilitations can be ascribed to testing of a different chemical blend (January 2020) and to leaky valves (November 2020). The flow reversal had a pronounced effect on the pressure drop through the heat exchanger, which decreased ~ 1 m (at $Q = 8$ l/s) after the maintenance actions (Figure 4c). This indicates that the clogging material was partly made up of loose particles, which could be easily removed without rinsing chemicals. Consequently, the annual heat exchanger cleaning was deemed unnecessary before/during the heating season 2021/2022. However, the effectiveness of the flow reversals appeared to decrease with time, which led to a gradual pressure build-up during winter/spring 2021/2022.

Water quality

The hydrochemistry of the abstracted water did not change significantly during the extended step-discharge test displayed in Figure 5. The dissolved oxygen (DO) and electric conductivity (EC) sensors appeared to require some time initially to stabilize, but displayed little variation after that (DO ≤ 0.05 mg/l; $1950 < EC < 2000$ μ S/cm). The four water

samples were almost constant in dissolved iron (3.53–3.67 mg/l) and manganese (0.63–0.66 mg/l).

The concentration of suspended solids increased with pumping rate. Figure 6 displays turbidity measurements and particle counting of water samples taken during two step-discharge tests. The particle counts showed a marked increase at 90% pumping rate (i.e., $Q = 12.9$ – 13.5 l/s).

Turbidity trends were harder to identify during the step-discharge tests (Figure 6). The turbidity varied considerably both during and between the two step-discharge tests. This is probably due to analytical errors, with inevitable contact with oxygen during sampling and too long storage periods (i.e., a few hours) before analysis. This may have facilitated oxidation and precipitation of the initially dissolved iron. Thus, turbidity measurements performed in laboratory does not seem like a reliable method to determine suspended solids loading.

Optimizing submersible pump regulation

SPF_M data presented in Figure 3 indicates that the groundwater pumping rate should be kept as low as possible, but without freezing the groundwater or the secondary circuit fluid (eq. 2) with regards to heat performance.

Differences in SPF_M between winter (January–April) 2021 and 2022 may be related to clogging of the heat exchanger. The heat exchanger was less clogged in 2021, after the rehabilitation in January 2021 (Figure 4c). Clogging material is a less efficient heat conductor than the steel plates of the heat exchanger and will thus increase the temperature difference between the groundwater and secondary circuit fluid in the heat exchanger (Kerner 2011). This will lower the evaporation temperature of the heat pump and lower the heat pump’s coefficient of performance (COP_{HP}) (Stene 2001). Temperature measurements on the in- and outlet of the groundwater and secondary circuit of the heat exchanger are therefore advised to monitor clogging (Kerner 2011). The temperature sensors $T1$ – $T4$ (Figure 1) at Lena terrasse are inaccurate. Still, measurements at $T4$ (i.e., a proxy for the heat pump evaporation temperature) were lower in January–April 2022 (4.2 ± 0.7 °C) than the same period in 2021 (4.7 ± 0.8 °C), despite similar pumping rates Q and heat

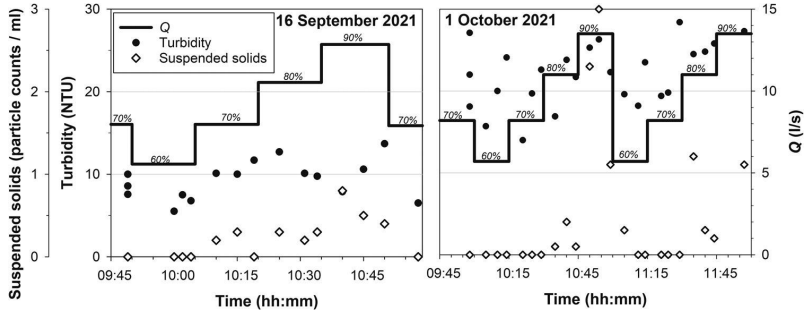


Fig. 6. Turbidity and suspended solids (from manual particle counting) of water samples taken during two step discharge tests at Lena terrasse 16 September (*left*) and 1 October (*right*) 2021. Percentages refer to pumping frequency relative to the maximum.

delivery P (Figure 3). This underlines the importance of performing heat exchanger rehabilitation also from a heat performance point of view.

The effect of operating conditions (i.e., heat exchanger plate shear stress, τ) on clogging rate ($d\Delta p_{HE}/dt$) of the heat exchanger is shown in Figure 7a. Literature suggests that the clogging risk is larger at lower τ (Novak 1982, 1983; Kerner 2011). This implies that the clogging rate ($d\Delta p_{HE}/dt$) will decrease as the heat exchanger becomes more and more clogged, since τ is proportional to Δp_{HE} (eq. 4). To account for this, the baseline shear stress τ' , prior to clogging $d\Delta p_{HE}$ in the period $dt = t_n - t_{n-1}$, was calculated as (eq. 4 and 5)

$$\tau' = \frac{(B_{HE, n-1} Q_m + C_{HE, n-1} Q_m^2) \cdot d_h}{4L} \quad (7)$$

where $B_{HE, n-1}$ and $C_{HE, n-1}$ are the heat exchanger loss coefficients at time t_{n-1} and Q_m is the median pumping rate in the period $dt = t_n - t_{n-1}$. The heat exchanger manufacturer provided values for $d_h = 10.4$ mm and $L = 1384$ mm. τ' was plotted versus $d\Delta p_{HE}/dt$ in the period $dt = t_n - t_{n-1}$.

The τ recommendations (Novak 1982, 1983; Kerner 2011) seem applicable for Lena terrasse's heat exchanger, with the largest clogging rate observed when the operating conditions are "poor" ($\tau < 25$ Pa), see Figure 7a. This corresponds to an event in June 2021 when the pumping rate was kept constant and low (~ 5.6 l/s) over a long period (Figure 4). Thus, keeping pumping rates $Q \geq 6$ l/s seems reasonable when it comes to heat exchanger clogging.

There are less obvious trends between the median pumping rate (Q_m) for any period $dt = t_n - t_{n-1}$ and injection well clogging rate ($d\Delta p_{inj}/dt$), see Figure 7b. According to Olsthoorn (1982)

$$\frac{d\Delta p_{inj}}{dt} \propto Q^2 \quad (8)$$

for an injection well suffering from mechanical clogging by sediment particles. This relationship is not observed between 5.6-11.9 l/s median pumping rates.

At higher pumping rates ($Q > 12$ -13 l/s), the suspended solids concentrations of the extracted groundwater increase, see Figure 6. $Q = 12$ -13 l/s corresponds to entrance velocities v_e in the range 1.26-1.37 cm/s through the 6 meter long

161 mm inner diameter production well screen with 31.3% perforation. This is well below typical literature values for $v_{crit} \geq 3$ cm/s (Williams 1985; Driscoll 1986). However, $v_e = 1.26$ -1.37 cm/s are in the same range as critical groundwater flow velocities to mobilize adhesive, subsurface particles with $d < 0.2$ mm (Muckenthaler 1989). The production well filter was naturally developed after drilling in May 2014, and has measured consistently high non-linear loss coefficients ($C_{prod} = 14285 \pm 5636$ s²/m⁵) in the measurement period (2019-2022). Some of the non-linear losses could be related to elevated flow velocities past the pump motor, caused by a too large submersible pump (OD = 139.5 mm) relative to the production well diameter (ID = 158 mm) (Gjengedal et al. 2021). However, high and stable C-values (≥ 1900 s²/m⁵) may also indicate improper well design (Walton 1962). Improper production well design (i.e., screen slot dimensions) or deficient well development could explain the observed suspended solids trends, and why critical velocities for aquifer matrices (Muckenthaler 1989) seem more applicable than customized production well threshold values (Williams 1985; Driscoll 1986).

Alternatively, some of the suspended solids could stem from corrosion of the production well steel, accelerated by the saline water quality (EC = 1950-2000 μ S/cm, see Figure 5). Regardless of the cause, higher suspended solids loading would increase the injection well's mechanical clogging risk. Despite sparse suspended solids monitoring, pumping rates should be kept ≤ 12 l/s, at least until a decrease in suspended solids loadings has been documented.

The clogging rate of both heat exchanger and injection well seems to be dependent on time since last rehabilitation (Figure 4b and c). Increasing clogging rate with time could correspond to the oxidation of iron. Oxidation of iron will usually accelerate with time due to the self-catalytic effect of iron oxides on oxidation of iron (Tamura, Goto, and Nagayama 1976). Especially, the kinetics will speed up if the iron oxide surfaces inhabit *iron-oxidizing bacteria* (IOB), gaining energy solely or partly from oxidation of iron (Houben and Treskatis 2007). The observation of high dissolved iron concentrations, iron oxide incrustations and specialized IOB at Lena terrasse (Stenvik et al. 2022b) backs up the hypothesis of iron oxides causing the observed

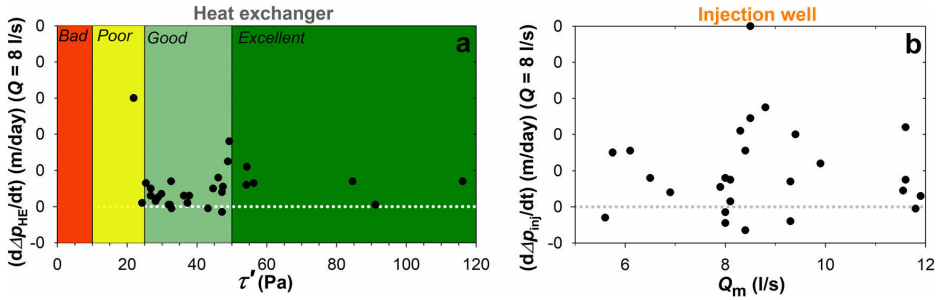


Fig. 7. Operating conditions for heat exchanger (a) and injection well (b) versus clogging rate ($d\Delta p_i/dt$) in the period $dt = t_n - t_{n-1}$. τ' = background plate shear stress prior to clogging (eq. 7). Heat exchanger plate shear stress (τ) categories (“bad”, “poor”, “good” and “excellent”) are from Novak (1982, 1983) and Kerner (2011). Q_m = median pumping rate in the period ($dt = t_n - t_{n-1}$).

clogging acceleration. van Beek, Breedveld, and Stuyfzand (2009) advice pumping production wells suffering from iron oxide clogging continuously (i.e., not on/off or with variable speed drive) to restrict mixing of vertical redox zones. Furthermore, increasing pumping rates during step-discharge tests lead to larger water table drawdowns. Consequently, the flow toward the well filter becomes more vertically oriented, and more water entering from the shallow part of the aquifer would be expected (Kruseman, de Ridder, and Verweij 1990). It would thus have been expected to see changes in the hydrochemistry if the production well extracted water from different vertical redox and/or fresh-/saltwater zones. Since this does not occur in the Lena terrasse GWHP (Figure 5), the vertical hydrochemical variation around the production well filter was deemed minimal, and changing the pumping rate seems unproblematic from a chemical mixing point of view. Still, the bacteria nutrition and turbulence generally increase with pumping rate, which both may speed up iron oxide encrustation. Consequently, operating the pump at variable but low pumping rates does seem appropriate with regards to iron oxide clogging.

It has been demonstrated that lower pumping rates also increases the risk of vacuum pressures in the groundwater circuit at Lena terrasse. However, it is economically more profitable to avoid vacuum pressures through design measures (e.g., constricting the flow in the injection pipe), instead of constantly operating the GWHP system at elevated pumping rates (Stenvik et al. 2022a).

Overall, operating the submersible pump at Lena terrasse at the lowest possible pumping rate between 6 and 12 l/s seems to be the optimum regulation strategy. Here, “possible” means “without freezing the groundwater or secondary circuit fluid”. Thus, the pumping rate should be adjusted according to the heating demand.

The effect of variable speed drive of the submersible pump on clogging rate is hard to determine from the Lena terrasse monitoring data. This is because the pumping rate mostly has been kept constant over longer periods. Still, comparison of Δp_i before and after step-discharge tests shows that the injection well benefits while the heat exchanger is slightly impeded by the tests. These implications

should be further investigated by performing and analyzing longer periods with a more variable pumping scheme.

Even with improved operation of the submersible pump, the heat exchanger and injection well are likely to require frequent rehabilitation measures. The ease of performing the flow reversal justifies adding it to the GWHP operating scheme. Although extending the longevity of rehabilitations, flow reversals cannot fully replace chemical CIP rinsing according to Müller-Steinhagen (2010). The increasing pressure drop across the heat exchanger during winter 2021/2022 despite performing flow reversals testifies to this. Though, more frequent flow reversals may further extend the periods between rehabilitation actions.

The clogging develops rather rapidly in the heat exchanger, and especially the injection well, after rehabilitations. This indicates that not all iron oxides are removed during rehabilitations, which leaves self-catalytic surfaces “available” for rapid oxidation and precipitation of iron. It is recommended that rehabilitation of both the heat exchanger and the injection well are tested with a new chemical rinsing method, using the reducing agent *sodium dithionite* ($\text{Na}_2\text{S}_2\text{O}_4$). This chemical has proven to be very effective in dissolving even mature iron oxides (Houben 2003), and could help to prolong the operational periods between rehabilitation actions.

Conclusions

From the presented investigations we conclude that:

- The monthly performance factor (SPF_M) for the groundwater heat pump (GWHP) system at Lena terrasse in Melhus, Norway is higher at lower pumping rates (Q).
- The heat exchanger and injection well suffer from clogging. The heat exchanger clogging rate increases at $Q < 6$ l/s, while the suspended solids concentrations increase at $Q > 12$ -13 l/s. The latter involves risk of mechanical clogging by sediments in the injection well. Clogging rate appears to be independent of the pumping rate in the range 6-12 l/s.

- Hydrochemistry does not seem to change with pumping rate, indicating that vertical redox mixing does not accelerate if the pumping rate is varied.
- The clogging rate of both the heat exchanger and the injection well increases with time after rehabilitation, resembling the self-catalytic effect of iron oxides on oxidation of iron. This matches previous studies which have revealed iron oxide incrustations in the same GWHP system.
- It is advised that the Lena terrasse GWHP system operate the submersible groundwater pump in the range $6 \leq Q \leq 12$ l/s. The pumping rate should be minimized, but be high enough to avoid freezing the groundwater or secondary circuit fluid, meaning Q should be adjusted to the heating demand.

Disclosure statement

No potential conflict of interest was reported by the authors.

Funding

This work was supported by the Regional Research Funds in Mid-Norway under grant number 284965; Norwegian University of Science and Technology (including St. Olav's Hospital - Trondheim University Hospital). The funding sources were not involved in the study design, writing of the report; nor in the decision to submit the article for publication.

Notes on contributors

Lars A. Stenvik, M.Sc, is a PhD candidate.

Randi K. Ramstad, PhD, is an Associate Professor II.

Bjørn S. Frengstad, PhD, is a Professor.

ORCID

Lars A. Stenvik  <http://orcid.org/0000-0002-0627-8770>

Randi K. Ramstad  <http://orcid.org/0000-0001-9614-636X>

Data availability statement

The authors agree to share their research data. These will be made available at a Mendeley Data repository (reserved doi: 10.17632/pc69rcs94y.1).

Acknowledgments

This study was conducted as part of the research project Optimal Utilization of Groundwater for Heating and Cooling in Melhus 2 (ORMEL 2). This project is a cooperation

between Melhus municipality, the Norwegian University of Science and Technology, Asplan Viak AS, the Geological Survey of Norway and Gjølvaag AS, receiving funding from the Regional Research Funds in Mid-Norway. We would like to thank all the involved institutions and persons for cooperation and financial support. A special thanks is directed to Gry Tangvik Amundsen, former janitor at Lena terrasse's GWHP system, for always welcoming our field visits and for constructive discussions. Finally, the authors would like to thank the two reviewers for their constructive comments and feedback.

References

- Bakema, G. 2001. *Well and borehole failures and solutions in underground thermal energy storage. 2/9805/GW*. Arnhem, Netherlands: IF Technology.
- Banks, D. 2012. *An introduction to thermogeology: Ground source heating and cooling*. 2nd ed. Oxford: Wiley-Blackwell.
- Banks, D., and D. Birks. 2020. Heat from the ground. *Geoscientist* 30 (2):12–7. doi:10.1144/geosci2020-070
- Çengel, Y. A., and J. M. Cimbala. 2010. *Fluid mechanics: fundamentals and applications*. 2nd ed. Boston: McGraw-Hill.
- Driscoll, F. G. 1986. *Groundwater and wells*. 2nd ed. St. Paul, MN: Johnson Division.
- Du, X., H. Zhang, X. Ye, and Y. Lu. 2018. Flow velocity effects on Fe(III) clogging during managed aquifer recharge using urban storm water. *Water* 10 (4):358. doi:10.3390/w10040358
- Eggen, G., and G. Vangsnes. 2005. Heat pump for district cooling and heating at Oslo airport, Gardermoen. In 8th IEA Heat Pump Conference 2005: global advances in heat pump technology, applications, and markets. Conference proceedings, ed. M. Axell. Borås: IEA Heat Pump Centre.
- Gaut, A., and K. Ellingsen. 1992. *Grunnvannsmuligheter i Norge. GiN-veileder nr. 8 [Groundwater exploitation potential in Norway]*. Trondheim, Norway: Skrifter 107, Geological Survey of Norway.
- Gjengedal, S., R. K. Ramstad, B. O. Hilmo, and B. S. Frengstad. 2020. Fouling and clogging surveillance in open loop GSHP systems: A systematic procedure for fouling and clogging detection in the whole groundwater circuit. *Bulletin of Engineering Geology and the Environment* 79 (1):69–82. doi:10.1007/s10064-019-01556-5
- Gjengedal, S., L. A. Stenvik, R. K. Ramstad, J. I. Ulfnes, B. O. Hilmo, and B. S. Frengstad. 2021. Online remote-controlled and cost-effective fouling and clogging surveillance of a groundwater heat pump system. *Bulletin of Engineering Geology and the Environment* 80 (2):1063–72. doi:10.1007/s10064-020-01963-z
- Hilmo, B. O., and R. Gurigard. 2017. Rehabilitering av filterbrønner – erfaringer fra Norge [Rehabilitation of groundwater wells - experience from Norway]. Paper presented at Grundvattendagarna, Uppsala, Sweden, 7–8 November.
- Houben, G. 2003. Iron oxide incrustations in wells. Part 2: Chemical dissolution and modeling. *Applied Geochemistry* 18 (6):941–54. doi:10.1016/S0883-2927(02)00185-3
- Houben, G. 2006. The influence of well hydraulics on the spatial distribution of well incrustations. *Ground Water* 44 (5):668–75. doi: 10.1111/j.1745-6584.2006.00216.x.
- Houben, G., and C. Treskatis. 2007. *Water well rehabilitation and reconstruction*. New York: McGraw-Hill.
- Huisman, L., and T. N. Olsthoorn. 1983. *Artificial groundwater recharge*. Marshfield: Pitman Publishing Inc.
- Jacob, C. E. 1947. Drawdown test to determine effective radius of artesian well. *Transactions of the American Society of Civil Engineers* 112 (1):1047–64. doi:10.1061/TACEAT.0006033

- Jenne, E. A., O. Andersson, and A. Willemsen. 1992. *Well, hydrology, and geochemistry problems encountered in ATEs systems and their solutions*. SAE Technical Paper 929153. Warrendale: SAE International.
- Kerner, J. 2011. Compact, high-efficiency heat exchangers: Understanding fouling. *Chemical Engineering* 118 (6):35–41.
- Kruseman, G. P., N. A. de Ridder, and J. M. Verweij. 1990. *Analysis and evaluation of pumping test data*. 2nd ed. Wageningen: International Institute for Land Reclamation and Improvement.
- Martin, R., ed. 2013. *Clogging issues associated with managed aquifer recharge methods*. Australia: IAH Commission on Managing Aquifer Recharge.
- Muckenthaler, P. 1989. Ergänzende Modellvorstellungen Für Erosions- Und Suffosion kriterien [Supplementary model presentations for erosion and suffosion criteria]. *Wasserwirtschaft* 79 (7/8):405–9.
- Müller-Steinhagen, H. 2010. C4 fouling of heat exchanger surfaces. In *VDI heat atlas*, ed. VDI-Gesellschaft Verfahrenstechnik und Chemieingenieurwesen. 2nd ed., 79–104. Berlin: Springer Berlin Heidelberg.
- Novak, L. 1982. Comparison of the Rhine River and the Öresund Sea water fouling and its removal by chlorination. *Journal of Heat Transfer* 104 (4):663–9. doi:10.1115/1.3245183
- Novak, L. 1983. Fouling in plate heat exchangers and its reduction by proper design. In *Heat exchangers: Theory and practice*, ed. J. Taborek, G. F. Hewitt, and N. Afgan, 871–83. Washington: Hemisphere Pub. Corp.
- Olsthoorn, T. N. 1982. *The clogging rate of recharge wells, main subjects*. KIWA-communications 72. Rijswijk, Netherlands: KIWA.
- Pérez-Paricio, A., and J. Carrera. 1998. Operational guidelines regarding clogging. In *Artificial recharge of groundwater*, ed. J. H. Peters, 441–5. London: CRC Press.
- Riise, M. H. 2015. Praktisk guide for grunnvarmeanlegg basert på oppumpet grunnvann [Practical guide for ground water heat pump systems]. Master thesis., Norwegian University of Science and Technology.
- Stene, J. 2001. Varmepumper: grunnleggende varmpumpeteknikk [Heat pumps: Engineering Basics]. STF84 A97302, SINTEF Energi, Klima- og kuldeteknikk, Trondheim, Norway.
- Stenvik, L. A., S. Gjengedal, R. K. Ramstad, and B. S. Frengstad. 2022a. How to avoid gas clogging in groundwater heat pump systems: A case study from the Lena terrasse system in Melhus, Norway. *Bulletin of Engineering Geology and the Environment* 81 (4):152. doi:10.1007/s10064-022-02652-9
- Stenvik, L. A., S. Gjengedal, R. K. Ramstad, and B. S. Frengstad. 2022b. Hydrochemical and biotic control on iron incrustations in groundwater heat pump systems: Case study from a saline, anoxic aquifer in Melhus, Norway. *Geothermics* 100:102349. doi:10.1016/j.geothermics.2022.102349
- Stuyfzand, P. J., and J. Osma. 2019. Clogging issues with aquifer storage and recovery of reclaimed water in the brackish werribee aquifer, Melbourne, Australia. *Water (Basel)* 11 (9):1807. doi:10.3390/w11091807
- Tamura, H., K. Goto, and M. Nagayama. 1976. The effect of ferric hydroxide on the oxygenation of ferrous ions in neutral solutions. *Corrosion Science* 16 (4):197–207. doi:10.1016/0010-938X(76)90046-9
- van Beek, C. G. E. M. 1989. Rehabilitation of clogged discharge wells in the Netherlands. *Quarterly Journal of Engineering Geology* 22 (1):75–80. doi:10.1144/GSL.QJEG.1989.022.01.06
- van Beek, C. G. E. M., R. Breedveld, and P. J. Stuyfzand. 2009. Preventing two types of well clogging. *Journal - American Water Works Association* 101 (4):125–34. doi:10.1002/j.1551-8833.2009.tb09880.x
- Walton, W. C. 1962. Selected analytical methods for well and aquifer evaluation. Bulletin 49, Illinois State Water Survey, Urbana, Illinois.
- Williams, D. E. 1985. Modern techniques in well design. *Journal - American Water Works Association* 77 (9):68–74. doi:10.1002/j.1551-8833.1985.tb05608.x
- Zeppenfeld, K. 2005. Untersuchungen über den Einfluss der Strömungsgeschwindigkeit auf die Kalkabscheidung aus calciumhaltigen Wässern [Studies of the effect of the flow velocity on calcium carbonate precipitation from water containing calcium]. *Vom Wasser* 103 (2):11–9.

Paper VII

Laboratorietesting av en kjemikalie som reduserer og løser opp jernoksid. Vurdering av anvendelighet til brønnrensing

Av Lars Aaberg Stenvik

Lars Aaberg Stenvik er sivilingeniør i hydrogeologi og stipendiat ved NTNU, Institutt for geovitenskap og petroleum.

Summary

Laboratory testing of a chemical which reduces and dissolves iron oxide incrustations. Assessment of applicability to well rehabilitation. Groundwater often contains dissolved iron which will be oxidized in contact with oxygen to form iron oxide precipitates. The precipitates will incrust and clog wells, and necessitate well cleaning. International experience has shown that a combination of chemical and mechanical cleaning yields the best results. Chemical well cleaning is seldom applied in Norway, due to environmental concerns. The reducing chemical (sodium) dithionite ($\text{Na}_2\text{S}_2\text{O}_4$) has previously demonstrated high dissolution capacity of synthetic iron oxides, reacts at neutral pH, and leaves relatively non-hazardous residues. This article presents a laboratory experiment with dissolution of iron oxide incrustations from an open-loop ground source heat pump system in Melhus, Norway in a mixture of dithionite and bicarbonate. This resulted in 37-45 wt.-% of the incrustations being dissolved, and a comparable reaction efficiency as with synthetic iron oxides. The chemicals are relatively cheap. Cleaning effect, environmental concerns and economy indicate that the chemicals should be tested on Norwegian wells. Still, some technical challenges must be overcome before the method can be applied.

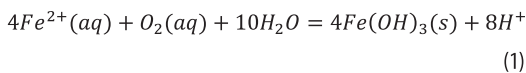
Sammendrag

Grunnvann inneholder ofte løst jern som ved kontakt med oksygen feller ut som jernoksider. I grunnvannsbrønner medfører dette gjentetting av f.eks. brønnfiltre, og behov for brønnrensing. Internasjonal erfaring har vist at kombinasjonen av kjemiske og mekaniske rensemetoder gir best effekt. Kjemisk rens er lite brukt i norske brønner. Den reduserende kjemikalien (natrium)-dithionitt ($\text{Na}_2\text{S}_2\text{O}_4$) virker under nøytral pH, gir relativt ufarlige uorganiske restprodukter, og har tidligere vist god oppløsningsevne på syntetiske jernoksider. I denne artikkelen presenteres et laboratorieforsøk med oppløsning av jernoksid-utfellinger fra et grunnvarmeanlegg i Melhus i dithionitt, bufret med bikarbonat. Resultatene viser at 37-45 vekt-% av utfellingsprøven hadde blitt oppløst etter to timer, og sammenlignbar reaksjonseffektivitet (mengde forbrukt vs. tilsatt kjemikalie) som med syntetiske jernoksider. Kjemikaliene er relativt billige og lett tilgjengelige. Renseeffekt, miljøsinn og økonomi tilsier at kjemikalien først bør uttestes på grunnvarmebrønner. Enkelte tekniske utfordringer knyttet til utføring av rens må løses før metoden kan anvendes i Norge.

Introduksjon

Løste og suspenderte stoffer i grunnvannet kan felle ut i brønner som tar ut eller infiltrerer vann. Dette medfører større friksjonsmotstand per utpumpet vannvolum, økte pumpekostnader, og i verste fall gjentetting av brønnene. Særlig er jernoksid-utfellinger et verdensomspennende problem for grunnvannsbrønner (Houben & Treskatis, 2007), både til drikkevanns- (van Beek, 1989; Banks, 1992; Walter, 1997; Dimkić et al., 2012; Bustos Medina et al., 2013), irrigasjons- (Stuetz & McLaughlan, 2004), drenerings- (Weidner et al., 2012) og grunnvarmeførmål (Lindblad-Pässe, 1986; Bakema, 2001; Woyessa, 2012; Riise, 2015; Possemiers et al., 2016).

Ved oksygenfattige betingelser vil jern reduseres og løses som Fe^{2+} -ioner i grunnvannet. Dersom det jernrike grunnvannet kommer i kontakt med oksygen (O_2) vil Fe^{2+} -ionene oksideres til Fe^{3+} -ioner. Rundt nøytral grunnvannspH vil Fe^{3+} danne uløselige, oransje/rustrøde jern(hydr)oksider (Houben, 2004):

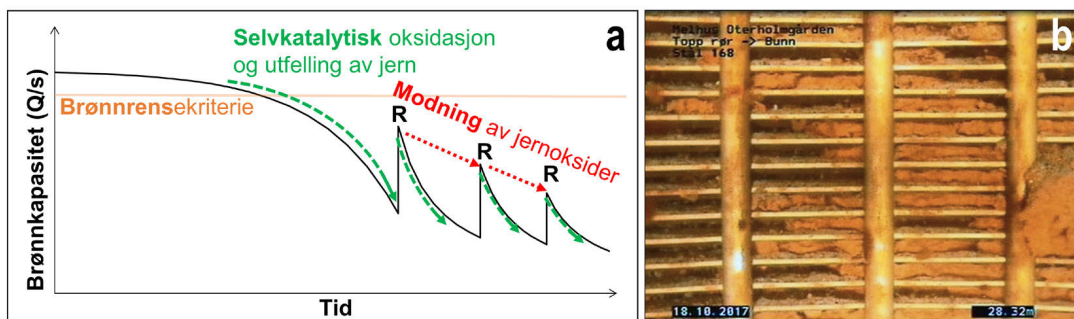


Under uttak av grunnvann er det fare for at reaksjonen i ligning 1 finner sted. Uttaksbrønner fungerer ofte som en «redoks-kortslutning» der dypt, jern-rikt grunnvann mixes med grunt, oksygenrikt grunnvann (van Beek, 1989). Mixing kan også forkomme som følge av horisontale vannkvalitetsvariasjoner (Stuetz & McLaughlan, 2004). Videre er det fare for at det

utpumpede grunnvannet kommer i kontakt med oksygen ved transport gjennom lekkende rør(komponenter) (Bakema, 2001). Dette forklarer hvorfor brønnsystemer som pumper jernrikt vann ofte opplever gjentettingsproblemer i filtre, pumper, rør og varmevekslere, og behov for kostbare rensetiltak (Houben & Treskatis, 2007).

Det amorfte jernhydroksidet *ferrihydratt* ($Fe(OH)_3$) som først dannes vil med tiden modnes til den mer stabile forbindelsen goethitt ($FeOOH$) (Houben, 2003a). Modningen innebærer en re-krySTALLISERING der overflatearealet og vanninnholdet minker. Re-krySTALLISERINGEN bruker måneder til år, og skjer raskere ved høyere pH (Schwertmann & Murad, 1983). I et brønnens-perspektiv vil goethitt med sitt lave overflateareal være vanskeligere å løse og fjerne enn ferrihydratt (Houben, 2003b). Brønnrehabilitering bør derfor utføres før en for stor andel utfellingene har modnet til goethitt. Dersom derimot rehabilitering utføres for sent, vil det bli vanskelig å gjenopprette brønnens opprinnelige uttakskapasitet, se Figur 1a.

Akkurat hvor ofte en brønn bør renses er vanskelig å si på generelt grunnlag. Det finnes likevel enkelte veiledende tall, både for tidsintervall mellom rehabiliteringer og hvor stor nedgang i *spesifikk brønnkapasitet* Q/s som kan tolereres før tiltak iverksettes. Her representerer Q pumperate, og s senkning eller heving av grunnvannsspeilet lokalt, henholdsvis i en uttaks- eller injeksjonsbrønn. Houben & Treskatis (2007) hevder en bør forvente å måtte rens



Figur 1. Brønnkapasitet (Q/s) logget mot tid for en brønn med jernoksid-utfellinger. R = rehabilitering. Modifisert etter Houben (2004) (a). Bilde fra kamerainspeksjon av brønnfilter tilknyttet grunnvarmesystem i Melhus (Foto: Gjøvaag AS) (b).

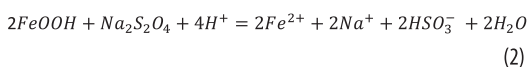
løsmassebrønner mellom hvert hele og femte år. Det er uenighet hvor stor Q/s -nedgang som kan tolereres før rehabilitering utføres. Forskjellige forfattere har foreslått at brønnen bør rehabiliteres etter 10% (McLaughlan, 2002, i Houben & Treskatis, 2007), 20% (Houben & Treskatis, 2007), 25% (Driscoll, 1989, i Houben & Treskatis, 2007) og 30% (Hilmo & Gurigard, 2017) kapasitetsnedgang. Q og s er derfor to essensielle parametere å overvåke, for å vurdere om og når brønnen bør renses, se Figur 1a.

Like mye som «når», er «hvordan» en brønn renses essensielt. Brønnrensing deles inn i to hovedkategorier: kjemiske og mekaniske metoder. Mekanisk rens deles videre inn i termiske, hydrauliske og impuls-metoder (Houben & Treskatis, 2007). Alle metodene har til hensikt å løsne og fjerne utfellingene fra brønnen, ut fra informasjon om hvor og hva slags utfelling som tetter igjen brønnen. Kamerainspeksjon av brønner kan avsløre hvor i brønnen utfellingene er konsentrert, samt bidra til å karakterisere utfellingene, se Figur 1b. Vannkjemiske målinger og mineralogiske analyser av utfellingsmaterialet vil hjelpe med å fastsette utfellingstype. Ut fra denne informasjonen, kan en eller flere passende kjemisk eller mekanisk rensesprosedyr(e) velges. Erfaring tilsier at best brønnrenseeffekt oppnås ved en kombinasjon av kjemisk og mekanisk rens (van Beek, 1989; Houben & Treskatis, 2007).

Jernoksidens kjemiske egenskaper gir enkelte implikasjoner for hvordan brønner med denne typen utfelling bør renses. Ligning 1 viser at jernoksider er mer løselig ved lavere pH og mer reduserende (dvs. mer oksygenfattige) forhold. Aktuelle renskjemikalier er dermed sterke syrer og reduserende midler. Videre oksiderer og utfeller løst jern lettere når det er adsorbent til jernoksidoverflater. Jernoksid-utfellingene gir også grobunn for forskjellige *jernoksiderende bakterier*, som nyttiggjør seg av energien fra oksidasjon av jern til egen metabolisme (Houben & Treskatis, 2007). Dette medfører en *selvkatalytisk* effekt, der oksidasjon og utfelling av jern skjer raskere etter hvert som mer jern allerede har oksidert og utfelt (Tamura et al.,

1976). Dette stemmer også med praktiske erfaringer, der brønner som sliter med jernoksid-utfelling ofte kan driftes uten problemer over flere år før problemene oppstår og raskt forverres (Houben, 2004), se Figur 1a. Den selvkatalytiske effekten understreker også viktigheten av å få rensert bort alle jernoksid-utfellingene under brønnrensing. Hvis ikke vil en i verste fall øke utfellingsraten, pga. mer jernoksid-overflateareal frigjøres, og raskt måtte renses brønnen igjen, se Figur 1a etter rens (R).

Laboratorietesting av diverse syrer og reduserende midler, viste at det reduserende middelet (*natrium*)dithionitt ($\text{Na}_2\text{S}_2\text{O}_4$) løste opp både fersk ($\text{Fe}(\text{OH})_3$) og modnet (FeOOH) jernoksid mest effektivt. Reaksjonsligningen er gitt ved (Houben, 2003b):



der HSO_3^- er *bisulfitt*. Ifølge Mehra & Jackson (1960) løser dithionitt jernoksider mest effektivt rundt nøytral pH. Derfor bufres reaksjonen med (natrium)bikarbonat (NaHCO_3). Restproduktet fra denne reaksjonen er jern, natrium, sulfat (oksidert sulfitt) og bikarbonat, altså relativt ufarlige, uorganiske forbindelser som allerede finnes naturlig i grunnvannet. Dithionitt bufret med bikarbonat utgjør dermed mindre risiko for skade på brønnmaterialet og naturmiljø enn alternative rensedmidler, f.eks. sterke syrer (Houben & Treskatis, 2007). Disse egenskapene gjør dithionitt til et attraktivt brønnrensekjemikalie. Kombinasjonen av dithionitt og bikarbonat med kompleksdannere som hindrer re-utfelling av det løsnede jernet, har blitt patentert som *Aixtractor*® 2.0. *Aixtractor*® 2.0 har sammen med seksjonsvis filtertrekking (hydraulisk rens) vist gode resultater også i praksis (Stuyfzand, 2007; Treskatis & Purnpää-Schäfer, 2013).

I norsk sammenheng er overvåking og rehabilitering av brønner et forsømt område. Banks (1992) avdekket i en spørreundersøkelse for norske grunnvannsverk «deprimerende» lav grad av overvåking og planer for rehabilitering. Denne tendensen virker å vedvare nærmere

30 år etter (Hilmo & Gurigard, 2017; Stenvik, 2020). Følgelig oppdages ofte gjentetningsproblemer for sent, og uten gode rutiner for å rense brønnene. Alternativet blir da ofte å bore nye brønner.

Så vidt forfatteren bekjent, virker det også å være en viss (sunn) skepsis mot å tilføre (rense) kjemikalier til grunnvannsmagasinet, særlig til drikkevannskilder, men uten nødvendigvis å vurdere hver enkelt kjemikalies kost mot nytte. Som et alternativ har en kombinert termisk og hydraulisk rensemetode blitt utviklet av Hilmo & Gurigard (2017). Metoden omfatter at varmt vann (nær 100 °C) tappes i brønnen over tid (≥ 12 timer), før seksjonsvis mammutpumping med trykkluft utføres opp og ned langs brønnfilteret.

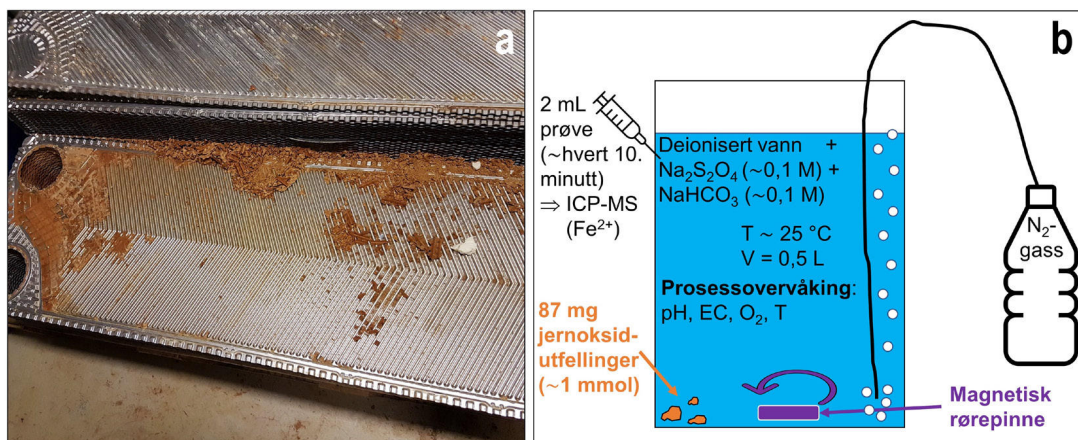
Denne artikkelen har til hensikt å løfte fram viktigheten av jevnlig overvåking og vedlikehold av grunnvannsbrønner, med særlig fokus på vedlikehold. Laboratorietesting av en reduserende kjemikalies evne til å løse opp jernoksidutfellinger fra et åpent grunnvarmeanlegg i Melhus vil bli presentert. Praktisk bruk av rensekjemikalien vil også gjennomgås ut fra et kost-nytte-perspektiv for en grunnvarmebrønn i Melhus, sammenlignet med den kombinerte hydrauliske og termiske renseprosedyren til Hilmo & Gurigard (2017).

Metode

Vann iblandet natriumdionitt og -bikarbonats evne til å redusere og løse opp jernoksidutfellinger ble undersøkt, ved hjelp av et laboratorieeksperiment inspirert av Houben (2003b). Til forskjell fra Houben (2003b) ble det i dette eksperimentet ikke brukt syntetisk framstilte jernoksider, men jernoksidutfellinger innhentet i felt.

Jernoksidutfellinger fra varmeveksleren til Lena terrasses grunnvarmeanlegg i Melhus ble prøvetatt under rens høsten 2018, se Figur 2a. XRD-analyse av materialet viste at den krystalline delen (10%) av prøven hovedsakelig bestod av goethitt (FeOOH), med mindre mengder sideritt (FeCO_3) og kvarts (SiO_2). ICP-MS-analyse av den samme utfellingsprøven oppløst i HNO_3 -syre indikerte at mellom 59 og 71% av materialet bestod av jernoksider, avhengig av mengdeforholdet mellom amorf ferrihydritt ($\text{Fe}(\text{OH})_3$) og modnet goethitt (FeOOH) (Stenvik et al., 2022).

Eksperimentoppsettet og -prosedyren er vist i Figur 2b. Et beger med deionisert vann ($V = 0,5$ L) ble tilsatt 8,71 g ~ 50 mmol) natriumdionitt (Thermo Scientific, $\geq 85\%$ renhet) og 4,20 g ~ 50 mmol) natriumbikarbonat (VWR Chemicals, $\geq 99\%$ renhet). Kjemikaliene fikk god tid til å løses i vannfasen før eksperimentet. En magnetisk rørepinne ble brukt for å sirkulere



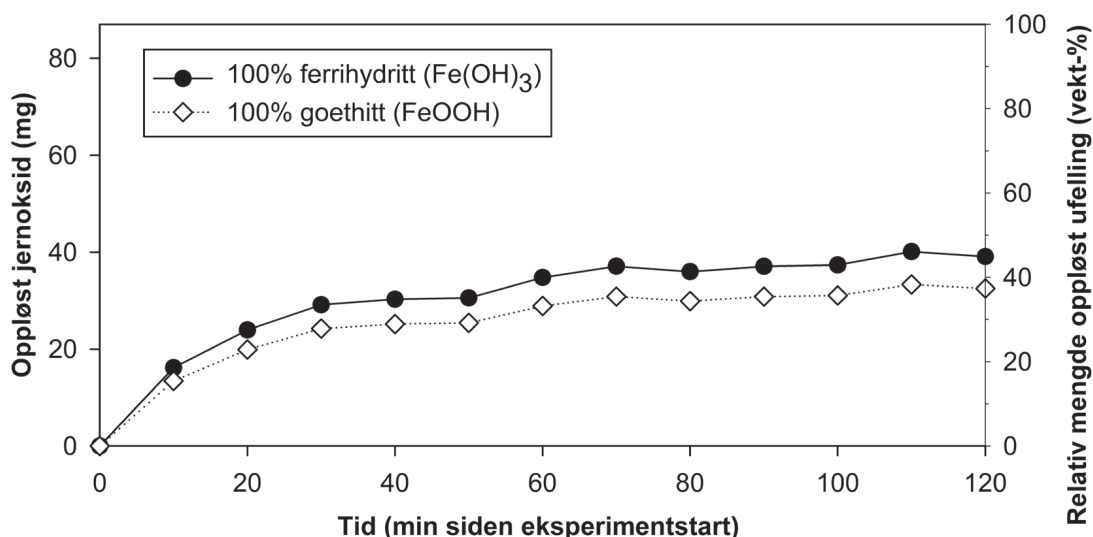
Figur 2. Jernoksidutfellinger fra varmeveksler tilknyttet åpent grunnvarmesystem i Melhus (Foto: Randi Kalskin Ramstad) (a). Eksperimentoppsett inspirert av Houben (2003b) (b).

vannet i karet, mens nitrogen-gass (N_2) kontinuerlig boblet inn i bunnen av karet for å holde vannet oksygenfritt. Videre ble 87 mg (~1 mmol goethitt) utfellingsmateriale tilsatt begeret. Det molare størrelsesforholdet mellom ditionitt/bikarbonat og jernoksid (50:1) var høyere enn i ligning 2, for å sørge for å ha overskudd av kjemikalie som kunne reagere med jernoksidene. Med jevne mellomrom (~hvert tiende minutt) ble det tatt vannprøver (2 mL) som ble filtrert (0,2 μ m). 1 mL av vannprøven ble pipetert i et prøveglass, fortynnet 1:9 med en 0,1M HNO_3 -løsning, og analysert for Fe^{2+} -innhold med ICP-MS (Perkin Elmer ELAN DRC II). Fe^{2+} -innholdet, og molvekt av $Fe(OH)_3$ og $FeOOH$, ble brukt til å omregne til vekt-% oppløst jernoksidutfelling relativt til total mengde tilsatt utfellingsprøve (87 mg). I tillegg ble prosessparameterne pH (WTW Sensolyt 900-P), elektrisk konduktivitet (EC) (WTW TetraCon 925/C), løst oksygen (O_2) (WTW FDO 925) og temperatur (T) (alle tre forannevnte sensorer) målt med jevne mellomrom (~hvert 40. minutt). Eksperimentets varte ca. 2 timer, og ble utført i kjemisk-/mineralogisk laboratorium ved Institutt for geovitenskap og petroleum, NTNU.

Resultater

Måling av prosessparameterne O_2 , pH, EC og T forsikret at oppløsningseksperimentet gikk etter planen. O_2 -målingene ($\leq 0,1$ mg/L) viste at nitrogen-gassen effektivt tømte prøvebeholderen for atmosfærisk gass, mens temperaturmålingene viste at eksperimentet ble utført ved stabil temperatur (~24-25 °C). pH holdt seg ca. nøytral gjennom eksperimentet, som anbefalt av Mehra & Jackson (1960). Riktignok falt pH fra 7,3 til 6,9 gjennom eksperimentet. Den elektriske ledningsevnen økte gjennom hele eksperimentet, men med avtakende rate mot slutten av målingene. Dette tyder på at mye jernoksid ble redusert og oppløst innledningsvis, men at reaksjonen etter hvert avtok.

ICP-MS-målinger av konsentrasjon løst jern, omregnet til relativ mengde oppløst utfelling, stemmer overens med elektrisk ledningsevne-målingene, se Figur 3. Mesteparten av jernet ble løst under første halvdel av eksperimentet, men mengde utfelt jern økte gjennom hele eksperimentet. Enkelte unntak med nedgang i mengde løst jern (f.eks. mellom 70 og 80 minutter) tyder på konsentrasjonsvariasjoner i løsningen og/eller unøyaktigheter i prøvetakingen. Til sammen ble 0,37 mmol jernoksid, tilsvarende mellom



Figur 3. Faktisk og relativ mengde oppløst jernoksid (total mengde utfelling = 87 mg) vs. tid i løsning bestående av deionisert vann, natriumditionitt og natriumbikarbonat. Oppløst mengde jernoksider ble beregnet ut fra ICP-MS-analyse av Fe^{2+} , og antakelse om at løst jern stammet fra ferrihydritt (øvre grense) og goethitt (nedre grense).

37-45 vekt-% av utfellingsprøven, oppløst av vann-ditionitt-bikarbonat-løsningen.

Diskusjon

Den oppløste mengden jernoksider (37-45%) i dette eksperimentet er lavere enn den estimerte mengden jernoksider (59-71%) i en sammenlignbar prøve (Stenvik et al., 2022). Dette kan ha flere mulige forklaringer:

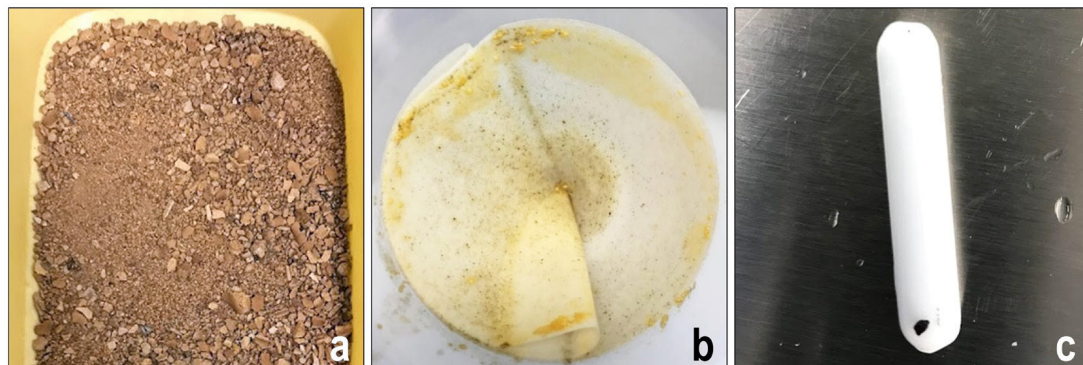
- 1) Siden prøvetaking i 2018 har prøven blitt lagret i romtemperatur i en ikke lufttett boks. Dette medfører fare for at prøven kan ha blitt modnet til å bestå av mer goethitt under eksperimentet i mai 2022 enn under prøvetaking i 2018. Ettersom goethitt har mindre overflateareal og er mer stabil enn ferrihydritt, vil modnet jernoksid være vanskeligere å løse opp med $\text{Na}_2\text{S}_2\text{O}_4$.
- 2) Naturlige variasjoner i mengde jernoksider i utfellingsprøven kan også forekomme. En tidligere XRD-analyse har vist at utfellingene fra Lena terrasse bestod av mest jernoksid, men mindre mengder sideritt (FeCO_3) og kvarts (SiO_2) (Stenvik et al., 2022). Utfellingsprøven fra Lena terrasse ser ut til å være relativt inhomogen, se Figur 4a. Dette underbygger risikoen for naturlige variasjoner i mineralinnhold.
- 3) Avviket mellom oppløst (37-45%) og beregnet (59-71%) (Stenvik et al., 2022) mengde jernoksider kan også skyldes feilberegninger. ICP-MS-analyse av utfelling

oppløst i HNO_3 ligger til grunn for beregning av mengden jernoksid i utfellingsprøven (59-71%). Her ble det antatt at alt løst jern ($\text{Fe}^{2+}/\text{Fe}^{3+}$) stammet fra jernoksid (Stenvik et al., 2022). Det er likevel fare for at oppløsning av syreløselig FeCO_3 bidro til et overdrevet estimat. $\text{Na}_2\text{S}_2\text{O}_4$ løser derimot ikke FeCO_3 . Dermed er ikke ICP-MS-analyser av utfellingene oppløst i HNO_3 og $\text{Na}_2\text{S}_2\text{O}_4$ nødvendigvis sammenlignbare.

Sammenligning mellom oppløst mengde jernoksider i dette eksperimentet med tidligere estimert jernoksid-konsentrasjon i utfellingene har derfor begrenset relevans.

Rensekjemikalie- og jernoksid-løsningen ble filtrert gjennom et $0,45 \mu\text{m}$ -filter etter eksperimentet. Dette førte til at en mengde mindre, sorte sedimenter, i tillegg til oransje jernoksid-lignende slam, ble filtrert ut, se Figur 4b. Filtre-ringen skjedde en stund etter at eksperimentet ble fullført. Deler av jernoksid-slammet bestod derfor trolig av re-utfelt jern, etter at N_2 -gass ikke lenger holdt løsningen oksygen-fri. Noe av det sorte materialet festet seg til den magnetiske rørepinnen, se Figur 4c. Dette materialet bestod trolig av *magnetitt* (Fe_3O_4) korrodert fra brønn-systemet.

Den filtrerte utfellingsprøven etter rens virker mer inndelt etter mineralfaser (Figur 4b og c) enn utfellingsprøven før rens (Figur 4a). Få av de



Figur 4. Sammenligning av utfellingsprøve før (venstre) og etter (midten, høyre) laboratorieforsøk. Bildet i midten viser filteret ($0,45 \mu\text{m}$) som kjemikalieløsningen ble silt gjennom etter eksperimentet, mens bildet til høyre viser den magnetiske rørepinnen med magnetiske deler fra utfellingsprøven som har festet seg (svart bit på bunnen).

filtrerte sedimentene så ut til å være omgitt av en oransje hinne med jernoksid. Natriumditiotionitt- og bikarbonat-blandingen ser dermed ut til å ha en god evne til å løse jernoksid-utfellinger fra silikatholdige sedimenter, noe som er hovedformålet ved kjemisk rensing av et brønnfilter.

Mengden oppløst jernoksid relativt til total mengde jernoksid utfellinger virker å være noe lavere i dette eksperimentet ($37\% / 59\% = 63\%$), sammenlignet med mengden oppløst syntetisk jernoksid (75-100%) i laboratorieforsøket til Houben (2003b). Likevel er *reaksjonseffektiviteten* (*RE*) sammenlignbar for eksperimentet i denne ($RE = 0,37\%$) og Houben (2003b) sin studie ($RE = 0,38-0,5\%$), etter samme reaksjonstid (to timer) og med samme mengde $\text{Na}_2\text{S}_2\text{O}_4$ tilsatt (~50 mmol):

$$RE(\%) = \frac{Na_2S_2O_4 \text{ forbrukt (mol)}}{Total Na_2S_2O_4 \text{ tilsatt (mol)}} * 100\% \quad (3)$$

$$= \frac{0,5 * \text{løst jernoksid (mol)}}{Total Na_2S_2O_4 \text{ tilsatt (mol)}} * 100\%$$

der løst jern leses av Figur 3. Lavest *RE* i Houben (2003b) sitt laboratorieforsøk ble oppnådd for modnede goethitter med lite overflateareal. Dette indikerer at ditionitt har tilnærmet like god evne til å løse naturlige som syntetiske goethitt-utfellinger, men at det kreves et relativt høyt forholdstall mellom mengde tilsatte kjemikalier og utfellinger. Ditionitts gode renssevne for jernoksider (Houben, 2003b) rettferdiggjør derfor en vurdering av kjemikalienes anvendelighet til norske brønner gjentattet av jernoksid-utfellinger.

Ditionitts anvendelighet som brønnrensemetode

Anvendeligheten av ditionitt og bikarbonat som brønnrensemetode avhenger av økonomiske, tekniske og miljømessige forhold, i tillegg til kjemisk oppløsningssevne.

Det er økonomisk fordelaktig dersom kjemisk rensing med ditionitt ikke øker kostnadene vesentlig sammenlignet med gjeldende rensemetode(r). Returbrønnen til grunnvarmeanlegget på Lena terrasse i Melhus har blitt rensert med Hilmo and Gurigard (2017) sin termiske

og hydrauliske metode, senest i juni 2021. Femten timers drift av dieseldrevet fyrkjel til å varme opp vann som ble tappet i returbrønnen kostet da 5850 kr. Her bør det også nevnes at drivstoff-prisene har økt med 61-62% mellom juni 2021 til juni 2022 (Statistisk sentralbyrå, 2022). Mengden kjemikalier som kreves per brønn vil avhenge av mengde utfellinger i brønnfilteret. Cleanwells GbR (u.å.) angir likevel som en tommelfingerregel at $c = 30$ g Aixtractor 2.0° kreves per liter med borehull som skal behandles. Returbrønnen til det åpne grunnvarmeanlegget på Lena terrasse i Melhus har borehulldiameter (\varnothing) på 168 mm og filterrørlengde (l_f) på 10 m. Med andre ord kreves det $\pi\varnothing^2 / 4 * l_f * c \approx 6,6$ kg Aixtractor 2.0° til rens av brønnen. Dersom ekvimolart forhold mellom NaHCO_3 og $\text{Na}_2\text{S}_2\text{O}_4$ antas i Aixtractor 2.0°, som i eksperimentet i denne studien, kreves det ca. 2,2 kg NaHCO_3 og 4,4 kg $\text{Na}_2\text{S}_2\text{O}_4$. Ifølge et pristilbud fra VWR (mai 2022) koster 10 kg $\text{Na}_2\text{S}_2\text{O}_4$ 4800 kr og 5 kg NaHCO_3 1250 kr ekskl. mva. uten bedriftsavtale. Med merverdiavgift på 25% kan derfor renseskjemiene antas å koste ≤ 7600 kr. Kjemisk rens med ditionitt og bikarbonat virker derfor økonomisk konkurransedyktig med den termiske delen av rensemetoden til Hilmo & Gurigard (2017).

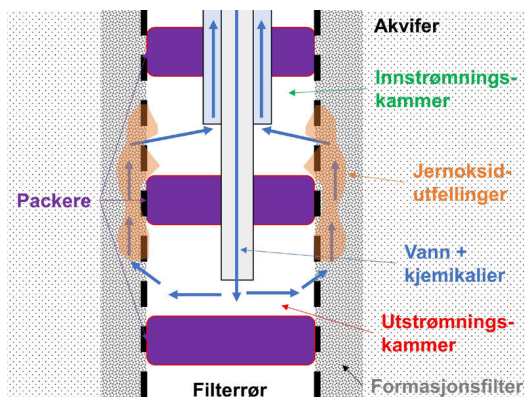
Videre har den kombinerte termiske og hydrauliske rensemetoden til Hilmo & Gurigard (2017) slitt med å rehabilitere returbrønnen på Lena terrasses tilbake til opprinnelig kapasitet (Q/s). Kapasiteten reduseres også raskt etter rens, slik at returbrønnen nå renses årlig. Lignende problemer er også erfart ved grunnvarmeanlegget til Oslo lufthavn på Gardermoen (Woyessa, 2012). Dette tyder på at filtrene er tettet igjen med modnede, tungtløselige jernoksid-utfellinger, som bidrar til rask selvkatalytisk oksidasjon og utfelling av jern etter rens. Brønneierne bør derfor vurdere å teste ut en ny brønnrensemetode, f.eks. en kombinert kjemisk og mekanisk rens med ditionitt.

Det er mer usikkerhet knyttet til den praktiske gjennomføringen av brønnrens med ditionitt og bikarbonat. Houben & Treskatis (2007) anbefaler at kjemikalieblandingen

sirkuleres gjennom vertikalt avgrensede deler av brønnfilteret med et *multikammer packer-system*, se Figur 5. Sirkuleringen oppnås ved å injisere kjemikalier i et utstrømningskammer, og pumpe blandingen ut fra et separat innstrømningskammer. Etter forfatterens kjennskap er ingen norske bore- eller (brønn)rensefirmaer i besittelse av et slikt eller lignende packer-system(er). Systemet må spesialbygges, og kreve både investeringskostnader og teknisk kompetanse. Erfaringer fra bl.a. Finland og Tyskland der lignende systemer har blitt bygget vil derfor være verdifulle til design og bygging av packer-systemet.

Miljømessig vil termiske rensemetoder ofte være gunstigere enn kjemiske rensemetoder. For eksempel kan nærliggende drikkevannsbrønner være i drift mens termisk brønnrens utføres (Hilmo & Gurigard, 2017). Videre er termisk forurensing av naturmiljø antakeligvis et mindre problem enn kjemikalieforurensing. Det må framheves at restproduktene av rensing med $\text{Na}_2\text{S}_2\text{O}_4$ og NaHCO_3 er relativt ufarlige, uorganiske forbindelser med høye eller ingen grenseverdier i Drikkevannsforskriften (2016), og nøytral pH. Akviferer som kun brukes til grunnvarmeformål, f.eks. Melhus akviferen, bør derfor kunne gis tillatelse til uttesting av kjemisk brønnrensing med ditionitt.

Aixtractor 2.0[®] inneholder i tillegg til $\text{Na}_2\text{S}_2\text{O}_4$ og NaHCO_3 en kompleksdanner som



Figur 5. Multikammer packer-system brukt til seksjonsvis brønnrens. Kjemikalieblanding sirkuleres fra utstrømnings-, via formasjonsfilteret med utfellinger, til innstrømningskammeret. Modifisert etter Detay (1997), i Houben & Treskatis (2007).

sikrer at det oppløste jernet forblir løst, og ikke re-utfeller. Dette kan medføre større vanskeligheter med å få tillatelse til bruk av kjemikalien. Forfatteren anbefaler derfor at en blanding utelukkende bestående av $\text{Na}_2\text{S}_2\text{O}_4$ og NaHCO_3 først uttestes, før mer komplekse kjemikalieblandinger eventuelt vurderes nødvendige.

Konklusjon

Det utførte laboratorieforsøket viser at en løsning bestående av 0,5 L deionisert vann, $\sim 0,1$ M av reduktanten $\text{Na}_2\text{S}_2\text{O}_4$ og bufret med $\sim 0,1$ M NaHCO_3 evnet å løse 37-45 vekt-% av en utfellingsprøve (87 mg) fra et åpent grunnvarmesystem i Melhus. Utfellingsprøven bestod hovedsakelig av goethitt og ferrihydritt, og mindre mengder kvarts og sideritt. Selv om tilsynelatende ikke all jernoksid i utfellingsprøven ble oppløst, var reaksjonseffektiviteten sammenlignbar med et tidligere laboratorieeksperiment med syntetiske jernoksider. I sistnevnte laboratorieeksperiment, der flere kjemikalier ble uttestet, viste natriumditionitt ($\text{Na}_2\text{S}_2\text{O}_4$) seg å ha best renssevne for jernoksider. Med tanke på oppløsningssevne virker derfor ditionitt som et foretrukket valg til kjemisk brønnrensing av jernoksidutfellinger.

Anvendeligheten av ditionitt avgjøres av økonomiske, tekniske og miljømessige forhold. Prisen på ditionitt-kjemikalier er konkurransedyktig med oppvarmingskostnader relatert til termisk brønnrensing. Rensing med ditionitt er mer krevende teknisk, ettersom sirkulering av renskjemikalier gjennom brønnfilteret bør utføres med et spesialbygget *multikammer packer-system*. Miljømessig gir rensing med ditionitt og bikarbonat de ufarlige restproduktene jern, natrium, sulfat og bikarbonat, og nøytral pH. Dette er fordelaktig sammenlignet med andre kjemiske rensmidler, både mtp. fare for spredning i naturmiljøet og skade på brønnmaterialet. Tillatelse til testing av kjemikalien i akviferer som brukes til åpne grunnvarmesystemer bør derfor kunne gis. Utprøving anbefales derfor i grunnvarmebrønner der termisk og/eller hydraulisk brønnrensing ikke har gitt ønsket renseseffekt.

Takksigelser

Det presenterte arbeidet er en del av forskningsprosjektet ORMEL 2 (Optimal ressursutnyttelse av grunnvann til oppvarming og kjøling i Melhus), støttet av Regionalt forskningsfond Midt-Norge (tildelingsnummer 284965). ORMEL 2 er et samarbeid mellom Norges teknisk-naturvitenskapelige universitet (NTNU), Norges geologiske undersøkelse (NGU), Asplan Viak AS, Melhus kommune og Gjøvaag AS. Jeg vil takke alle involverte partnere i forskningsprosjektet for deres støtte. Spesielt vil jeg takke professor Bjørn Frengstad og førsteamanuensis II Randi Kalskin Ramstad ved Institutt for geovitenskap og petroleum, NTNU for oppfordring og støtte til å gjennomføre laboratorieeksperimentet. Videre rettes det en stor takk til senioringeniør Laurentius Tjihuis og overingeniør Torill Sørløkk ved kjemisk-/mineralogisk laboratorium ved Institutt for geovitenskap og petroleum, NTNU, for støtte under planlegging og gjennomføring av laboratorieforsøket.

Referanser

Bakema, G. (2001). *Well and Borehole Failures and Solutions in Underground Thermal Energy Storage* (2/9805/GW). Arnhem, NL: IF Technology.

Banks, D. (1992). *Grunnvannsbrønner: kontroll, vedlikehold, rehabilitering*. GiN-veileder 13 (Skrifter 108). Trondheim: NGU

Bustos Medina, D.A., van den Berg, G.A., van Breukelen, B.M., Juhasz-Holerman, M., & Stuijffzand, P.J. (2013). Iron hydroxide clogging of public supply wells receiving artificial recharge: Near-well and in-well hydrological and hydrochemical observations. *Hydrogeology Journal*, 21(7), 1393-1412. <https://doi.org/10.1007/s10040-013-1005-0>

Cleanwells GbR. (u.å.). *AIXTRACTOR 2.0® brochure*. Hentet 10. mai 2022 fra http://cleanwells.de/downloads/en/aixtractor_2_en.pdf

Detay, M. (1997). *Water Wells - Implementation, Maintenance and Restoration*. London, UK: John Wiley and Sons.

Dimkić, M., Pušić, M., Obradović, V., & Kovačević, S. (2012). The effect of certain biochemical factors on well clogging under suboxic and mildly anoxic conditions. *Water Sci Technol*, 65(12), 2206-2212. <https://doi.org/10.2166/wst.2012.129>

Drikkevannsforskriften. (2016). *Forskrift om vannforsyning og drikkevann* (FOR-2016-12-22-1868). Lovdata. <https://lovdata.no/dokument/SF/forskrift/2016-12-22-1868>

Driscoll, F.G. (1989). *Groundwater and wells* (2. utgave). St. Paul, US: Johnson Division.

Hilmo, B. O., & Gurigard, R. (2017). Rehabilitering av filterbrønner – erfaringer fra Norge. *Grundvattendagarna*, 7.-8. november 2017, Uppsala, Sverige.

Houben, G. (2003a). Iron oxide incrustations in wells. Part 1: genesis, mineralogy and geochemistry. *Applied Geochemistry*, 18(6), 927-939. [https://doi.org/10.1016/S0883-2927\(02\)00242-1](https://doi.org/10.1016/S0883-2927(02)00242-1)

Houben, G. (2003b). Iron oxide incrustations in wells. Part 2: chemical dissolution and modeling. *Applied Geochemistry*, 18(6), 941-954. [https://doi.org/10.1016/S0883-2927\(02\)00185-3](https://doi.org/10.1016/S0883-2927(02)00185-3)

Houben, G. (2004). Modeling the Buildup of Iron Oxide Encrustations in Wells. *Groundwater*, 42(1), 78-82. <https://doi.org/10.1111/j.1745-6584.2004.tb02452.x>

Houben, G., & Treskatis, C. (2007). *Water well rehabilitation and reconstruction*. New York, US: McGraw-Hill.

Lindblad-Pässe, A. (1986). *Järnutfällningsproblem i grundvattenvärmsystem* (R109:1986). Stockholm: Statens råd för byggnadsforskning.

McLaughlan, R. (2002). *Managing water well deterioration*. Lisse, NL: Balkema.

Mehra, O.P., & Jackson, M.L. (1960). Iron oxide removal from soils and clays by a dithionite-citrate system buffered with sodium bicarbonate. *Clays and Clay Minerals*, 5, 317-327. <https://doi.org/https://doi.org/10.1016/B978-0-08-009235-5.50026-7>

Possemiers, M., Huysmans, M., Anibas, C., Batelaan, O., & Steenwinkel, J. (2016). Reactive transport modeling of redox processes to assess Fe.sub.3 precipitation around aquifer thermal energy storage wells in phreatic aquifers. *Environmental Earth Sciences*, 75(8), 1. <https://doi.org/10.1007/s12665-016-5398-7>

Riise, M. H. (2015). *Praktisk guide for grunnvarmeanlegg basert på oppumpet grunnvann*. [Masteroppgave]. NTNU, Trondheim.

Schwertmann, U., & Murad, E. (1983). Effect of pH on the Formation of Goethite and Hematite from Ferrihydrite. *Clays and Clay Minerals*, 31(4), 277-284. <https://doi.org/10.1346/CCMN.1983.0310405>

Statistisk sentralbyrå. (2022). *Sal av petroleumsprodukt og flytande biodrivstoff*. Hentet 10. mai 2022 fra <https://www.ssb.no/statbank/table/09654/>

Stenvik, L. A. (2020). Utfellingsproblemer med jern og mangan i norske drikkevannsbrønner [Eng: Iron and manganese incrustations in Norwegian groundwater works. In Norwegian]. *Kommunalteknikk* (4). https://issuu.com/kommunalteknikk/docs/6kt_4-20/s/11415728

Stenvik, L. A., Gjengedal, S., Ramstad, R. K., & Frengstad, B. S. (2022). Hydrochemical and biotic control on iron incrustations in groundwater heat pump systems: Case study from a saline, anoxic aquifer in Melhus, Norway. *Geothermics*, 100. <https://doi.org/https://doi.org/10.1016/j.geothermics.2022.102349>

Stuetz, R., & McLaughlan, R. (2004). Impact of localised dissolved iron concentrations on the biofouling of environmental wells. 49(2), 107-113. <https://doi.org/10.2166/wst.2004.0100>

Stuyfzand, P. (2007). Naar een effectievere diagnose, therapie en preventie van chemische put- en drainverstopping [Norsk: Mot mer effektiv diagnostisering, vedlikehold og forebygging av kjemiske brønntuffellinger. På nederlandsk]. *H2O*, 8, 44-47. <https://edepot.wur.nl/343238>

Tamura, H., Goto, K., & Nagayama, M. (1976). The effect of ferric hydroxide on the oxygenation of ferrous ions in neutral solutions. *Corrosion Science*, 16(4), 197-207. [https://doi.org/10.1016/0010-938X\(76\)90046-9](https://doi.org/10.1016/0010-938X(76)90046-9)

Treskatis, C., & Puronpää-Schäfer, P. (2013). Keeping up the flow. *WorldWater*, 15-17. <http://cleanwells.de/downloads/fachartikel/WORLDWATER%202014.pdf>

van Beek, C. G. E. M. (1989). Rehabilitation of clogged discharge wells in the Netherlands. *Quarterly journal of engineering geology and hydrogeology*, 22(1), 75-80. <https://doi.org/10.1144/GSL.QJEG.1989.022.01.06>

Walter, D. A. (1997). *Geochemistry and microbiology of iron-related well-screen encrustation and aquifer biofouling in Suffolk County, Long Island, New York* (Water-Resources Investigations Report 97-4032). Coram, New York, US: U.S. Geological Survey. <https://doi.org/10.3133/wri974032>

Weidner, C., Henkel, S., Lorke, S., Rude, T. R., Schüttrumpf, H., & Klauder, W. (2012). Experimental Modelling of Chemical Clogging Processes in Dewatering Wells. *Mine Water and the Environment*, 31(4), 242-251. <https://doi.org/10.1007/s10230-012-0188-2>

Woyessa, A. O. (2012). *Identification of hydrochemical processes in the screen environment in shallow geothermal wells from Gardermoen University of Oslo*. Oslo.



SAMFUNNSLØSNINGER FOR VANN OG MILJØ

Det er Swecos jobb å utnytte den beste fagkompetansen og være din flerfaglige rådgiver innen:

- Konsekvensutredninger
- VA-planer og utredninger
- Vannressursplaner
- Hydrologiske undersøkelser
- VA-modellering
- Avløpsrensaneanlegg
- Vannbehandlingsanlegg
- VA-transportssystemer i åpne grøfter
- VA-transportssystemer med grøttefrie løsninger
- Overvannshåndtering
- Miljøundersøkelser
- Miljøøkonomi og -ledelse

www.sweco.no

SWECO 

Paper **VIII**



Elevated manganese concentrations in groundwater wells after longtime abstraction with bank filtration: developing and testing of a sorption model for Ringerike waterworks, Norway

Lars A. Stenvik¹ · Bernt Olav Hilmo² · Bjørn S. Frengstad¹

Received: 22 December 2021 / Accepted: 1 September 2022 / Published online: 6 October 2022
© The Author(s) 2022

Abstract

Groundwater abstraction wells located in aquifers hydraulically connected with rivers or lakes will induce bank filtration if the water level in the aquifer is lowered below the surface-water level. Many groundwater works utilize this induced infiltration to increase the abstraction capacity of their wells. Unfortunately, infiltration of organic-rich surface water may alter the aquifer's redox geochemistry, and mobilize iron and/or manganese. Ringerike groundwater works in southeastern Norway operates with bank filtration. Manganese concentrations in the abstracted water began to increase 19 years after the start of operations, and stabilized at an elevated level 8 years later. The estimated manganese retardation ($R_{\text{sorp}} = 45 \pm 18$) from a simplified advection-sorption model is comparable to the observed manganese retardation range $36 < R_{\text{obs}} < 50$, assuming a groundwater residence time $t_{\text{gw}} \sim 200$ days. The advection-sorption model is based on limited sediment composition and hydrochemical data, which introduces significant uncertainty to R_{sorp} . However, R_{sorp} and R_{obs} in the same range, and the good fit between PHREEQC simulated and observed data, indicates that sorption is a possible explanation for the delayed breakthrough of elevated manganese concentrations in Ringerike waterworks' production wells. Comparable bank filtration schemes are advised to establish observation well(s) between the bank filtration and production well field for early detection of sorption fronts. This would facilitate (1) longer time available for remediation measures and their evaluation, and (2) less manganese to be desorbed during the remediation stage.

Keywords Manganese · Water supply · Bank filtration · Reactive transport · Retardation

Introduction

Bank filtration refers to infiltration of surface water into an unconfined aquifer, induced by groundwater abstraction. Groundwater abstraction will draw down the water level in the aquifer, whereby infiltration is induced if the water level in the aquifer is lowered below the water level of a hydraulically connected river or lake. The filtration through the aquifer sediments will improve the infiltrated water quality hygienically (e.g., remove pathogens and organic matter; Hiscock and Grischek 2002; Kvitsand et al. 2017). Furthermore, the induced infiltration will increase the abstraction

capacity from small aquifers, by supplementing the groundwater recharge from precipitation and natural groundwater flow (Knutsson 2008). Bank filtration is therefore often used for drinking-water pretreatment (Dillon 2005).

A downside to bank filtration is the possible alteration of redox conditions in the aquifer, which may increase the iron (Fe^{2+}) and manganese (Mn^{2+}) concentrations in the abstracted water (Farnsworth and Hering 2011). Elevated iron and manganese concentrations lead to undesired color and taste, which needs costly treatment if the water is to be used for drinking purposes (Ellingsen 1992). This is because iron and manganese are oxidized and precipitate as oxide minerals in contact with oxygen. The precipitates may furthermore incrust and clog well filters, distribution pipes, etc., forcing costly remediation (Houben and Treskatis 2007). Followingly, groundwater sources with high iron and manganese concentrations are sought avoided for drinking-water purposes.

The alteration of redox conditions in aquifers during bank filtration can be ascribed to an increased influx of

✉ Lars A. Stenvik
lars.a.stenvik@ntnu.no

¹ Norwegian University of Science and Technology, S. P. Andersens vei 15A, N-7491 Trondheim, Norway

² Asplan Viak AS, Abels gate 9, 7030 Trondheim, Norway

organic matter. If enough organic matter infiltrates, the degradation will deplete the water of oxygen and nitrate, and in turn reduce manganese ($\text{Mn}^{3+/4+}$) oxides and iron (Fe^{3+}) oxides to soluble Fe^{2+} and Mn^{2+} ions (Stumm and Morgan 1996; see Fig. 1), resulting in a reducing zone near the bank, characterized by high dissolved Fe^{2+} and Mn^{2+} concentrations. The degradation of organic matter also produces carbon dioxide gas which is dissolved in water to form carbonic acid. The acid dissolves carbonate minerals, which may further increase dissolved iron and manganese concentrations. The transport of iron and manganese toward the abstraction well may be delayed by sorption to aquifer sediments. The composition of ions adsorbed to aquifer sediments reflects the dissolved concentrations (Appelo and Postma 2005). Thus, increasing dissolved manganese concentrations would lead to ion exchange of manganese for other cations initially adsorbed to the aquifer sediments, causing a manganese “sorption front” moving towards the production well area, with a velocity that is slower than the average groundwater flow rate (Fig. 1). Water-table oscillations around the abstraction well(s) will oxygenate the groundwater, leading to a more oxic zone in this part of the aquifer. Precipitation of oxide minerals in the aquifer around the abstraction wells may hinder the breakthrough of elevated iron and manganese concentrations in the abstracted water (Farnsworth and Hering 2011). If, however, dissolved iron and manganese reaches the abstraction well, they may be oxidized in the well filter through mixing with shallow, oxygen-rich groundwater, causing the aforementioned clogging issues (Houben and Treskatis 2007).

The redox characteristics of iron and manganese differ from one another. Manganese is more easily reduced than iron, and requires more oxygen to be oxidized. Furthermore, oxidation of manganese is kinetically slower than oxidation of iron (Stumm and Morgan 1996), which explains why

elevated dissolved concentrations of manganese is more common than elevated concentrations of iron in bank filtration abstraction wells (Farnsworth and Hering 2011).

Some bank filtration schemes abstract water low in manganese for many years before manganese concentrations start to increase (see Table 1). The retardation R of manganese transport can be defined as (Appelo and Postma 2005)

$$R_{\text{obs}} = \frac{t_{\text{Mn}}}{t_{\text{gw}}} \quad (1)$$

where t_{Mn} is the bank filtration operation time before elevated manganese concentrations occurred and t_{gw} is the aquifer residence time of the abstracted groundwater. The data in Table 1 indicate retardation R_{obs} ranging from single- to three-digit magnitude.

Delayed occurrences of elevated manganese concentrations in bank filtration settings have demanded numerous and often complex explanations (see Table 1 and Fig. 1). Many authors have attributed the retardation of manganese transport to sorption to aquifer sediments (Thomas et al. 1994; Petrunic et al. 2005; Farnsworth and Hering 2011). Oren et al. (2007) developed a manganese sorption model for sewage infiltration into an aquifer in the Dan Region, Israel, based on the composition of cations in solution and the aquifer sediments’ cation exchange capacity. The aim was to assess whether the modeled manganese retardation due to sorption resembled the observed retardation in nearby observation wells. Since the modeled manganese retardation resembled the observed one, Oren et al. (2007) concluded that sorption was the probable cause of manganese breakthrough after a time lag of 8–12 years.

The organic content of the infiltrating surface water and the aquifer sediments can also induce changes to manganese concentrations with time. Seasonal changes in the organic loading of recharge water and lithological variation led to seasonal and spatial changes in dissolved manganese

Fig. 1 Geochemical processes related to manganese (and iron) during groundwater abstraction with bank filtration

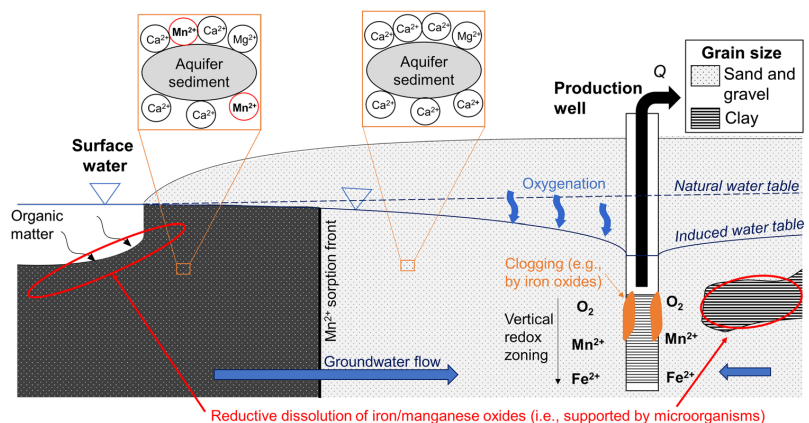


Table 1 Occurrence of elevated manganese concentrations after longtime operation of groundwater works with bank filtration. The reference “Waterworks” refers to data retrieved directly from operators at the waterworks

Country	Location of waterworks	Aquifer deposit ^a	Start (year)	Elevated Mn ²⁺ (year)	Travel time	Retardation explanation	Reference
Canada	New Brunswick	Glacio.	1955 (1968 ^b)	1971	Months-years	<ul style="list-style-type: none"> • Sorption • Delay by microbes 	Thomas et al. (1994) Petrunic et al. (2005) Dawe (2006)
Norway	Bø	Glacio.	1978	^c	Days-months	-	Kraft (2011)
	Kongsberg	Glacio.	1984	^c	~3 months	-	Waterworks
	Kongsvinger	Glacio.	1970	^c	-	-	Waterworks
	Lillehammer	Glacio.	1982 (1993 ^b)	2000–2002	15–60 days	<ul style="list-style-type: none"> • Varying sediment composition • New flow path 	Segar (1994) Holmström et al. (2010)
	Ringerike	Glacio.	1987	2006	~200 days ^d	• (Sorption) ^e	Vestland (2012)
	Sauherad	Glacio.	1994	^c	-	-	Waterworks
	Seljord	Glacio./ fluvial	1990	^c	-	-	Waterworks
USA	Rhode Island	Glacio.	1953	1965–1967	90 days-2 years	-	Silvey and Johnston (1977)

^aUnconsolidated sand and/or gravel. Glacio. = glaciofluvial

^bNew production well inducing new flow path starts to operate

^cAfter multiple years of operation, but uncertainty with regards to exact year of problem occurrence

^dBased on hydraulic conductivity $K = 10^{-3}$ m/s, effective porosity $n = 20\%$, hydraulic gradient = 0.5% and travel length = 500 m (Vestland 2012)

^eSuggested explanation is not based on geochemical calculations (Stenvik and Hilmo 2020)

concentrations, respectively, in an alluvial aquifer connected to the Lot River in south of France (Bourg and Bertin 1994). The spatial changes were due to low-permeability clay lamellas, which impeded the groundwater flow rate and led to longer residence time and more reducing conditions. Variation in lithology and the drilling of a new production well that induced new groundwater flow paths were used to explain increasing manganese concentrations after longtime operation at Lillehammer waterworks, Norway (Holmström et al. 2010). Similarly, increasing recharge of organic-rich river water to the aquifer, following drilling of a new production well and increasing pumping rate, was used to explain increasing groundwater manganese concentrations in New Brunswick, Canada, between 1971–1989 (Thomas et al. 1994).

Thomas et al. (1994) and Petrunic et al. (2005) also pointed to the microbial community as part of the explanation for elevated manganese concentrations. The microbial community needs time to adapt to a new redox regime (i.e., build a community of manganese-reducing bacteria), which will increase the reduction rate of manganese oxides with time.

Well clogging also may induce changes to the abstracted water quality. Incrustations usually form in the top portion of the well filter first, where inflow rates are highest, and then gradually expand downwards as the well filter clogs. This will lead to abstraction of deeper groundwater, which is often

more anoxic and higher in iron and manganese, with time (Houben and Treskatis 2007).

It is also noteworthy that all occurrences listed in Table 1 are related to glaciofluvial aquifers, though previous studies have had limited emphasis on this aspect. Despite many possible explanations for increasing manganese concentrations after longtime operation, the retardation explanation is often not properly settled (see Table 1). This article investigates whether sorption can explain the elevated manganese concentrations after longtime groundwater abstraction with bank filtration at Ringerike waterworks. A simplified advection-sorption model is developed based on existing aquifer sediment data and new hydrochemical field and laboratory measurements of the abstracted water. The model is validated by comparison with records of manganese concentrations in the production wells in the period 2006–2021, and other geochemical data. Strategies to monitor future bank filtration schemes with regards to disclosing risk of and source of elevated manganese concentrations are also presented.

Study area

The Kilemoen aquifer and Ringerike waterworks

The study area comprises the Holocene ice marginal delta Kilemoen, deposited ~10,500 years ago during the last

deglaciation (Vorren and Mangerud 2006). The deposit consists of glaciofluvial, unconsolidated sand and gravel, partially covered by and with lamellas of marine clay deposited when seawater inundated the area (see Fig. 2). The glaciofluvial deposit makes up an unconfined aquifer hydraulically connected to River Begna, with >30 m saturated thickness (Vestland 2012). The regional natural groundwater gradient follows the river from north to south, with groundwater recharge north of and discharge south of Kilemoen. Kilemoen comprises many kettle holes, with one of these deemed favorable for Ringerike waterworks' production well field (Klemetsrud 1985).

Ringerike waterworks started its operation in 1987 with three production wells (no. 1–3) pumping 80–90 L/s on average (see Table 2). Initially, the riverbed was deemed too impermeable for bank filtration; thus, a sand filter for pretreatment of river water and two infiltration wells were established near the riverbank (see “Tjorputten” in Fig. 2) to increase the abstraction capacity (Ellingsen and Finsrud 1990). Though, the sand filter and infiltration wells have

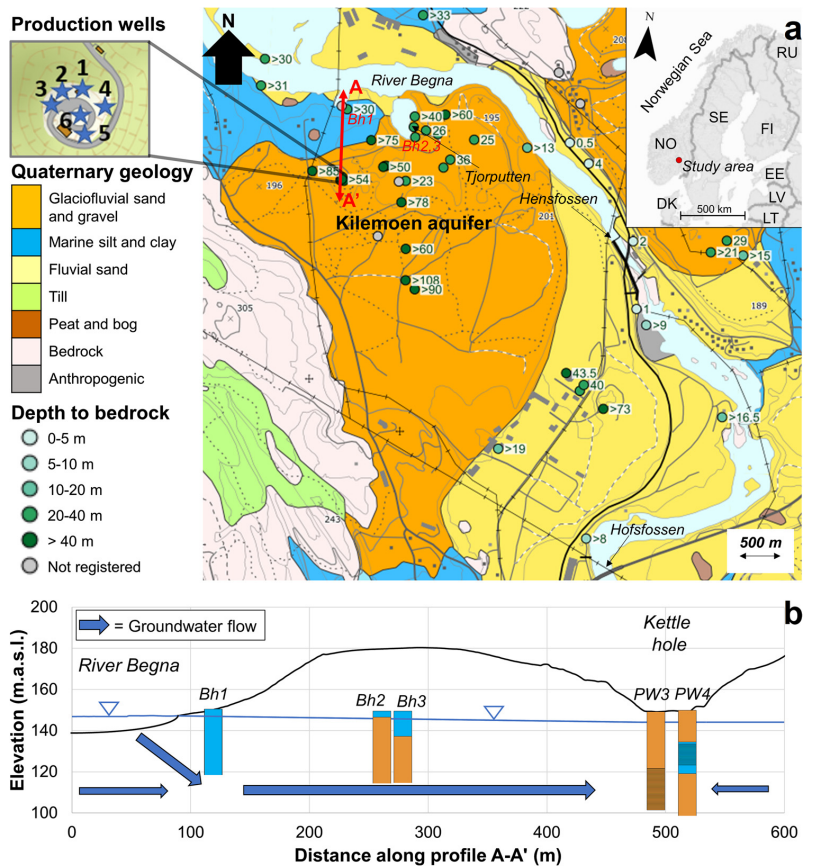
been used very sparsely. The precipitation recharge is estimated to be 13 L/s at Kilemoen (Vestland 2012). Stable water levels, while water is pumped out at 80–90 L/s from the aquifer, indicate that bank filtration is active somewhere along the Kilemoen-Begna interface. Now it is assumed that most of the bank filtration occurs north of the production well and in the Tjorputten area.

Table 2 Basic information about production wells in kettle hole at Ringerike waterworks

Well	Operational since (year)	Total depth (m)	Screened depth (m)	Q (L/s)
PW1	1987	47	27–47	16–21
PW2	1987	43	23–43	16–21
PW3	1987	47	27–47	16–21
PW4	2007	33	23–33	^a
PW5	2007	27	16–26	14–19
PW6	2009	33	23–33	14–19

^aCurrently not in operation due to problems with sand production

Fig. 2 **a** Map of the study area. Production wells at Ringerike waterworks in enlarged section. Modified from (Geological Survey of Norway 2021). **b** Profile of the Kilemoen aquifer. Based on drilling logs by Skarphagen (1982) and Klemetsrud (1985). Production well (PW) screen depths are indicated by horizontal lines. Proportional groundwater flow is indicated conceptually. Elevation data retrieved from Norwegian Mapping Authority (2021)



Elevated manganese concentrations: Previous investigations

The dissolved manganese concentrations in the production wells started to increase in 2006 (Fig. 3a), initiating investigations to disclose the problem cause. Test drillings in 2006–2007 showed increasing iron and manganese levels with depth both in the production well kettle hole and near the riverbank at Tjorputten (see Fig. 3b). The total organic carbon (TOC) levels in the aquifer (TOC = 0.1–1.2 mg/L; Fig. 3b) were lower than the yearly average in River Begna in the period 1994–2014 (TOC = 3.27 ± 0.84 mg/L; sampled at Hensfossen in Fig. 2; Lindholm et al. 2015). The depletion of TOC is probably due to oxidation of organic matter from the river water, coupled with the reduction of iron and manganese oxides in a zone near the riverbank. However, this requires that oxygen and nitrate are depleted during infiltration. The river TOC levels equal a *chemical oxygen demand* COD = 8.72 ± 2.23 mg/L, which is below the oxygen saturation at 5–10 °C (11–13 mg/L). The infiltrating water may however not be fully oxygen saturated, which would facilitate reductive dissolution of oxides.

Elevated manganese concentrations in PW1–PW3 and increasing manganese concentrations with depth (Fig. 3b) led to the drilling of three new, shallower production wells south of the existing wells in 2007 (PW4 and PW5) and 2009 (PW6; see Table 2 and Fig. 2). The new production wells have consistently measured lower manganese concentrations than the older ones. Problems with sand pumping in PW4, probably due to the PW4 well screen's proximity to a clay lamella, see Fig. 2(b), has kept this well partly out of operation. Meanwhile the manganese concentrations in PW1–PW3 continued to increase after 2006, unconstrained by operational measures, including increased use of infiltration wells and installing variable speed drive pumps in the production wells. Each production well comprises a piezometric well drilled right next to it. None of these piezometric wells have indicated substantial production well clogging (i.e., increasing difference in drawdown in piezometric and production well). Nevertheless, mechanical rehabilitation by brushing and jetting was deployed in 2007 without affecting the manganese concentrations. Eventually, the problems of elevated manganese concentrations constrained a new 100 million NOK (~10 million EUR) water treatment facility in 2018, which has delivered water of satisfactory quality to the water distribution system (Brugger and Paskert 2020).

In a review of iron and manganese issues related to Norwegian groundwater works, a reducing zone near the riverbank combined with retardation by sorption to aquifer sediments was suggested as a possible explanation to increasing manganese concentrations after longtime operation at Ringerike waterworks (Stenvik and Hilmo

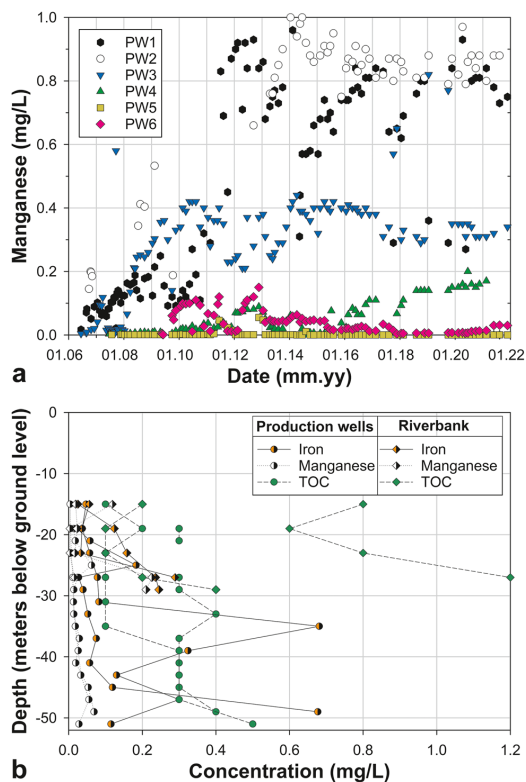


Fig. 3 a Manganese concentration in production wells at Ringerike waterworks vs. time. For location of production wells (PW1–PW6) see Fig. 2. Modified from Stenvik and Hilmo (2020). b Depth profiles of dissolved concentrations of iron and manganese in two test wells drilled in the production well field kettle hole (December 2006) and two test wells near the riverbank at Tjorputten (August 2007). Data retrieved from Tormod Tobiassen (operator at Ringerike waterworks) and Hilmo (2007). Note: Iron concentrations are inaccurate due to the inconsistent filtration procedure used for the water samples

2020). The lack of detailed calculations and hydrochemical measurements hampered this analysis, but set the stage for a more in-depth analysis of the manganese issues at Ringerike waterworks.

Materials and methods

Hydrochemistry data

The raw groundwater quality from five pumping wells (PW1–PW3, PW5, PW6) at Ringerike waterworks was investigated separately by field measurements and water sampling in October 2021. Sensors measuring dissolved

oxygen (DO; WTW FDO 925), pH (WTW Sensolyt 900-P), electrical conductivity (EC; WTW TetraCon 925/C), oxidation-reduction potential (ORP) (Sensolyt ORP 900-P) and temperature (all sensors) were submerged in a flow-through cell and connected to a WTW Multi 3630 IDS digital meter (Fig. 4). The digital meter performed automatic readings every 30 s for ~1 h, while the flow rate through the cell was kept at ~0.1 L/s. ORP was recalculated to redox potential relative to the standard hydrogen electrode (Eh) by a correction factor given by the electrode supplier. Alkalinity was determined by GRAN titration (Stumm and Morgan 1996) with a Merck MColor-test. Additionally, water samples were taken from each of the field measured production wells. The water samples were first filtered with a 0.45- μm membrane, then acidified with 0.1M HNO_3 , and analyzed for major cations and anions by inductively coupled mass spectrometry (ICP-MS; Agilent 8800 ICP-MS Triple Quad) at the Department of Chemistry, NTNU, Norway. The accuracy of the ICP-MS instrument (i.e., %-error (absolute) between expected and measured value) was determined from analysis of freshwater reference material.

Results from field measurements and water samples were used as input for the geochemical software PHREEQC v. 3.7.2a (Parkhurst and Appelo 2013) to calculate mineral saturation indices and the electrical balance between cations and anions. Equilibrium constants used for calculating mineral saturation indices were retrieved from the “PHREEQC.DAT” database.

Manganese sorption model

One-dimensional (1D) transport of manganese in an aquifer, assuming neglectable dispersion, can be described with the *advection-reaction* equation:

$$\frac{\partial[\text{Mn}^{2+}]}{\partial t} = \pm \sum_{i=1}^n P_i - v \frac{\partial[\text{Mn}^{2+}]}{\partial x} - S \quad (2)$$

where $[\text{Mn}^{2+}]$ is the manganese concentration, t is time, x is distance from the riverbank in the flow direction, P_i is the rate of chemical precipitation/dissolution reaction involving manganese, v is the average groundwater flow velocity and S is the rate of manganese adsorption.

Adsorption and desorption of dissolved ions (ion exchange) occur instantaneously and can be treated as equilibrium processes if the flow rate is slow enough and if there are no stagnant zones in the porous medium (Appelo and Postma 2005). The groundwater flow velocity at Ringelike is relatively high ($v = 2.5$ m/day, Vestland 2012), but comparable to the flow velocity ($v = 1.5$ m/day) in the Dan Region, Israel, where ion exchange equilibrium

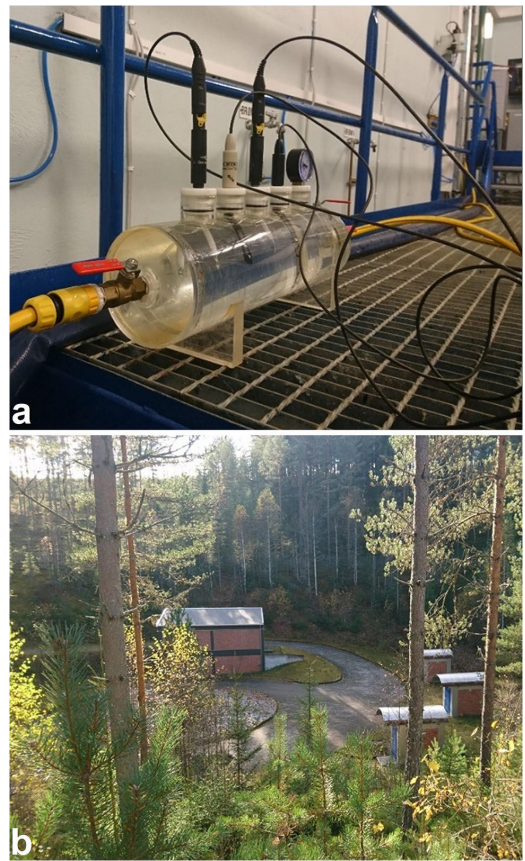


Fig. 4 a Flow-through cell during measurement. b Kettle hole where Ringelike waterworks’ production wells are located. Pump houses above production well 1-3 to the right

was assumed for a similar transport model (Oren et al. 2007). The ion exchange equilibrium assumption facilitates relating the change in dissolved concentration with time ($\frac{\partial[\text{Mn}^{2+}]}{\partial t}$) to the adsorption rate S with a manganese *distribution coefficient* K_d (Appelo and Postma 2005):

$$S = K_d \cdot \frac{\partial[\text{Mn}^{2+}]}{\partial t} \quad (3)$$

Equation 2 can be further simplified by assuming that reductive dissolution of manganese oxides only occurs near the riverbank (i.e., at $x = 0$), and that no other manganese precipitation/dissolution reaction occurs in the aquifer. Inserting Eq. (3) into Eq. (2), combined with mathematical manipulation and the definition of retardation from Eq. (1), yields the *sorption retardation equation* (Appelo and Postma 2005):

$$R_{sorp} = 1 + K_d \quad (0 < x \leq L) \tag{4}$$

where L (~500 m) is the length from the recharge area to the production well area. K_d depends on the total *cation exchange capacity* (CEC) of the aquifer sediments, and the composition of cations in solution and their relative tendency to ion exchange for each other:

$$K_d = \frac{\beta_{Mn} \cdot CEC}{[Mn^{2+}]} \tag{5}$$

where β_{Mn} is the proportion of sorption sites taken up by manganese. Under circum-neutral pH conditions, the CEC primarily depends on the organic matter and clay (<2 μ m) concentration of the aquifer matrix (Breeuwsma et al. 1986, in Appelo and Postma 2005):

$$CEC \left(\frac{meq}{100 \text{ g dry soil}} \right) = 0.7 \cdot (wt. - \%clay) + 3.5 \cdot (wt. - \%organic \text{ carbon}) \tag{6}$$

Grain-size distributions from 40 test drillings in the Kilemoen aquifer demonstrated 39 drillings with no clay, and one with ~10% clay content (Klemetsrud 1985; Skarphagen 1982). The mean $\pm 2 \times$ standard deviations clay content was approximated to $0.25 \pm 0.25\%$, since the clay did not appear to be normally distributed. The organic carbon content was not measured in any of the sediment samples from Kilemoen. However, two sediment samples from a glaciofluvial aquifer (Gardermoen, ~50 km direct distance away) of the same age as Kilemoen contained 0.17 and 0.21% ($0.19 \pm 0.06\%$) organic carbon (Woyessa 2012). These values, together with an effective porosity $n = 20\%$ (Vestland 2012) and bulk dry aquifer density $\rho_b = 2.12 \text{ g/cm}^3$ (i.e., assuming an aquifer matrix consisting of pure quartz), were used to estimate $CEC = 0.089 \pm 0.029 \text{ eq/L water}$. The estimated CEC, together with measured $[Mn^{2+}]$ and β_{Mn} calculated from cation concentrations in PW1–PW3, were used to calculate K_d (Eq. 5) and R_{sorp} (Eq. 4). See section S1 in the electronic supplementary material (ESM) for calculation of β_{Mn} and detailed deduction of equations.

The sorption processes for PW1–PW3 were also simulated with the ADVECTION, EXCHANGE, and

SOLUTION modules in PHREEQC (see Fig. 5). The 500 m aquifer section between the riverbank and production well area was represented by 50 reaction cells, with each cell representing a groundwater solution in equilibrium with cation exchange sites with the average $CEC = 0.089 \text{ eq/L water}$. Cell 1–50 was initially equilibrated with groundwater quality as measured in PW1–PW3, except for the manganese concentrations. A $[Mn^{2+}] = 0.007 \text{ mg/L}$ measured at Hofsfossen (Bækken et al. 2011) in River Begna (Fig. 2) was chosen to represent the prebank filtration ($t = 0$) aquifer conditions. This value resembled the minimum manganese concentrations measured in the production wells (Fig. 3a). Thus, initially very little manganese was adsorbed. The bank filtration process was simulated by shifting the solutions to increasing cell numbers, and the introduction of a new groundwater quality (cell 0) into cell 1. The solution in cell 0 did not change during the simulation, and comprised manganese concentrations as measured in PW1–PW3. The simulation comprised 4,000 shifts, which equaled $4,000/50 = 80$ abstracted pore volumes. Abstracted pore volumes equal time since the start of the simulation/operation (t) divided by groundwater residence time (t_{gw}). See section S2 of the ESM for the PHREEQC script.

Results

The measured raw groundwater chemistry of the production wells at Ringerike waterworks is presented in Table 3. The water samples' charge balance between cations and anions was not always satisfactory, with imbalance decreasing with increasing total dissolved solids (electrical conductivity). The accuracy of the ICP-MS instrument was generally higher for cations (1.2–4.3 %-error) than anions (66.4 %-error for SO_4^{2-} ; 7.1 %-error for Cl^- ; see section S3 of the ESM for details). Comparing with previous water samples (Hilmo 2007; Vestland 2012), the field measured alkalinity values were slightly higher in this study. The charge imbalances could thus be due to systematic errors in the anion measurements. Still, the charge imbalances for

Fig. 5 Conceptual build-up of the PHREEQC advection-sorption model for production wells PW1–PW3 at Ringerike waterworks. CEC = cation exchange capacity

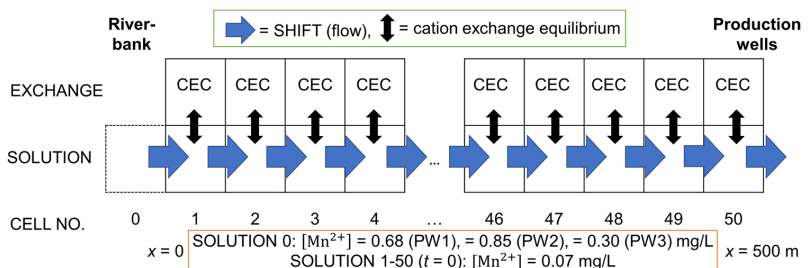


Table 3 Raw groundwater chemistry 12–14 October 2021 at Ringerike waterworks. *Eh* redox potential referring to the normal hydrogen electrode, *DO* dissolved oxygen, *EC* electrical conductivity, *Temp.* temperature, *Alk* alkalinity

Parameter	PW1 ^a	PW2 ^a	PW3 ^a	PW5 ^a	PW6 ^a
pH ^b	6.77 ± 0.04	7.00 ± 0.03	6.94 ± 0.02	6.74 ± 0.02	6.80 ± 0.03
Eh (mV) ^b	362 ± 5	343 ± 7	337 ± 5	404 ± 28	365 ± 23
DO (mg/L) ^b	1.23 ± 0.01	0.31 ± 0.01	0.67 ± 0.01	6.73 ± 0.01	2.38 ± 0.20
EC (μS/cm) ^b	149 ± 1	189 ± 3	160 ± 1	82 ± 1	120 ± 0.1
Temp. (°C) ^b	7.4 ± 0.2	7.2 ± 0.1	6.9 ± 0.1	6.7 ± 0.1	7.2 ± 0.1
Alk (mmol/L) ^c	1.3 ± 0.2	1.6 ± 0.1	1.4 ± 0.2	0.9 ± 0.2	1.2 ± 0.4
Fe ²⁺ (mg/L) ^d	0.01 ± 0.00	0.00 ± 0.00	0.01 ± 0.00	0.00 ± 0.00	0.01 ± 0.00
Mn ²⁺ (mg/L) ^d	0.68 ± 0.01	0.85 ± 0.02	0.30 ± 0.00	0.00 ± 0.00	0.03 ± 0.00
Na ⁺ (mg/L) ^d	3.88 ± 0.02	5.58 ± 0.09	5.47 ± 0.03	2.35 ± 0.03	3.39 ± 0.06
Mg ²⁺ (mg/L) ^c	3.84 ± 0.06	4.46 ± 0.06	4.35 ± 0.03	1.92 ± 0.03	2.93 ± 0.09
Ca ²⁺ (mg/L) ^d	15.41 ± 0.12	20.12 ± 0.22	15.43 ± 0.09	8.38 ± 0.12	13.30 ± 0.21
K ⁺ (mg/L) ^d	2.22 ± 0.03	2.29 ± 0.04	1.98 ± 0.02	1.41 ± 0.01	1.82 ± 0.03
Cl ⁻ (mg/L) ^d	2.80 ± 0.40	4.59 ± 0.25	4.81 ± 0.29	1.03 ± 0.09	1.97 ± 0.08
SO ₄ ²⁻ (mg/L) ^d	6.02 ± 0.04	8.15 ± 0.08	9.53 ± 0.13	4.61 ± 0.04	6.26 ± 0.11
Charge balance ^e	-8.0%	-5.5%	-10.1%	-17.9%	-11.6%

^aEach well was sampled and field measured once ($n = 1$)

^bValues given as mean $\pm 2 \times$ standard deviations (SD) during ~ 1 h of continuous measurement (every 30 s) in flow through cell.

^cValues given as mean $\pm 2 \times$ SD of three Gran titrations

^dValues given as mean \pm root square deviation of ICP-MS instrument measurements

^e $\frac{\sum \text{Cations} - \sum \text{Anions}}{\sum \text{Cations} + \sum \text{Anions}}$ (in equivalents)

the production wells of highest interest (PW1–PW3) were between -5.5 and -10.1% , and thus deemed acceptable for further analysis.

All production wells abstract a circumneutral, Ca–HCO₃ water quality. There is however a marked difference between the deeper (PW1–PW3) and shallower (PW5–PW6) wells, both with regards to electrical conductivity and concentrations of redox-sensitive species. The deeper wells display higher electrical conductivity, higher manganese and lower dissolved oxygen values, indicative of a more reductive redox environment in the deeper parts of the aquifer. Still, wells of similar depth display different hydrochemistry—for instance, the manganese concentrations were two times higher in PW1 than PW3. This could relate to the ratio of bank filtration to native groundwater in the abstracted water. PW1–PW2 probably produce higher ratios of bank filtrated water than PW3 (Fig. 2).

Calculations of mineral saturation indices (SI) with PHREEQC show that all abstracted water at Ringerike waterworks is undersaturated (i.e., $SI < 0$) both with respect to manganese oxides (MnOOH) and manganese and calcium carbonates (MnCO₃, CaCO₃, see Table 4). Thus, the groundwater will tend to dissolve rather than precipitate these minerals. It is also noteworthy that redox potentials ($0.3 \leq Eh \leq 0.4$ V) were comparable for all wells, despite oxygen concentrations ranging from 0.3 to 6.7 mg/L (Table 4). Oxidation of manganese at pH ~ 7 occurs at $Eh \geq 0.6$ V (Appelo and Postma 2005). This implies that oxygenation, which probably occurs in the vicinity of the abstraction wells

(Farnsworth and Hering 2011), is not sufficient to trigger oxidation of manganese. This can be explained by oxidation of manganese's slow kinetics, as compared with iron (Stumm and Morgan 1996). The redox potentials are well within levels where oxidation of iron is expected to occur ($Eh > 0$ V), indicating iron oxides as the stable iron phase (Appelo and Postma 2005), and explaining the low iron concentrations in the abstracted water (see Table 3).

The K_d and R_{sorp} for production wells PW1–PW3 were estimated to be 44 ± 18 and 45 ± 18 , respectively. The uncertainties in the estimates were relatively large ($\sim 40\%$) and dependent on (1) the uncertainty of clay content, (2) the uncertainty of organic matter content of the soil, and (3) variation in the cation composition (β_{Mn} , [Mn²⁺]) of the groundwater (see Eqs. 4–6). Their relative importance to the uncertainty were calculated to be 25% (clay), 36% (organic

Table 4 Saturation indices for rhodochrosite (MnCO₃), manganite (MnOOH) and calcite (CaCO₃)

Production well	Saturation index (SI)		
	MnCO ₃	MnOOH	CaCO ₃
PW1	-0.56	-3.57	-1.68
PW2	-0.17	-3.16	-1.26
PW3	-0.73	-3.86	-1.49
PW6	-1.91	-4.79	-1.75

matter) and 39% (cation composition), demonstrating that the cause of uncertainty is relatively evenly distributed.

PHREEQC-simulated concentrations of calcium, chloride and manganese in PW2 are displayed in Fig. 6. Calcium first increases due to ion exchange, with manganese replacing calcium at exchange sites. Chloride values remain constant since anions do not participate in sorption processes. Manganese concentrations start to increase after ~20–30 abstracted pore volumes. The “S-shaped” curvature of the simulated manganese concentrations, with a gradual increase in manganese concentrations up until a maximum level, is due to K_d 's dependency on the solute concentration of manganese and other cations (Eq. 5). Ca^{2+} and other major cations (Mg^{2+} , K^+ , Na^+) decrease, while manganese concentrations increase. This is because cation exchange sites are becoming saturated with respect to manganese. Consequently, less major cations become desorbed. When ion exchange equilibrium is reached in the entire aquifer (i.e., after ~50 abstracted pore volumes), manganese concentrations stabilize meanwhile Ca^{2+} and other cations return to its level at time zero (= 0 abstracted pore volumes).

Discussion

Simulated manganese concentrations from the PHREEQC sorption model are plotted versus observed concentrations in Fig. 7. The simulated (R_{sorp}) and observed (R_{obs}) manganese retardation is read off as the number of abstracted pore volumes before manganese concentrations start to increase

and stabilize at an elevated level. The observed manganese concentrations resemble the curvature of the simulated ones. An especially good fit is observed for PW2 ($R^2 = 0.90$), while simulations for PW1 ($R^2 = -0.08$) and PW3 ($R^2 = -0.82$) predict breakthrough of the sorption front later than the observed increase in manganese concentrations. This indicates that the sorption capacity of the aquifer sediments is sufficient to delay manganese transport to the production wells in the Kilemoen aquifer, and that it serves as a possible explanation for the observed retardation of manganese

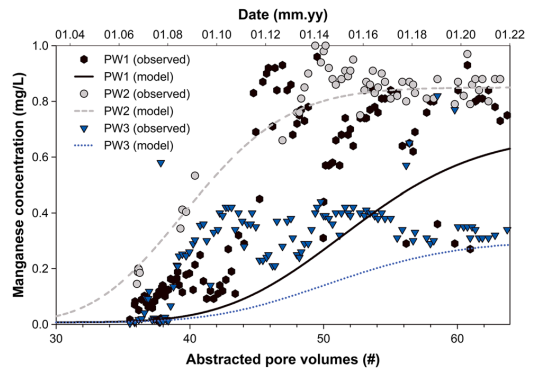
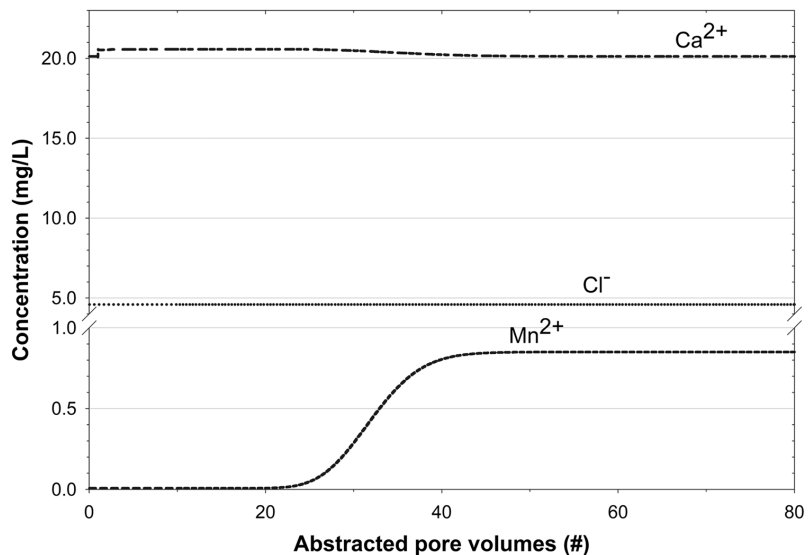


Fig. 7 PHREEQC-simulated (“model”) and observed manganese concentrations in production wells PW1–PW3 plotted vs. abstracted pore volumes = t/t_{gw} , where t = time since start of operation/simulation and t_{gw} = groundwater residence time. Abstracted pore volumes matched with date, assuming $t_{gw} = 200$ days, and start of operation on 1 January 1987

Fig. 6 PHREEQC simulated concentrations of Ca^{2+} , Cl^- and Mn^{2+} in production well PW2 versus numbers of abstracted pore volumes = t/t_{gw} , where t = time since start of simulation and t_{gw} = groundwater residence time



($36 < R_{\text{obs}} < 50$) in PW1–PW3. Similar conclusions were made by Oren et al. (2007) based on R_{sorp} resembling R_{obs} .

The calculated R_{sorp} and PHREEQC modeled sorption retardation only represent rough estimates, due to simplifications and sparse input data, especially associated with the CEC value. Firstly, the model assumes that neither mineral precipitation nor dissolution occurs between the riverbank and production well area ($0 < x \leq L$). The manganese mineral subsaturations (Table 4) indicate that manganese may be (reductively) dissolved in the water phase near the abstraction wells, in addition to near the riverbank. The manganese retardation due to sorption R_{sorp} would represent an underestimate if manganese-containing minerals dissolve closer to the abstraction well than the model assumes. Furthermore, silicate and carbonate dissolution adding cations to the groundwater is expected to occur between the riverbank and abstraction wells. For instance, all water samples in Table 4 are undersaturated with respect to calcite. Water samples indicate higher ratios of dissolved manganese to other cations in test wells near the riverbank (Hilmo 2007) than in the production wells (Table 3). A larger proportion of manganese to other cations would increase the relative tendency of manganese to occupy sorption sites (β_{Mn}), and thus increase the manganese sorption retardation R_{sorp} .

Furthermore, the clay concentrations vary considerably, as shown on the map and in drilling logs in Fig. 1. In all, 39 out of 40 test sediment samples displayed no clay present, which could indicate groundwater flow paths with no clay present. In this case, the average R_{sorp} for PW1–PW3 would be reduced to 36 ± 14 , which would lead to a better fit of the modeled to observed data for PW1 and PW3 (see Fig. 7).

Lastly, no organic matter measurements were available for the Kilemoen aquifer. Instead, the analysis relied on two sediment samples from another aquifer (Gardermoen, ~50 km direct distance away) of the same age (~10,500 years old).

Other retardation explanations should also be tested before concluding whether sorption is the main controller of manganese transport in the Kilemoen aquifer. Since the abstraction wells have not experienced severe clogging issues, changes in water quality due to new inflow paths around the production wells are thus not probable. This is also as expected from the subsaturation with respect to manganese oxides and carbonates (Table 4) and low iron concentrations (Table 3). Manganese oxide and carbonate subsaturations also increase the risk of a manganese sorption front reaching the production wells, since no precipitation sequestration of manganese can be expected (Farnsworth and Hering 2011). Thus, mineral saturation calculations strengthen the hypothesis of sorption controlling the elevated manganese concentrations after longtime operation.

Additionally, the operational scheme did not change (e.g., establishing of new production wells or increasing pumping

rate) prior to the increasing manganese concentrations in 2006. The introduction of a new groundwater flow path leading to extraction of groundwater with longer residence time and/or more reductive conditions is thus deemed unlikely. This further points to sorption as the most probable cause of delayed manganese increase in the production wells.

Laboratory experiments by Petrunic et al. (2005) showed that the microbial community needed time to adapt to changing redox conditions. Still, the microbial activity could not explain the delayed manganese enrichment alone, neither in the laboratory experiments nor the bank filtration scheme at New Brunswick, Canada (see Table 1). Regular measurements of the inorganic (CO_2 , Ca^{2+} , alkalinity, pH) and organic (TOC) carbonate system would be valuable to assess delays in microbial community growth, as one would expect more CO_2 and less TOC in the water when the microbial activity intensifies. Unfortunately, however, sparse carbonate-system measurements have been collected from the Ringerike waterworks.

The authors deem sorption as the most probable cause of delayed elevated manganese concentrations. This is because neither introduction of a new flow path, either locally around the production wells or in the aquifer, nor changes in the microbial community seem to be able to explain the retardation alone and/or in a more satisfactory manner than the presented sorption model shown in Fig. 7. Still, more data on sediment composition (organic and clay content) and water quality over time would have reduced the uncertainty associated with this conclusion.

The estimated TOC value for the Kilemoen aquifer seems representative of other glaciofluvial aquifers in Norway. Five sediment samples from a younger glaciofluvial aquifer (~10,200–10,500 years old, Olsen 2008) in Lillehammer, Norway, displayed a median (range) of $\text{TOC} = 0.26\%$ (0.08–1.07%; Holmström et al. 2010). Two sediment samples from an older glaciofluvial deposit (~12,500 years old (Vorren and Mangerud 2006)) displayed loss on ignition $\text{LOI} = 0.15$ and 0.42% (Riise 2015; Stenvik et al. 2022). TOC values of 0.09 and 0.24% could be estimated from the LOI values by dividing with van Bommel's factor (= 1.724) (Holmström et al. 2010). Despite relatively sparse data, the measured TOC values indicate that Norwegian glaciofluvial aquifers can have a significant Mn^{2+} sorption retardation capacity, which may be further increased if clay is present (Eq. 6).

Mn^{2+} retardation due to sorption and changes in the microbial community may explain why all occurrences (known to the authors) of elevated manganese concentrations after longtime bank filtration have occurred in glaciofluvial deposits (see Table 1). Additionally, manganese retardation due to sorption was observed during sewage reclamation by infiltration to the aquifer in the Dan Region, Israel (Oren et al. 2007). For all these manganese retardation cases, there seems to be limited or at least less organic

material in the depositional environment than the infiltrating water. This implies that more oxic groundwater conditions prevailed during natural prebank filtration conditions, which limited dissolved and hence adsorbed manganese in the aquifer. Furthermore, the aquifer formations had excess manganese sorption capacity available when the redox geochemistry changed (i.e., when abstraction wells in the aquifer induced bank filtration).

Monitoring of sorption fronts in bank filtration settings

If the elevated manganese concentrations are due to a sorption front moving from the bank filtration to the production well area, water quality sampling in an observation well between the bank filtration and production well area would be valuable.

The observation well would facilitate both detection of the sorption before it reaches the production well(s) and assessment of the degree of success of in-situ remediation measures. The location of the observation well has certain implications: the closer to the infiltration area the observation well is located, the longer time is available to implement the remedies and the sooner remediation actions can be evaluated, if these actions are applied in the bank filtration area (e.g., establishing an infiltration basin/well). Sooner implementation of remedies is also of great significance, since the amount of adsorbed manganese must first be desorbed and flushed out of the aquifer before the aquifer returns to its original state with low manganese concentrations. This could explain why measures that were undertaken at Ringerike waterworks in 2006–2007 (i.e., running the sand filter and infiltration wells near the riverbank) did not reduce the manganese concentrations in the short term.

According to Fig. 6, a manganese sorption front would result in a gradual increase in manganese, meanwhile other cation concentrations gradually decrease. Thus, major cations versus dissolved manganese time series could indicate whether sorption causes the delayed breakthrough of manganese in observation/production wells. Regular water quality sampling should be performed in the observation wells, both by field measurements (pH, O_2 , EC, Eh, T, alkalinity) in a flow-through cell and water samples for laboratory analysis (major cations and anions, iron and manganese, TOC), to keep track of the water quality versus time. The authors suggest at least one full water quality assessment per year.

The example from Ringerike waterworks demonstrates the value of water quality monitoring of bank filtration schemes. Issues with elevated Mn^{2+} concentrations, the

operational scheme and aquifer conditions at Ringerike are representative of many other Norwegian waterworks (Table 1). Similar bank filtration waterworks in glaciofluvial aquifers in Norway and abroad are thus advised to implement the aforementioned monitoring during operation.

Conclusions

The elevated concentrations of manganese in the Kilemoen aquifer are most likely caused by reductive dissolution of manganese oxides near the riverbank, induced by bank filtration of organic-rich river water. This is deduced from depth-specific water sampling near the riverbank, which displays higher iron and manganese and lower TOC values in the groundwater compared with the river water.

Manganese concentrations in the production wells at Ringerike waterworks ~500 m away from the riverbank started to increase 19–27 years after start of operation, depending on the well location. This equals a retardation in the range $36 < R_{obs} < 50$, assuming groundwater residence time $t_{gw} \sim 200$ days. Similar retardation ($R_{sorp} = 45 \pm 18$) was estimated with a simplified advection-sorption model, considering sorption as the only retardation factor. This shows retardation due to sorption is a possible explanation to the observed manganese retardation, although rather large uncertainty is associated with the rather sparse input data and simplified advection-reaction model.

For similar bank filtration schemes, it is recommended to establish an observation well between the production well area and the riverbank that is water sampled and field measured regularly to monitor possible manganese sorption fronts moving toward the production well field. This would enable planning and evaluation of measures to reduce manganese concentrations before they break through to the production well field. Locating the observation well closer to the riverbank will (1) allow more time to execute remediation measures and more rapid evaluation of these and (2) require less manganese to be desorbed and flushed out of the aquifer during remediation.

Supplementary Information The online version contains supplementary material available at <https://doi.org/10.1007/s10040-022-02538-w>.

Acknowledgements We would like to thank all the involved institutions and persons for cooperation and financial support. Many thanks to Tormod Tobiassen, operator at Ringerike waterworks, for hospitality, and acquisition and sharing of data, and Berit Aaberg and Gunnar Stenvik for cheap car rental during field work. Furthermore, a big thanks is directed to David L. Parkhurst, scientist emeritus at the US Geological Survey, for helpful input on PHREEQC modeling. Lastly, we offer many thanks for the constructive comments from the editor and four reviewers.

Funding Open access funding provided by NTNU Norwegian University of Science and Technology (incl St. Olavs Hospital - Trondheim University Hospital). This study is part of the research project Optimal Utilization of Groundwater for Heating and Cooling in Melhus 2 (ORMEL 2), which is a cooperation between Melhus municipality, the Norwegian University of Science and Technology, Asplan Viak AS, the Geological Survey of Norway and Gjøvaag AS, receiving funding from the Regional Research Funds in Mid-Norway.

Declarations

Conflict of interest statement On behalf of all authors, the corresponding author states that there is no conflict of interest.

Open Access This article is licensed under a Creative Commons Attribution 4.0 International License, which permits use, sharing, adaptation, distribution and reproduction in any medium or format, as long as you give appropriate credit to the original author(s) and the source, provide a link to the Creative Commons licence, and indicate if changes were made. The images or other third party material in this article are included in the article's Creative Commons licence, unless indicated otherwise in a credit line to the material. If material is not included in the article's Creative Commons licence and your intended use is not permitted by statutory regulation or exceeds the permitted use, you will need to obtain permission directly from the copyright holder. To view a copy of this licence, visit <http://creativecommons.org/licenses/by/4.0/>.

References

- Appelo CAJ, Postma D (2005) *Geochemistry, groundwater and pollution*, 2nd edn. Balkema, Amsterdam
- Bækken T, Kile MR, Skryseth LM, Eriksen TE (2011) Resipientundersøkelse av Begna, Randselva og Tyrifjorden i 2010 i forbindelse med utslipp fra Norske Skog Follum ASA og Huhtamaki Norway AS [Recipient survey of Begna, Randselva and Tyrifjorden in 2010 in response to pollution from Norske Skog Follum ASA and Huhtamaki Norway AS]. NIVA report 6189-2011, Norwegian Institute for Water Research (NIVA), Oslo, Norway. https://niva.brage.unit.no/niva-xmliui/bitstream/handle/11250/215520/6189-2011_72dpi.pdf. Accessed Sept 2022
- Bourg ACM, Bertin C (1994) Seasonal and spatial trends in manganese solubility in an alluvial aquifer. *Environ Sci Technol* 28(5):868–876. <https://doi.org/10.1021/es00054a018>
- Breuwisma A, Wösten H, Vleeshouwer J, Slobbe A, Bouma J (1986) Derivation of land qualities to assess environmental problems from soil surveys. *Soil Sci Soc Am J* 50(1):186–190. <https://doi.org/10.2136/sssaj1986.03615995005000010035x>
- Brugger M, Paskert P (2020) Groundwater plant with treatment system to remove manganese. *Water Solutions* (2). <https://www.hydrogroup.de/fileadmin/redakteur/pdf/fachberichte/twa/2020-02-water-solutions-groundwater-plant-with-system-to-remove-manganese.pdf>. Accessed Sept 2022
- Dawe MR (2006) Assessing infiltration velocities during riverbank filtration. MSc Thesis, University of New Brunswick, Fredericton, NB, Canada
- Dillon P (2005) Future management of aquifer recharge. *Hydrogeol J* 13(1):313–316. <https://doi.org/10.1007/s10040-004-0413-6>
- Ellingsen K (1992) Grunnvannskvalitet: problemer og tiltak [Groundwater quality: problems and preventive measures]. GiN guide no. 12. Skrifter 106, Geological Survey of Norway, Trondheim, Norway. https://www.ngu.no/upload/Publikasjoner/Skrifter/GiN-veileder_nr12.pdf. Accessed Sept 2022
- Ellingsen K, Finsrud R (1990) Grunnvannsanlegg - eksempler [Groundwater works: examples] GiN-guide no. 5, Skrifter 101, Geological Survey of Norway, Trondheim, Norway. https://www.ngu.no/upload/Publikasjoner/Skrifter/GiN-veileder_nr5.pdf. Accessed Sept 2022
- Farnsworth CE, Hering JG (2011) Inorganic geochemistry and redox dynamics in bank filtration settings. *Environ Sci Technol* 45(12):5079–5087. <https://doi.org/10.1021/es2001612>
- Geological Survey of Norway (2021) GRANADA: Nasjonal grunnvannsdatabase [GRANADA: national groundwater database]. http://geo.ngu.no/kart/granada_mobil/. Accessed 23 June 2021
- Hilmo BO (2007) Undersøkelserboringer ved Tjorputten: oppsummering av resultater og forslag til videre arbeid [Test drillings at Tjorputten: summary of results and proposals for further work]. 514555 – Nye brønner til Ringerike vannverk, Asplan Viak AS, Trondheim, Norway. https://www.ngu.no/upload/Publikasjoner/Eksterne-grunnvannsrapporter/VRL46_2008_010a_ful.pdf. Accessed Sept 2022
- Hiscock KM, Grischek T (2002) Attenuation of groundwater pollution by bank filtration. *J Hydrol* 266(3):139–144. [https://doi.org/10.1016/S0022-1694\(02\)00158-0](https://doi.org/10.1016/S0022-1694(02)00158-0)
- Holmström P, Rudolph-Lund K, Sørli JE (2010) Korgen vannverk: hydrogeologisk og vannkjemisk tilstandsvurdering av brønner [Korgen waterwork: hydrogeological and hydrochemical assessment of groundwater wells]. NGI report 20081232-00-1-R, Norwegian Geotechnical Institute (NGI), Oslo
- Houben G, Treskatis C (2007) *Water well rehabilitation and reconstruction*. McGraw-Hill, New York
- Klemetsrud T (1985) Ringerike vannverk - Kilemoen: pilotboringer i grop 8, og ved Tjorputten [Ringerike waterwork - Kilemoen: pilot drilling in kettle hole 8 and at Tjorputten]. NGU report 86009, Geological Survey of Norway, Oslo, Norway. <https://www.ngu.no/publikasjon/ringerike-vannverk-kilemoen-pilotboringer-i-grop-8-og-ved-tjorputten>. Accessed Sept 2022
- Knutsson G (2008) Hydrogeology in the Nordic countries. Episode 31. <https://doi.org/10.18814/epiugs/2008/v31i1/020>
- Kraft P (2011) Beskyttelse av råvannskilden til Bø vannverk [Protection of Bø waterworks' groundwater source]. 522947 – Reguleringsplan for beskyttelse av Bø vannverk, Asplan Viak AS, Ås, Norway. http://webhot3.gisline.no/GisLinePlanarkiv/0821/02_32_2009/Dokumenter/Beskyttelsesplan.pdf. Accessed Sept 2022
- Kvitsand HML, Myrmet M, Fiksdal L, Østerhus SW (2017) Evaluation of bank filtration as a pretreatment method for the provision of hygienically safe drinking water in Norway: results from monitoring at two full-scale sites. *Hydrogeol J* 25(5):1257–1269. <https://doi.org/10.1007/s10040-017-1576-2>
- Lindholm M, Vogelsang C, Engebretsen A, Kværnø S, Eggested HO, Selvik JR (2015) Forurensningsregnskap for Ringerike kommune [Accounting for pollution in Ringerike municipality]. NIVA report 6873-2015, NIVA, Oslo, Norway. https://niva.brage.unit.no/niva-xmliui/bitstream/handle/11250/285876/6873-2015_72dpi.pdf?sequence=3&isAllowed=y. Accessed Sept 2022
- Norwegian Mapping Authority (2021) Høydedata [Elevation data]. <https://hoydedata.no/LaserInnsyn/>. Accessed 27 Oct 2021
- Olsen L (2008) Kwartærgeologi i Lillehammer kommune: beskrivelse til løsmassekart M 1:50 000 [Quaternary geology in Lillehammer municipality: description to map M 1:50 000]. NGU report 2008.031, Geological Survey of Norway, Trondheim, Norway. https://www.ngu.no/upload/Publikasjoner/Rapporter/2008/2008_031.pdf. Accessed Sept 2022
- Oren O, Gavrieli I, Burg A, Guttman J, Lazar B (2007) Manganese mobilization and enrichment during soil aquifer treatment (SAT) of effluents, the Dan Region Sewage Reclamation Project

- (Shafdan). *Israel Environ Sci Technol* 41(3):766–772. <https://doi.org/10.1021/es060576+>
- Parkhurst DL, Appelo CAJ (2013) Description of input and examples for PHREEQC version 3: a computer program for speciation, batch-reaction, one-dimensional transport, and inverse geochemical calculations. *US Geol Surv Tech Methods* 6-A43. <https://pubs.usgs.gov/tm/06/a43/>. Accessed Sept 2022
- Petrunic BM, MacQuarrie KTB, Al TA (2005) Reductive dissolution of Mn oxides in river-recharged aquifers: a laboratory column study. *J Hydrol* 301(1):163–181. <https://doi.org/10.1016/j.jhydr.2004.06.022>
- Riise MH (2015) Praktisk guide for grunnvarmeanlegg basert på oppumpet grunnvann [Practical guide for ground water heat pump systems]. MSc Thesis, Norwegian University of Science and Technology, Trondheim, Norway. <https://ntnuopen.ntnu.no/ntnu-xmlui/handle/11250/2350389>. Accessed Sept 2022
- Segar D (1994) A groundwater vulnerability study of the Korgen waterworks, Lillehammer kommune. NGU report 94.010, Geological Survey of Norway, Trondheim, Norway. <https://www.ngu.no/publikasjon/groundwater-vulnerability-study-korgen-waterworks-lillehammer-kommune>. Accessed Sept 2022
- Silvey WD, Johnston HE (1977) Preliminary study of sources and processes of enrichment of manganese in water from University of Rhode Island supply wells. *US Geological Survey Open file Rep* 77-561. <http://pubs.er.usgs.gov/publication/ofr77561>. Accessed Sept 2022
- Skarphagen H (1982) Grunnvannsanlegg Kilemoen. Vedrørende undersøkelserboringer i forbindelse med plassering av infiltrasjonsbrønner ved Tjørputten [Test drilling for infiltration wells at Tjørputten]. NGU report O-82055, Geological Survey of Norway, Oslo, Norway. <https://www.ngu.no/en/publikasjon/grunnvannsanlegg-kilemoen-vedr-rende-unders-kelsesboringer-i-forbindelse-med-plassering>. Accessed Sept 2022
- Stenvik LA, Hilmo BO (2020) Jern- og manganproblematikk ved grunnvannsutttak med eksempler fra Ringerike og Sunndal vannverk [Iron and manganese problems under groundwater abstraction with cases from Ringerike and Sunndal waterworks]. *Vann* 55(2):151–161. <https://vannforeningen.no/dokumentarkiv/jern-og-manganproblematikk-ved-grunnvannsutttak-gjennomgang-med-eksempler-fra-ringerike-og-sunndal-vannverk/>. Accessed Sept 2022
- Stenvik LA, Gjengedal S, Ramstad RK, Frenstad BS (2022) Hydrochemical and biotic control on iron incrustations in groundwater heat pump systems: case study from a saline, anoxic aquifer in Melhus, Norway. *Geothermics* 100. <https://doi.org/10.1016/j.geothermics.2022.102349>
- Stumm W, Morgan JJ (1996) *Aquatic chemistry: chemical equilibria and rates in natural waters*, 3rd edn. Wiley, Chichester, England
- Thomas NE, Kan KT, Bray DI, MacQuarrie KTB (1994) Temporal changes in manganese concentrations in water from the Fredericton aquifer, New Brunswick. *Groundwater* 32(4):650–656. <https://doi.org/10.1111/j.1745-6584.1994.tb00901.x>
- Vestland M (2012) Klausuleringsplan for Ringerike vannverk Kilemoen [Protection plan for Ringerike waterworks Kilemoen]. 529119 – Hydrogeologisk rådgivning - Ringerike vannverk, Asplan Viak AS, Trondheim, Norway. <https://webdav.ringerike.kommune.no/webdav/Formannskapssaker%20-%20h%C3%B8st%202012-%20v%C3%A5r%202015/14%2003%2011/44-14-01%20Tilleggsnotat%20sak%2044%20Vedlegg.pdf>. Accessed Sept 2022
- Vorren TO, Mangerud J (2006) Istider kommer og går [Ice ages come and go]. In: Ramberg IB, Bryhni I, Nøttvedt A (eds) *Landet blir til: Norges geologi* [The making of a land: geology of Norway]. Norsk Geological Society, Trondheim, Norway
- Woyessa AO (2012) Identification of hydrochemical processes in the screen environment in shallow geothermal wells from Gardermoen. MSc Thesis, University of Oslo, Oslo, Norway. <https://www.duo.uio.no/handle/10852/12561>. Accessed Sept 2022

Publisher's note Springer Nature remains neutral with regard to jurisdictional claims in published maps and institutional affiliations.

ISBN 978-82-326-6385-9 (printed ver.)
ISBN 978-82-326-6879-3 (electronic ver.)
ISSN 1503-8181 (printed ver.)
ISSN 2703-8084 (online ver.)



NTNU

Norwegian University of
Science and Technology